frontiers | Research Topics

New insights into prostate cancer: New biomarkers, molecular mechanisms, and therapeutic approaches

Edited by
Anna Perri, Vittoria Rago and Guadalupe Maya-Núñez

Published in
Frontiers in Endocrinology
Frontiers in Pharmacology

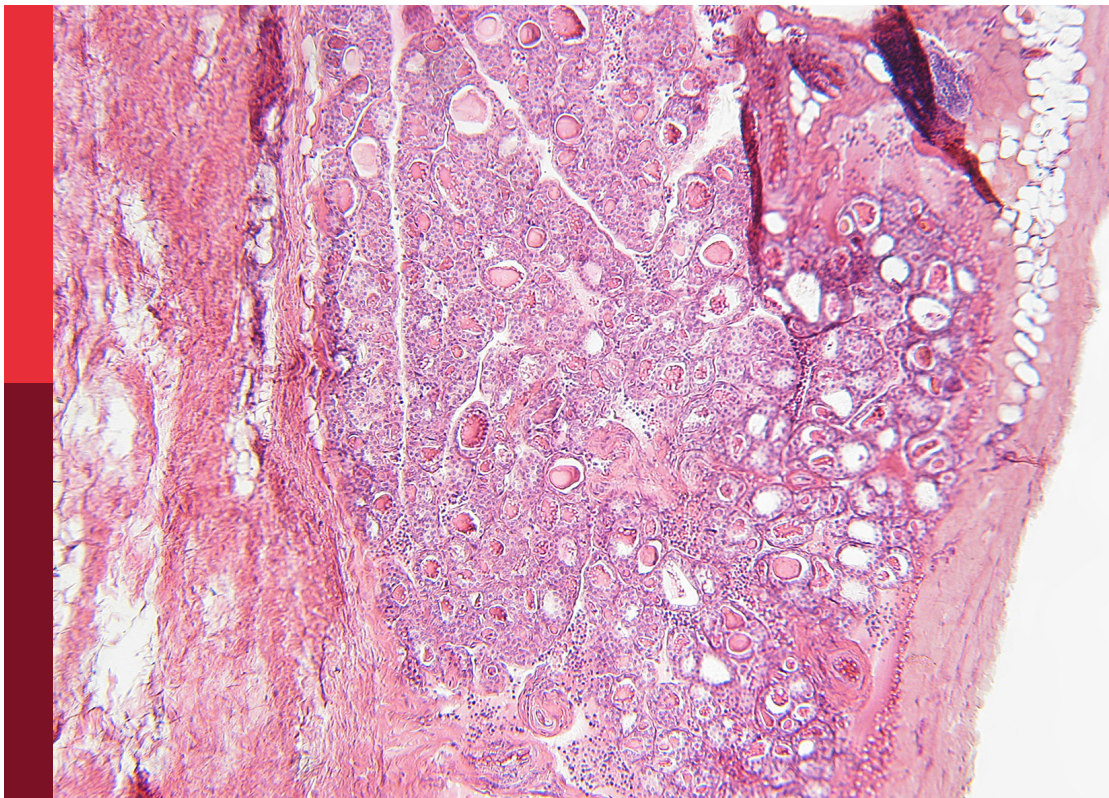

ISSN 1664-8714
ISBN 978-2-8325-5258-2
DOI 10.3389/978-2-8325-5258-2

About Frontiers

Frontiers is more than just an open access publisher of scholarly articles: it is a pioneering approach to the world of academia, radically improving the way scholarly research is managed. The grand vision of Frontiers is a world where all people have an equal opportunity to seek, share and generate knowledge. Frontiers provides immediate and permanent online open access to all its publications, but this alone is not enough to realize our grand goals.

Frontiers journal series

The Frontiers journal series is a multi-tier and interdisciplinary set of open-access, online journals, promising a paradigm shift from the current review, selection and dissemination processes in academic publishing. All Frontiers journals are driven by researchers for researchers; therefore, they constitute a service to the scholarly community. At the same time, the *Frontiers journal series* operates on a revolutionary invention, the tiered publishing system, initially addressing specific communities of scholars, and gradually climbing up to broader public understanding, thus serving the interests of the lay society, too.

Dedication to quality

Each Frontiers article is a landmark of the highest quality, thanks to genuinely collaborative interactions between authors and review editors, who include some of the world's best academicians. Research must be certified by peers before entering a stream of knowledge that may eventually reach the public - and shape society; therefore, Frontiers only applies the most rigorous and unbiased reviews. Frontiers revolutionizes research publishing by freely delivering the most outstanding research, evaluated with no bias from both the academic and social point of view. By applying the most advanced information technologies, Frontiers is catapulting scholarly publishing into a new generation.

What are Frontiers Research Topics?

Frontiers Research Topics are very popular trademarks of the *Frontiers journals series*: they are collections of at least ten articles, all centered on a particular subject. With their unique mix of varied contributions from Original Research to Review Articles, Frontiers Research Topics unify the most influential researchers, the latest key findings and historical advances in a hot research area.

Find out more on how to host your own Frontiers Research Topic or contribute to one as an author by contacting the Frontiers editorial office: frontiersin.org/about/contact

New insights into prostate cancer: New biomarkers, molecular mechanisms, and therapeutic approaches

Topic editors

Anna Perri — Magna Græcia University of Catanzaro, Italy

Vittoria Rago — University of Calabria, Italy

Guadalupe Maya-Núñez — Mexican Social Security Institute, Mexico

Citation

Perri, A., Rago, V., Maya-Núñez, G., eds. (2024). *New insights into prostate cancer: New biomarkers, molecular mechanisms, and therapeutic approaches*. Lausanne: Frontiers Media SA. doi: 10.3389/978-2-8325-5258-2

Table of contents

frontiers | Frontiers in Endocrinology

TYPE Editorial
PUBLISHED 24 July 2024
DOI 10.3389/fendo.2024.1453065

OPEN ACCESS

EDITED AND REVIEWED BY
Antonino Belfiore,
University of Catania, Italy

*CORRESPONDENCE
Anna Perri
anna.perri@unicz.it
Vittoria Rago
vittoria.rago@unical.it

RECEIVED 22 June 2024
ACCEPTED 08 July 2024
PUBLISHED 24 July 2024

CITATION
Perri A, Rago V and Maya-Núñez G (2024) Editorial: New insights into prostate cancer: new biomarkers, molecular mechanisms, and therapeutic approaches.
Front. Endocrinol. 15:1453065.
doi: 10.3389/fendo.2024.1453065

Editorial: New insights into prostate cancer: new biomarkers, molecular mechanisms, and therapeutic approaches

Anna Perri[1*], Vittoria Rago[2*] and Guadalupe Maya-Núñez[3]

[1]Department of Experimental and Clinical Medicine, Magna Graecia University, Catanzaro, Italy, [2]Department of Pharmacy, Health and Nutritional Sciences, University of Calabria, Rende (CS), Italy, [3]Unidad de Investigación Médica en Medicina Reproductiva, Coordinación de Investigación en Salud, Instituto Mexicano del Seguro Social, Mexico City, Mexico

KEYWORDS

prostate cancer (PCa), castration-resistant PCa (CRPC), biomarkers, androgen receptor, G protein-coupled estrogen receptor (GPER), positive surgical margins, bioactive compounds

Editorial on the Research Topic
New insights into prostate cancer: new biomarkers, molecular mechanisms, and therapeutic approaches

Prostate cancer (PCa) is the second most frequent cancer among men worldwide (1). PCa is considered curable when it is localized, but when it metastasizes the clinical treatment is complex. Androgen deprivation therapy (ADT) is a regular treatment for PCa patients; however, some of them develop castration-resistant PCa (CRPC), and despite several new treatment options, metastatic CRPC has a poor prognosis with a survival rate below 2–3 years (2).

The present Research Topic aims to present new emerging evidence in diagnostics and treatment of PCa.

The Prostate specific antigen (PSA) is a poor indicator of early PCa, particularly if its levels are between 4 and 20 ng/ml. Among other PCa serum markers, Sialic acid (SA) represents a potential candidate for tumor aggressiveness, as demonstrated in other types of cancer (3). Sun and Yan reported that in patients with PSA values between 4 and 20 ng/mL, the serum biochemical index, including SA, is a potential prediction marker for PCa. The authors suggested that SA levels could prevent unnecessary biopsies and biopsy-related morbidities. Furthermore, Sun et al., demonstrated that the serum SA levels in patients without treatment are positively correlated with bone metastases, consequently proposing that elevated SA levels before surgery could be an indicator of increased malignancy risk and advanced cancer stages. Cathepsins play a crucial role in preserving cellular homeostasis; however, under inflammatory conditions, they can drive cancer progression and other diseases (4, 5). The Mendelian randomization study of Cao et al., provided new

insights into the role of cathepsins in the diagnosis and treatment of benign prostate diseases (BPD), as they offered the first evidence of a genetic causal link between cathepsins and BPD.

The identification of new specific markers associated with cancer recurrence is critical in the management of PCa patients. The autophagy-related gene expression levels have great potential in predicting tumor recurrence risk and evaluating the response to treatment in PCa patients (6, 7). Kang et al., built a risk model using four anoikis-related genes that effectively predict the risk of recurrence and survival outcomes in PCa patients, confirming the clinical value of in-depth investigation of anoikis-related genes in PCa.

Drug resistance CRPC mechanisms due to AR splice variants, mutations, or glucocorticoid receptor (GR) substitution of AR function, is a common cause of treatment failure. The search for pharmacological agents to overcome this cancer resistance conducted to plant extracts research (8). Lam et al., demonstrated the efficacy of the bioactive compound YIV-818-A in overcoming drug resistance caused by AR variants and GR, by inhibiting AR and GR activities. Some studies elucidated the molecular mechanism underlying the anti-tumor effects of curcumin on both androgen-sensitive and -insensitive prostate cancer cells (9). The meta-analyses conducted by Wang et al. showed a favorable association between PCa and curcumin treatment, highlighting that the curcumin dosage potentially impacted the treatment efficacy. Overall these findings further reinforce the concept that dietary supplements could be used as chemoprevention agent for PCa, although further studies are needed to ascertain their use in the clinical practice.

G protein-coupled estrogen receptor (GPER) plays an important role in tumor development and metastasis, by activating different signaling pathways (10, 11). The GPER-mediated signaling in PCa is the hedgehog (Hh) pathway and has not been widely investigated. This signaling-pathway activation is associated with aggressiveness, metastasis, and relapse in triple-negative breast cancer, occurring *via* glioma-associated oncogene homolog (GLI) transcriptional factors (12). The study of Rico-Fuentes et al., performed on PCa samples with different prognostic grades demonstrated that GPER is highly expressed in the nucleus and its expression increases with the cancer progression. Furthermore, GPER's expression correlates with pGLI3 nuclear expression across different stage groups, suggesting that GPER could represent a new marker of tumor aggressiveness.

Insulin growth factor (IGF) signaling plays a key role in the development and progression of PCa. Consequently, targeting IGF signaling has been considered a potential therapeutic strategy for this cancer (13). Elemam et al., provided an overview of the main evidence on prostate tumorigenesis regulation *via* the IGF system, highlighting that drugs targeting the IGF family could represent a promising therapeutic approach in the management of advanced PCa.

Many researchers found a complex and close association between the immune system and PCa (14). Still, few studies have investigated the association between immune cells and the risk of PCa. Hao et al., identified immune cell phenotypes significantly associated with PCa, contributing to open new insights for exploring potential immunotherapeutic targets in PCa.

An increasing number of articles highlight the positive surgical margin (PSM) as a relevant parameter to make decisions for adjuvant treatment and predict patient outcomes after radical prostatectomy (RP), mainly in patients with localized PCa (15). Therefore, the factors influencing PSM should be considered by urologists during operation, regardless of the surgery approach (i.e. robot-assisted, laparoscopic, and open RP). The monocentric study of Wang et al. showed that PSM risk was increased in patients receiving hormonal therapy before the surgery compared with patients without treatment, highlighting that the resection extent should be accurately evaluated. In the past, the RP was rarely the first option for advanced PCa, but thanks to the introduction of robot-assisted RP, it has been reported that advanced PCa patients respond well to ADT therapy and have better progression-free survival after cytoreductive prostatectomy, suggesting that surgery might be an effective treatment option also for advanced PCa (16). Li et al. built a clinical features-based prognosis model demonstrating the benefits of surgery in patients with advanced PCa, and emphasizing that its accuracy may offer some reference on clinical decision-making.

In conclusion, this Research Topic presents interesting new evidence in the field of precision medicine for PCa diagnosis and treatment. Although relevant progress has been made, further studies are needed to better understand how to overcome castration resistance, find new predictors of tumor recurrences, and improve the survival rate.

Author contributions

AP: Writing – review & editing, Writing – original draft. VR: Writing – review & editing, Writing – original draft. GM-N: Writing – review & editing, Writing – original draft.

Conflict of interest

The authors declare that the research was conducted in the absence of any commercial or financial relationships that could be construed as a potential conflict of interest.

The author(s) declared that they were an editorial board member of Frontiers, at the time of submission. This had no impact on the peer review process and the final decision.

Publisher's note

References

1. Kaiser A, Haskins C, Siddiqui MM, Hussain A, D'Adamo C. The evolving role of diet in prostate cancer risk and progression. *Curr Opin Oncol*. (2019) 31:222–9. doi: 10.1097/CCO.0000000000000519

2. Nuhn P, De Bono JS, Fizazi K, Freedland SJ, Grilli M, Kantoff PW, et al. Update on systemic prostate cancer therapies: management of metastatic castration-resistant prostate cancer in the era of precision oncology. *Eur Urol*. (2019) 75:88–99. doi: 10.1016/j.eururo.2018.03.028

3. Zhang Z, Wuhrer M, Holst S. Serum sialylation changes in cancer. *Glycoconj J*. (2018) 35:139–60. doi: 10.1007/s10719-018-9820-0

4. Patel S, Homaei A, El-Seedi HR, Akhtar N. Cathepsins: Proteases that are vital for survival but can also be fatal. *BioMed Pharmacother*. (2018) 105:526–32. doi: 10.1016/j.biopha.2018.05.148

5. Miyake H, Hara I, Eto H. Serum level of cathepsin B and its density in men with prostate cancer as novel markers of disease progression. *Anticancer Res*. (2004) 24:2573–7.

6. Zhao X, Wang Z, Tang Z, Hu J, Zhou Y, Ge J, et al. An anoikis-related gene signature for prediction of the prognosis in prostate cancer. *Front Oncol*. (2023) 13:1169425. doi: 10.3389/fonc.2023.1169425

7. Wen C, Ge Q, Dai B, Li J, Yang F, Meng J, et al. Signature for prostate cancer based on autophagy-related genes and a nomogram for quantitative risk stratification. *Dis Markers*. (2022) 2022:7598942. doi: 10.1155/2022/7598942

8. Kallifatidis G, Hoy JJ, Lokeshwar BL. Bioactive natural products for chemoprevention and treatment of castration-resistant prostate cancer. *Semin Cancer Biol*. (2016) 40–41:160–9. doi: 10.1016/j.semcancer.2016.06.003

9. Termini D, Den Hartogh DJ, Jaglanian A, Tsiani E. Curcumin against prostate cancer: current evidence. *Biomolecules*. (2020) 10:1536. doi: 10.3390/biom10111536

10. Ramírez-de-Arellano A, Pereira-Suárez AL, Rico-Fuentes C, López-Pulido EI, Villegas-Pineda JC, Sierra-Diaz E. Distribution and effects of estrogen receptors in prostate cancer: associated molecular mechanisms. *Front Endocrinol (Lausanne)*. (2021) 12:811578. doi: 10.3389/fendo.2021.811578

11. Rago V, Romeo F, Giordano F, Ferraro A, Carpino A. Identification of the G protein-coupled estrogen receptor (GPER) in human prostate: expression site of the estrogen receptor in the benign and neoplastic gland. *Andrology*. (2016) 4:121–7. doi: 10.1111/andr.12131

12. Xu T, Ma D, Chen S, Tang R, Yang J, Meng C, et al. High GPER expression in triple-negative breast cancer is linked to pro-metastatic pathways and predicts poor patient outcomes. *NPJ Breast Cancer*. (2022) 8:100. doi: 10.1038/s41523-022-00472-4

13. Liu G, Zhu M, Zhang M, Pan F. Emerging role of IGF-1 in prostate cancer: A promising biomarker and therapeutic target. *Cancers (Basel)*. (2023) 15:1287. doi: 10.3390/cancers15041287

14. Molina OE, LaRue H, Simonyan D, Hovington H, Têtu B, Fradet V, et al. High infiltration of CD209+ dendritic cells and CD163+ macrophages in the peritumor area of prostate cancer is predictive of late adverse outcomes. *Front Immunol*. (2023) 14:1205266. doi: 10.3389/fimmu.2023.1205266

15. Chapin BF, Nguyen JN, Achim MF, Navai N, Williams SB, Prokhorova IN, et al. Positive margin length and highest Gleason grade of tumor at the margin predict for biochemical recurrence after radical prostatectomy in patients with organ-confined prostate cancer. *Prostate Cancer Prostatic Dis*. (2018) 21:221–7. doi: 10.1038/s41391-017-0019-4

16. Rajwa P, Zattoni F, Maggi M, Marra G, Kroyer P, Shariat SF, et al. Cytoreductive radical prostatectomy for metastatic hormone-sensitive prostate cancer-evidence from recent prospective reports. *Eur Urol Focus*. (2023) 9:637–41. doi: 10.1016/j.euf.2023.01.011

frontiers | Frontiers in Endocrinology

TYPE Original Research
PUBLISHED 14 August 2023
DOI 10.3389/fendo.2023.1188944

OPEN ACCESS

EDITED BY
Aarti Mathur,
Johns Hopkins Medicine, United States

REVIEWED BY
Mauricio Rodriguez-Dorantes,
National Institute of Genomic Medicine (INMEGEN), Mexico
Yingbo Huang,
University of Minnesota, United States

*CORRESPONDENCE
Lei Yan
yanlei5309@126.com

RECEIVED 18 March 2023
ACCEPTED 28 July 2023
PUBLISHED 14 August 2023

CITATION
Sun J and Yan L (2023) The diagnostic effectiveness of serum sialic acid predicts both qualitative and quantitative prostate cancer in patients with prostate-specific antigen between 4 and 20 ng/mL. *Front. Endocrinol.* 14:1188944. doi: 10.3389/fendo.2023.1188944

The diagnostic effectiveness of serum sialic acid predicts both qualitative and quantitative prostate cancer in patients with prostate-specific antigen between 4 and 20 ng/mL

Jingtao Sun and Lei Yan*

Department of Urology, Qilu Hospital of Shandong University, Jinan, China

Introduction: This study aimed to evaluate the predictive value of the serum biochemical index, including alkaline phosphatase (AKP), lactate dehydrogenase (LDH), α-L-fucosidase (AFU), serum sialic acid (SA), and fibrinogen (FIB), for prostate cancer (PCa) and clinically significant prostate cancer (CSPCa) in patients with a prostate-specific antigen (PSA) value between 4 and 20 ng/mL.

Patients and methods: This study retrospectively examined the clinical data of 408 eligible patients who underwent prostate biopsies in our hospital between March 2015 and July 2022. CSPCa was defined as a "Gleason grade group of≥2". For analyzing the association between PCa/CSPCa and serum biochemical index, univariable logistic regression and multivariable logistic regression were conducted. Based on the multivariable logistic regression model, we constructed models and compared the area under the curve (AUC). We generated the nomogram, the ROC curve, the DCA curve, and the calibration curve for PCa.

Results: Overall, we studied 271 patients with PCa (including 155 patients with CSPCa) and 137 non-PCa patients. Patients with PCa were more likely to consume alcohol, have higher total PSA (TPSA) values, and have lower free PSA (FPSA) and free/total PSA (f/T) values. There were higher TPSA values and lower f/T values in the CSPCa group when compared with the non-CSPCa group. The univariate logistic regression analyses did not show significant results. However, AKP, AFU, SA, TPSA, and FPSA all retain significant significance when all factors are included in multifactor logistic regression analysis. This finding suggests that the exposure factor exhibited an independent effect on the outcome after controlling for other factors, including the potential confounding effects that may have been underestimated. Through ROC curves, we found that SA and TPSA levels are more powerful predictors. In contrast, there is a lack of excellent predictive value for PCA and CSPCa using Age, AFU, FIB, and FPSA.

Conclusion: In our study, serum biochemical index is a potential prediction tool for PCa and CSPCa for patients with PSA values between 4 and 20 ng/mL.

Additionally, the new serum biochemical index SA is also useful when diagnosing PCa and CSPCa, as we conclude in our study.

KEYWORDS

serum sialic acid, prostate cancer, prostate biopsy, diagnosis, treatment

1 Introduction

Worldwide, prostate cancer is the second leading cause of cancer-related death among men after lung cancer (1). The incidence of prostate cancer continued to rise slowly from 2014 through 2018. Over the past decade, the proportion of prostate cancer cases diagnosed at a distant stage has increased from 3.9% to 8.2% (2). Prostate-specific antigen (PSA) is an important biomarker for detecting prostate cancer. But PSA tests are not sensitive enough to detect prostate cancer early (PCA) because of their low specificity (3). In other words, most patients undergo unnecessary and potentially harmful follow-up tests, like biopsies, especially if their PSA level is between 4.0 and 20.0 ng/ml (4). The need for more specific biomarkers is, therefore, necessary to compensate for this defect. Many biomarkers of PCa have been developed successively, such as Prostate Health Index (PHI), prostate cancer antigen 3 (PCA3), four-kallikrein panel (4K), transmembrane protease serine 2-ERG (TMPRSS2-ERG), ExoDx Prostate Intelliscore and SelectMDx (5, 6). There are, however, a few disadvantages to these experimental methods, making them unsuitable for routine PCa detection (7).

Certain systemic serum biochemical indexes have been recognized as being important in promoting and advancing tumor progression in recent years. Tumor-related serum biochemical indexes, including alkaline phosphatase (AKP), lactate dehydrogenase (LDH), α-L-fucosidase (AFU), serum sialic acid (SA), and fibrinogen (FIB), have gained attention as diagnostic tools for tumors (8–10). Despite this, the study on the effects of multiple biochemical indices combined on tumor growth is not comprehensive.

In glycoproteins and glycolipids, SA is a series of hydroxylated monosaccharides containing nine carbon atoms at methylated non-reduction terminals In glycoproteins and glycolipids, SA is a series of hydroxylated monosaccharides containing nine carbon atoms at the methylated non-reduction terminals (11). There has been substantial evidence to demonstrate that cancer is associated with high serum levels of sialic acid, which have been seen in cancer patients in numerous studies (12), for instance, oral cancer (13), breast cancer (14), ovarian cancer (15) and cholangiocarcinoma (16).

A primary objective of our study was to investigate whether the SA could be used at the PSA level of 4.0 to 20.0 ng/mL to predict PCa and CSPCa. We validated the diagnostic efficacy of the AKP, LDH, AFU, and FIB in PCa and CSPCa as well.

2 Materials and methods

2.1 Patient selection information collection

From March 2015 to July 2022, we obtained information from the electronic medical record system about all patients who underwent prostate biopsies with PSA levels of 4.0-20.0ng/mL in our hospital. Blood tests were performed within 2 weeks before biopsies on all patients for the serum PSA derivative (TPSA and fPSA). Our study excluded patients with any one or more of the following conditions: (I) Patients with hematological diseases, known infections, and other malignancies; (II) Patients who had undergone prostate surgery (such as transurethral resection) before their biopsies; (III) Pathologically diagnosed patients with prostatic intraepithelial neoplasms and atypical small acinar proliferations; (IV) Patients with incomplete clinical data. Following that, we collected the following information from the medical records of eligible patients: age, history of tobacco (SH) and alcohol use (AH), blood test results with alkaline phosphatase (AKP), lactate dehydrogenase (LDH), α-L-fucosidase (AFU), fibrinogen (FIB), and prostate-specific antigen (PSA).

2.2 Blood biochemical measurement

Before receiving any clinical intervention, each patient had his venous blood drawn in the early morning after fasting for 12 hours. We stored blood samples in test tubes that contained clot activator and gel. Blood samples coagulated naturally at room temperature during the experiment. Following that, the samples were centrifuged at 2000 rpm for 10 minutes. A Roche Cobas 8000 automatic analyzer was used to determine SA concentrations after the serum had been separated. AKP concentrations in the normal range ranged from 45.00 U/dL to 125.00 U/L.The normal range for LDH concentration was 120.00 U/dL to 230.00 U/L. In terms of AFU concentration, the normal range was less than 40.00 U/L. The concentration of SA was normally between 45.6 mg/dL and 75.4 mg/dL.

2.3 Fibrinogen measurement

Surgical procedures are routinely preceded by the collection of blood samples from patients to measure plasma fibrinogen levels.

Fibrinogen levels in the blood were determined by the Clauss (17) method using bovine thrombin (100 NIHU/mL). Plasma fibrinogen levels between 2-4 g/L were considered normal.

2.4 Biopsy method and pathological examination

Using 3.0 T scanner, two uroradiologists with at least three years of experience performed prostate mpMRI before undergoing biopsies. Imaging assessments were retrospectively performed by experienced surgical team members to determine biopsy methods based on imaging findings. Lastly, local anesthesia was used to perform transrectal biopsies or transperineal biopsies on all patients. Prostate biopsies incorporated 12 + 3 cores (based on 12 systematic cores, and the remaining core at the suspicious MRI area that was visualized by cognitive fusion biopsies). After the biopsy specimens were collected, they were analyzed within a week by two experienced urologists following the ISUHP (International Society of Urological Pathology) consensus guidelines.

2.5 Data management

Based on the histopathological results, patients were categorized as non-PCa groups or PCa groups. Moreover, we separated the patients into CSPCa and non-CSPCa groups. It was defined as "clinically significant prostate cancer (CSPCa)" when referring to the Gleason grade group of≥2. After fasting for 12 hours, each patient was given five milliliters of venous blood in the early morning before any clinical intervention was carried out. To test the clot activator and gel, a blood sample was stored at room temperature and naturally coagulated. After centrifugation at 2000 rpm for 10 minutes, the samples were collected.

2.6 Statistical analysis

Normality tests were conducted on all continuous variables. In the case of continuous variables that passed the normality test, Student's t-tests were used, whereas Mann-Whitney U-tests were used in the case of continuous variables with skewed distributions. For continuous variables with normal distribution, the mean+SD was reported, and for continuous variables with skewed distribution, the median (IQR) was reported. Numbers (percentages) were reported for categorical variables after Chi-square tests were conducted. We performed univariate and multivariate logistic regression analyses to identify the independent predictors of PCa and CSPCa. The final model selection was performed using a backward stepdown selection process. Significant results were determined by a p-value of less than 0.05. An analysis of the ROC curve, DCA curve, and calibration curves was carried out to determine the validity of the PCa risk nomogram we developed for prostate biopsy. Differences in AUC were compared with the DeLong test. Statistical analyses were conducted using IBM SPSS (Version 19.0) and R (Version 4.1.0) software.

3 Results

3.1 Patient demographics eligible for participation in the program

The study included a total of 408 patients who met the entry criteria. 271 patients were diagnosed with PCa (including 155 patients with CSPCa). As shown in Table 1, the patients were classified according to their characteristics and laboratory values.

Besides TPSA (8.27 vs 10.49, p<0.01), the SA (57.70 vs 53.60, p<0.01), FPSA (1.41 vs 1.24, p=0.02) and f/T (0.18 vs 0.25, p<0.01) of the non-PCa group were significantly higher than those of the PCa group. Furthermore, PCa patients also had a higher proportion of smokers in their group as compared to non-PCa patients (Table 1).

As compared to the non-CSPCa group, the CSPCa group had higher levels of LDH and TPSA. In contrast, CSPCa groups had lower f/T values. In terms of SH, SA, and FPSA, however, there was no significant difference between the two groups. Further, there were no statistically significant differences in age, AH, AFU, and FIB between PCa and non-PCa groups, nor between CSPCa and non-CSPCa groups (Table 1).

3.2 Univariable and multivariable analyses of clinical indicators

In order to determine the predictive factors for clinical indicators, we conducted both univariate and multivariate logistic regression analyses. Furthermore, we conducted a collinearity analysis in multiple regression to comprehensively assess the variables that could be included in the model. The results of the collinearity analysis indicate that there is no interaction among the factors. The univariate logistic regression analyses yielded insignificant findings, with the exception of smoking history and TPSA level. The final model selection was made using a backward stepdown selection process. Significantly, AKP, AFU, SA, TPSA, and FPSA maintained statistical significance when subjected to multifactor logistic regression analysis that included all factors (refer to Table 2, PCa vs non-PCa, all VIF < 5.000). This finding suggests that the exposure factor exhibited an independent effect on the outcome after controlling for other factors, including the potential confounding effects that may have been underestimated.

Similarly, in the CSPCa groups versus the non-CSPCa groups, factors other than TPSA were not significant in the univariate logistic regression analysis. The multifactor logistic regression, however, revealed statistical significance for AFU, SA, FIB, and TPSA (Table 2, all VIF < 5.000). We also plot forest maps of multivariate regression analysis as shown in Figure 1.

TABLE 1 Characteristic baseline.

Variable (n=408)	Non-PCa (n=137)	PCa (n=271)	p Value	Non-CSPCa (n=253)	CSPCa (n=155)	p Value
Age, year	68.00(63.00,73.00)	68.00(63.00,74.00)	0.99	69.00(63.00,74.00)	68.00(62.00,74.00)	0.33
SH (%)			0.04			0.84
Y	54.00(39.40)	80.00(29.50)		84.00(33.20)	50.00(32.30)	
N	83.00(60.60)	191.00(70.50)		169.00(66.80)	105.00(67.70)	
AH (%)			0.10			0.46
Y	51.00(37.20)	79.00(29.20)		84.00(33.20)	46.00(29.70)	
N	86.00(62.80)	192.00(70.80)		169.00(66.80)	109.00(70.30)	
AKP,U/L	70.00(60.00,82.00)	66.50(56.25,78.00)	0.10	68.00(56.00,79.00)	67.00(58.25,82.00)	0.47
LDH,U/L	192.00(173.00,221.00)	187.50(168.00,211.00)	0.22	186.00(168.75,211.00)	194.00(172.00,218.00)	0.08
AFU,U/L	17.00(13.00,22.00)	17.00(13.25,21.00)	0.94	17.00(13.00,21.50)	17.00(14.00,22.00)	0.61
SA,mg/dL	57.70(51.40,66.60)	53.60(49.73,59.73)	<0.01	54.70(50.60,62.20)	54.30(48.88,60.65)	0.15
FIB,g/L	3.17(2.75,3.63)	3.00(2.65,3.42)	0.07	2.98(2.62,3.48)	3.11(2.70,3.49)	0.26
TPSA,ng/mL	8.27(6.24,11.42)	10.49(7.72,13.76)	<0.01	8.74(6.91,11.89)	10.88(8.01,14.86)	<0.01
FPSA,ng/mL	1.41(1.03,1.80)	1.24(0.80,1.83)	0.02	1.29(0.93,1.76)	1.28(0.80,2.00)	0.66
f/T	0.18(0.13,0.25)	0.12(0.08,0.18)	<0.01	0.16(0.11,0.21)	0.12(0.08,0.17)	<0.01

Data are presented as median (P25, P75) or n (%). SH, smoking history; AH, alcohol history; AKP, Alkaline phosphatase; LDH, Lactate dehydrogenase; AFU, α-L-fucosidase; SA, Serum sialic acid; FIB, Fibrinogen; TPSA, total prostatic specifific antigen; fPSA, free prostatic specifific antigen; f/T, free/total prostatic specifific antigen ratio; PCa, prostate cancer; CSPCa, clinically signifificant prostate cancer, which was defifined as Gleason grade ≥ 2.

3.3 ROC curve analysis of variables

We analyzed ROC-AUC for Age, AFU, SA, FIB, TPSA, and FPSA to evaluate specific diagnostic variables for PCa and CSPCa. The detailed results of the analysis are presented in Table 3, Figures 2, 3. As calculated using the parameters of the analysis, the TPSA had the highest predictive value for PCa values (AUC=0.6253, 95% CI: 0.5683–0.6824). The AUC values for the Age, AFU, SA, FIB, and FPSA were 0.5004 (95% CI: 0.4419–0.5589), 0.5025 (95% CI: 0.4383–0.5668), 0.6125 (95% CI: 0.5515–0.6788, 0.5638 (95% CI: 0.4953–0.6323), and 0.5726 (95% CI: 0.5149–0.6303), respectively. In the group of CSPCa, the ROC curve analysis showed that the AUCs of Age, AFU, SA, FIB, and TPSA were 0.5004 (95% CI: 0.4419–0.5589), 0.5025 (95% CI: 0.4383–0.5668), 0.6152 (95% CI: 0.5515–0.6788), 0.5638 (95% CI: 0.4953–0.6323) and 0.6253(95% CI: 0.5683–0.6824), respectively. As a result, TPSA can diagnose both PCa and CSPCa with the highest degree of certainty. Moreover, the SA level is one of the most powerful predictors, although not as effective as TPSA. In contrast, there is a lack of excellent predictive value for PCA and CSPCa using Age, AFU, FIB, and FPSA.

3.4 Development of a nomogram for PCa prediction

To intuitively show the predictive value of the serum biochemical index for PCa, a nomogram was developed to predict the probability of PCa according to all significant factors for PCa and CSPCa occurrence (Figure 4A). In PCa prediction, the ROC curve showed good discrimination, and the AUC for the nomogram was 0.685 (CI:0.541-0.771) (Figure 4B). Moreover, the DCA curves and calibration curves revealed good agreement between predicted and observed PCa probabilities (Figures 4C, D).

4 Discussion

In this study, a retrospective analysis of prostate biopsies conducted on patients with PSA values ranging from 4.0 to 20.0ng/mL has been conducted. And we found that patients with PCa had significantly lower SA when compared with non-PCa patients. Further, the SA showed a high predictive value in the multivariable prediction model for PCa and CSPCa. AFU and FIB also demonstrated high predictive values in PCa and CSPCa multivariable prediction models, but they were not as accurate as SA in predicting PCa and CSPCa. In contrast, other serum biochemical indices, such as AKP and LDH, were insufficient for the diagnosis of PCa and CSPCa.

In more and more studies, it has come to light that serum biochemical-related cells and serum biochemical-related substances in cancer patients will undergo a series of changes as the disease progresses. These factors are closely related to the diagnosis and prognosis of cancers, such as AKP (18), LDH (19, 20), AFU (21), SA (21, 22), and FIB (23).

In the current state of prostate cancer screening, PSA is the most commonly used index (24, 25), Despite this, PCa and BPH were difficult to distinguish at PSA values between 4 and 20 ng/

TABLE 2 Univariable and multivariable analyses of clinical indicators.

PCa	Colinearity	Univariable Regression Analysis		Multivariable Regression Analysis		CSPCa	Univariable Regression Analysis		Multivariable Regression Analysis	
	VIF	OR (95% CI)	*p* Value	OR (95% CI)	*p* Value		OR (95% CI)	*p* Value	OR (95% CI)	*p* Value
Age, year	1.050	0.999(0.973-1.025)	0.92	/	/		0.984(0.959-1.010)	0.218	/	/
SH (%)	1.759	0.644(0.418-0.990)	0.045	/	/		0.958(0.625-1.468)	0.844	/	/
Y										
N										
AH (%)	1.745	0.694(0.449-1.071)	0.099	/	/		0.849(0.551-1.309)	0.459	/	/
Y										
N										
AKP,U/L	1.095	1.002(0.997-1.007)	0.484	/	/		1.001(0.997-1.005)	0.633	/	/
LDH,U/L	1.056	0.998(0.993-1.003)	0.398	/	/		1.004(0.999-1.009)	0.119	/	/
AFU,U/L	1.055	1.009(0.973-1.045)	0.637	1.086(1.028-1.147)	0.003		1.016(0.980-1.052)	0.390	1.063(1.018-1.110)	0.005
SA,mg/dL	1.539	0.997(0.989-1.005)	0.493	0.896(0.855-0.938)	0.000		1.003(0.995-1.011)	0.517	0.944(0.910-0.980)	0.003
FIB,g/L	1.505	0.947(0.768-1.168)	0.613	2.187(1.169-4.092)	0.014		1.087(0.885-1.334)	0.426	2.160(1.243-3.754)	0.006
TPSA,ng/mL	1.245	1.183(1.082-1.293)	0.000	1.184(1.083-1.293)	0.000		1.115(1.060-1.173)	0.000	1.134(1.064-1.209)	0.000
FPSA,ng/mL	1.353	0.860(0.709-1.042)	0.124	0.739(0.556-0.980)	0.036		1.062(0.879-1.282)	0.534	/	/
F-PSA/PSA	1.027	0.937(0.843-1.012)	0.232	/	/		1.003(0.908-1.109)	0.947	/	/

SH, smoking history; AH, alcohol history; AKP, Alkaline phosphatase; LDH, Lactate dehydrogenase; AFU, α-L-fucosidase; SA, Serum sialic acid; FIB, Fibrinogen; TPSA, total prostatic specific antigen; fPSA, free prostatic specific antigen; f/T, free/total prostatic specific antigen ratio; PCa, prostate cancer; CSPCa, clinically significant prostate cancer, which was defined as Gleason grade ≥ 2; OR, odds ratio; CI, confidence interval.

mL in some cases. As the gold standard, prostate biopsies required patients to tolerate greater pain, and it was possible that false negatives would result in microscopic prostate cancer not being detected. By contrast, the SA test had the advantage of being safe, low-cost, easy to implement, and generalizable in clinical settings.

As a terminal component of the non-reducing end of carbohydrate chains of glycoproteins and glycolipids, the yields of plasma SA typically increase during cancer progression. Sialic acid, while not a specific marker for one disease, has promise as a means to monitor disease progression and a measure of treatment effectiveness (26). The use of SA has been demonstrated to

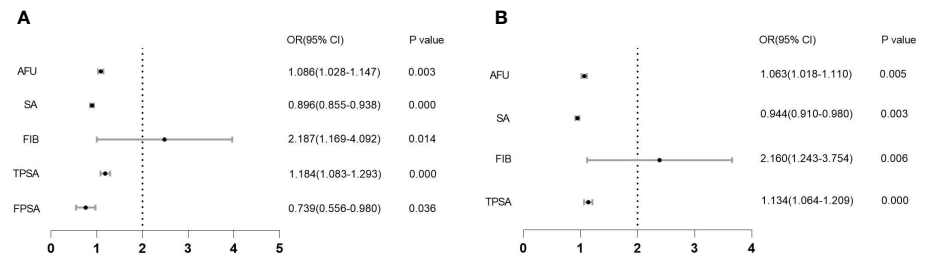

FIGURE 1
Forest map of multivariate regression analysis. **(A)**: Forest map between PCa and non-PCa; **(B)**: Forest map between CSPCa and non-CSPCa.

TABLE 3 ROC curve analysis of variables.

Variables	AUC	95% CI	Cut-Off	Sensitivity	Specifficity	Youden Index
PCa						
Age	0.5004	0.4419-0.5589	72.500	0.322	0.730	0.062
AFU	0.5025	0.4383-0.5668	11.500	0.909	0.157	0.066
SA	0.6152	0.5515-0.6788	42.850	0.966	0.047	0.013
FIB	0.5638	0.4953-0.6323	4.945	0.043	0.989	0.032
TPSA	0.6253	0.5683-0.6824	8.720	0.661	0.569	0.230
FPSA	0.5726	0.5149-0.6303	1.785	0.271	0.754	0.025
CSPCa						
Age	0.5004	0.4419-0.5589	72.500	0.323	0.696	0.019
AFU	0.5025	0.4383-0.5668	11.500	0.921	0.139	0.060
SA	0.6152	0.5515-0.6788	85.500	0.048	0.986	0.034
FIB	0.5638	0.4953-0.6323	2.995	0.574	0.518	0.092
TPSA	0.6253	0.5683-0.6824	9.015	0.697	0.526	0.223

AFU, α-L-fucosidase; SA, Serum sialic acid; FIB, Fibrinogen; TPSA, total prostatic specifific antigen; fPSA, free prostatic specifific antigen; PCa, prostate cancer; CSPCa, clinically signifificant prostate cancer, which was defifined as Gleason grade ≥ 2.

facilitate the growth of prostate cancer as well as bone metastases from the prostate in many studies (10, 12, 27, 28). SA has yet to be proven to be a predictive biomarker for PCa and CSPCa in patients with a PSA value between 4 and 20 ng/m, however. Ultimately, our findings suggest that PCa/CSPCa with a PSA value between 4 and 20 ng/mL detection is significantly correlated with a lower SA level. FIB and AFU are significant diagnoses for prostate cancer, but they cannot be used as effectively as SA for diagnosing PCa and CSPCa with PSA between 4.0 and 20.0 ng/mL.

Our postulations regarding the role of SA in the metastasis of prostate adenocarcinoma primarily encompass the following factors (Figure 5). Firstly, the complement system constitutes a crucial component of innate immunity. Within this system, the H-factor serves as a pivotal regulatory protein (29). The anionic adhesion domain on factor H (30, 31) can selectively identify sialic acid or certain sulfated mucopolysaccharides and other detrimental molecules present on the surface of host cells. Upon binding to sialic acid on the surface of host cells, the H-factor effectively impedes the activation of the complement pathway, thus preventing any potential damage resulting from complement system activation (32). Furthermore, the sialylation of tumors serves to conceal active ligands on the surface of tumor cells that would otherwise bind to them. Additionally, sialylation on the surface of tumor cells can impede the formation of immune synapses between tumor cells and NK cells, thereby diminishing the cytotoxicity of NK cells towards tumors (33). This phenomenon could potentially be attributed to the incapacity of the activating receptor NKG2D on the surface of natural killer cells to identify activated ligands that have undergone modification by sialic acid on the surface of neoplastic cells (34–36), or to the substantial negative charge that sialic acid carries on the cell membrane surface. Additionally, the excessive expression of sialoglycans on the surface of malignant cells may facilitate evasion of immune surveillance by disrupting cytotoxic T lymphocyte activation and cytotoxicity mechanisms. Several pertinent studies have validated that gangliosides, specifically GD1a, present on the surface of tumor cells, can impede the transportation and exocytosis of cytoplasmic particles in CTL (37, 38), Consequently, this inhibition impedes the perforin, granzyme, and other contents of cytoplasmic particles from executing their function on target cells, thereby hindering the mediation of target cell death. Furthermore, the high sialylation of Fas on the surface of tumor cells can obstruct tumor cell apoptosis mediated by Fas and FasL (39, 40). Extant literature has established that the α-2,6 glycosidic bond-linked sialic acid present on the surface of lung cancer cells can stimulate the production of immunosuppressive cytokine TGF by Siglec-15 positive monocyte macrophages-β (transforming growth factor-β). Additionally, the sialoglycan on the surface of tumor cells impedes the secretion of TNF-α by Siglec-9 positive macrophages while promoting the secretion of IL-10. The co-expression of sialic acid on tumor cells and Siglec on macrophages plays a crucial role in determining the cytokine profile, thereby influencing the onset and progression of immune evasion in tumors. Furthermore, mucin, a high molecular weight glycoprotein, has been identified as a potential regulator of immune response. Specifically, studies have demonstrated that heavily sialylated mucins can bind to Siglecs on dendritic cells, leading to inhibition of their activation. Additionally, mucin 1 has been shown to promote the maturation of immature dendritic cells through aggregation. Nonetheless, these dendritic cells exhibit incomplete functionality, as they are unable to generate interleukin 12 (IL-12) or elicit an immune response from T cells (41, 42). Upon exposure to sialyltransferase, mucin 2 and sialic acid α-2,6 glycosidic bond linkage can attach to the surface of monocyte-derived dendritic cells via sigelec-3, leading to apoptosis induction.

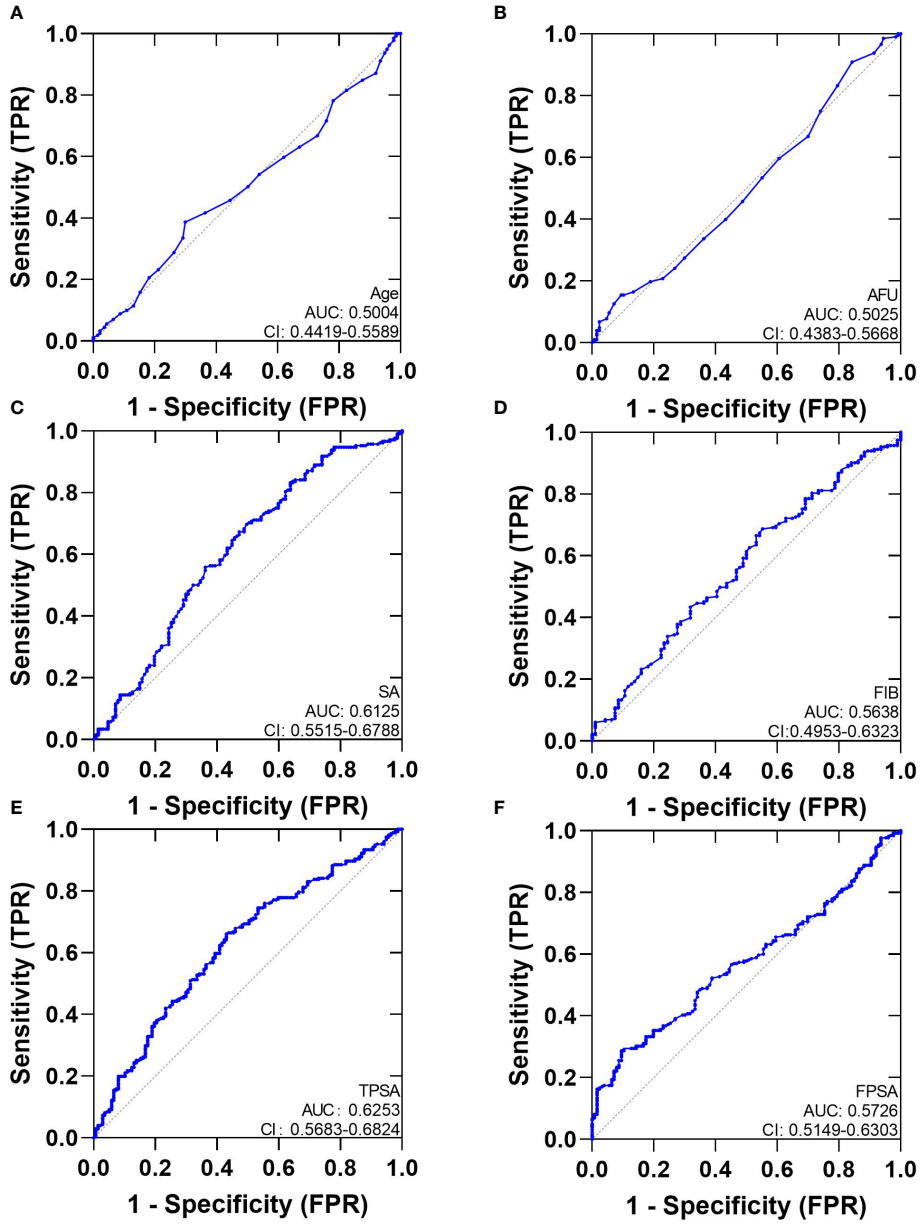

FIGURE 2
The AUC curves of Serum Biochemical Index, TPSA and FPSA. **(A)**: The AUC curves of Age; **(B)**: The AUC curves of AFU; **(C)**: The AUC curves of SA; **(D)**: The AUC curves of FIB; **(E)**: The AUC curves of TPSA; **(F)**: The AUC curves of FPSA.

Furthermore, binding with sigelec-9 results in a reduction in IL-12 production. To conclude, sialic acid has the ability to facilitate tumor immune evasion through various mechanisms, including the attenuation of immune cell activity, disruption of complement system activation, and stimulation of immunosuppressive cytokine release.

The results of clinical examination can help clinicians to diagnose and treat diseases. But many external factors, such as the storage time of blood, the standard use of instruments, and so on, can affect the results and lead to errors. To avoid these contradictions and ensure the validity of the test results, we arrange the test sequence reasonably and test the blood sample within the best time. If the quality of the blood sample has changed as it has been stored longer, the blood will be collected again for retesting.

Nevertheless, a few limitations should be considered in this study. First, since our work was based on a retrospective study conducted at a single center, there may have been some statistically selective bias in the results. The second limitation is that despite our strict enrolling criteria, we were unable to completely exclude conditions like varicose veins in the lower limbs, atherosclerosis, and others which might impact SA levels. Additionally, because the sample size was limited, we did not distinguish between the biopsy strategies. Finally, all the data were collected from Qilu Hospital of Shandong University, so the results may have limitations in general application.

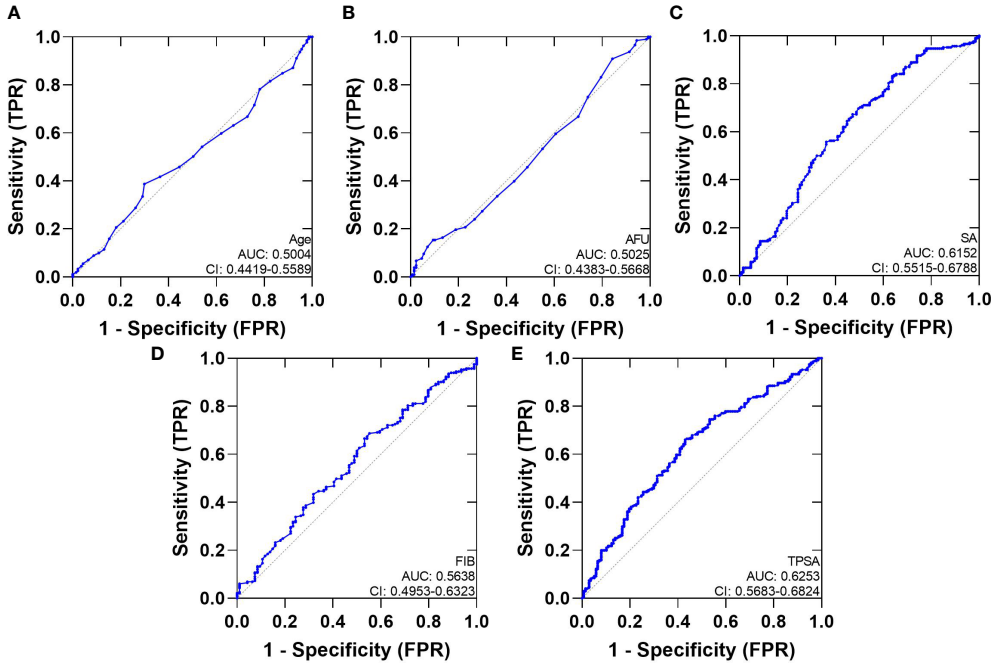

FIGURE 3
The AUC curves of Serum Biochemical Index and TPSA. **(A)**: The AUC curves of Age; **(B)**: The AUC curves of AFU; **(C)**: The AUC curves of SA; **(D)**: The AUC curves of FIB; **(E)**: The AUC curves of TPSA.

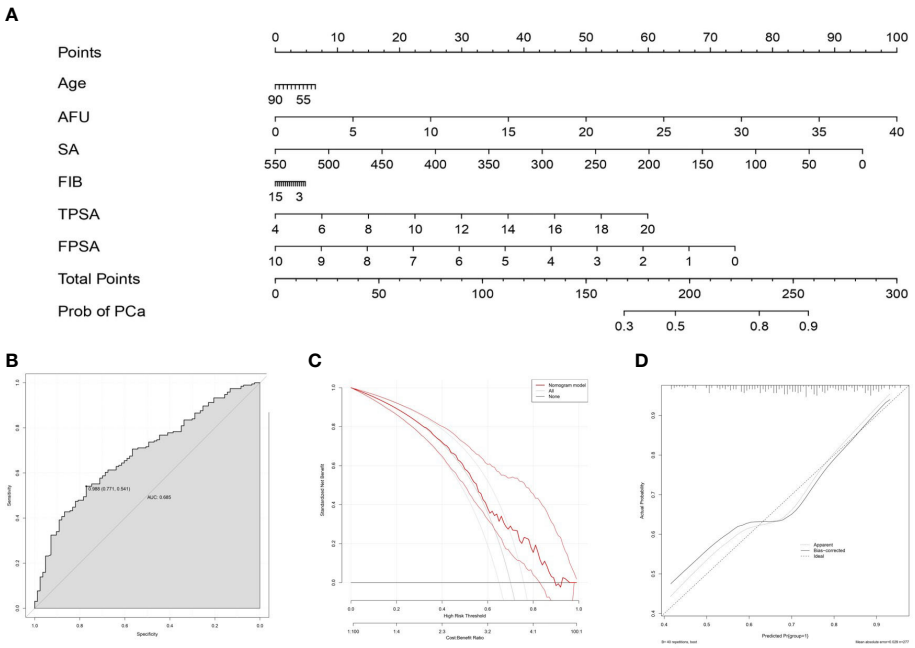

FIGURE 4
Nomogram for predicting PCa based on the training cohort. **(A)**: The prostate biopsy nomogram was developed in the training cohort, with age, AFU, SA, FIB, TPSA, and FPSA incorporated. ROC curve **(B)**, DCA curve **(C)** and calibration curve **(D)** for assessing the discrimination and calibration of the nomogram in predicting the probabilities of PCa.

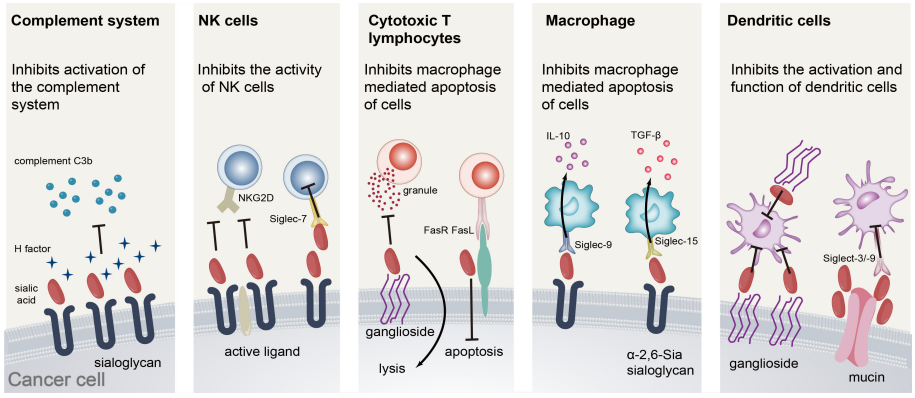

FIGURE 5
The mechanism of sialic acid promoting the occurrence and development of prostate cancer.

5 Conclusion

The SA is a significant predictor of PCa and CSPCa diagnoses in patients with PSA levels between 4.0 and 20.0ng/mL, according to our study. It is possible that in real clinical practice, they will help prevent unnecessary biopsies and biopsy-related morbidities. FIB and AFU had high predictive values for PCa and CSPCa, but they did not perform as well as SA in predicting these diseases.

Data availability statement

The raw data supporting the conclusions of this article will be made available by the authors, without undue reservation.

Ethics statement

The studies involving human participants were reviewed and approved by the Institutional Ethics Review Board of Qilu Hospital of Shandong University. Written informed consent for participation was not required for this study in accordance with the national legislation and the institutional requirements.

Author contributions

JS performed the data analyses and wrote the manuscript. JS and LY participated in the collection of samples and clinical data. LY participated in the study design and revising of the manuscript. All authors have read and agreed to the published version of the manuscript.

Conflict of interest

The authors declare that the research was conducted in the absence of any commercial or financial relationships that could be construed as a potential conflict of interest.

Publisher's note

References

1. Kang Y, Song P, Fang K, Yang B, Yang L, Zhou J, et al. Survival outcomes of low prostate-specific antigen levels and T stages in patients with high-grade prostate cancer: a population-matched study. *J Cancer* (2020) 11(22):6484–90. doi: 10.7150/jca.40428

2. Siegel RL, Miller KD, Fuchs HE, Jemal A. Cancer statistics, 2022. *Ca-a Cancer J Clin* (2022) 72(1):7–33. doi: 10.3322/caac.21708

3. Qu YS, Adam BL, Yasui T, Ward MD, Cazares LH, Schellhammer PF, et al. Boosted decision tree analysis of surface-enhanced laser desorption/ionization mass spectral serum profiles discriminates prostate cancer from noncancer patients. *Clin Chem* (2002) 48(10):1835–43. doi: 10.1093/clinchem/48.10.1835

4. . (!!! INVALID CITATION !!! [4, 5]).

5. Hendriks RJ, van Oort IM, Schalken JA. Blood-based and urinary prostate cancer biomarkers: a review and comparison of novel biomarkers for detection and treatment decisions. *Prostate Cancer Prostatic Di* (2017) 20(1):12–9. doi: 10.1038/pcan.2016.59

6. Duffy MJ. Biomarkers for prostate cancer: prostate-specific antigen and beyond. *Clin Chem Lab Med* (2020) 58(3):326–39. doi: 10.1515/cclm-2019-0693

7. Narayan VM. A critical appraisal of biomarkers in prostate cancer. *World J Urol* (2020) 38(3):547–54. doi: 10.1007/s00345-019-02759-x

8. Ind T, Iles R, Shepherd J, Chard T. Serum concentrations of cancer antigen 125, placental alkaline phosphatase, cancer-associated serum antigen and free beta human chorionic gonadotrophin as prognostic markers for epithelial ovarian cancer. *Br J Obstet Gynaecol* (1997) 104(9):1024–9. doi: 10.1111/j.1471-0528.1997.tb12061.x

9. Tatekawa Y, Kemmotsu H, Mouri T, Joe K, Ohkawa H. A case of pediatric ovarian dysgerminoma associated with high serum levels and positive immunohistochemical staining of neuron-specific enolase. *J Pediatr Surg* (2004) 39 (9):1437–9. doi: 10.1016/j.jpedsurg.2004.05.023

10. Zhang C, Yan L, Song H, Ma Z, Chen D, Yang F, et al. Elevated serum sialic acid levels predict prostate cancer as well as bone metastases. *J Cancer* (2019) 10(2):449–57. doi: 10.7150/jca.27700

11. Chittemsetti S, Manchikatla PK, Guttikonda V. Estimation of serum sialic acid in oral submucous fibrosis and oral squamous cell carcinoma. *J Oral Maxillofac Pathol JOMFP* (2019) 23(1):156. doi: 10.4103/jomfp.JOMFP_239_18

12. Zhang Z, Wuhrer M, Holst S. Serum sialylation changes in cancer. *Glycoconj J* (2018) 35(2):139–60. doi: 10.1007/s10719-018-9820-0

13. Dadhich M, Prabhu V, Pai VR, D'Souza J, Harish S, Jose M. Serum and salivary sialic acid as a biomarker in oral potentially Malignant disorders and oral cancer. *Indian J Cancer* (2014) 51(3):214–8. doi: 10.4103/0019-509X.146720

14. Hoganryan A, Fennelly JJ, Jones M, Cantwell B, Duffy MJ. Serum sialic-acid and cea concentrations in human-breast cancer. *Br J Cancer* (1980) 41(4):587–92. doi: 10.1038/bjc.1980.101

15. Dedova T, Braicu EI, Sehouli J, Blanchard V. Sialic acid linkage analysis refines the diagnosis of ovarian cancer. *Front Oncol* (2019) 9. doi: 10.3389/fonc.2019.00261

16. Wongkham S, Bhudhisawasdi V, Chau-in S, Boonla C, Muisuk K, Kongkham S, et al. Clinical significance of serum total sialic acid in cholangiocarcinoma. *Clinica Chimica Acta* (2003) 327(1-2):139–47. doi: 10.1016/S0009-8981(02)00371-6

17. Clauss A. Rapid physiological coagulation method in determination of fibrinogen. *Acta haematol* (1957) 17(4):237–46. doi: 10.1159/000205234

18. Lima Moura S, Pallares-Rusinol A, Sappia L, Marti M, Pividori MI. The activity of alkaline phosphatase in breast cancer exosomes simplifies the biosensing design. *Biosensors Bioelectron* (2022) 198:113826. doi: 10.1016/j.bios.2021.113826

19. Ding J, Karp JE, Emadi A. Elevated lactate dehydrogenase (LDH) can be a marker of immune suppression in cancer: Interplay between hematologic and solid neoplastic clones and their microenvironments. *Cancer Biomarkers* (2017) 19(4):353–63. doi: 10.3233/CBM-160336

20. Wang H, Wang M-S, Zhou Y-H, Shi J-P, Wang W-J. Prognostic values of LDH and CRP in cervical cancer. *Onco Targets Ther* (2020) 13:1255–63. doi: 10.2147/OTT.S235027

21. Zhang C, Liu J, Chao F, Wang S, Li D, Han D, et al. Alpha-L-fucosidase has diagnostic value in prostate cancer with "Gray-zone PSA" and inhibits cancer progression via regulating glycosylation. *Front Oncol* (2021) 11. doi: 10.3389/fonc.2021.742354

22. Mikkonen JJW, Singh SP, Akhi R, Salo T, Lappalainen R, Gonzalez-Arriagada WA, et al. Potential role of nuclear magnetic resonance spectroscopy to identify salivary metabolite alterations in patients with head and neck cancer. *Oncol Lett* (2018) 16 (5):6795–800. doi: 10.3892/ol.2018.9419

23. Qian X, Wang H, Ren Z, Jin F, Pan SY. The value of NLR, FIB, CEA and CA19-9 in colorectal cancer. *Zhonghua yu fang yi xue za zhi [Chinese J Prev medicine]* (2021) 55 (4):499–505. doi: 10.3760/cma.j.cn112150-20200805-01094

24. Wang MC, Valenzuela LA, Murphy GP, Chu TM. Purification of a human-prostate specific antigen. *Invest Urol* (1979) 17(2):159–63.

25. Oesterling JE, Jacobsen SJ, Klee GG, Pettersson K, Piironen T, Abrahamsson PA, et al. Free, complexed and total serum prostate-specific antigen - the establishment of appropriate reference ranges for their concentrations and ratios. *J Urol* (1995) 154 (3):1090–5. doi: 10.1016/S0022-5347(01)66984-2

26. Cheeseman J, Kuhnle G, Stafford G, Gardner RA, Spencer DIR, Osborn HMI. Sialic acid as a potential biomarker for cardiovascular disease, diabetes and cancer. *Biomarkers Med* (2021) 15(11):911–28. doi: 10.2217/bmm-2020-0776

27. Xie G-S, Li G, Li Y, Pu J-X, Huang Y-H, Li J-H, et al. Clinical association between pre-treatment levels of plasma fibrinogen and bone metastatic burden in newly diagnosed prostate cancer patients. *Chin Med J* (2019) 132(22):2684–9. doi: 10.1097/CM9.0000000000000506

28. Michalakis K, Ilias I, Triantafyllou A, Polymeris A, Kastriotis I, Chairakaki A-D, et al. Detection of prostate cancer by sialic acid level in patients with non-diagnostic levels of prostate-specific antigen. *Maturitas* (2012) 73(4):325–30. doi: 10.1016/j.maturitas.2012.07.016

29. Ferreira VP, Pangburn MK, Cortes C. Complement control protein factor H: The good, the bad, and the inadequate. *Mol Immunol* (2010) 47(13):2187–97. doi: 10.1016/j.molimm.2010.05.007

30. Csincsi AI, Kopp A, Zoeldi M, Banlaki Z, Uzonyi B, Hebecker M, et al. Factor H-related protein 5 interacts with pentraxin 3 and the extracellular matrix and modulates complement activation. *J Immunol* (2015) 194(10):4963–73. doi: 10.4049/jimmunol.1403121

31. Renner B, Laskowski J, Poppelaars F, Ferreira VP, Blaine J, Antonioli AH, et al. Factor H related proteins modulate complement activation on kidney cells. *Kidney Int* (2022) 102(6):1331–44. doi: 10.1016/j.kint.2022.07.035

32. Schmidt CQ, Ederveen ALH, Harder MJ, Wuhrer M, Stehle T, Blaum BS. Biophysical analysis of sialic acid recognition by the complement regulator Factor H. *Glycobiology* (2018) 28(10):765–73. doi: 10.1093/glycob/cwy061

33. Zucker-Franklin D, Nabi ZF. Phorbol ester-induced loss of cell surface sialic acid enhances target cell sensitivity to cytolysis by natural killer (NK) cells. *Trans Assoc Am Phys* (1987) 100:339–46.

34. Ding H, Yang X, Wei Y. Fusion proteins of NKG2D/NKG2DL in cancer immunotherapy. *Int J Mol Sci* (2018) 19(1):177. doi: 10.3390/ijms19010177

35. Zingoni A, Molfetta R, Fionda C, Soriani A, Paolini R, Cippitelli M, et al. NKG2D and its ligands: "One for all, all for one". *Front Immunol* (2018) 9. doi: 10.3389/fimmu.2018.00476

36. Frazao A, Rethacker L, Messaoudene M, Avril M-F, Toubert A, Dulphy N, et al. NKG2D/NKG2-ligand pathway offers new opportunities in cancer treatment. *Front Immunol* (2019) 10. doi: 10.3389/fimmu.2019.00661

37. Bellamy A, Davison AN, Feldmann M. Derivation of ganglioside-specific t-cell lines of suppressor or helper phenotype from cerebrospinal-fluid of multiple-sclerosis patients. *J Neuroimmunol* (1986) 12(2):107–20. doi: 10.1016/0165-5728(86)90024-X

38. Lee HC, Wondimu A, Liu Y, Ma JSY, Radoja S, Ladisch S. Ganglioside inhibition of CD8(+) T cell cytotoxicity: interference with lytic granule trafficking and exocytosis. *J Immunol* (2012) 189(7):3521–7. doi: 10.4049/jimmunol.1201256

39. Contini P, Ghio M, Merlo A, Brenci S, Filaci G, Indiveri F, et al. Soluble HLA class I/CD8 ligation triggers apoptosis in EBV-specific CD8(+) cytotoxic T lymphocytes by Fas/Fas-ligand interaction. *Hum Immunol* (2000) 61(12):1347–51. doi: 10.1016/S0198-8859(00)00212-3

40. Rode M, Balkow S, Sobek V, Brehm R, Martin P, Kersten A, et al. Perforin and Fas Act together in the induction of apoptosis, and both are critical in the clearance of lymphocytic choriomeningitis virus infection. . *J Virol* (2004) 78(22):12395–405. doi: 10.1128/JVI.78.22.12395-12405.2004

41. Ishida A, Ohta M, Toda M, Murata T, Usui T, Akita K, et al. Mucin-induced apoptosis of monocyte-derived dendritic cells during maturation. *Proteomics* (2008) 8 (16):3342–9. doi: 10.1002/pmic.200800039

42. Beatson R, Tajadura-Ortega V, Achkova D, Picco G, Tsourouktsoglou T-D, Klausing S, et al. The mucin MUC1 modulates the tumor immunological microenvironment through engagement of the lectin Siglec-9. *Nat Immunol* (2016) 17(11):1273–81. doi: 10.1038/ni.3552

frontiers | Frontiers in Pharmacology

TYPE Original Research
PUBLISHED 04 October 2023
DOI 10.3389/fphar.2023.1244655

OPEN ACCESS

EDITED BY
Guadalupe Maya-Núñez,
Mexican Social Security Institute (IMSS), Mexico

REVIEWED BY
Chun-Han Chen,
Taipei Medical University, Taiwan
Ulises Daniel Orlando,
National Scientific and Technical Research Council (CONICET), Argentina
Dongbo Xu,
University at Buffalo, United States

*CORRESPONDENCE
Yung-Chi Cheng,
✉ yccheng@yale.edu

†These authors have contributed equally to this work

RECEIVED 22 June 2023
ACCEPTED 20 September 2023
PUBLISHED 04 October 2023

CITATION
Lam W, Arammash M, Cai W, Guan F, Jiang Z, Liu S-H, Cheng P and Cheng Y-C (2023), YIV-818-A: a novel therapeutic agent in prostate cancer management through androgen receptor downregulation, glucocorticoid receptor inhibition, epigenetic regulation, and enhancement of apalutamide, darolutamide, and enzalutamide efficacy. *Front. Pharmacol.* 14:1244655. doi: 10.3389/fphar.2023.1244655

YIV-818-A: a novel therapeutic agent in prostate cancer management through androgen receptor downregulation, glucocorticoid receptor inhibition, epigenetic regulation, and enhancement of apalutamide, darolutamide, and enzalutamide efficacy

Wing Lam[1†], Mohammad Arammash[1†], Wei Cai[1,2†], Fulan Guan[1], Zaoli Jiang[1], Shwu-Huey Liu[3], Peikwen Cheng[3] and Yung-Chi Cheng[1*]

[1]Department of Pharmacology, Yale University School of Medicine, New Haven, CT, United States, [2]School of Pharmaceutical Sciences, Hunan University of Medicine, Huaihua, China, [3]Yiviva, Inc, New York, NY, United States

Introduction: Prostate cancer is the second leading cause of cancer death among men in the United States. Castration-Resistant Prostate Cancer (CRPC) often develops resistance to androgen deprivation therapy. Resistance in CRPC is often driven by AR variants and glucocorticoid receptor (GR). Thus, drugs that target both could be vital in overcoming resistance.

Methods: Utilizing the STAR Drug Discovery Platform, three hundred medicinal plant extracts were examined across 25 signaling pathways to identify potential drug candidates. Effects of the botanical drug YIV-818-A, derived from optimized water extracts of Rubia cordifolia (R.C.), on Dihydrotestosterone (DHT) or Dexamethasone (DEX) induced luciferase activity were assessed in 22RV1 cells harboring the ARE luciferase reporter. Furthermore, the key active compounds in YIV-818-A were identified through activity guided purification. The inhibitory effects of YIV-818-A, RA-V, and RA-VII on AR and GR activities, their impact on AR target genes, and their roles in modifying epigenetic status were investigated. Finally, the synergistic effects of these compounds with established CRPC drugs were evaluated both *in vitro* and *in vivo*.

Results: YIV-818-A was found to effectively inhibit DHT or DEX induced luciferase activity in 22RV1 cells. Deoxybouvardin (RA-V) was identified as the key active compound responsible for inhibiting AR and GR activities. Both YIV-818-A and RA-V, along with RA-VII, effectively downregulated AR and AR-V proteins through inhibiting protein synthesis, impacted the expression of AR target genes, and modified the epigenetic status by reducing levels of Bromodomain and Extra-

Terminal proteins (Brd2/Brd4) and H3K27Ac. Furthermore, these compounds exhibited synergistic effects with apalutamide, darolutamide, or enzalutamide, and suppressed AR mediated luciferase activity of 22RV1 cells. Co-administration of YIV-818-A and enzalutamide led to a significant reduction of 22RV1 tumor growth in vivo. Different sources of R.C. had variable levels of RA-V, correlating with their potency in AR inhibition.

Discussion: YIV-818-A, RA-V, and RA-VII show considerable promise in addressing drug resistance in CRPC by targeting both AR protein and GR function, along with modulation of vital epigenetic markers. Given the established safety profile of YIV-818-A, these findings suggest its potential as a chemopreventive agent and a robust anti-prostate cancer drug.

KEYWORDS

YIV-818-A, AR, GR, prostate cancer, apalutamide, darolutamide, and enzalutamide

Introduction

Prostate cancer is the second leading cause of cancer death among men in the United States. According to the National Cancer Institute over 3 million men in the United States are living with prostate cancer, with 288,300 additional cases and 34,700 deaths expected in 2023. Androgen receptor (AR) signaling plays a key role in development of Benign prostatic hyperplasia (BPH) and prostate cancer (Shiota et al., 2011; Gioeli and Paschal, 2012; Mills, 2014; Wong et al., 2014; Tan et al., 2015). Therefore, androgen or Androgen R targeted therapy has become a major focus for the prevention and treatment of benign prostate hyperplasia and cancer. In addition to surgical interventions, luteinizing hormone-releasing hormone (LHRH) agonist analogues have emerged as a cornerstone of prostate cancer treatment since the mid-1980s. The development of Castration-Resistant Prostate Cancer (CRPC) is inevitable following the long-term treatment of androgen deprivation therapy. For the treatment of metastatic castration-resistant prostate cancer before chemotherapy, in 2011 the FDA approved abiraterone, which targets CYP17A1—a critical enzyme in extragonadal and testicular androgen synthesis. Enzalutamide, which has a higher affinity than first generation antagonists for the AR ligand-binding pocket, was approved by FDA for non-metastatic and metastatic CRPC (Rice et al., 2019). Later on, apalutamide and darolutamide, which have higher selectivity and potency against AR with reductions in brain penetrance, were also approved by FDA for treatment of non-metastatic prostate cancer (Rice et al., 2019).

Many mechanisms for CRPC are proposed and some are responsible for abiraterone resistance and enzalutamide resistance. Resistance mechanisms include altering the metabolic enzymes expression favorable for DHT synthesis, AR gene amplification (Shiota et al., 2011), AR mutation/truncation of LBD (Ligand Binding Domain) (Koivisto et al., 1997; Li et al., 2013). AR splice variants (AR-V) could be commonly (19%–59%) of patients with AR-positive metastatic CRPC (Antonarakis et al., 2014; Lu et al., 2015; Pomerantz et al., 2015). In addition, AR mutations enabling the AR to use other steroid hormones such as glucocorticoids (Buchanan et al., 2001), and the glucocorticoid receptor (GR) replacing AR function (Arora et al., 2013; Shah et al., 2017).

Creating a multi-targeted medication that can simultaneously hinder both the androgen receptor variants and glucocorticoid receptor action holds the potential to overcome drug resistance, extend the duration of treatment efficacy, and ultimately enhance the therapeutic outcomes for prostate cancer patients. Through our STAR (Signal, Transduction, Activity, and Response) Drug Discovery Platform, we studied the effects of three hundred medicinal plant extracts across 25 signaling pathways to identify a drug candidate to target the androgen signaling pathway. YIV-818-A, optimized water extracts of *Rubia cordifolia* (R.C.), was discovered as a novel drug candidate. YIV-818-A, Deoxybouvardin (RA-V), or RA-VII were found to have the ability to effectively target both the androgen receptor and glucocorticoid receptor by down-regulating the androgen receptor protein, impairing the glucocorticoid receptor function, and reducing Brd2/Brd4 levels and H3K27Ac levels, which play a crucial role in AR and GR function. Additionally, the compounds showed synergistic effects with apalutamide, darolutamide, and enzalutamide in inhibiting androgen receptor activity and suppressing the growth of 22RV1 cells. Co-administration of YIV-818-A and enzalutamide also resulted in a marked reduction of 22RV1 tumor growth *in vivo*. In conclusion, YIV-818-A, RA-V, or RA-VII hold promise for overcoming current drug resistance and could be used for the treatment of androgen-dependent disease and castration-resistant prostate cancer (CRPC).

Materials and methods

Rubia Cordifolia extract preparation methods and standards

YIV-818-A (*Rubia Cordifolia* (batch number, Y1830) water extract spray dried powder) 100 mg/mL was extracted with 1 mL HPLC grade water and heated at 80°C for 30 min. The herbal extract was centrifuged at 12,000 rpm in desktop centrifuge at room temperature for 5 min. The supernatant was transferred into a 2 mL tube and used as a 100 mg/mL. RA-V, RA-VII and RA-XI standard compounds were purchased from Chemfaces.com and were dissolved in DMSO.

Purification of the active compound with anti-AR activity from *Rubia Cordifolia*

25 g of YIV-818-A was extracted in 100 mL HPLC grade water at 80°C for 30 min. The extract of YIV-818-A was then centrifuged at 10,000 rpm for 10 min and the supernatant was passed through a solid phase column (Millipore-Sigma, Discovery DSC18 10 g). The column was washed sequentially with 50 mL 10% EtOH and 50 mL 30% EtOH and finally 30 mL 50% EtOH was used to elute the fraction containing. The 50% EtOH fraction was vacuum dried and re-dissolved in 3 mL 50% EtOH before passing through a second solid phase column (Millipore-Sigma, Discovery DSC18 10 g). The second column was then washed with 30 mL 0.1% formic acid, 30 mL 10:90 [(Methanol:Acetonitrile 88:12): (0.1% formic acid)], 30 mL 30:70 [(Methanol:Acetonitrile 88:12): (0.1% formic acid)], and 30 mL 45:55 [(Methanol:Acetonitrile 88:12): (0.1% formic acid)]. A fraction was collected by eluting with 30 mL 60: 40 [(Methanol:Acetonitrile 88:12): (0.1% formic acid)] and was vacuum dried. Next, the dried material was dissolved and treated with 0.2 N NaOH in a 50% methanol solution (5 mL) for 10 min. The NaOH treated fraction was passed through a C18 column and eluted with AM60 and AM75 as procedure used in the second column. AM75 fraction was then vacuum dried. The dried AM75 fraction was re-dissolved in 3 mL 50% EtOH and then passed through a C18 column (2.5 cm diameter x 50 cm length packed with Discovery DSC18 resin). The C18 column was washed with a gradient of acetonitrile:water from 10% to 80% (100 fractions, 5 mL per each fraction). All collected fractions were then vacuum dried and dissolved in EtOH for the AR luciferase assay and Western blotting. The fractions which successfully inhibited the AR activity and downregulate the AR and CycD1 protein of 22RV1 cells were subjected to UHPLC Q-Exactive Orbitrap MS for analysis (Thermo Fisher Scientific, Bremen, Germany). The fraction with the purified active compound with $[M+H]^+$ m/z = 757.3549 (positive mode) was dissolved in $CDCl_3$ and subjected to NMR analysis (Bruker Daltonics, Bremen, Germany) for chemical structure determination.

UHPLC Q-Exactive Orbitrap MS condition

A Dionex Ultimate 3000 UHPLC and the Q-Exactive Focus Orbitrap MS was connected via an electrospray ionization (ESI) source. The fractions were performed on a Thermo Scientifific Hypersil GOLD™ aQ (100 mm × 2.1 mm, 1.9 mm) at the flow rate of 0.3 mL/min. The mobile phases consisted of 0.1% formic acid aqueous solution (solvent A) and acetonitrile (solvent B) with the following gradient program: 0–2 min, 95%–90% A; 2–5 min, 90%–80% A; 5–10 min, 80%–75% A; 10–12 min, 75%–45% A; 12–20 min, 45%–20% A; 20–25 min, 20%–5% A; 25–26 min, 5%–95% A; 26–30 min, 95% A. The sample injection volume was 2 μL. The key mass spectrometer was running at positive mode with the mass range at m/z 120–1,000. The key parameters were as follows: spray voltage, 3.5 kV (+); the sheath gas flow rate, 35 arb; aux gas flow rate, 10 arb; capillary temperature, 320°C; heater temperature, 350°C; resolution, 70,000. Data acquisition and processing were carried out with the Xcalibur version 4.2.

Prostate cancer cell culturing methods

22RV1 and LNCaP prostate cancer cells were grown in corning T75 cell culture flasks in RPMI1640 media supplemented with 5% FBS, 50 μg/mL Kanamycin in a 37°C, 5% CO_2 incubator.

Establishment of PSA luciferase reporter in 22RV1, LNCaP and PC3 cells and overexpression of GR in LNCaP cells

The 22RV1, LNCaP and PC3 cell lines were stably transfected with a PGL4.2 luciferase reporter (Promega, Madison, USA). This reporter contains a sequence (3xgtaattgcagaacagcaagtgctagctctc) representing the wild type of Androgen Response Element (ARE) derived from the Prostate-Specific Antigen (PSA) promoter. As a control, cells were also transfected with the PGL4.2 luciferase reporter that does not include the PSA promoter. This transfection was accomplished using Lipofectamine 3000 (Thermo Fisher Scientific, Waltham, MA). Stable clones were selected and maintained with puromycin (0.5 μg/mL). DHT (25 nM) and DEX (50 nM) was used to stimulate androgen receptor activity for a 24-hour period. The pcDNA5 plasmid (Thermo Fisher Scientific, Waltham, MA), carrying the full open reading frame of GR, was transfected into LNCaP cells, and hygromycin (50 μg/mL) was employed to select and maintain stable clones.

Luciferase assay

10^4 reporter cells per well of 96-well plate were seeded in RPMI1640 media supplemented with 5% dialysis activated carbon treated FBS, 50 μg/mL Kanamycin in a 37°C, 5% CO2 incubator for 48 h. Cells were treated with herbal extracts at 30, 100, 300, and 600 μg/mL for 24 h in a 37°C-CO_2 incubator. DHT (25 nM) was used to stimulate androgen receptor activity. Dexamethasone (50 nM) was used to stimulate glucocorticoid receptor activity. Cells were lysed using luciferase lysis buffer after which luciferase buffer with luciferin was added to generate luminescence. Luminescence was recorded using a luminescence microplate reader. The IC_{50} is the concentration of treatment agent required to reduce the measured luminescence to half of its maximal value. IC_{50} was determined by the median-effect equation of the Chou-Talalay method (Chou and Talalay, 1977).

Drug-drug interaction analysis

Isobologram plots based on combination index (Chou and Talalay, 1977) were used to determine additive, synergistic, and antagonistic interactions of the combinations. Isobologram plots: (D)1/(Dχ)1 against (D)2/(Dχ)2 in which (Dχ)1 and (Dχ)2 represented concentrations of each drug alone to exert 50% inhibition, while (D)1 and (D)2 were concentrations of drugs in combination to achieve 50% inhibition. Different ratio of two herbs were used to determine their combination effects. Additive interaction: Points on the diagonal line. Synergistic interaction: Points below the diagonal line. Antagonistic interaction: Points above the diagonal line.

Western blotting

Cell lysis was performed using 2x SDS sample buffer (62.5 mM Tris-HCl, 2% SDS, 10% glycerol, 50 mM DTT, and 0.05% bromophenol blue). Cell lysates were sonicated for 10 s to shear DNA. Cell extracts were then electrophoresed through 10% SDS-polyacrylamide gels and transferred to 0.2 µm nitrocellulose membranes (Bio-Rad Laboratories, Hercules, CA) with a Miniprotein II transferring apparatus (Bio-Rad). The non-specific interaction of membrane was blocked with 5% non-fat milk and probed in TBS-T buffer (1x TBS buffer, 0.2% Tween 20) containing. Monoclonal rabbit anti-AR (1:5000), was used to detect the androgen receptor (Abcam #133273), Glucocorticoid Receptor (D8H2) XP® Rabbit mAb #3660, ERα Antibody (F-10): sc-8002, BRD4 (E2A7X) Rabbit mAb #13440, Brd2 (D89B4) Rabbit mAb #5848, PARP (46D11) Rabbit mAb #9532, Acetyl-Histone H3 (Lys27) (D5E4) XP® Rabbit mAb #8173 and a monoclonal actin antibody diluted 1:2500 (Sigma, St. Louis, MO) was used to detect β-actin as the internal control to normalize protein loading. The membranes were then incubated with horseradish peroxidase-conjugated anti-mouse IgG and anti-rabbit IgG (1: 5,000; Sigma). Enhanced chemiluminescence reagents (Perkin-Elmer Life Science Products, Boston, MA) were used to visualize the immunoreactive bands and the densities of protein bands were scanned analyzed using ImageJ software from the NIH.

Real time quantitative PCR (RT-qPCR) for mRNA expression

RNA was extracted from herb treated cells using the Roche High Pure RNA isolation kit. cDNA was then generated from RNA samples using a Bio-rad iScript Advanced cDNA synthesis kit for RT-qPCR. qPCR was performed using human AR, KLK2, PSA, CycD1 and β-actin primers (Table 1) and iTaq™ Universal SYBR® Green Supermix in a CFX PCR machine (Bio-rad). Duplicate well were performed for each sample, and the entire experiment was repeated three times Relative mRNA expression was calculated based on the change of the threshold cycle relative to the internal control, β-actin, using a standard curve generated by purified PCR products.

TABLE 1 Primer sequences for qRT-PCR analysis.

Gene	Forward/ Reverse	DNA sequence
Human AR	F1	CCTGGCTTCCGCAACTTACAC
	R1	GGACTTGTGCATGCGGTACTCA
Human KLK2	F1	GGTGGCTGTGTACAGTCATGGAT
	R1	TGTCTTCAGGCTCAAACAGGTTG
Human PSA	F1	ACCAGAGGAGTTCTTGACCCCAAA
	R1	CCCCAGAATCACCCGAGCAG
Human CycD1	F1	CCATCCAGTGGAGGTTTGTC
	R1	AGCGTATCGTAGGAGTGGGA
Human β-actin	F1	GCCACGGCTGCTTCCAGCTCC
	R1	TTGTGCTGGGTGCCAGGGCAGTGA

Animal studies

22RV1 cells (2×10^6 cells in 100 µL Matrigel, BD Biosciences) were transplanted subcutaneously into 8-week-old female NCR-nude mice (Taconic Biosciences, Inc., Rensselaer, NY). Body weight, tumor size, and mortality of the mice were monitored daily. After 10–14 days, mice with tumor sizes of 180 mm^3 were selected. Tumor volume was examined by using the formula length × $width^2$ × π/6. Each group consisted of five mice. YIV-818-A was administered orally for 7 days (500 mg/kg po, BID) and/or enzalutamide was administered orally for 7 days (5 mg/kg po, QD). In the control groups, mice were administered water orally. All animal experiments were carried out in accordance with the relevant guidelines and regulations approved Yale University Institutional Animal Care and Use Committee (IACUC) protocol. Animal experimental protocols were approved by Yale University Institutional Animal Care and Use Committee (IACUC). Animal studies were carried out in compliance with the ARRIVE guidelines.

Detection of PSA protein of plasma of animal

PSA (Total)/KLK3 Human ELISA Kit (Thermofisher Scietific) was used to detect PSA protein of plasma collected from animal using PST tube with heparin (BD biosciences) according to the manual provided in the kit.

Statistical analysis

Two-way ANOVA analysis (GraphPad Prism 9) was employed to discern differences between two data curves. Additionally, t-tests (Microsoft Excel) were conducted to ascertain statistical significance between group comparisons. Differences were considered statistically significant at $p < 0.05$.

Results

Deoxybouvardin (RA-V) is the active compound of *Rubia cordifolia* responsible for inhibiting AR activity and downregulating AR protein

YIV-818A water extract was fractionized using C18 columns with different gradients of methanol and acetonitrile (please see detail in materials and methods). The eluted fractions (F9 to F15) from the final C18 column had a relatively strong inhibitory effect on AR driven luciferase activity and could also downregulate AR/AR-V (AR splice variants) protein of 22RV1 (Supplementary Figures S1A, B). Fraction 11 had a single peak (highest intensity amount of F9 to F15) with $[M+H]^+$ m/z = 757.3549 that was detected using high resolution LC-MS (Supplementary Figure S1C). By marching to chemical database, $[M+H]^+$; calcd for Deoxybouvardin (RA-V) $C_{40}H_{49}N_6O_9$ is 757.3555 which is closest to our detected mass (m/z = 757.3549) of the purified compound. RA-V was purchased from a commercial source and was subjected to LCMS. Both chemicals of F11 and RA-V

10.3389/fphar.2023.1244655

A	IC_{50} for ARE-luciferase reporter									
Cells	22RV1			LNCaP		LNCaP-GR			PC3	
Ligand	-	+DHT	+DEX	-	+DHT	-	+DHT	+DEX	-	DEX
Enzalutamide(ENZ), uM	240±45	13.6±4	>250	>250	0.58±0.22	>250	0.38±0.24	>250	>250	>250
YIV-818-A, ug/ml	250±27	25±7	50±16	>250	17.9±2.7	>250	12.2±4	34.6±9.5	>250	35.4±8.3
RA-V, nM	50±15	15±4	22±5	>100	5.3±1.4	>100	4.1±1.3	7.8±2.2	40±19	5.7±2.3
RA-VII, nM	25.5±4	5.5±2.5	13.5±5	>30	2.8±0.2	>30	2.4±0.5	5.6±2.3	32±9	3.6±0.6
RA-XI, nM	>250	>250	>250	>250	>250	>250	>250	>250	>250	>250

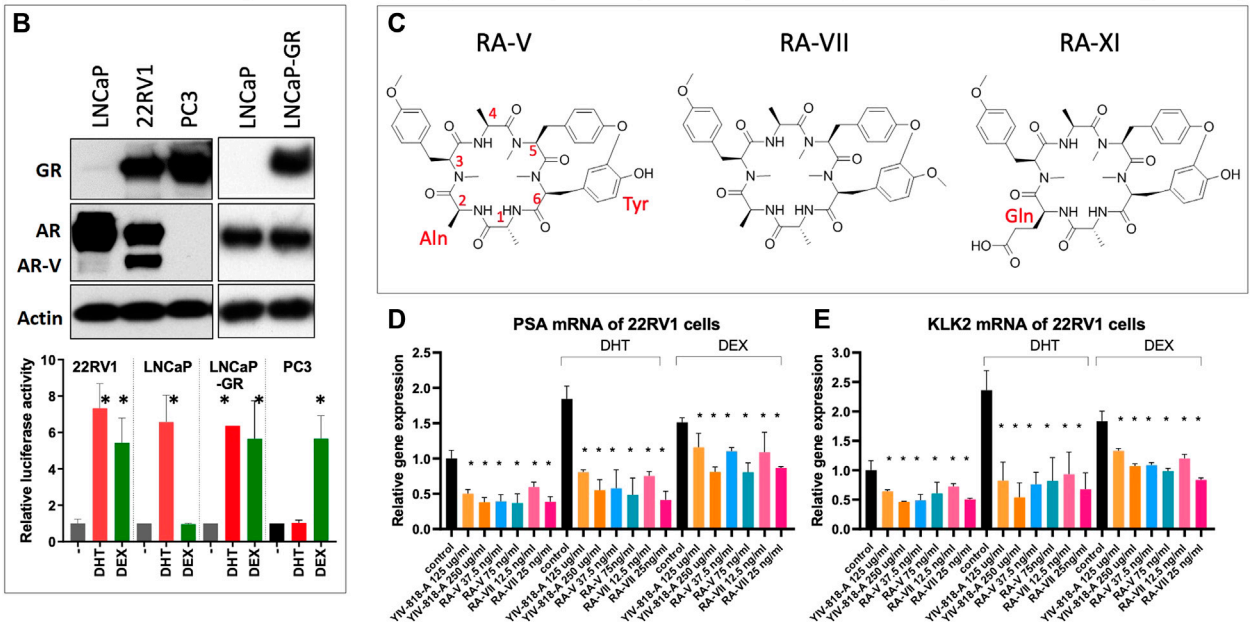

FIGURE 1
Comparing the potencies of enzalutamide, YIV-818-A, RA-V, RA-VII and RA-XI on LNCaP and 22RV1 AR luciferase reporter cells. **(A)** Effect of YIV-818-A, RA-V, RA-VII, RA-XI, and enzalutamide on AR luciferase reporter activity of 22RV1 cells without or with DHT or with DEX and LNCAP cells without or with DHT. LNCaP cells and 22RV1 cells, carrying AR-luciferase reporter, were treated with YIV-818-A, RA-V, RA-VII, RA-XI and enzalutamide in absence or presence of DHT or DEX for 24 h. Values are IC_{50} (dose of herbal extract or compound required for 50% inhibition of the luciferase activity as comparing to control). **(B)** Western blotting for the protein expression of GR, AR, AR-V (AR splice variants) and actin (upper panel) and luciferase activity with or without DHT or DEX (lower panel) of 22RV1, LNCaP, LNCaP-GR and PC3 cells and. GAPDH was used as protein loading control for normalization. **(C)** Chemical structures of RA-V, RA-VII and RA-XI. RT-qPCR analysis for the effect of YIV-818-A, RA-V, RA-VII on mRNA expression of PSA **(D)** and KLK2 **(E)** of 22RV1 cells with or without DHT and DEX. *p*-value (*t*-test) less than 0.05 (Control with or with DHT or DEX vs. Treatment) was highlighted with (*) in the figure. Details of experimental procedures are given in *Materials and methods*.

had some retention time with $[M+H]^+$ m/z = 757.3549 (Supplementary Figure S1C). They also had the same mass spectrum $[M+H]^+$ m/z = 757.3549, $[M+Na]^+$ m/z = 779.3364 (Supplementary Figure S1D). In addition, ^{1}H-NMR and ^{13}C-NMR analysis confirmed the chemical of F11 (dissolved in $CDCl_3$) had same chemical shifts with Deoxybouvardin (RA-V) (Supplementary Table S1) as previously reported (Itokawa et al., 1983). Please see other NMR spectrum including ^{1}H, ^{13}C, DEPT90, DEPT135, COSY, HMBC, HSQC, NOESY in Supplementary Data for NMR analysis.

YIV-818-A, RA-VII and RA-V could inhibit both DHT and DEX induced luciferase activity of prostate cancer cells

In Figure 1A, the presence of DHT resulted in a remarkable 23-fold increase in enzalutamide resistance in the castration-resistant prostate cancer cell line, 22RV1 (Sramkoski et al., 1999), 1999), compared to the IC_{50} observed in LNCaP cells. This finding is consistent with previous studies (Li et al., 2013; Nakazawa et al., 2014) suggesting that AR splice variants in 22RV1 cells (Figure 1B), which possess a truncated ligand-binding domain, maintain continuous activity and are unresponsive to enzalutamide binding. RA-VII and RA-XI are both hexapeptide analogs of RA-V (Figure 1C). RA-XI was detected in YIV-818-A and other batches of RC, while RA-VII was barely detected in any batch of RC. Intriguingly, up to 250 nM of RA-XI did not inhibit luciferase activity in any assay, whereas RA-V, similar to YIV-818-A, effectively inhibited both DHT- and Dex-induced luciferase activity in both LNCaP and 22RV1 cells (Figure 1A). Furthermore, RA-VII exhibited higher potency than RA-V in all luciferase assays (Figure 1A).

YIV-818A demonstrated enhanced inhibitory action in 22RV1 cells in the presence of DHT, suggesting a potential heightened susceptibility of wild type AR to YIV-818A in these cells (Figure 1A). Notably, both RA-V and RA-VII showed only slight differences in IC_{50} values with or

without DHT in 22RV1 cells, indicating their enhanced targeting proficiency for both AR and AR-V (AR splice variants) (Figure 1A). The above results indicate that the presence of DHT can significantly impact enzalutamide resistance in 22RV1 cells and support the notion that YIV-818A, RA-V, and RA-VII effectively inhibit AR and AR-V (AR splice variants) activity in prostate cancer cells. The IC_{50} values for YIV-818-A, RA-V, and RA-VII in 22RV1 cells were discerned to be 1 to 3 times higher than those in LNCaP cells under DHT influence (Figure 1A). Even though YIV-818-A, RA-V, and RA-VII may not completely counteract the drug resistance portrayed by AR-V (AR splice variants) bearing 22RV1 cells, they exhibited IC_{50} values significantly bridging the gap between LNCaP and 22RV1 cells, unlike enzalutamide. This represents a substantial advancement over the striking 23-fold IC_{50} disparity observed with enzalutamide. Consequently, our data suggests that YIV-818-A, RA-V, and RA-VII may possess potential to target prostate tumors bearing either wild type AR or AR-V (AR splice variants), thereby promising to substantially attenuate, if not completely nullify, the drug resistance manifested in 22RV1 cells.

Additionally, it has been reported that around 30% of enzalutamide-resistant patients exhibit overexpression of the glucocorticoid receptor (GR), which can substitute for AR function and activate downstream targets of the androgen receptor. In our study, we observed that enzalutamide was unable to inhibit GR-mediated luciferase activity in the AR luciferase reporter assay using 22RV1 cells that express GR (Figure 1A). In contrast, YIV-818-A effectively suppressed dexamethasone (Dex)-induced luciferase activity in 22RV1 cells. To further investigate the inhibitory effects of YIV-818A, RA-V, and RA-VII on GR-driven activity, we compared the actions of Enzalutamide, YIV-818A RA-V, and RA-VII in three different cell lines: LNCaP cells that only express AR and respond solely to DHT, LNCaP-GR cells that express both AR and GR and respond to both DHT and DEX, and PC3 cells that only express GR and respond solely to DEX (Figure 1B). As shown in Figure 1A, enzalutamide could only inhibit DHT-induced luciferase activity in LNCaP and LNCaP-GR cells but had no effect on DEX-induced luciferase activity in LNCaP-GR or PC3 cells. In contrast, YIV-818A RA-V and RA-VII were able to inhibit DEX-induced luciferase activity in LNCaP-GR or PC3 cells (Figure 1A). In conclusion, our findings demonstrate that YIV-818A RA-V and RA-VII could effectively inhibit both DHT-driven AR activity and DEX-driven GR activity in prostate cancer cells.

In addition to luciferase reporter assays, we further confirmed that YIV-818-A, RA-V and RA-VII could inhibit DHT or DEX triggered endogenous AR target gens; *PSA* and *KLK2* of 22RV1 cells by using qRT-PCR (Figures 1D, E).

Overall, our findings suggest that YIV-818-A, RA-V, and RA-VII hold promise as potential treatments for prostate cancers with AR, AR-V (AR splice variants) and might be beneficial in enzalutamide-resistant cases with GR overexpression.

YIV-818-A, RA-V and RA-VII could downregulate AR, AR-V (AR splice variants), CycD1 protein through inhibiting protein synthesis

Based on the LC-MS analysis, it was determined that the water extract of YIV-818-A at 250 μg/mL contained approximately 75 ng/mL of RA-V. As a result, we utilized a concentration range of YIV-818-A spanning from 28 μg/mL to 250 μg/mL, and a concentration range of RA-V from 8.3 ng/mL to 75 ng/mL, to treat 22RV1 cells with or without DHT for a duration of 24 h (Figure 2A). These specific concentration ranges were chosen to ensure effective exposure of the cells to YIV-818-A and RA-V while considering their respective potencies (Figure 2A). As depicted in Figure 2A, RA-V exhibited similar potency to YIV-818-A in downregulating AR (full-length), AR-V (AR splice variants), and cyclin D1 protein in 22RV1 cells, both with and without DHT. Based on these results, RA-V appears to be the key compound in YIV-818-A responsible for downregulating AR, AR-V (AR splice variants), and cyclin D1 in 22RV1 cells. In comparison, RA-VII required 25 ng/mL to achieve similar effects as those produced by 75 ng/mL of RA-V (Figure 2A). Consequently, RA-VII demonstrated approximately three times greater potency than RA-V in downregulating AR, AR-V (AR splice variants), and cyclin D1 in 22RV1 cells. YIV-818-A, RA-V, or RA-VII were also capable of downregulating AR and cyclin D1 protein in LNCaP cells (Supplementary Figure S2). YIV-818-A, RA-V, or RA-VII had no effect on GR protein expression and GR nuclear localization in 22RV1 cells in the presence of dexamethasone (dex) (Supplementary Figures S3A, B). These findings suggest that YIV-818-A, RA-V, or RA-VII might exhibit selectivity in downregulating certain hormone receptor proteins.

In Figures 2B, C, YIV-818-A, RA-V, or RA-VII did not significantly impact AR and cyclin D1 mRNA expression in 22RV1 cells. This suggests that the downregulation of AR and cyclin D1 protein by YIV-818-A, RA-V, or RA-VII is not mediated through mRNA regulation. Since Bouvardin and SVC112, analogs of RA-V and RA-VII, have previously been identified as protein translation inhibitors that can inhibit *de novo* protein synthesis (Zalacain et al., 1982; Chan et al., 2004; Keysar et al., 2020), we investigated whether YIV-818-A, RA-V, or RA-VII could inhibit AR by suppressing its protein synthesis. In Figure 2D and Supplementary Figure S4, we demonstrated that YIV-818-A, RA-V, or RA-VII could inhibit the incorporation of puromycin into newly synthesized polypeptides of 22RV1 cells. When puromycin-labeled polypeptides were pulled down for Western blot analysis, the levels of newly synthesized AR, AR-V (AR splice variants), and cyclin D1, but not GR and actin, were decreased by YIV-818-A, RA-V, or RA-VII treatments (Figure 2E). In conjunction with the above results, we provide evidence that YIV-818-A, RA-V, or RA-VII downregulate AR, AR-V (AR splice variants), and cyclin D1 primarily through protein synthesis inhibition, rather than mRNA regulation.

YIV-818-A, RA-V and RA-VII could affect epigenetic status by inhibiting BRD protein expression and H3K27 acetylation

The BET (Bromodomain and Extra-Terminal Domain) subfamily of bromodomain proteins plays a crucial role in AR and GR-dependent enhancer activation, leading to the transcription of target genes regulated by these receptors (Asangani et al., 2014; Nagarajan et al., 2014; Shah et al., 2017). By recognizing acetylated histones (H3K27Ac) on enhancer regions, BET proteins facilitate the recruitment of

10.3389/fphar.2023.1244655

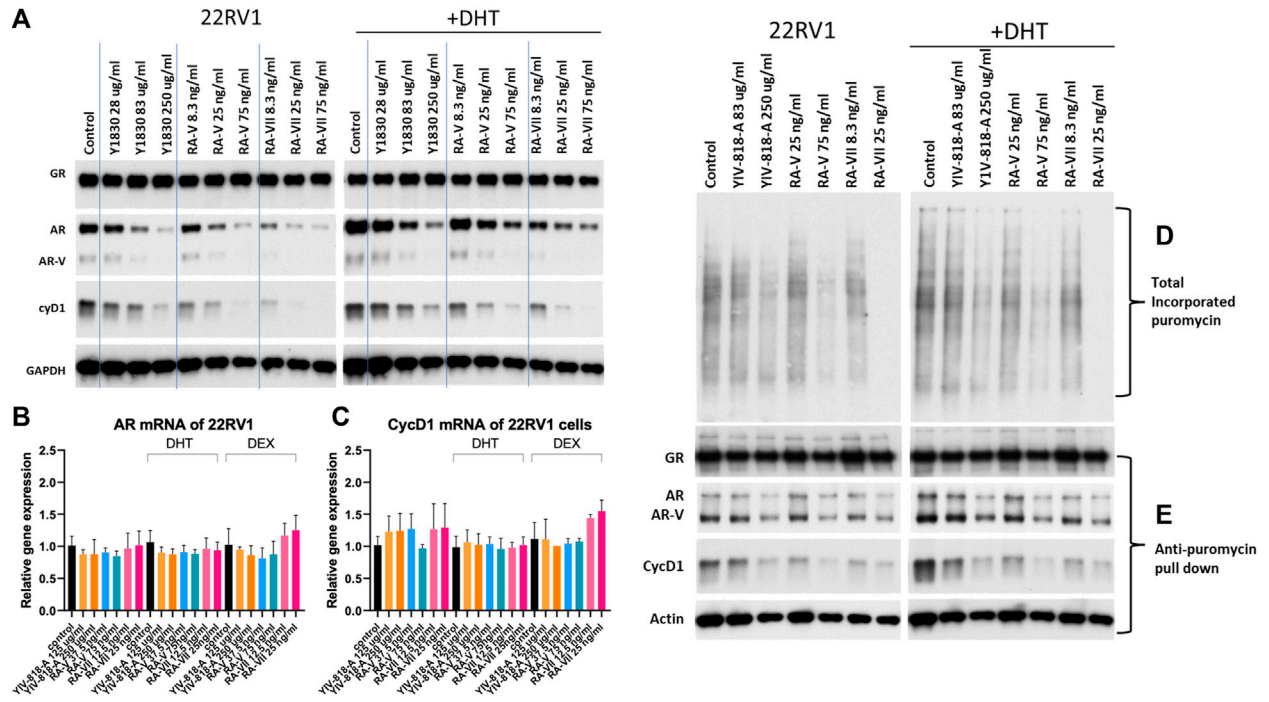

FIGURE 2
Effect of YIV-818-A, RA-V or RA-VII on GR, AR, AR-V (AR splice variants) and CycD1 protein expression and AR and CycD1 mRNA expression of 22RV1 cells as. **(A)** Western blotting for protein expression of GR, AR, AR-V (AR splice variants) and CycD1 of 22RV1 following treatment of YIV-818-A, RA-V or RA-VII without or with DHT (25 nM) for 24 h. Specific antibodies were used to determine the protein expression in Western blotting. GAPDH was used as protein loading control for normalization. 22RV1 cells were treated with YIV-818-A, RA-V or RA-VII for 24 h without or with DHT. Total RNA was extracted for RT-qPCR using specific primers for AR**(B)** and CycD1**(C)**. β-actin mRNA was used for normalization. All results were normalized to no ligand control. **(D)** Western blotting for detection of *de novo* synthesis polypeptides of 22RV1 cells. Puromycin (1uM) was used to label newly translated polypeptides of 22RV1 cells in presence of YIV-818-A, RA-V or RA-VII without and with DHT (25 nM) for 45 min. Monoclonal Anti-puromycin antibody was used to detect puromycin incorporated polypeptides. **(E)** Western blotting for detection of newly translated AR, AR-V (AR splice variants) and CycD1. After puromycin labeling, 22RV1 cells were lysed in IP buffers. Anti-puromycin antibody and protein-A/G magnetic beads were used to pull down newly synthesis polypeptides and then specific antibodies for AR, CycD1 and Actin were used to detect pull down AR, AR-V (AR splice variants), CycD1 and Actin **(E)**. Details of experimental procedures are given in *Materials and methods*.

AR or GR transcriptional machinery, leading to the activation of target gene expression and the promotion of cell-specific responses to androgens and glucocorticoids (Asangani et al., 2014; Nagarajan et al., 2014; Shah et al., 2017). BET inhibitors have been demonstrated to suppress breast and prostate cancer cell growth. Treatment with YIV-818-A, RA-V, or RA-VII led to a decrease in Brd2 and Brd4 protein expression in 22RV1 cells, both with and without DHT (Figure 3). Moreover, YIV-818-A, RA-V, or RA-VII reduced histone 3 lysine 27 acetylation (H3K27Ac), which is required for BRD binding at enhancers, but did not affect H3K9Ac or K14Ac (Figure 3).

These findings suggest that YIV-818-A, RA-V, or RA-VII might reduce the binding of Brd proteins to promoter/enhancer regions of AR and GR target genes, thereby impacting their transcription. Additionally, the downregulation of Brd proteins and H3K27Ac could represent one mechanism of action through which YIV-818-A, RA-V, or RA-VII inhibit GR transcriptional activity. These results also imply that YIV-818-A, RA-V, or RA-VII are not pan-inhibitors for histone acetyltransferases (HAT), but rather may selectively inhibit the transcription of a subset of genes that are dependent on H3K27Ac.

YIV-818-A, RA-V or RA-VII exhibit synergistic inhibition of AR activity in 22RV1 cells and LNCaP cells upon combination with enzalutamide, apalutamide, and darolutamide

Given that YIV-818-A, RA-V, or RA-VII exhibit distinct mechanisms of action in inhibiting AR compared to the FDA-approved androgen inhibitors, enzalutamide, apalutamide, and darolutamide used in prostate cancer treatments, we speculated that YIV-818-A, RA-V, or RA-VII might have the potential to synergistically enhance the therapeutic effects of enzalutamide, apalutamide, or darolutamide.

To assess drug interactions between YIV-818-A, RA-V, or RA-VII and the current drugs, we performed an isobologram analysis based on the combination index. Our results demonstrated that combinations of YIV-818-A, RA-V, or RA-VII with enzalutamide, apalutamide, or darolutamide exhibited synergistic effects (most data points from all treatments fell below the red-diagonal line of the isobologram plots) in inhibiting DHT-driven AR activity in both 22RV1 and LNCaP cells (Figures 4A, B). Therefore, YIV-818-A, RA-V, or RA-VII showed potential to enhance the efficacy of

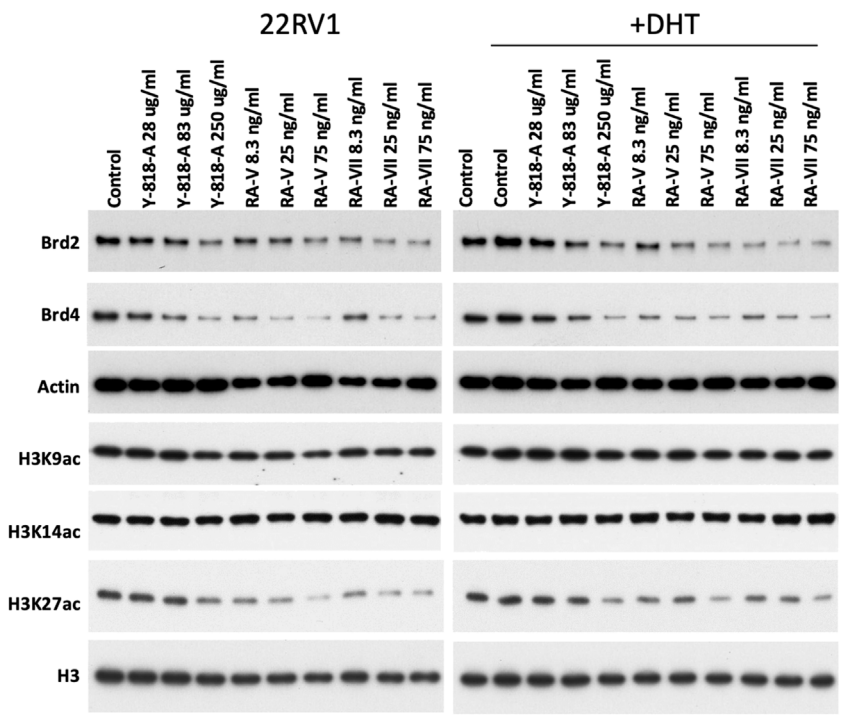

FIGURE 3
Effects of YIV-818-A, RA-V or RA-VII on protein expression of Brd2, Brd4 and histone acetylation at lysine 9, 14 and 27 of 22RV1 cells without or with DHT. Western blotting for protein expression of Brd2, Brd4, H3K9ac, H3K14ac, H3K27ac of 22RV1 following treatment of YIV-818-A, RA-V and RA-VII without or with DHT (25 nM) for 24 h. Specific antibodies were used to determine the protein expression in Western blotting. Actin and Histone 3 (H3) was used as protein loading control for normalization. Details of experimental procedures are given in *Materials and methods*.

enzalutamide, apalutamide, or darolutamide in the treatment of prostate cancers.

YIV-818-A enhanced enzalutamide action against 22RV1 tumor growth *in vivo*. The compelling *in vitro* evidence of synergistic AR activity inhibition by YIV-818-A and enzalutamide led us to explore their combined efficacy in an *in vivo* setting. We proceeded to validate this hypothesis using a 22RV1 xenograft model in nude mice.

Oral administration of YIV-818-A (500 mg/kg, twice daily) resulted in a significant deceleration of tumor growth ($p = 0.018$). On the other hand, enzalutamide (5 mg/kg, once daily) was not found to substantially decrease the growth of 22RV1 tumors in the nude mice (Figure 5A). However, a strikingly pronounced inhibition of 22RV1 tumor growth ($p < 0.0001$) was observed when YIV-818-A and enzalutamide were co-administered (Figure 5A). It is important to note that the treatments with YIV-818-A and/or enzalutamide had no discernible impact on the body weight of the test subjects (Figure 5B). In a deeper examination of the tumor tissue, we observed a considerable decrease in the mRNA expression levels of PSA and KLK2 - known target genes of AR - in response to the combined therapy of YIV-818-A and enzalutamide (Figures 5C, D). Furthermore, we also noted a reduction in PSA protein levels in plasma following this combined treatment ($p < 0.007$) (Figure 5E).

These results robustly align with our *in vitro* findings and indicate that a combined therapeutic approach with YIV-818-A and enzalutamide could offer an enhanced strategy to inhibit the growth of prostate cancer.

RA-V can serve as a quality control marker to select *Rubia cordifolia*

27 different batches of *Rubia cordifolia* (R.C.) and YIV-818-A water extracts were used to treat 22RV1-AR-luciferase reporter cells in present of DHT for 24 h. Results indicated that different batches of *Rubia cordifolia* (R.C.) had different potency in inhibiting DHT triggered AR activity (Figure 6A). The RA-V content of different batches was measured using LCMS. The content of RA-V of different batches was correlated to AR inhibition (%) using Pearson correlation. Results indicated that the content of RA-V of *Rubia cordifolia* (R.C.) had some degree of correlation to the AR inhibition (%) ($R = 0.819$) (Figure 6B). Therefore, the RA-V content of a specific batch of *Rubia cordifolia* (R.C.) could be used to predict its potency of AR inhibition. An increased content of RA-V in the batches of *Rubia cordifolia* (R.C.) increased the likelihood of stronger AR activity inhibition.

Discussion

Enzalutamide, apalutamide, and darolutamide are second-generation androgen receptor (AR) blockers approved for both non-metastatic and metastatic castration-resistant prostate cancer (CRPC) (Cattrini et al., 2022). These drugs significantly extend metastasis-free survival to about 36–40 months, compared to 14.7–18.4 months in the placebo groups (Cattrini et al., 2022). However, grade 3 adverse events or higher occur in

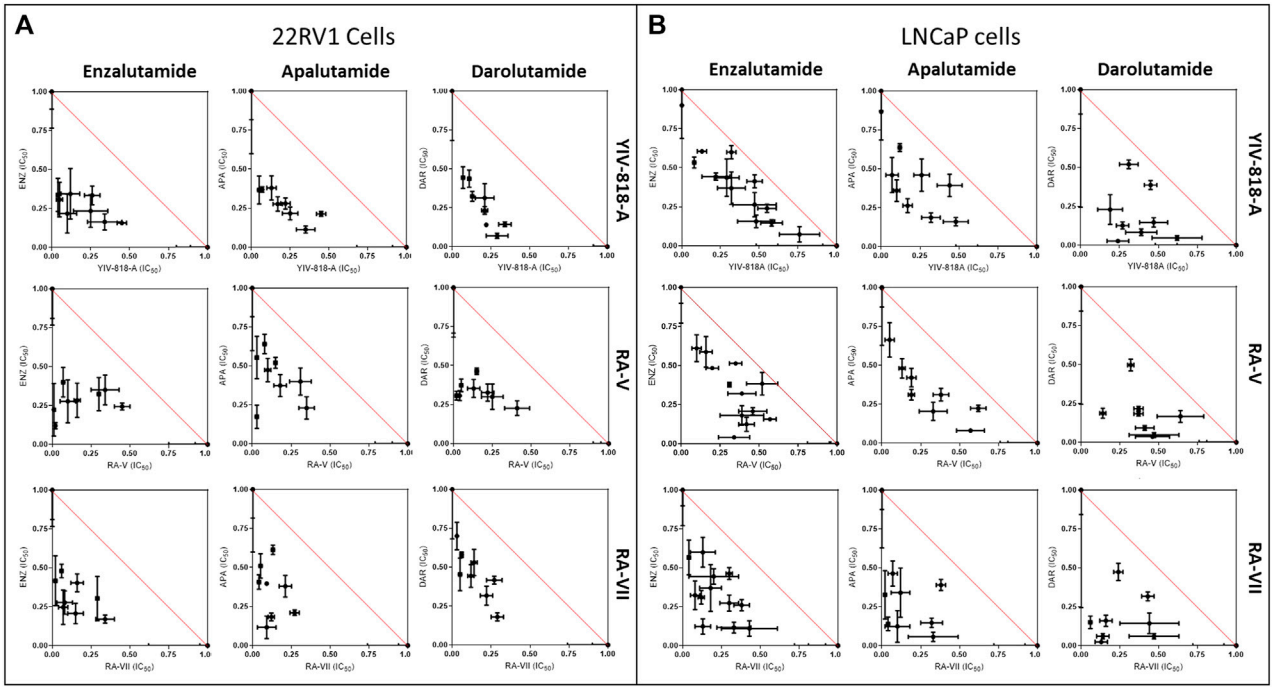

FIGURE 4
Interaction of YIV-818-A, RA-V or RA-VII with enzalutamide (ENZ), apalutamide (APA) or darolutamide (DAR) on inhibiting DHT induced AR mediated luciferase activity of 22RV1 cells **(A)** and LNCaP cells **(B)**. Isobologram plots were used to determine additive, synergistic, and antagonistic interactions of the combinations. Additive interaction: Points on the red-diagonal line. Synergistic interaction: Points below the red-diagonal line. Antagonistic interaction: Points above the red-diagonal line. Details of experimental procedures are given in *Materials and methods*.

approximately 25% of patients, with fatigue, hypertension, diarrhea, and weight loss being the most common side effects. Furthermore, enzalutamide carries a risk of causing seizure activity (Cattrini et al., 2022). Drug resistance, often manifested through AR splice variants, mutations, or glucocorticoid receptor (GR) substitution of AR function, is a common cause of treatment failure (Rice et al., 2019).

In this study, we present YIV-818-A and its active component, RA-V, as novel compounds capable of inhibiting both AR and GR activity. Similarly, RA-VII, a bicyclic hexapeptide analog of RA-V, exhibits comparable activity. Our Western blotting results reveal that YIV-818-A, RA-V, or RA-VII can reduce AR protein levels and diminish mRNA expression of AR target genes such as PSA and KLK2. Previous research demonstrated that SVC112, an analog of RA-VII, selectively reduces Cyclin D1 (CycD1) protein levels by obstructing protein translation in Head and Neck Squamous Carcinoma (Keysar et al., 2020). Furthermore, RA-V has been found to impede protein translational elongation by inhibiting the connection of the eukaryotic elongation factor 2 (eEF2) to ribosomes (Stickel et al., 2015). In alignment with these findings, our study reveals that YIV-818-A, RA-V, or RA-VII are also capable of inhibiting AR and CycD1 protein synthesis. This downregulation of AR and CycD1 proteins seems to be predominantly driven by the inhibition of protein synthesis rather than mRNA regulation. Taking into consideration the half-lives of AR and GR proteins - approximately 3 h (Syms et al., 1985) and 23 h (Dong et al., 1988) respectively, the pronounced AR protein downregulation following treatment with YIV-818-A, RA-V, or RA-VII can potentially be explained. It is plausible that the shorter half-life of AR proteins facilitates more noticeable effects from the treatments, as compared to GR proteins.

Interestingly, the inhibition of glucocorticoid receptor (GR) activity by YIV-818-A, RA-V, or RA-VII does not appear to directly correspond with protein downregulation. This led us to hypothesize that these compounds might be influencing the cofactors associated with the GR protein. Supporting this premise, our findings revealed that the levels of bromodomain proteins (Brd) and histone 3 lysine 27 acetylation (H3K27ac) were attenuated by YIV-818, RA-V, and RA-VII. Considering the pivotal role of Brd and H3K27ac in AR and GR-dependent enhancer activation and target gene transcription (Asangani et al., 2014; Nagarajan et al., 2014; Shah et al., 2017), this might represent one potential mechanism by which YIV-818-A, RA-V, or RA-VII inhibit GR activity. As part of future research, the utilization of a ChIP sequencing assay could provide valuable insights and further validate our hypothesis, determining if YIV-818A, RA-V, and RA-VII indeed affect GR activity by diminishing Brd and H3K27ac levels.

Notably, YIV-818-A, RA-V, or RA-VII have all exhibited a synergistic effect with enzalutamide, apalutamide, or darolutamide in the inhibition of AR activity, both in cell culture and *in vivo* (using the YIV-818 and enzalutamide combination in 22RV1, CRPC cells). By virtue of their ability to downregulate AR-V (AR splice variants) and hinder the GR activity of CRPC cells, the combination of these compounds with enzalutamide, apalutamide, or darolutamide might considerably decrease the chance of drug resistance development. Moreover, a potential reduction in drug dosage could possibly

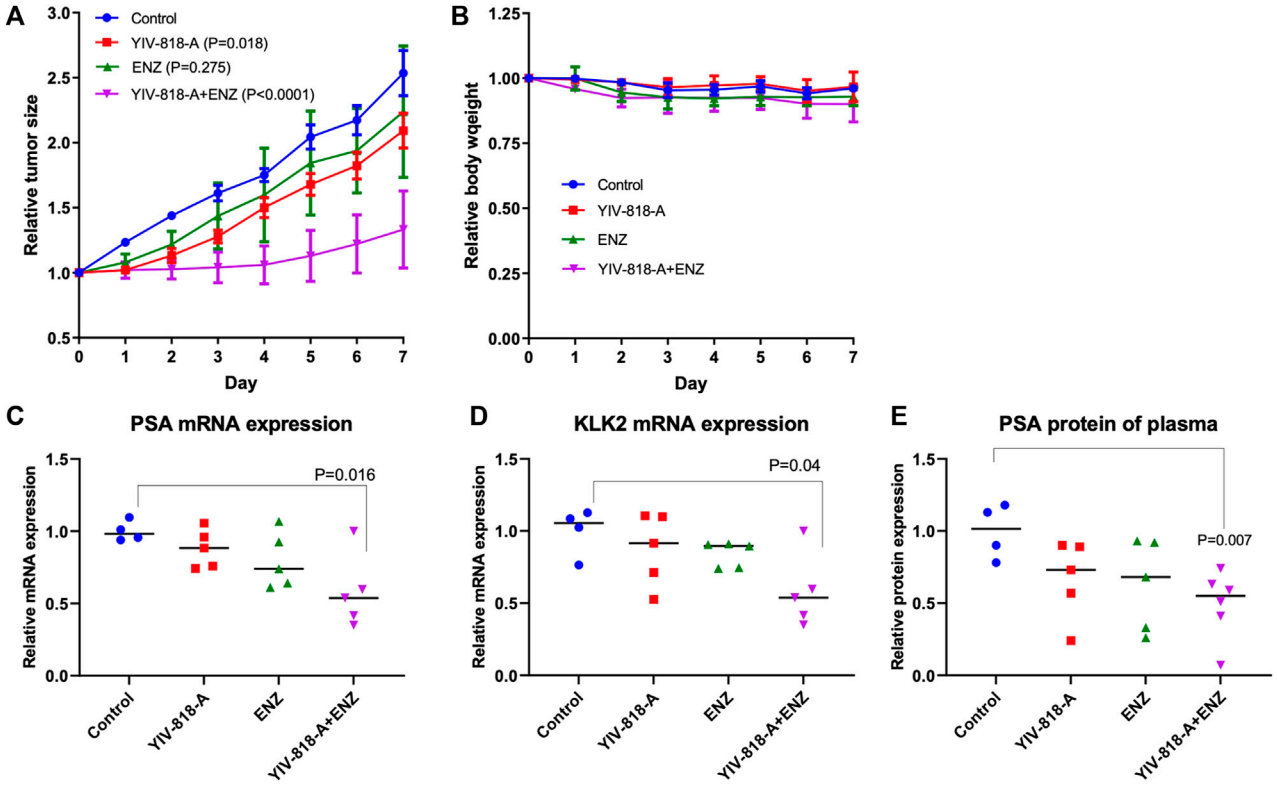

FIGURE 5
Effect of YIV-818-A and/or enzalutamide on 22RV1 tumor growth of NCR-nude mice. **(A)** Effect of YIV-818-A (500 mg/kg, PO, BID) and/or enzalutamide (5 mg/kg, PO, QD) on 22RV1 tumor growth of NCR-nude mice. **(B)** Effect of YIV-818-A and/or enzalutamide on animal body weight during the treatments. qRT-PCR analysis for PSA mRNA **(C)** and KL2 mRNA **(D)** of 22RV1 tumor following the treatments. **(E)** PSA protein detection of plasma of animal following the treatments. ELISA was used to detect PSA protein of plasma. Two-way ANOVA analysis was employed to discern differences between two data curves. Additionally, t-tests were conducted to ascertain statistical significance between group comparisons. Details of experimental procedures are given in *Materials and Methods*.

mitigate adverse effects experienced by patients. Therefore, YIV-818-A, RA-V, or RA-VII represent a promising approach to augment the therapeutic impact of enzalutamide, apalutamide, and darolutamide.

Furthermore, palbociclib, abemaciclib, and ribociclib, which are CDK4/6 inhibitors, are approved for the treatment of metastatic CRPC (Kase et al., 2020). Cyclin D1 (CycD1) serves as an activator for CDK4/6 kinases (Morgan, 1997). Upon the loss of CycD1, CDK4/6 kinases become inactive, thus unable to phosphorylate Rb (Bertoli et al., 2013). This hypophosphorylated Rb represses E2F, resulting in cell cycle progression arrest (Dick and Rubin, 2013). Since YIV-818-A, RA-V, or RA-VII downregulate CycD1, they may mirror the action of palbociclib, abemaciclib, and ribociclib in halting cell growth. Therefore, the potential application of YIV-818-A, RA-V, or RA-VII in the treatment of metastatic CRPC warrants further investigation.

At least twenty-four distinct bicyclic hexapeptides have been discovered and isolated from *Rubia cordifolia* (R.C.) (Shan et al., 2016). Existing research suggests that some of these bicyclic hexapeptides exhibit cytotoxic effects against tumor cells, P-388 leukemia cells, SGC-7901 human gastric adenocarcinoma cells, A-549 human non-small cell lung carcinoma cells, as well as HeLa (human cervical carcinoma) and KB (human epithelial carcinoma) cells (Itokawa et al., 1984; Lee et al., 2008a; Zhao et al., 2011). Moreover, a plethora of new bicyclic hexapeptides have been synthesized with an aim to enhance their anti-tumor activity (Lee et al., 2008a; Lee et al., 2008b; Hitotsuyanagi et al., 2011; Keysar et al., 2020).

Our study underlines the varying potency of different bicyclic hexapeptides, such as RA-V, RA-VII, or RA-XI, in inhibiting AR and GR. It is intriguing to note how a seemingly minor change, such as substituting glutamic acid at the 2nd position of the hexapeptide (as in RA-XI) instead of alanine (as in RA-V or RA-VII), can significantly reduce the anti-AR and anti-GR activity of RA-XI. This could be attributed to the bulky carboxylic acid group of glutamic acid potentially impeding its binding to the target molecule. On the other hand, the presence of a CH3 group on the tyrosine at position 6 in RA-VII appears to enhance its anti-AR and anti-GR activity compared to RA-V, which has an H group at the same position. The region spanning the 2nd to 6th positions could dictate the hexapeptide's orientation towards its target, but this hypothesis warrants further investigation. A comprehensive study exploring the structure-activity relationship of this class of compounds in relation to AR should be pursued further. Such efforts could pave the way for the identification of more potent compounds with high selectivity towards AR, GR, or certain epigenetic states.

In addition to AR, AR-V (AR splice variants), and GR, prostate cancer progression and drug resistance involve a myriad of

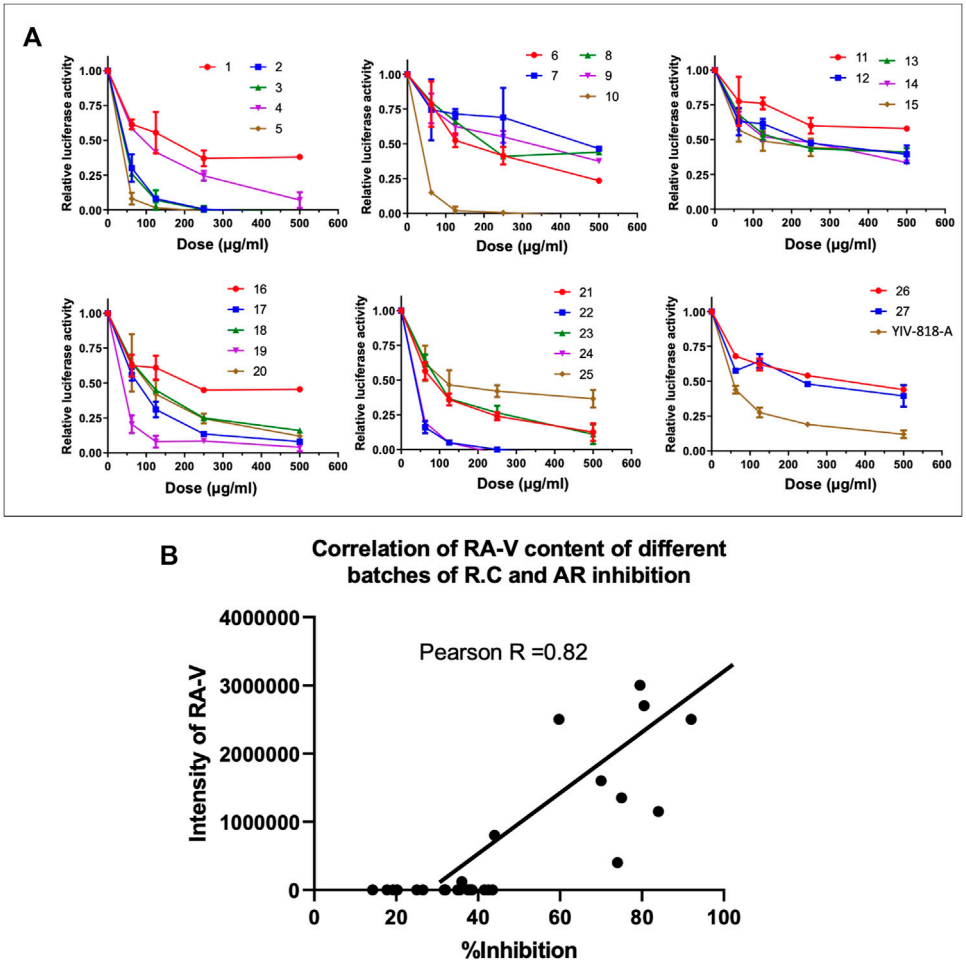

FIGURE 6
Correlation between RA-V of *Rubia cordifolia* (R.C.) and AR Inhibition in 22RV1 Cells. **(A)** Effect of different batches of RC on AR driven luciferase activity of 22RV1 in presence of DHT. **(B)** Pearson correlation analysis for the content of RA-V of different batches of *Rubia cordifolia* (R.C.) and AR inhibition (%). Details of experimental procedures are given in *Materials and Methods*.

alternative mechanisms that have been extensively studied (Vander Ark et al., 2018). Notably, ACSL4 (acyl-CoA synthetase long-chain family member 4) has emerged as a significant player, as its high expression has been linked to promoting prostate cancer growth, invasion, and hormonal resistance, thereby contributing to disease aggressiveness (Wu et al., 2015). Another critical factor is AKR1C3, which plays a pivotal role in androgen-related pathways. This enzyme is responsible for metabolizing androstenediones into more-active androgens like testosterone or dihydrotestosterone, influencing androgen signaling in prostate cancer cells (Liu et al., 2015). Moreover, uncontrolled IL6/JAK/STAT3 signaling has been implicated in enzalutamide resistance. This pathway can transactivate androgen signaling, leading to reduced responsiveness to antiandrogen therapies like enzalutamide (Handle et al., 2016). Additionally, the transcription factor SOX2 has been found to promote lineage plasticity and antiandrogen resistance in prostate cancer cases lacking TP53 and RB1 tumor suppressor genes, contributing to the development of more aggressive and enzalutamide resistant phenotypes (Mu et al., 2017). Understanding these diverse mechanisms and their impact on prostate cancer progression is crucial for developing more effective therapeutic approaches. Exploring how YIV-818A, RA-V, and RA-VII interact with these targets can provide valuable insights into their potential as treatment options for prostate cancer, especially in cases with multiple resistance mechanisms. Targeting these alternative pathways could open new avenues for personalized and combination therapies, ultimately leading to improved outcomes for prostate cancer patients.

Rubia cordifolia (R.C) has a long-standing history of safe usage in Asia as a dietary supplement designed to improve health. *Rubia cordifolia* (R.C.) has been recognized for its diverse biological properties, including promoting coagulation, modulating the immune system, providing anti-inflammatory and neuroprotective effects, acting as an antioxidant, and exhibiting anti-tumor properties (Shan et al., 2016). However, its potential impact on androgen receptor (AR) and glucocorticoid receptor (GR) signaling in the treatment of prostate cancer has been largely overlooked. Our research presents compelling evidence to suggest that *Rubia cordifolia* (R.C.) may inhibit the growth of prostate

cancer by disrupting AR and GR signaling. Thus, *Rubia cordifolia* (R.C.) emerges as a potentially powerful therapeutic agent for prostate cancer treatment or as a chemopreventive measure. This promising prospect is deserving of further investigation and consideration in future research endeavors.

We identified RA-V, a component of YIV-818-A, as the agent responsible for inhibiting AR and GR. However, we observed considerable variation in the quantity of RA-V present in *Rubia cordifolia* (R.C.) across different batches. Interestingly, the amount of RA-V present in *Rubia cordifolia* (R.C.) showed a strong correlation with AR inhibition across different batches. This suggests that RA-V could serve as a chemical marker to select high-potency *Rubia cordifolia* (R.C.) batches for development in the treatment or prevention of prostate cancer.

In summary, YIV-818-A, RA-V, or RA-VII show potential in overcoming the drug resistance encountered in castration-resistant prostate cancer (CRPC) cells caused by AR variants and GR. This is achieved by down-regulating AR protein, inhibiting GR function, and influencing epigenetic regulation. Agents such as YIV-818-A, RA-V, and RA-VII could potentially enhance the therapeutic effect of FDA-approved androgen inhibitors—enzalutamide, apalutamide, or darolutamide—against castration-resistant prostate cancer (CRPC). Moreover, RA-V, found in *Rubia cordifolia* (R.C.), could serve as a chemical marker for quality control in the preparation of this herbal supplement. Given the longstanding safe usage of *Rubia cordifolia* (R.C.) in Asia as a dietary supplement for health improvement, YIV-818-A could potentially be developed as a chemoprevention agent and/or anti-cancer drug for the treatment of prostate cancer.

Data availability statement

The original contributions presented in the study are included in the article/Supplementary Material, further inquiries can be directed to the corresponding author.

Ethics statement

The animal study was reviewed and approved by Yale University Institutional Animal Care and Use Committee (IACUC).

Author contributions

WL established cell lines and did luciferase assays, Western blotting, qRT-PCR, isolation of active compounds and co-wrote the manuscript. MA did Western blotting, purifying active compound, correlation analysis and co-wrote the manuscript. WC did high resolution LC-MS analysis, NMR, chemical structure analysis. FG did animal studies. ZJ did animal studies. S-HL provided YIV-818-A and co-wrote the manuscript. PC provided YIV-818-A and co-wrote the manuscript. Y-CC supervised the project and co-wrote the manuscript. All authors contributed to the article and approved the submitted version.

Funding

This work was supported by Yiviva and a research gift from the National Foundation for Cancer Research, USA.

Acknowledgments

Y-CC is a fellow of the National Foundation for Cancer Research (USA).

Conflict of interest

Y-CC is the inventor of YIV-818-A for cancer treatment. The patent is owned by Yale University. Yale University has licensed this patent to Yiviva. S-HL and PC are employees of Yiviva. WL is a consultant for Yiviva.

The remaining authors declare that the research was conducted in the absence of any commercial or financial relationships that could be construed as a potential conflict of interest.

Publisher's note

Supplementary material

The Supplementary Material for this article can be found online at: https://www.frontiersin.org/articles/10.3389/fphar.2023.1244655/full#supplementary-material

References

Antonarakis, E. S., Lu, C., Wang, H., Luber, B., Nakazawa, M., Roeser, J. C., et al. (2014). AR-V7 and resistance to enzalutamide and abiraterone in prostate cancer. *N. Engl. J. Med.* 371, 1028–1038. doi:10.1056/NEJMoa1315815

Arora, V. K., Schenkein, E., Murali, R., Subudhi, S. K., Wongvipat, J., Balbas, M. D., et al. (2013). Glucocorticoid receptor confers resistance to antiandrogens by bypassing androgen receptor blockade. *Cell* 155, 1309–1322. doi:10.1016/j.cell.2013.11.012

Asangani, I. A., Dommeti, V. L., Wang, X., Malik, R., Cieslik, M., Yang, R., et al. (2014). Therapeutic targeting of BET bromodomain proteins in castration-resistant prostate cancer. *Nature* 510, 278–282. doi:10.1038/nature13229

Bertoli, C., Skotheim, J. M., and De Bruin, R. A. (2013). Control of cell cycle transcription during G1 and S phases. *Nat. Rev. Mol. Cell Biol.* 14, 518–528. doi:10.1038/nrm3629

Buchanan, G., Greenberg, N. M., Scher, H. I., Harris, J. M., Marshall, V. R., and Tilley, W. D. (2001). Collocation of androgen receptor gene mutations in prostate cancer. *Clin. Cancer Res.* 7, 1273–1281.

Cattrini, C., Caffo, O., De Giorgi, U., Mennitto, A., Gennari, A., Olmos, D., et al. (2022). Apalutamide, darolutamide and enzalutamide for nonmetastatic castration-resistant prostate cancer (nmCRPC): A critical review. *Cancers (Basel)* 14, 1792. doi:10.3390/cancers14071792

Chan, J., Khan, S. N., Harvey, I., Merrick, W., and Pelletier, J. (2004). Eukaryotic protein synthesis inhibitors identified by comparison of cytotoxicity profiles. *RNA* 10, 528–543. doi:10.1261/rna.5200204

Chou, T. C., and Talalay, P. (1977). A simple generalized equation for the analysis of multiple inhibitions of Michaelis-Menten kinetic systems. *J. Biol. Chem.* 252, 6438–6442. doi:10.1016/s0021-9258(17)39978-7

Dick, F. A., and Rubin, S. M. (2013). Molecular mechanisms underlying RB protein function. *Nat. Rev. Mol. Cell Biol.* 14, 297–306. doi:10.1038/nrm3567

Dong, Y., Poellinger, L., Gustafsson, J. A., and Okret, S. (1988). Regulation of glucocorticoid receptor expression: Evidence for transcriptional and posttranslational mechanisms. *Mol. Endocrinol.* 2, 1256–1264. doi:10.1210/mend-2-12-1256

Gioeli, D., and Paschal, B. M. (2012). Post-translational modification of the androgen receptor. *Mol. Cell Endocrinol.* 352, 70–78. doi:10.1016/j.mce.2011.07.004

Handle, F., Erb, H. H., Luef, B., Hoefer, J., Dietrich, D., Parson, W., et al. (2016). SOCS3 modulates the response to enzalutamide and is regulated by androgen receptor signaling and CpG methylation in prostate cancer cells. *Mol. Cancer Res.* 14, 574–585. doi:10.1158/1541-7786.MCR-15-0495

Hitotsuyanagi, Y., Lee, J. E., Kato, S., Kim, I. H., Kohashi, H., Fukaya, H., et al. (2011). Per-N-methylated analogues of an antitumor bicyclic hexapeptide RA-VII. *Bioorg Med. Chem.* 19, 2458–2463. doi:10.1016/j.bmc.2011.02.003

Itokawa, H., Takeya, K., Mihara, K., Mori, N., Hamanaka, T., Sonobe, T., et al. (1983). Studies on the antitumor cyclic hexapeptides obtained from Rubiae radix. *Chem. Pharm. Bull. (Tokyo)* 31, 1424–1427. doi:10.1248/cpb.31.1424

Itokawa, H., Takeya, K., Mori, N., Takanashi, M., Yamamoto, H., Sonobe, T., et al. (1984). Cell growth-inhibitory effects of derivatives of antitumor cyclic hexapeptide RA-V obtained from Rubiae radix (V). *Gan* 75, 929–936.

Kase, A. M., Copland, J. A., Iii, and Tan, W. (2020). Novel therapeutic strategies for CDK4/6 inhibitors in metastatic castrate-resistant prostate cancer. *Onco Targets Ther.* 13, 10499–10513. doi:10.2147/OTT.S266085

Keysar, S. B., Gomes, N., Miller, B., Jackson, B. C., Le, P. N., Morton, J. J., et al. (2020). Inhibiting translation elongation with SVC112 suppresses cancer stem cells and inhibits growth in Head and Neck squamous carcinoma. *Cancer Res.* 80, 1183–1198. doi:10.1158/0008-5472.CAN-19-3232

Koivisto, P., Kononen, J., Palmberg, C., Tammela, T., Hyytinen, E., Isola, J., et al. (1997). Androgen receptor gene amplification: A possible molecular mechanism for androgen deprivation therapy failure in prostate cancer. *Cancer Res.* 57, 314–319.

Lee, J. E., Hitotsuyanagi, Y., Fukaya, H., Kondo, K., and Takeya, K. (2008a). New cytotoxic bicyclic hexapeptides, RA-XXIII and RA-XXIV, from Rubia cordifolia L. *Chem. Pharm. Bull. (Tokyo)* 56, 730–733. doi:10.1248/cpb.56.730

Lee, J. E., Hitotsuyanagi, Y., Nakagawa, Y., Kato, S., Fukaya, H., and Takeya, K. (2008b). Design and synthesis of a bis(cycloisodityrosine) analogue of RA-VII, an antitumor bicyclic hexapeptide. *Bioorg Med. Chem. Lett.* 18, 6458–6461. doi:10.1016/j.bmcl.2008.10.064

Li, Y., Chan, S. C., Brand, L. J., Hwang, T. H., Silverstein, K. A., and Dehm, S. M. (2013). Androgen receptor splice variants mediate enzalutamide resistance in castration-resistant prostate cancer cell lines. *Cancer Res.* 73, 483–489. doi:10.1158/0008-5472.CAN-12-3630

Liu, C., Lou, W., Zhu, Y., Yang, J. C., Nadiminty, N., Gaikwad, N. W., et al. (2015). Intracrine androgens and AKR1C3 activation confer resistance to enzalutamide in prostate cancer. *Cancer Res.* 75, 1413–1422. doi:10.1158/0008-5472.CAN-14-3080

Lu, J., Lonergan, P. E., Nacusi, L. P., Wang, L., Schmidt, L. J., Sun, Z., et al. (2015). The cistrome and gene signature of androgen receptor splice variants in castration resistant prostate cancer cells. *J. Urol.* 193, 690–698. doi:10.1016/j.juro.2014.08.043

Mills, I. G. (2014). Maintaining and reprogramming genomic androgen receptor activity in prostate cancer. *Nat. Rev. Cancer* 14, 187–198. doi:10.1038/nrc3678

Morgan, D. O. (1997). Cyclin-dependent kinases: Engines, clocks, and microprocessors. *Annu. Rev. Cell Dev. Biol.* 13, 261–291. doi:10.1146/annurev.cellbio.13.1.261

Nagarajan, S., Hossan, T., Alawi, M., Najafova, Z., Indenbirken, D., Bedi, U., et al. (2014). Bromodomain protein BRD4 is required for estrogen receptor-dependent enhancer activation and gene transcription. *Cell Rep.* 8, 460–469. doi:10.1016/j.celrep.2014.06.016

Nakazawa, M., Antonarakis, E. S., and Luo, J. (2014). Androgen receptor splice variants in the era of enzalutamide and abiraterone. *Horm. Cancer* 5, 265–273. doi:10.1007/s12672-014-0190-1

Pomerantz, M. M., Li, F., Takeda, D. Y., Lenci, R., Chonkar, A., Chabot, M., et al. (2015). The androgen receptor cistrome is extensively reprogrammed in human prostate tumorigenesis. *Nat. Genet.* 47, 1346–1351. doi:10.1038/ng.3419

Rice, M. A., Malhotra, S. V., and Stoyanova, T. (2019). Second-generation antiandrogens: From discovery to standard of Care in castration resistant prostate cancer. *Front. Oncol.* 9, 801. doi:10.3389/fonc.2019.00801

Shah, N., Wang, P., Wongvipat, J., Karthaus, W. R., Abida, W., Armenia, J., et al. (2017). Regulation of the glucocorticoid receptor via a BET-dependent enhancer drives antiandrogen resistance in prostate cancer. *Elife* 6, e27861. doi:10.7554/eLife.27861

Shan, M., Yu, S., Yan, H., Chen, P., Zhang, L., and Ding, A. (2016). A Review of the Botany, Phytochemistry, Pharmacology and Toxicology of Rubiae Radix et Rhizoma. *Molecules* 21 (12), 1747. doi:10.3390/molecules21121747

Shiota, M., Yokomizo, A., and Naito, S. (2011). Increased androgen receptor transcription: A cause of castration-resistant prostate cancer and a possible therapeutic target. *J. Mol. Endocrinol.* 47, R25–R41. doi:10.1530/JME-11-0018

Sramkoski, R. M., Pretlow, T. G., 2nd, Giaconia, J. M., Pretlow, T. P., Schwartz, S., Sy, M. S., et al. (1999). A new human prostate carcinoma cell line, 22Rv1. *Vitro Cell Dev Biol Anim* 35, 403–409. doi:10.1007/s11626-999-0115-4

Stickel, S. A., Gomes, N. P., Frederick, B., Raben, D., and Su, T. T. (2015). Bouvardin is a radiation modulator with a novel mechanism of action. *Radiat. Res.* 184, 392–403. doi:10.1667/RR14068.1

Syms, A. J., Norris, J. S., Panko, W. B., and Smith, R. G. (1985). Mechanism of androgen-receptor augmentation. Analysis of receptor synthesis and degradation by the density-shift technique. *J. Biol. Chem.* 260, 455–461. doi:10.1016/s0021-9258(18)89753-8

Tan, M. E., Li, J., Xu, H. E., Melcher, K., and Yong, E. (2015). Androgen receptor: Structure, role in prostate cancer and drug discovery. *Acta Pharmacol. Sin.* 36, 3–23. doi:10.1038/aps.2014.18

Vander Ark, A., Cao, J., and Li, X. (2018). Mechanisms and approaches for overcoming enzalutamide resistance in prostate cancer. *Front. Oncol.* 8, 180. doi:10.3389/fonc.2018.00180

Wong, Y. N., Ferraldeschi, R., Attard, G., and De Bono, J. (2014). Evolution of androgen receptor targeted therapy for advanced prostate cancer. *Nat. Rev. Clin. Oncol.* 11, 365–376. doi:10.1038/nrclinonc.2014.72

Wu, X., Deng, F., Li, Y., Daniels, G., Du, X., Ren, Q., et al. (2015). ACSL4 promotes prostate cancer growth, invasion and hormonal resistance. *Oncotarget* 6, 44849–44863. doi:10.18632/oncotarget.6438

Zalacain, M., Zaera, E., Vazquez, D., and Jimenez, A. (1982). The mode of action of the antitumor drug bouvardin, an inhibitor of protein synthesis in eukaryotic cells. *FEBS Lett.* 148, 95–97. doi:10.1016/0014-5793(82)81250-7

Zhao, S. M., Kuang, B., Fan, J. T., Yan, H., Xu, W. Y., and Tan, N. H. (2011). Antitumor cyclic hexapeptides from rubia plants: History, chemistry, and mechanism (2005-2011). *Chim. (Aarau)* 65, 952–956. doi:10.2533/chimia.2011.952

frontiers | Frontiers in Endocrinology

TYPE Original Research
PUBLISHED 24 October 2023
DOI 10.3389/fendo.2023.1270594

OPEN ACCESS

EDITED BY
Anna Perri,
Magna Græcia University of Catanzaro, Italy

REVIEWED BY
Savio Domenico Pandolfo,
Federico II University Hospital, Italy
Eliane Gouvêa Oliveira-Barros,
Juiz de Fora Federal University, Brazil

*CORRESPONDENCE
Jianxing Li
ljxa01048@btch.edu.cn
Nianzeng Xing
xingnianzeng@126.com

†These authors have contributed equally to this work

RECEIVED 01 August 2023
ACCEPTED 21 September 2023
PUBLISHED 24 October 2023

CITATION
Wang F, Zhang G, Tang Y, Wang Y, Li J and Xing N (2023) Analysis of risk factors for positive surgical margin after laparoscopic radical prostatectomy with and without neoadjuvant hormonal therapy. *Front. Endocrinol.* 14:1270594. doi: 10.3389/fendo.2023.1270594

Analysis of risk factors for positive surgical margin after laparoscopic radical prostatectomy with and without neoadjuvant hormonal therapy

Fangming Wang[1†], Gang Zhang[1†], Yuzhe Tang[1†], Yunpeng Wang[2], Jianxing Li[1*] and Nianzeng Xing[3*]

[1]Department of Urology, Tsinghua University Affiliated Beijing Tsinghua Changgung Hospital, Tsinghua University Clinical Institute, Beijing, China, [2]Department of Outpatient, The Second Medical Center & National Clinical Research Center for Geriatric Diseases, Chinese PLA General Hospital, Beijing, China, [3]Department of Urology, National Cancer Center/National Clinical Research Center for Cancer/Cancer Hospital, Chinese Academy of Medical Sciences and Peking Union Medical College, Beijing, China

Background: Positive surgical margins (PSM) is not only an independent risk factor for recurrence, metastasis, and prognosis, but also an important indicator of adjuvant therapy for prostate cancer (PCa) patients treated with radical prostatectomy (RP). At present, there are few reports analyzing risk factors of PSM in laparoscopic RP (LRP), especially for those PCa cases who accepted neoadjuvant hormonal therapy (NHT). Hence, the aim of the current study was to explore risk factors for PSM after LRP in PCa patients with and without NHT.

Methods: The clinicopathological data of patients who underwent LRP from January 2012 to July 2020 was retrospectively analyzed. Risk factors for PSM after LRP in NHT and non-NHT groups were respectively explored.

Results: The overall PSM rate was 33.3% (90/270), PSM rate was 39.3% (64/163) in patients without NHT and 24.3% (26/107) in those with NHT. The apex was the most common location of PSM in non-NHT group (68.8%, 44/64), while the fundus was the most common location of PSM in NHT group (57.7%, 15/26). Multiple logistic regression revealed that body mass index (BMI), PSA, ISUP grade after LRP, pathological stage T (pT) and pathological lymph node status (pN) were independent factors affecting the PSM for patients without NHT (OR=1.160, 95% CI:1.034-1.301, p=0.011; OR=3.385, 95%CI:1.386-8.268, p=0.007; OR=3.541, 95%CI:1.008-12.444, p=0.049; OR=4.577, 95%CI:2.163-9.686, p<0.001; OR=3.572, 95%CI:1.124-11.347, p=0.031), while pT, pN, and lymphovascular invasion (LVI) were independent risk factors affecting PSM for patients with NHT (OR=18.434, 95%CI:4.976-68.297, p<0.001; OR=7.181, 95%CI:2.089-24.689, p=0.002; OR=3.545, 95%CI:1.109-11.327, p=0.033).

Conclusions: The apex was the most common location in NHT group, and BMI, PSA, ISUP after LRP, pT and pN were independent risk factors affecting PSM for NHT patients; while the fundus was the most common location in non-NHT group, and pT, pN, and LVI were independent risk factors affecting PSM for non-NHT patients.

KEYWORDS

neoadjuvant hormonal therapy, positive surgical margin, laparoscopic radical prostatectomy, risk factors, prostate cancer

Introduction

Prostate cancer (PCa) is the second most common cancer and the fifth most common cause of cancer death among men worldwide in 2020 (1). Although there are emerging diagnostic biomarkers for the detection of PCa (2, 3), PCa is usually diagnosed by prostate biopsy prompted by a blood test to measure prostate-specific antigen (PSA) levels and/or digital rectal examination. Localized PCa can be cured by radical prostatectomy (RP) or radiotherapy. PCa relapses after RP are treated with salvage radiotherapy and/or androgen deprivation therapy (ADT) for local relapse, or with ADT combined with chemotherapy for systemic relapse. Advanced PCa often progresses despite ADT and is then considered castration-resistant and incurable. Patients with localized disease at a low to intermediate risk of recurrence generally have a favorable outcome of 99% overall survival for 10 years if the disease is treated at an early stage (4). As mentioned, RP is the most common treatment options for localized PCa, and increasingly used as an important step for the treatment of advanced local, and even early metastatic cases when indicated (5). Postoperative histopathology report of RP specimens including pathological stage T (pT), lymph node status (pN), grade, perineural invasion (PNI), lymphovascular invasion (LVI), and positive surgical margin (PSM) is of crucial importance to clarify the stage, make decisions for adjuvant treatment, and predict patient outcome after RP (6, 7). A PSM is defined as cancer at the inked margin of the specimen. This can follow from incising into the extraprostatic cancer in patients with extracapsular extension or by incision into an otherwise organ-confined cancer (8). Although controversial, most studies validated that PSM is an independent risk factor for biochemical recurrence, local recurrence, distant metastasis, and prognosis (9–11), and exerts stressful impact on patients and family members (12). Moreover, PSM is an important indicator for postoperative adjuvant hormonal therapy or radiotherapy after RP (13, 14). Therefore, urologists should be familiar with factors influencing PSM and spare no effort to avoid the occurrence of PSM during operation. At present, studies reporting risk factors of PSM mainly focused on robot-assisted LRP and open RP, and there are few reports analyzing risk factors of PSM in conventional LRP. Besides, almost all studies exploring risk factors of PSM excluded PCa cases which have accepted neoadjuvant hormonal therapy (NHT). Until now, it remains largely unknown which clinicopathological parameters could be risk factors for PSM in PCa patients treated with NHT prior to RP. Hence, the aim of the current study was to describe the locations of PSM and the clinicopathological characteristics including BMI, PSA, grade, stage, PNI, and LVI and identify the independent risk factors affecting PSM of RP specimen in the Chinese PCa patients who underwent conventional LRP with and without NHT, respectively. Our results could have clinical implications for the prediction of PSM and guidance of individual LRP surgery, postoperative adjuvant therapy, and evaluation of prognosis.

Materials and methods

General information

A total of 275 patients with PCa who underwent extraperitoneal LRP and pelvic lymph node dissection performed by the same surgeon in Tsinghua University Affiliated Beijing Tsinghua Changgung Hospital and Cancer Hospital and Chinese Academy of Medical Sciences and Peking Union Medical College between January 2012 and October 2020 were reviewed. Inclusion criteria of the study were pathologically confirmed prostate adenocarcinoma in LRP specimen. Exclusion criteria of the study were (1) medical history of receiving any radiotherapy or chemotherapy before LRP; (2) LRP converted to open operation. For the present study, we withdrew 2 patients who underwent radiotherapy and 3 cases whose LRP procedures converted into open surgical procedures, and collected 270 PCa cases who met the recruitment standard and were identified for analysis. Mean age was 67.4 ± 6.7 years, mean body mass index (BMI) was 25.4 ± 3.2 kg/m^2. Median preoperative PSA was 15.3 (9.0-28.7) ng/ml, median preoperative prostate volume was 35.2 (23.0-46.2) ml. All demographic and clinicopathological data including age, BMI, hypertension, diabetes mellitus, history of pelvic surgery, preoperative PSA, prostate volume, the interval between biopsy and RP, NHT treatment, and postoperative pathological results including pT and pN, ISUP (international society of urological pathology) grade, PSM and exact locations, PNI, and LVI were collected from the hospital information system.

Definitions

All LRP samples were routinely sent to the pathological department for diagnosis, and were fixed, serially sectioned and processed according to the well-established protocols. Pathologic factors analyzed included grade and tumor stage, PSM, PNI, and LVI. The cancer grade assessment was performed according to the ISUP 2014 classification system (15). The pT was evaluated on the basis of a prostatectomy specimen according to the American Joint Committee on Cancer (AJCC) TNM classification of malignant tumors in 2017 (AJCC, pT2-T4, Nx,0,1) (16). pT1+pT2 were categorized as localized PCa and pT3+pT4 were categorized as locally advanced PCa. PSM was defined as tumor extending to the inked surface of the prostatectomy specimen that the surgeon has cut across (17). The apex, fundus, body, and vas deferens or seminal vesicles are four locations of PSM in the pathological report. PNI is defined as cancer tracking along or around a nerve within the perineural space (18). PNI was defined as the invasion of cancer cells in, around, and through the nerves. Diagnostic criterion for LVI was defined as the presence of tumor cells within an endothelial-lined space that is usually devoid of a muscular wall (www.cap.org/protocols-and-guidelines/cancerreporting-tools/cancer-protocol templates). The pathology of the presence of PSM, PNI, and LVI was reviewed by 2 senior pathologists through comprehensive analysis of H&E staining results. For controversial cases, a third pathologist was invited to reach group agreement.

Statistical analysis

Data were expressed as means ± SD or median with interquartile range for continuous variables and number (percentage) for categorical variables. The differences between continuous variables were analyzed by unpaired t-tests or MannWhitney U tests as appropriate. Categorical variables were analyzed by $\chi 2$-test. At first, all PCa subjects were divided into two groups according to whether receiving NHT or not: non-NHT and NHT groups, and clinicopathological variables including PSM were compared between the two groups. Then all cases were divided into two groups according to PSM status: non-PSM and PSM groups, and clinicopathological variables were compared between the two groups. Significant clinicopathological risk factors for PSM examined by univariate logistic regression analysis were further analyzed by multivariate logistic regression analysis to determine the independent risk factors of PSM in non-NHT and NHT groups, respectively. All tests were two-sided and a p-value <0.05 was considered significant. The statistical analyses were performed with SPSS version 22.0 software (Chicago, IL, USA).

Results

Characteristics of non-NHT and NHT patients

The clinicopathological characteristics of the enrolled PCa subjects were shown in Table 1.The mean age was 67.4 ± 6.7 years, mean BMI was 25.4 ± 3.2 kg/m^2. Median preoperative PSA was 15.3 (9.0-28.7) ng/ml, median preoperative prostate volume was 35.2 (23.0-46.2) ml. The overall PSM rate was 33.3% (90/270), and the accumulated distribution of locations was as following: apex (62.2%, 56/90), fundus (41.1%, 37/90), body (37.8%, 34/90), vas deferens/seminal vesicles (7.8%, 7/90).

Among all 270 PCa patients, 163 did not receive NHT and 107 received NHT. Among NHT patients, 82 cases accepted maximal androgen blockade (MAB) therapy with median course of 3 months; 3 cases accepted simple castration therapy with median course of 3 months; 22 cases accepted anti-androgen monotherapy (AAM) with median course of 1 month. The PSM rate of non-NHT and NHT group was 39.3% (64/163), 24.3% (26/107), respectively,

TABLE 1 Baseline characteristics of the PCa subjects underwent LRP according to the NHT stratification.

	All subjects (n=270)	Non-NHT (n=163)	NHT (n=107)	p value
Demographic characteristics				
Age (years)	67.4 ± 6.7	66.7 ± 6.8	68.4 ± 6.4	**0.032**
BMI (kg/m^2)	25.4 ± 3.2	25.0 ± 3.2	26.0 ± 3.2	**0.017**
Hypertension (n (%))	116 (43.0%)	72 (44.2%)	44 (41.1%)	0.706
Diabetes mellitus (n (%))	55 (20.6%)	33 (20.5%)	22 (20.8%)	0.959
Pelvic surgery history (n (%))	20 (7.4%)	13 (8.0%)	7 (6.5%)	0.813
Clinicopathological parameters				
PSA (ng/ml)	15.3 (9.0-28.7)	11.6 (7.7-21.2)	23.4 (12.3-45.6)	**<0.001**
ISUP grade of biopsy (n (%))				**<0.001**
1	58 (22.2)	40 (25.6)	18 (17.1)	

(Continued)

10.3389/fendo.2023.1270594

TABLE 1 Continued

	All subjects (n=270)	Non-NHT (n=163)	NHT (n=107)	p value
2	61 (23.4)	46 (29.5)	15 (14.3)	
3	57 (21.8)	36 (23.1)	21 (20.0)	
4	46 (17.6)	23 (14.7)	23 (21.9)	
5	39 (14.9)	11 (7.1)	28 (26.7)	
Without biopsy	9 (3.3)	7 (4.3)	2 (1.9)	
Prostate volume (ml)	35.2 (23, 46.2)	36.7 (28.2,46.9)	29.8 (21.4,45.8)	**0.041**
Interval time from puncture to LRP (days)	51.0 (36.0-105.5)	42.0 (32.0-55.3)	100.0 (52.0-178.0)	**<0.001**
ISUP after LRP (n (%))				**<0.001**
1	35 (13.0)	26 (16.0)	9 (8.4)	
2	69 (25.6)	52 (31.9)	17 (15.9)	
3	72 (26.7)	48 (29.4)	24 (22.4)	
4	22 (8.1)	10 (6.1)	12 (11.2)	
5	72 (26.7)	27 (16.6)	45 (42.1)	
Pathological stage (n (%))				0.767
T1+T2	156 (57.8)	93 (57.1)	63 (58.9)	
T3+T4	114 (42.2)	70 (42.9)	44 (41.1)	
N (n (%))				**0.036**
N0	234 (86.7)	147 (90.2)	87 (81.3)	
N1	36 (13.3)	16 (9.8)	20 (18.7)	
M (n (%))				**0.003**
M0	254 (94.1)	159 (97.5)	95 (88.8)	
M1	16 (5.9)	4 (2.5)	12 (11.2)	
PSM (n (%))	90 (33.3)	64 (39.3%)	26 (24.3)	**0.011**
PSM locations (n (%))				0.123
apex	28 (31.1)	24 (37.5)	4 (15.4)	
apex+fundus	11 (12.2)	7 (10.9)	4 (15.4)	
apex+body	8 (8.9)	8 (12.5)	0	
apex+fundus+body	5 (5.6)	3 (4.7)	2 (7.7)	
apex+fundus+vas deferens/seminal vesicles	4 (4.4)	2 (3.1)	2 (7.7)	
fundus	11 (12.2)	6 (9.4)	5 (19.2)	
fundus+body	5 (5.6)	4 (6.3)	1 (3.8)	
fundus+body+vas deferens	1 (1.1)	0	1 (3.8)	
body	15 (16.7)	9 (14.1)	6 (23.1)	
vas deferens/ seminal vesicles	2 (2.2)	1 (1.6)	1 (3.8)	
Accumulated PSM locations (n (%))				**0.048**
apex	56 (62.2)	44 (68.8)	12 (46.2)	
fundus	37 (41.1)	22 (34.4)	15 (57.7)	

(Continued)

TABLE 1 Continued

	All subjects (n=270)	Non-NHT (n=163)	NHT (n=107)	p value
body	34 (37.8)	24 (37.5)	10 (38.5)	
vas deferens/ seminal vesicles	7 (7.8)	3 (4.7)	4 (15.4)	
PNI (n (%))	180 (66.7)	105 (64.4)	75 (70.1)	0.333
LVI (n (%))	37 (13.7)	18 (11.0)	19 (17.8)	0.117

Data are expressed as n (%), mean ± SD, or median (interquartile range). The bold value indicated statistical significance. PCa, prostate cancer; LRP, laparoscopic radical prostatectomy; NHT, neoadjuvant hormonal therapy; BMI, body mass index; PSA, prostate-specific antigen; ISUP, International Society of Urological Pathology; M, metastasis; PSM, positive surgical margin; PNI, perineural invasion; LVI, lymphovascular invasion.

and the difference was significantly different (p=0.011). The apex was the most common location of PSM in non-NHT group (68.8%, 44/64), while the fundus was the most common location of PSM in NHT group (57.7%, 15/26). There were significant statistical difference in terms of age, BMI, PSA, ISUP grade of biopsy and after LRP, prostate volume, the interval between biopsy and RP, pN status, and metastasis between non-NHT and NHT groups (p=0.032, p=0.017, p<0.001, p<0.001, 0.041, p<0.001, p=0.036, p=0.003, respectively), while there were no significant difference regarding pT, PNI, and LVI between the two groups (p=0.767, 0.333, 0.117, respectively).

Relation of PSM with the clinicopathological characteristics of PCa

As shown in Table 2, the percentages of locally advanced PCa (pT3+pT4), pN (+), cases without NHT and cases with LVI were significantly higher in PSM group (n=90), when compared with non-PSM group (n=180) (p<0.001, p=0.004, p=0.012, p=0.015).

There were no significant difference in terms of age, BMI, hypertension, diabetes, history of pelvic surgery, PSA before biopsy, ISUP grade before biopsy and after LRP, prostate volume, the interval between biopsy and RP, metastasis, and PNI between non-PSM and PSM groups (all p>0.05).

Correlation of clinicopathological variables with the presence of PSM in PCa patients without NHT

We performed univariate and multivariate logistic regression analysis to evaluate the correlations of clinicopathological variables with PSM in non-NHT group. As shown in Table 3, BMI, PSA before biopsy, ISUP grade after LRP, pT, and pN were found to be significantly and positively correlated with the presence of PSM in univariate logistic regression analysis (p<0.05). In the stepwise multivariate regression analysis, we added and adjusted confounding factors including age, BMI, hypertension, diabetes, history of pelvic surgery, prostate volume, and ultimately revealed that the correlations of BMI, PSA before biopsy, ISUP grade after LRP, pT, and pN with PSM remained significant after adjustment for confounding factors (OR=1.160, 95%CI:1.034-1.301, p=0.011; OR=3.385, 95%CI:1.386-8.268, p=0.007;OR=3.541, 95%CI:1.008-12.444, p=0.049; OR=4.577, 95%CI:2.163-9.686, p<0.001; OR=3.572, 95%CI:1.124-11.347, p=0.031, respectively).

Correlation of clinicopathological variables with the presence of PSM in PCa patients with NHT

As shown in Table 4, ISUP grade of biopsy, pT, pN, and LVI were found to be significantly and positively correlated with the presence of PSM (p<0.05) in PCa patients with NHT in univariate logistic regression analysis. In the stepwise multivariate regression analysis, only pT, pN, and LVI remained significantly correlated with the presence of PSM after adjusting the mentioned confounding factors in NHT group (OR=18.434, 95%CI: 4.976-68.297, p<0.001; OR=7.181, 95%CI: 2.089-24.689, p=0.002; OR=3.545, 95%CI:1.109-11.327, p=0.033).

Discussion

LRP is the most common treatment option for localized and locally advanced PCa in China. The desirable outcomes after RP are to achieve “trifecta” including oncological outcomes, continence, and potency (19). Afterwards, some urologists presented the new concept of “pentafecta” outcomes, which includes complications and PSM on top of the traditional trifecta outcomes (20). No matter “trifecta” or “pentafecta” standard is adopted, controlling oncological outcomes is the most important task of LRP. However, PSM occurred in postoperative pathological result, which would influence the controlling of oncological outcomes and affect the prognosis unfavorably. Therefore, knowing the common location and risk factors of PSM is crucial and has great clinical value for developing the surgical strategy and guiding adjuvant therapy after LRP. Our current study firstly demonstrated the locations of PSM and investigated the correlation between clinicopathological parameters and PSM in PCa patients who underwent LRP with and without NHT, and demonstrated that BMI, PSA, ISUP grade after LRP, pT and pN were independent risk factors affecting PSM for patients without NHT, while pT, pN, and LVI were independent risk factors affecting PSM for patients with NHT. Our results have clinical

TABLE 2 Relation of PSM with the clinicopathological characteristics of PCa patients underwent LRP.

	Non-PSM (N=180)	PSM (N=90)	p value
Age (years)	67.0 ± 6.6	68.2 ± 6.8	0.180
BMI (kg/m^2)	25.3 ± 3.2	25.7 ± 3.3	0.292
Hypertension (n (%))	78 (67.2)	38 (32.8)	0.897
Diabetes mellitus (n (%))	38 (69.1)	17 (30.9)	0.872
Pelvic surgery history (n (%))	12 (60.0)	8 (40.0)	0.623
PSA (ng/ml)	14.0 (8.5-27.3)	18.1 (9.5-30.1)	0.068
PSA group (n (%))			0.181
<10ng/ml	55 (73.3)	20 (26.7)	
10-20ng/ml	50 (68.5)	23 (31.5)	
>20ng/ml	59 (60.2)	39 (39.8)	
Missing (n)	16	8	
ISUP grade of biopsy (n (%))			0.219
1	41 (70.7)	17 (29.3)	
2	46 (75.4)	15 (24.6)	
3	37 (64.9)	20 (35.1)	
4	29 (63.0)	17 (37.0)	
5	21 (53.8)	18 (46.2)	
Without biopsy	6	3	
Prostate volume (ml)	38.1 ± 19.9	39.0 ± 19.2	0.722
Interval time from puncture to LRP (days)	51.0 (36.0-117.0)	50.5 (35.5-79.3)	0.284
ISUP after LRP (n (%))			0.205
1	26 (74.3)	9 (25.7)	
2	49 (71.0)	20 (29.0)	
3	49 (68.1)	23 (31.9)	
4	16 (72.7)	6 (27.3)	
5	40 (55.6)	32 (44.4)	
Pathological stage (n (%))			**<0.001**
T1+T2	128 (82.1)	28 (17.9)	
T3+T4	52 (45.6)	62 (54.4)	
N (n (%))			**0.004**
N0	164 (70.1)	70 (29.9)	
N1	16 (44.4)	20 (55.6)	
M (n (%))			0.786
M0	170 (66.9)	84 (33.1)	
M1	10 (62.5)	6 (37.5)	
NHT (n (%))			**0.012**
Yes	81 (75.7)	26 (24.3)	
No	99 (60.7)	64 (39.3)	
PNI (n (%))			0.494
Yes	117 (65.0)	63 (35.0)	
No	63 (70.0)	27 (30.0)	
LVI (n (%))			**0.015**
Yes	18 (48.6)	19 (51.4)	
No	162 (69.5)	71 (30.5)	

Data are expressed as n (%), mean ± SD, or median (interquartile range). The bold value indicated statistical significance. PSM, positive surgical margin; PCa, prostate cancer; LRP, laparoscopic radical prostatectomy; BMI, body mass index; PSA, prostate-specific antigen; ISUP, International Society of Urological Pathology; M, metastasis; NHT, neoadjuvant hormonal therapy; PNI, perineural invasion; LVI, lymphovascular invasion.

implications for the prediction of PSM and guidance of operation especially for those receiving NHT.

At present, there were many studies reporting PSM rate globally. As summarized in Table 5 (21–29), PSM rate exceeded 25% in Chinese PCa patients, while PSM range was approximately 12-16.3% in the counterpart of other countries, the difference of which can be explained by the more advanced PCa percentages in China than other countries. The overall PSM rate was 33.3%, and PSM without NHT was 39.3% in our study, which were a little higher than those reported in some other centers in China (26–28). Tumor location within the prostate can influence the risk of PSM. In the current study, there were four locations of PSM according to the pathological report: apex, fundus, body, and vas deferens/seminal vesicles. Of the 90 cases of PSM, the apex accounted the largest proportion, the only and accumulated proportion of apex were 31.1% and 62.2%, respectively. Our results were in consistent with one study reporting that the apex accounted for 59.1% among all PSM locations after LRP (21). We summarized three reasons for the high PSM of apex: (a) The apex is deep and closely neighbored with deep dorsal vein complex, erectile nerve, and rectum, and thus relatively difficult to get exposed during operation; (b) The apex lacks of barrier of capsule, resulting in more susceptible to tumor invasion; (c) There are many variations in the shape of the urethral of apex, cutting perpendicular to urethral may increase the risks of tumor residue. Tumors located at the ventral or dorsal part of the prostate may also have different influence on PSM rate, which needs further study.

The risk factors for PSM reported by different centers were different (Table 5), and the subjects of almost all these studies analyzed were the PCa cases without NHT. As the advanced PCa accounts higher in China than the developed countries, the percentage of PCa patients receiving NHT may increase with the promotion and application of NHT. The protocol of NHT includes MAB, castration, and AAM, lasting 3-9 months before surgery. In our study, 39.6% of cases received NHT. Among the 107 patients with NHT, 82 cases accepted MAB therapy with median course of 3

TABLE 3 Logistic regression analysis for correlation of clinicopathological variables with the presence of PSM in PCa patients without NHT.

	univariate mode OR (95%CI)	p value	Multivariate mode OR (95%CI)	p value
Age	1.026 (0.978-1.076)	0.292		
BMI	1.112 (1.003-1.233)	**0.044**	1.160 (1.034-1.301)	**0.011**
Hypertension	0.876 (0.464-1.652)	0.682		
Diabetes	1.228 (0.564-2.673)	0.605		
History of pelvic surgery	0.667 (0.196-2.263)	0.516		
PSA before puncture	1.033 (1.006-1.061)	**0.017**	1.031 (1.003-1.059)	**0.028**
<10ng/ml	Reference		Reference	
10-20ng/ml	1.720 (0.751-3.940)	0.200	1.401 (0.572-3.432)	0.460
>20ng/ml	3.663 (1.563-8.587)	**0.003**	3.385 (1.386-8.268)	**0.007**
ISUP grade of biopsy				
1	Reference			
2	0.657 (0.265-1.625)	0.363		
3	1.491 (0.597-3.725)	0.392		
4	1.282 (0.451-3.641)	0.641		
5	2.000 (0.519-7.703)	0.314		
preoperative prostate volume	1.008 (0.991-1.025)	0.350		
Interval time from puncture to LRP (days)	1.002 (0.998-1.006)	0.380		
ISUP after LRP				
1	Reference		Reference	
2	1.093 (0.396-3.014)	0.864	0.966 (0.317-2.946)	0.952
3	1.750 (0.638-4.802)	0.277	1.762 (0.558-5.563)	0.334
4	0.563 (0.097-3.267)	0.521	0.236 (0.021-2.648)	0.242
5	3.273 (1.054-10.158)	**0.040**	3.541 (1.008-12.444)	**0.049**
postoperative pathological stage T	3.833 (1.975-7.440)	**<0.001**	4.577 (2.163-9.686)	**<0.001**
pathological lymph node involvement	3.902 (1.287-11.833)	**0.016**	3.572 (1.124-11.347)	**0.031**
M	4.820 (0.490-47.387)	0.177		
PNI	1.222 (0.630-2.369)	0.533		
LVI	2.728 (0.997-7.460)	0.051	2.803 (0.961-8.175)	0.059

Univariate and multivariate logistic regression analysis were performed. The multivariate model was adjusted for age, BMI, hypertension, diabetes, history of pelvic surgery, prostate volume. The bold value indicated statistical significance. The dependent variable was PSM of PCa. PSM, positive surgical margin; PCa, prostate cancer; NHT, neoadjuvant hormonal therapy; BMI, body mass index; PSA, prostate-specific antigen; ISUP, International Society of Urological Pathology; LRP, laparoscopic radical prostatectomy; M, metastasis; PNI, perineural invasion; LVI, lymphovascular invasion.

months; 3 cases accepted castration therapy with median course of 3 months; 22 cases accepted AAM with median course of 1 month. The protocol and duration of NHT were influenced by many factors such as doctor's suggestion, economic status of the family, and psychological demands of the patient.

Our study demonstrated that BMI, PSA, ISUP grade after LRP, pT and pN were independent risk factors affecting PSM for patients without NHT. Of note, BMI can reflect the infiltration of pelvic fat. For obese patients, pelvic fat can increase the difficulty of separation due to adhesion and increase the risk of PSM. However, the influence was relatively little with only OR value of 1.16. Previously conducted studies did not find BMI was an independent risk factor for PSM (21, 23, 24, 26–29). Therefore, the influence of BMI on PSM may be negligible. In addition to BMI, certain patient factors including history of pelvic surgery, and anatomical variations can impact the risk of PSM. However, in our study, we find that the correlation of pelvic surgery history with PSM was insignificant after adjustment for confounding factors, which could be explained by the small sample of cases with previous surgeries in the pelvic area. Secin FP, et al. (21) reported that preoperative PSA was an independent risk factor for PSM (OR=1.15, 1.04-1.28,p<0.01). Jason P. Izard, et al. (30) also

TABLE 4 Logistic regression analysis for correlation of clinicopathological variables with the presence of PSM in PCa patients with NHT.

	univariate mode	p value	Multivariate mode	p value
	OR (95%CI)		OR (95%CI)	
Age	1.057 (0.981-1.137)	0.144		
BMI	0.974 (0.846-1.121)	0.713		
Hypertension	1.067 (0.436-2.612)	0.888		
Diabetes	0.445 (0.120-1.651)	0.226		
History of pelvic surgery	4.727 (0.984-22.721)	0.052		
PSA before puncture	1.003 (0.993-1.012)	0.599		
<10ng/ml	Reference			
10-20ng/ml	0.600 (0.143-2.511)	0.484		
>20ng/ml	0.937 (0.284-3.087)	0.914		
ISUP grade of biopsy				
1	Reference		Reference	
2	1.231 (0.152-9.972)	0.846	1.205 (0.133-10.909)	0.868
3	1.333 (0.197-9.020)	0.768	1.288 (0.173-9.609)	0.805
4	3.500 (0.628-19.496)	0.153	3.627 (0.573-22.950)	0.171
5	6.000 (1.153-31.228)	**0.033**	5.718 (0.997-32.801)	0.050
preoperative prostate volume	0.988 (0.965-1.013)	0.346		
Interval time from puncture to LRP (days)	1.000 (1.000-1.001)	0.347		
ISUP after LRP				
1	Reference			
2	1.714 (0.152-19.359)	0.663		
3	0.727 (0.058-9.159)	0.805		
4	4.000 (0.363-44.113)	0.258		
5	4.414 (0.506-38.526)	0.179		
postoperative pathological stage T	14.75 (4.567-47.642)	**<0.001**	18.434 (4.976-68.297)	**<0.001**
pathological lymph node involvement	3.369 (1.205-9.418)	**0.021**	7.181 (2.089-24.689)	**0.002**
M	1.043 (0.260-4.183)	0.952		
PNI	1.576 (0.566-4.390)	0.384		
LVI	2.828 (0.992-8.064)	**0.052**	3.545 (1.109-11.327)	**0.033**

Univariate and multivariate logistic regression analysis were performed. The multivariate model was adjusted for age, BMI, hypertension, diabetes, history of pelvic surgery, prostate volume. The bold value indicated statistical significance. The dependent variable was PSM of PCa. PSM, positive surgical margin; PCa, prostate cancer; NHT, neoadjuvant hormonal therapy; BMI, body mass index; PSA, prostate-specific antigen; ISUP, International Society of Urological Pathology; LRP, laparoscopic radical prostatectomy; M, metastasis; PNI, perineural invasion; LVI, lymphovascular invasion.

reported that PSA was an independent risk factor for PSM, and the PSM rate of PCa patients with PSA<4.0, 4-9.9, and>10 ng/ml was 12%, 20%, and 28%, respectively. In line with these reports, our analysis showed that the OR of PSM for those with PSA>20ng/ml was 3.385. PSA was secreted by prostatic epithelial cells, and PSA elevation indicates that the highly aggressive PCa cells damage the tissue barrier, increasing the risk of PSM. Our result demonstrated that the OR of postoperative ISUP grade 5 for PSM was 3.54, which was consistent with the conclusions reached by Secin FP (21), Yang Rong (26), and Jason P. Izard (30). It is noteworthy that ISUP grade after LRP is generally higher than the biopsy ISUP grade for the same case, and could more objectively reflect the tumor grade. In our study, pT was an independent factor for PSM in non-NHT patients with the highest OR value among all risk factors (OR=4.577), which was partly in consistent with the studies (23, 27, 29) reporting pT was the only independent factor for PSM in PCa patients without NHT. We divided pT into localized (T1+T2) and locally advanced (T3+T4) stage, as advanced PCa break through the capsule or invade the neighbor tissues, therefore the PSM rate was higher in T3+T4 groups. Besides, we revealed that pN was also an independent risk factor for PSM in non-NHT patients, we believed that local lymph node involvement indicate the high

TABLE 5 Summary of literature reporting PSM rate and related independent risk factors for PSM in PCa patients underwent LRP.

Literature	Total cases (n)	PSM rate	Independent risk factors
Secin FP (21), 2007	407	12%	PSA, Gleason score, low volume, interfascial pathway
Sooriakumaran P (22), 2014	4918	16.3%	/
Yao Zhu (23), 2015	94	17%	pT
Wei Song (24), 2015	61	19.7%	TNM stage after puncture, PSA, positive percentage of the needle biopsy.
Louie-Johnsun MW (25), 2016	2943	15.9% (T2:9.8%; T3a:30.8%; T3b:39.2%)	/
Rong Yang (26), 2017	296	29.1%	Gleason score, PNI, number of positive cores in the biopsy specimen, and low prostate volume.
Zheng Zhang (27), 2019	177	32.2%	pT
Xiaojun Tian (28), 2019	418	34%	the percentage of positive cores in preoperative biopsy, clinical stage, f/t PSA, and age.
Pingxin Zhang (29), 2020	99	26.3%	pT
The current study, 2023	270	33.3%	
Without NHT	163	39.3%	BMI, PSA before needle biopsy, postoperative ISUP grade, pT and pN
With NHT	107	24.3%	pT, pN, and LVI

PSM, positive surgical margin; PCa, prostate cancer; LRP, laparoscopic radical prostatectomy; PSA, prostate-specific antigen; pT, pathological stage T; PNI, perineural invasion; f/t,free/total; NHT, neoadjuvant hormonal therapy; BMI, body mass index; ISUP, International Society of Urological Pathology; pN, pathological lymph node involvement; LVI, lymphovascular invasion. /, not reported.

aggressiveness of local tumor. It is challenging for surgeons to completely remove large and aggressive tumors while preserving negative surgical margins. Collectively, compared with previous studies (21–30), there exist differences and similarities regarding the risk factors for PSM in PCa cases without NHT in our study, which could be explained by the sample size, the surgeon experience and technique, and other factors.

Next, let's focus on those PCa patients with NHT. Naiki, et al. (31) reported that PSM rate was 27.8% (20/72) in PCa patients with NHT, which was consistent with our result demonstrating PSM rate was 24.3% in NHT groups. At present, it is generally recognized that NHT can reduce prostate volumes and stages, decrease PSA levels and PSM rate, but can't improve the long-term survival. The seemingly contradictory conclusion could be explained as follows: NHT could improve the local control of tumor, but could not eradicate the micrometastases (32). However, from another perspective, as NHT can reduce PSM rate, and PSM rate was closely correlated with biochemical recurrence and prognosis, NHT is inferred to improve prognosis. Therefore, the exact relationships among NHT, PSM and prognosis need further exploration.

In the current study, compared with non-NHT patients, the NHT counterparts were older and with higher BMI and ISUP grade before biopsy. In other words, the baseline parameters of the two groups were significantly different, which was the reason why we did not observe the decreasing effect of NHT on postoperative stage. Our research firstly demonstrated that pT, pN and LVI were independent risk factors for PSM in patients treated with NHT before LRP. Generally speaking, the frequency of pT, pN, and LVI would decrease after NHT, however, if one of these parameters was still positive after NHT, then the local invasion was supposed to be severe and increase the PSM rate.

It is noteworthy that the fundus rather than apex was the most common location for NHT patients, which was different from non-NHT patients. The could be explained as follows: on one hand, NHT reduced prostate volume, and thus made apex exposed more clearly during operation, helping to avoid PSM of apex; on the other hand, NHT could cause evident adhesion between prostate fundus and bladder neck, making the boundary difficult to distinguish and causing PSM. The cases in our study were all performed in extraperitoneal approach, and thus eliminated the bias caused by different surgery approaches.

Some studies reported that low prostate volume was an independent risk factor for PSM (21, 26), which was not observed in our study. Some researcher (27) believed that the smaller the prostate is, the larger the ratio between the tumor and the prostate, and the easier the tumor exceed the limited range of pathological staging and cause PSM. On the other hand, the smaller the prostate is, the wider the operation space, reducing the difficulty of surgery and risk of PSM. Therefore, we considered that the combined effect of the two factors is the reason why the low prostate volume was not the independent factor of PSM in our study. Moreover, the technique of surgeons was closely related to PSM, all LRP were performed by the same surgeon, who has proficient laparoscopic operation skills. The degree of neurovascular bundle (NVB) dissection was determined by the operating surgeon on the basis of the plane where the dissection took place. There are three degrees of NVB dissection: intrafascial (complete NVB sparing), interfascial (partial NVB sparing), and extrafascial (complete/almost complete NVB resection). Generally, in the current study, the surgeon preferred to spare NVB for the localized low to intermediate-risk cases, and do not spare NVB for the cases with extracapsular extension. In this way, we maximally reduced the bias caused by operation skills in our study.

The present study might have two potential clinical implications. First, urologists should dissect the urethral of the prostatic apex more carefully when performing LRP on PCa patients without NHT, and tackle the bladder neck more carefully when performing LRP on cases with NHT, respectively, to avoid PSM incidence as much as possible; second, preoperative BMI, PSA, biopsy grade, and stage could be used to predict the PSM of postoperative specimen and to estimate the prognosis, and the influencing factors should be considered by laparoscopic surgeons when planning the operation to decrease the incidence of PSMs.

Conclusions

In conclusion, our study first demonstrated that PSM rate was 24.3% and the fundus was the most common location of PSM in Chinese patients with NHT. The pT, pN, and LVI were independent factors affecting the PSM for Chinese patients with NHT. By comparison, PSM rate was 39.3% and the apex was the most common location of PSM in Chinese patients without NHT. BMI, PSA before needle biopsy, postoperative ISUP grade, pT and pN were independent factors affecting the PSM for patients without NHT. Our results provide reliable clinical implications for guidance of LRP and prediction of PSM especially for those PCa patients receiving NHT. For example, surgeons should pay more attention to the resection extent when tackling the boundary of prostate fundus and bladder neck in PCa patients with NHT, and use preoperative clinicopathological parameters to predict the PSM risks. The limitation of our study was that there might exist selection bias because the data analyzed in the study were derived from a single center, and studies from different hospitals are needed for validation of our results.

Data availability statement

The raw data supporting the conclusions of this article will be made available by the authors, without undue reservation.

Ethics statement

The studies involving humans were approved by Ethical committee of National Cancer Center. The studies were conducted in accordance with the local legislation and institutional requirements. The participants provided their written informed consent to participate in this study. Written informed consent was obtained from the individual(s) for the publication of any potentially identifiable images or data included in this article.

Author contributions

FW: Conceptualization, Data curation, Formal Analysis, Funding acquisition, Investigation, Methodology, Software, Validation, Visualization, Writing – original draft, Writing – review & editing. GZ: Writing – review & editing, Methodology, Validation, Investigation, Resources, Software. YT: Writing – review & editing, Methodology, Formal analysis, Resources, Software. YW: Investigation, Writing – original draft, Writing – review & editing. JL: Conceptualization, Formal Analysis, Methodology, Project administration, Supervision, Writing – review & editing. NX: Conceptualization, Funding acquisition, Project administration, Resources, Supervision, Writing – review & editing.

Funding

The authors declare financial support was received for the research, authorship, and/or publication of this article. This work was supported by grants from National Key R&D Program of China (Grant No.2022YFE0200800) awarded to NX, Research Fund for Tumors of Urinary System treatment in China (Grant No. 020) awarded to FW.

Conflict of interest

The authors declare that the research was conducted in the absence of any commercial or financial relationships that could be construed as a potential conflict of interest.

Publisher's note

References

1. Gandaglia G, Leni R, Bray F, Fleshner N, Freedland SJ, Kibel A, et al. Epidemiology and prevention of prostate cancer. *Eur Urol Oncol* (2021) 4(6):877–92. doi: 10.1016/j.euo.2021.09.006

2. Di Minno A, Aveta A, Gelzo M, Tripodi L, Pandolfo SD, Crocetto F, et al. 8-hydroxy-2-deoxyguanosine and 8-iso-prostaglandin F2α: putative biomarkers to assess oxidative stress damage following robot-assisted radical prostatectomy (RARP). *J Clin Med* (2022) 11(20):6102. doi: 10.3390/jcm11206102

3. Aveta A, Cilio S, Contieri R, Spena G, Napolitano L, Manfredi C, et al. Urinary microRNAs as biomarkers of urological cancers: A systematic review. *Int J Mol Sci* (2023) 24(13):10846. doi: 10.3390/ijms241310846

4. Rebello RJ, Oing C, Knudsen KE, Loeb S, Johnson DC, Reiter RE, et al. Prostate cancer. *Nat Rev Dis Primers* (2021) 7(1):9. doi: 10.1038/s41572-020-00243-0

5. Costello AJ. Considering the role of radical prostatectomy in 21st century prostate cancer care. *Nat Rev Urol* (2020) 17(3):177–88. doi: 10.1038/s41585-020-0287-y

6. Montironi R, van der Kwast T, Boccon-Gibod L, Bono AV, Boccon-Gibod L. Handling and pathology reporting of radical prostatectomy specimens. *Eur Urol* (2003) 44(6):626–36. doi: 10.1016/S0302-2838(03)00381-6

7. Thompson I, Thrasher JB, Aus G, Burnett AL, Canby-Hagino ED, Cookson MS, et al. Guideline for the management of clinically localized prostate cancer:2007 update. *J Urol* (2007) 177(6):2106–31. doi: 10.1016/j.juro.2007.03.003

8. Swindle P, Eastham JA, Ohori M, Kattan MW, Wheeler T, Maru N, et al. Do margins matter? The prognostic significance of positive surgical margins in radical prostatectomy specimens. *J Urol* (2005) 174(3):903–7. doi: 10.1097/01.ju.0000169475.00949.78

9. Pfitzenmaier J, Pahernik S, Tremmel T, Haferkamp A, Buse S, Hohenfellner M. Positive surgical margins after radical prostatectomy:do they have an impact on biochemical or clinical progression? *BJU Int* (2008) 102:1413–8. doi: 10.1111/j.1464-410X.2008.07791.x

10. Sachdeva A, Veeratterapillay R, Voysey A, Kelly K, Johnson MI, Aning J, et al. Positive surgical margins and biochemical recurrence following minimally-invasive

radical prostatectomy – an analysis of outcomes from a UK tertiary referral centre. *BMC Urol* (2017) 17:91. doi: 10.1186/s12894-017-0262-y

11. Chapin BF, Nguyen JN, Achim MF, Navai N, Williams SB, Prokhorova IN, et al. Positive margin length and highest Gleason grade of tumor at the margin predict for biochemical recurrence after radical prostatectomy in patients with organ-confined prostate cancer. *Prostate Cancer Prostatic Dis* (2018) 21:221–7. doi: 10.1038/s41391-017-0019-4

12. Hong YM, Hu JC, Paciorek AT, Knight SJ, Carroll PR. Impact of radical prostatectomy positive surgical margins on fear of cancer recurrence: results from CaPSURE. *Urol Oncol* (2010) 28:268–73. doi: 10.1016/j.urolonc.2008.07.004

13. Bolla M, van Poppel H, Tombal B, Vekemans K, Da Pozzo L, de Reijke TM, et al. Postoperative radiotherapy after radical prostatectomy for high-risk prostate cancer: long-term results of a randomised controlled trial (EORTC trial 22911). *Lancet* (2012) 380:2018–27. doi: 10.1016/S0140-6736(12)61253-7

14. Meeks JJ, Eastham JA. Radical prostatectomy: positive surgical margins matter. *Urol Oncol* (2013) 31(7):974–9. doi: 10.1016/j.urolonc.2011.12.011

15. Epstein JI, Egevad L, Amin MB, Delahunt B, Srigley JR, Humphrey PA, et al. The 2014 international society of urological pathology (ISUP) consensus conference on gleason grading of prostatic carcinoma: definition of grading patterns and proposal for a new grading system. *Am J Surg Pathol* (2016) 40(2):244–52. doi: 10.1097/PAS.0000000000000530

16. Buyyounouski MK, Choyke PL, McKenney JK, Sartor O, Sandler HM, Amin MB, et al. Prostate cancer - major changes in the American joint committee on cancer eighth edition cancer staging manual. *CA Cancer J Clin* (2017) 67(3):245–53. doi: 10.3322/caac.21391

17. Epstein JI, Amin M, Boccon-Gibod L, Egevad L, Humphrey PA, Mikuz G, et al. Prognostic factors and reporting of prostate carcinoma in radical prostatectomy and pelvic lymphadenectomy specimens. *Scand J Urol Nephrol Suppl* (2005) 216:34. doi: 10.1080/03008880510030932

18. Liebig C, Ayala G, Wilks JA, Berger DH, Albo D. Perineural invasion in cancer: A review of the literature. *Cancer* (2009) 115(15):3379–91. doi: 10.1002/cncr.24396

19. Patel VR, Coelho RF, Chauhan S, Orvieto MA, Palmer KJ, Rocco B, et al. Continence,potency and oncological outcomes after robotic-assisted radical prostatectomy: early trifecta results of a high-volume surgeon. *BJU Int* (2010) 106 (5):696–702. doi: 10.1111/j.1464-410X.2010.09541.x

20. Patel VR, Sivaraman A, Coelho RF, Chauhan S, Palmer KJ, Orvieto MA, et al. Pentafecta: a new concept for reporting outcomes of robot-assisted laparoscopic radical prostatectomy. *Eur Urol* (2011) 59(5):702–7. doi: 10.1016/j.eururo.2011.01.032

21. Secin FP, Serio A, Bianco FJ Jr, Karanikolas NT, Kuroiwa K, Vickers A, et al. Preoperative and intraoperative risk factors for side-specific positive surgical margins in laparoscopic radical prostatectomy for prostate cancer. *Eur Urol* (2007) 51(3):764–71. doi: 10.1016/j.eururo.2006.10.058

22. Sooriakumaran P, Srivastava A, Shariat SF, Stricker PD, Ahlering T, Eden CG, et al. A multinational, multi-institutional study comparing positive surgical margin rates among 22393 open, laparoscopic, and robot-assisted radical prostatectomy patients. *Eur Urol* (2014) 66(3):450–6. doi: 10.1016/j.eururo.2013.11.018

23. Zhu Y, Han C, Yang X, Dai B, Zhang H, Shi G, et al. Status of surgical margin: laparoscopic versus open radical prostatectomy. *J Mod Urol* (2015) 4):234–6.

24. Song W, Zhao Y, Jin X, Wang M, Zhang H. Study on factors of positive margins after transpepitoneal laparoscopic radical prostatectomy. *J Urol Clinician (Electronic Version)* (2015) 7(4):24–26.

25. Louie-Johnsun MW, Handmer MM, Calopedos RJ, Chabert C, Cohen RJ, Gianduzzo TR, et al. The Australian laparoscopic non robotic radical prostatectomy experience - analysis of 2943 cases (USANZ supplement). *BJU Int* (2016) 118 Suppl 3:43–8. doi: 10.1111/bju.13610

26. Yang R, Cao K, Han T, Zhang YF, Zhang GT, Xu LF, et al. Perineural invasion status, Gleason score and number of positive cores in biopsy pathology are predictors of positive surgical margin following laparoscopic radical prostatectomy. *Asian J Androl* (2017) 19(4):468–72. doi: 10.4103/1008-682X.173444

27. Zhang Z, Zhang K, Hong B, Zhang J, Zhou B, Gong K, et al. Risk factors for positive surgical margin after laparoscopic radical prostatectomy. *Chin J Clin Oncol* (2019) 46(06):39–42.

28. Tian XJ, Wang ZL, Li G, Cao SJ, Cui HR, Li ZH, et al. Development and validation of a preoperative nomogram for predicting positive surgical margins after laparoscopic radical prostatectomy. *Chin Med J* (2019) 132:928–34. doi: 10.1097/CM9.0000000000000161

29. Zhang P, Wang W, Ma J, Li X, Rexiati M, Wang Y, et al. Influencing factors of positive surgical margin after extraperitoneal laparoscopic radical prostatectomy. *J Mod Urol* (2020) 025(003):247–51.

30. Richters A, Derks J, Fossion LM, Kil PJ, Verhoeven RH, Aarts MJ, et al. Presence and number of positive surgical margins after radical prostatectomy for prostate cancer: effect on oncological outcome in a population-based cohort. *Urol Int* (2015) 95(4):472–7. doi: 10.1159/000441012

31. Naiki T, Kawai N, Okamura T, Nagata D, Kojima Y, Akita H, et al. Neoadjuvant hormonal therapy is a feasible option in laparoscopic radical prostatectomy. *BMC Urol* (2012) 12:36. doi: 10.1186/1471-2490-12-36

32. Wang J, Xue W. The progress of neoadjuvant therapy in prostate cancer. *Chin J Urol* (2020) 41(06):477–80.

frontiers | Frontiers in Endocrinology

TYPE Original Research
PUBLISHED 02 February 2024
DOI 10.3389/fendo.2024.1333284

OPEN ACCESS

EDITED BY
Anna Perri,
Magna Græcia University of Catanzaro, Italy

REVIEWED BY
Anna Kotulak-Chrząszcz,
Medical University of Gdansk, Poland
Chris Arnatt,
Saint Louis University, United States

*CORRESPONDENCE
Adrián Ramírez-de-Arellano
adrian.ramirez@academicos.udg.mx

RECEIVED 05 November 2023
ACCEPTED 11 January 2024
PUBLISHED 02 February 2024

CITATION
Rico-Fuentes C, López-Pulido EI, Pérez-Guerrero EE, Godínez-Rubí M, Villegas-Pineda JC, Villanueva-Pérez MA, Sierra-Díaz E, Zepeda-Nuño JS, Pereira-Suárez AL and Ramírez-de-Arellano A (2024) Positive correlation between the nuclear expression of GPER and pGLI3 in prostate cancer tissues from patients with different Gleason scores. *Front. Endocrinol.* 15:1333284. doi: 10.3389/fendo.2024.1333284

Positive correlation between the nuclear expression of GPER and pGLI3 in prostate cancer tissues from patients with different Gleason scores

Cecilia Rico-Fuentes[1,2], Edgar Iván López-Pulido[1], Edsaúl Emilio Pérez-Guerrero[2], Marisol Godínez-Rubí[3,4], Julio César Villegas-Pineda[2,5], Martha Arisbeth Villanueva-Pérez[6], Erick Sierra-Díaz[7], José Sergio Zepeda-Nuño[3], Ana Laura Pereira-Suárez[2,3] and Adrián Ramírez-de-Arellano[2*]

[1]Doctorado en Biociencias, Centro Universitario de los Altos, Universidad de Guadalajara, Tepatitlán de Morelos, Jalisco, Mexico, [2]Instituto de Investigación en Ciencias Biomédicas, Centro Universitario de Ciencias de la Salud, Universidad de Guadalajara, Guadalajara, Jalisco, Mexico, [3]Laboratorio de Patología Diagnóstica e Inmunohistoquimica, Centro de Investigación y Diagnóstico en Patología, Departamento de Microbiología y Patologia, Universidad de Guadalajara, Guadalajara, Jalisco, Mexico, [4]Departamento de Morfología, Centro Universitario de Ciencias de la Salud, Universidad de Guadalajara, Guadalajara, Jalisco, Mexico, [5]Departamento de Microbiología y Patología, Centro Universitario de Ciencias de la Salud, Universidad de Guadalajara, Guadalajara, Jalisco, Mexico, [6]Patología y Nefropatología, Centro de Diagnóstico e Investigación, Guadalajara, Jalisco, Mexico, [7]Departamento de Salud Pública, Centro Universitario de Ciencias de la Salud, División de Epidemiología, Unidad Médica de Alta Especialidad, Hospital de Especialidades, Centro Médico Nacional de Occidente, Universidad de Guadalajara, Guadalajara, Jalisco, Mexico

Prostate cancer (PCa) is the most prevalent cause of death in the male population worldwide. The G Protein-Coupled Estrogen Receptor (GPER) has been gaining relevance in the development of PCa. Hedgehog (Hh) pathway activation is associated with aggressiveness, metastasis, and relapse in PCa patients. To date, no studies have evaluated the crosstalk between the GPER and the Hh pathway along different group grades in PCa. We conducted an analysis of paraffin-embedded tissues derived from patients with different prognostic grade of PCa using immunohistochemistry. Expression and correlation between GPER and glioma associated oncogene homologue (GLI) transcriptional factors in the parenchyma and stroma of PCa tumors were evaluated. Our results indicate that GPER is highly expressed in the nucleus and increases with higher grade groups. Additionally, GPER's expression correlates with pGLI3 nuclear expression across different grade groups in PCa tissues; however, whether the receptor induces the activation of GLI transcriptional factors, or the latter modulate the expression of GPER is yet to be discovered, as well as the functional consequence of this correlation.

KEYWORDS

prostate cancer, GPER, GLI1, GLI3, hedgehog, prognostic categories

1 Introduction

Prostate cancer (PCa) is the most common non-skin malignancy in men and the fifth leading cause of cancer-related mortality worldwide (1). Even though the current treatments are effective, the molecular mechanisms related to metastasis, relapse, and treatment resistance are not fully understood. Elucidating these mechanisms would improve treatments and increase the therapeutic successes among PCa patients. For this reason, it is essential to focus on the molecules associated with this disease and the signaling pathways activated by them. Estrogens are critical hormones that regulate the development of hormone-sensitive tumors and growth disorders (2).

One of the hormonal receptors involved in PCa progression is the G protein-coupled estrogen receptor (GPER), an estradiol-activated receptor which has recently gained relevance in carcinogenesis because it promotes cell migration and invasion (3). Its role in cancer is still controversial; according to some authors GPER is protumoral (4), while others propose it as antitumoral (5), this suggests that the microenvironment might determine the effects and outcome of GPER functions. Indeed, this receptor acts through non-genomic signaling pathways related to cancer, such as mitogen-activated protein kinase (MAPK) (6), phosphoinositide 3-kinase (PI3K)/AKT (7), and hedgehog (Hh) pathway (8) in a cell-dependent manner.

Hh pathway is involved in wound healing, tissue regeneration and cell homeostasis maintenance in adults, its dysregulation is associated with cancer (9–11). Recently, a possible correlation has been suggested between high GPER expression and its overactivation of Hh signals increasing invasiveness and metastatic potential in triple-negative breast cancer (12); however, in PCa disease it has not been elucidated yet. These alterations are mainly mediated by glioma-associated oncogene homologue (GLI) transcriptional factors, which can be activated in a canonical (10) or non-canonical manner (9). GLI1 is a strong activator, whereas GLI3 has an activator/repressor domain, allowing it to act depending on the cellular context (13). Crosstalk with other pathways such as MAPK and PI3K can also activate GLI factors in a non-canonical manner (14). Therefore, GPER and activation of GLI factors probably contribute to the progression of PCa.

Amongst the GLI factors family, GLI1 and GLI3 are essential in various malignancies because they modulate cell self-renewal (15). GLI1 is involved metastatic and hormone refractory PCa (16) whilst GLI3 can either directly activate or repress target genes, including *Ptch*, *Cyclin D*, and *GLI1* (17) and its hyperactivation promotes growth and migration under depletion of androgens (18). Because the regulated expression of GLI1 and GLI3 is such a fundamental process and since dysregulation of such factors by GPER can contribute to the development and progression of PCa, it is necessary to focus on the underlying carcinogenic processes.

GLI factors are susceptible to posttranslational modifications such as phosphorylation, a phenomenon that modulates many intracellular pathways usually through crosstalk between GPER and EGFR (19). This variation between total and phosphorylated molecules leads to the upregulation of transcription genes involved in cancer invasiveness (20). However, this regulation has yet to be fully understood in PCa disease. The latter highlights the relevance to understand the phosphorylation status of GLI factors in the context of PCa.

Currently, there is a lack of information regarding the regulation that GPER exerts over GLI transcriptional factors in the context of cancer. A report suggests that an increase expression of GPER correlates with decreased nuclear GLI1 expression and unfavorable prognosis in breast cancer (21). To date, there is no evidence for a possible regulation of GLI3 by GPER. Thus, further research on the interaction between GPER and GLI transcriptional factors is needed to fully understand the mechanism involved.

Therefore, this work aimed to evaluate whether the expression of GPER in parenchyma and stromal tumor cells of PCa samples is associated with the expression and phosphorylation of GLI transcriptional factors; as well as to analyze if the expression of such factors changes according to the prognostic categories (grade groups).

2 Materials and methods

2.1 Tissue samples

We studied paraffin-embedded tissues derived from patients with different prognostic grade of PCa and that had been examined and archived at the Pathology and Nephropathology, Diagnosis and Research Center. Upon verification of the diagnosis and prognostics categories (group grades), the samples were transported to our laboratory and classified in four grade groups labelled 2,3,4, and 5 as follows: GS 7 (3 + 4) (N=9), GS 7 (4 + 3) (N=18), GS 8 (4 + 4) (N=11) and GS 9 (4 + 5) (N=15). Immunohistochemistry was performed at the Diagnostic Pathology and Immunohistochemistry laboratory at the University of Guadalajara, Mexico.

2.2 Automated immunohistochemistry

Formalin-fixed paraffin-embedded blocks of tissue samples were cut into 5μm sections, which were then immunostained with an automated BOND equipment (Leica Biosystems). A rabbit polyclonal primary antibody against GPER from Abcam (Cat. ab41565, Cambridge, UK) was used at a 1:200 dilution, followed by 15 minutes of incubation with EDTA buffer. GLI1 and pGLI1 from Santa Cruz (Cat.sc515781) and Biorbyt (Cat.orb503729), respectively, were used at a 1:100 dilution, followed by an incubation step with EDTA buffer for 15 minutes for GLI and 30 minutes for pGLI1. Finally, GLI3 from Santa Cruz (Cat.sc74478) and pGLI3 from Affinity Biosciences (Cat. AF7449) were used at a 1:100 dilution with 30 minutes of incubation with EDTA buffer and 30 minutes of incubation with citrate buffer, respectively. Diamond diluent from Cell Marque™ Tissue Diagnostics (Cat. 938B-05) and a DAB kit from Leica Biosystems, (Cat. DS9800) were used as antibody buffer and for detection, respectively.

The immunohistochemical analysis was performed with and Axioskop 2 plus light microscope (Carl Zeiss, Germany) coupled to a digital camera Coolsnap (Photometrics, Tucson, USA). Images were documented with Aperio LV1 scanner by Leica Biosystems and the percentage of cell positive analysis was made using Qupath version 0.2.3 software with an image type of brightfield (H-DAB). The analyses focused onto the nuclear and cytoplasmic staining and

were performed using cell analysis and positive cell detection with 40x magnification. Measurements were made in parenchyma and stroma of tumor tissues.

The images were analyzed in brightfield (H-DAB) using the Qupath version 0.2.3 software. Initially, the image was adjusted to a scale bar of 80µm or 40X magnification, then the tissue grid was displayed and the area of interest was selected. After that, measure is proceeded by the next sequence: analyze/cell detection/positive cell detection. At this point, intensity threshold parameters are showed and allows you to evaluate different cell compartment with +1, +2 and +3 intensities. The data is provided by the program and recorded in an excel file for analyzed it in a statistical package.

2.3 Statistical analysis

We used the R version 4.1.2. software (22). Comparison of percentage of positive cells between prognostic categories and nuclear or cytoplasmatic expression were performed with two-way ANOVA followed by Bonferroni correction as a *post hoc*. Differences were considered significant at p-value < 0.05.

3 Results

3.1 GPER´s expression increases in higher grade groups in prostate tissue samples

The expression of GPER was observed in tumoral and stromal prostate tissues, and its location in both cases predominated in the nucleus; however, it was also evidenced to a lesser extent in the cytoplasm (Figures 1A, C). In PCa tissues, the nuclear expression increased from grade groups 2 to 3 (p<0.05) and remained high in grade groups 4 and 5 samples. Likewise, GPER´s cytoplasmic expression increased significantly from grade groups 2 to 5 (p<0.001) and from grade groups 4 to 5 (p<0.01) in tumoral tissue (Figure 1B). In the stromal tissue, the nuclear expression in all our groups was observed and it did not change significantly throughout the different grade groups (Figure 1C); however, the cytoplasmic expression decreased considerable from grade groups 3 to 4 (p<0.001) while it increased from grade groups 4 to 5 (p<0.01) (Figure 1D).

3.2 GLI1 and pGLI1 expression predominates regardless of grades groups

GLI1 and pGLI1 were expressed in the nucleus and cytoplasm in both prostate tumor and stromal tissue (Figure 2). GLI1 was mainly expressed in the cytoplasm of tumoral cells, significant differences were found between grade 2 vs 5 in nuclei and cytoplasm of (p<0.05) and p<0.01) respectively (Figures 2A, B). In stromal tissue, GLI1 was expressed in both cellular compartments with no significant changes along the different groups (Figures 2C, D).

In the case of pGLI1 expression did not follow a pattern either across the grade groups or across tissue type or cellular localization. In tumoral tissues, pGLI1 was mainly expressed in grade groups 3 and 5 in both nucleus and cytoplasm; however, in grade groups 4 its expression was almost null and differed significantly when compared with grade groups 3 and 5 (p<0.0001 and p<0.001) respectively (Figures 2E, F). In stromal tissue, pGLI1 was mainly expressed in the nucleus of Gleason score 3 patients. Significant differences were found between grade groups 2 vs 3 (p<0.01) and 3 vs 4 (p<0.01) in the nuclear expression of pGLI1. No significative changes were observed in the pGLI1´s cytoplasmic expression in the tumoral tissue (Figures 2G, H).

3.3 High nuclear expression in pGLI3 as grade group increase in prostate tumor tissues

In contrast to the other transcription factors, GLI3 and pGLI3 were lightly observed in the tumoral and stromal tissues (Figure 3).

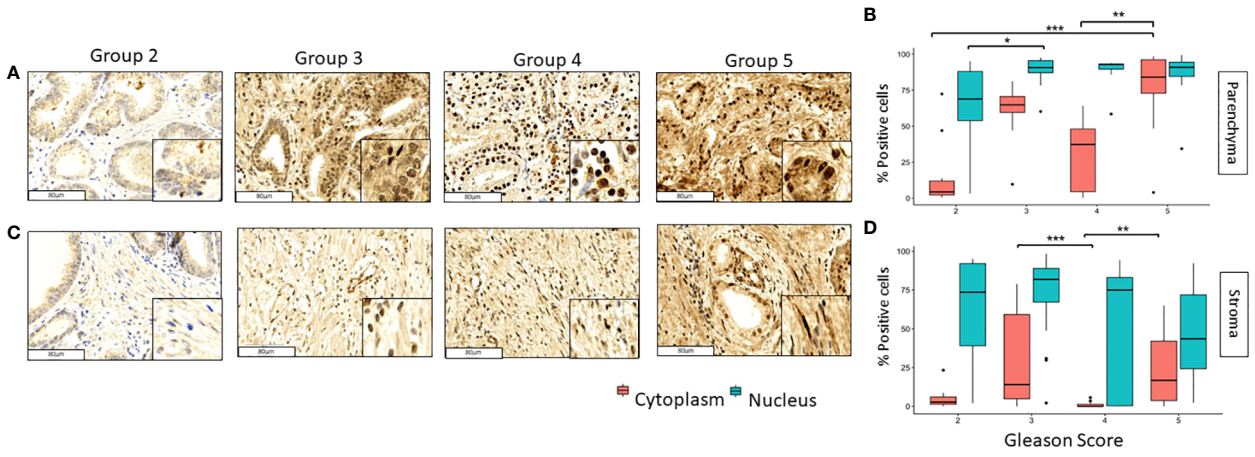

FIGURE 1
Expression of GPER in tumoral and stromal prostate tissue in different grade groups. Representative images of GPER in the parenchyma **(A, B)** and stromal **(C, D)** PCa tumor tissues by immunohistochemistry with HE staining (x200). Scale bar 80 µm. *=p<0.05, **=p<0.01, ***=p<0.001.

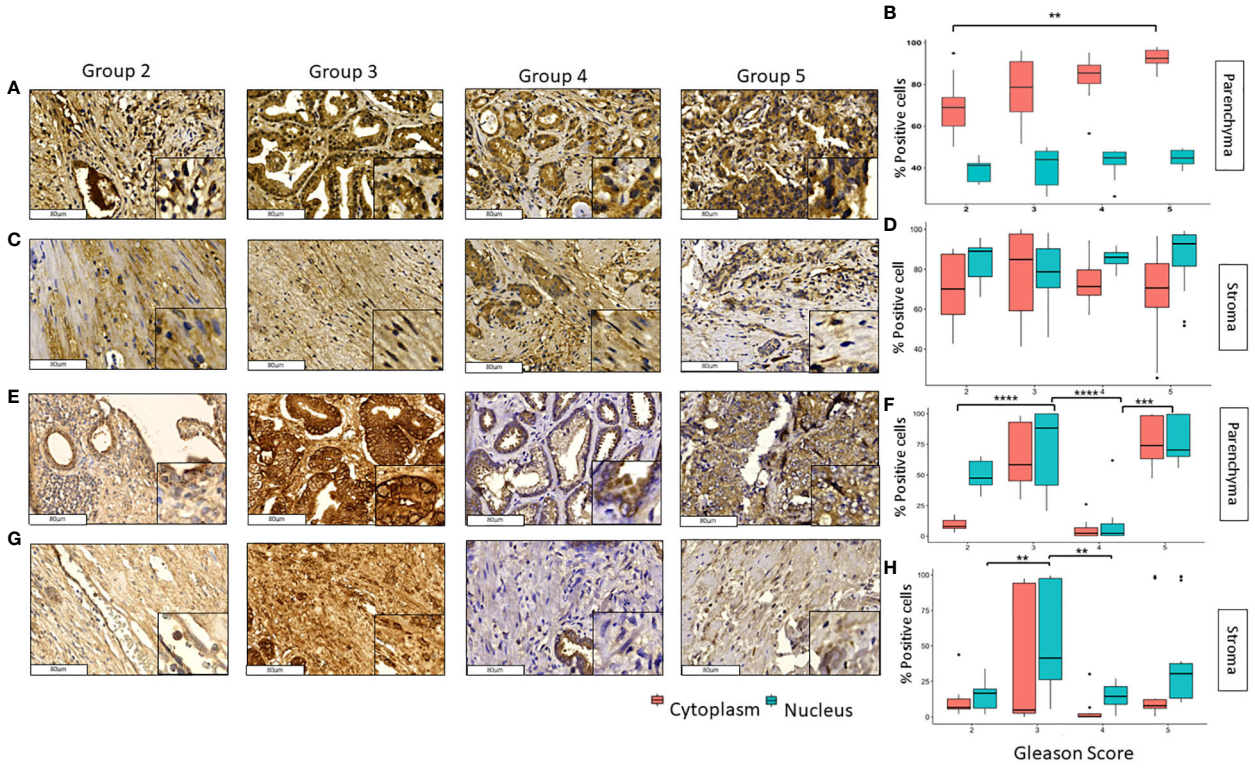

FIGURE 2
Expression of GLI1 and pGLI1 in tumoral and stromal prostate tissue in different grade groups. Representative images of GLI1 in the parenchyma **(A, B)** and stromal **(C, D)** tissues and pGLI1 in the parenchyma **(E, F)** and stromal **(G, H)** PCa tumor tissues by immunohistochemistry with HE staining (x200). Scale bar 80 µm. *=p<0.05, **=p<0.01, ***=p<0.001, ****=p<0.0001.

In tumoral tissue, the cytoplasmic expression of GLI3 decreases considerably from grade groups 2 to 5 and 3 to 5 (p<0.0001). The nuclear expression of GLI3 in these samples was low, and no significant changes were observed in the different groups (Figures 3A, B). As for the stromal tissue, GLI3 was absent in practically all group grades with non-significant p values among them (Figures 3C, D). Interestingly, nuclear pGLI3 increased significantly from grade groups 2 vs 3 (p<0.001) and 2 vs 4,5 (p<0.0001) in addition the cytoplasmic expression also increases from grades 2 vs 4 and 3 vs 4 (p<0.0001) (Figures 3E, F). Finally, the expression of pGLI3 decreases significantly from grade groups 3 to 5 (p<0.05) in stromal tissue (Figures 3G, H).

3.4 GPER positively correlates with pGLI3 factors in tumor tissues

A Pearson correlation revealed that in the tumoral tissue nuclear GPER positively correlates with nuclear pGLI3 (p<0.01) and negatively correlated with nuclear GLI3 (p<0.01). While cytoplasmic GPER positively correlates with cytoplasmic GLI1 and pGLI1 (p<0.01). Furthermore, there was a positive correlation in the expression of GPER vs pGLI1 and pGLI3 in the nuclear localization with a p<0.01 and p<0.001 respectively. Of note, these GLI transcriptional factors (pGLI1 and pGLI3) also correlated with each other (p<0.05). As for the cytoplasmic expression, we found that GLI1 was negatively correlated with GLI3 (p<0.01) whereas nuclear pGLI3 had a positive correlation with pGLI1 (p<0.001) (Figure 4A).

In stromal tissue, there was a positive correlation between nuclear GPER´s expression and GLI1´s in the cytoplasm (p<0.01). Also, the cytoplasmic expression of GPER was positively correlated with the nuclear pGLI3 (p<0.01). Moreover, nuclear pGLI1 and pGLI3 were positively correlated (p<0.01) (Figure 4B).

4 Discussion

PCa is the most common malignancy that impacts men's health, generating a pathological and molecular challenge in the understanding of the disease. GPER has been identified in parenchymal and stromal cells showing a dual role in proliferation depending on specific site of expression in reproductive tissues and regulates protumorigenic events by the activation of several signaling pathways (23). Hh pathway is a key signaling pathway involved in stemness and associated to relapse and bad prognosis (11) Not much is known about GPER and its regulation of Hh transcriptional factors, nevertheless, this receptor can trigger signaling cascades initiated in plasma membrane (24) leading to a pro-tumorigenic environment that promote angiogenesis (25); however, there is a limited information about biological significance

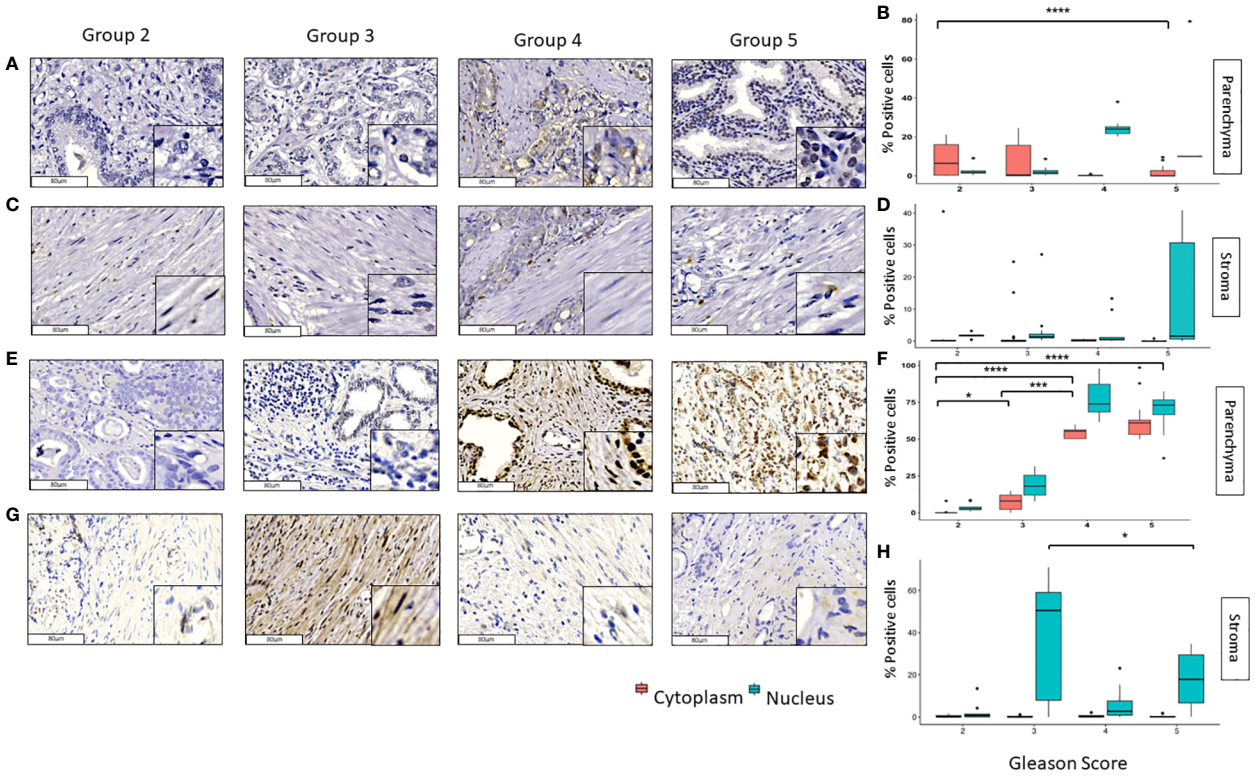

FIGURE 3
Expression of GLI3 and pGLI3 in tumoral and stromal prostate tissue in different grade groups. Representative images of GLI3 in the parenchyma **(A, B)** and stromal **(C, D)** PCa tumor tissues and pGLI3 in the tumoral **(E, F)** and stromal **(G, H)** PCa tumor tissues by immunohistochemistry with HE staining (x200). Scale bar 80 µm. *=p<0.05, **=p< 0.01, ***=p<0.001, ****=p<0.0001.

of GPER and relation with Hh pathways in PCa tissue. In this study, we evaluated the expression of GPER and its correlation of GLI factor involved in PCa tissues with different prognostic groups.

Our first result indicates that GPER´s expression remains in nuclear and increase in cytoplasmic compartments as grade groups proceed in tumor parenchyma, this phenomenon is discordant with Rago et al. studies where cytoplasmic GPER expression was highly observed in benign and decreases in prostate intraepithelial neoplasia lesions from Italian patients (26). A possible explanation might be the antibody used in both studies. Different epitopes are recognized by the antibodies, the antibody used in Rago´s research recognized extracellular domain (26) while the one

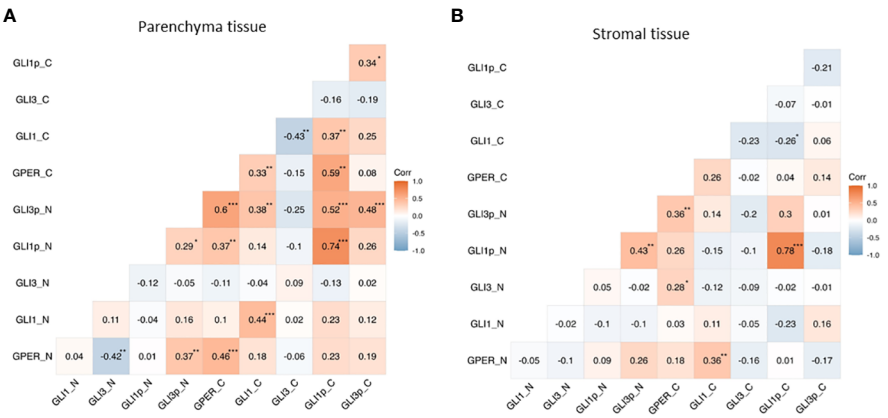

FIGURE 4
Correlation of GPER and GLI transcriptional factors in nuclear (N) and cytoplasmic (C) expression in the parenchyma and stromal PCa tissues. Heatmaps showing the correlation between the expression of GPER and GLI1, pGLI1, GLI3, and pGLI3 in parenchyma **(A)** and stromal **(B)** tissue. *p<0.05, **p<0.01, ***p<0.001.

we used can detect a protein ubiquitously expressed 27). Nuclear GPER was also reported by Marco Pupo et al. in breast cancer-associated fibroblasts, they suggest that GPER translocate through an importin-dependent mechanism and upregulated target genes like c-fos and CTGF induce by estrogens (28). Our results can lead to generate future perspectives performing cell fractions, to determine gene expression that GPER is activated in PCa tissues.

GPER may modulate the expression of genes (23) associated to the progression and development of PCa; however, further studies are needed to prove this hypothesis. Thus, targeting this receptor will provide a way to progress to a more precise approach to hormone-related disease detection and management.

Another fact was the presence of GPER expression in cytoplasm in tumoral and stroma PCa tissues, this remains as grade group proceed which agrees with Rago (26) and T Yu (29) studies. Several reports evidence GPER's modulation on clinical outcome, for instance Rago mentions that low expression of GPER is associated with high expression of pAKT and pCREB involved in cancer relapses (26); on the other hand, Yu et al. published that GPER confers multidrug resistance in CAFs through a cAMP/PKA/CREB dependent manner (29), therefore the expression of GPER is crucial to determine the level of aggressiveness in PCa tissues. Further analyses are required to demonstrate this fact in PCa.

In our results GLI1 full length (GLI1) was expressed mainly in cytoplasmic location in stroma and tumor tissue regardless of the grade group. This agrees with the observations made by Xing Liu et al., research which suggest that suppressor of fused protein (SUFU) has a negative regulation of Hh/GLI signaling activity, which arrests GLI1 proteins in cytoplasm and prevents their translocation to the nucleus (30). Therefore, SUFU protein affects transcription activity in cytoplasmic location (31). To date, still no evidence about correlation or interaction among GPER/SUFU/GLI1 in participation of diseases.

On the other hand, we found GLI1 phosphorylated (pGLI1) in tumor and stroma tissues where the expression was observed mainly in Gleason 7 (4 + 3) and 9 (4 + 5) (grade groups 3 and 5 respectively). Currently there are no reports about the behavior regarding presence and absence of pGLI1 along the different grade groups in prostate cancer tissues; however, pGLI1 is known to activate MAPK-ERK1/2 signaling in a SMO-independent manner that can be induced by stimulation of VEGFA secreted by cancer stromal cells in a paracrine manner in lung adenocarcinoma (13). Therefore, more studies are required to elucidate the importance of GPER/pGLI1 in tumor and stroma tissues.

Finally, we evaluated the expression of GLI3 full length (GLI3) in our samples. Slight expression was found in both compartments throughout grade groups. This was also observed by Diana Trnski et al., concluding that the processing of GLI3 into repressor transcriptional form is due to downregulation of GSK3β therefore cell proliferation decreases in colon cancer (30). Also GLI3 is degraded by proteasome induction of speckle-type POZ protein (SPO) (32) during CRCP androgen deprivation (18). Therefore, SPO and GSK3β are probably involved in downregulation or degradation of GLI3 and promotes tumor aggressiveness in PCa tissues.

Nevertheless, pGLI3 was observed in the nucleus of tumor parenchyma cells and, interestingly, its expression increased as the prognostic grade progresses. A few reports mention that phosphorylation of this transcriptional factor regulates positively (10) and negatively (33) in cancer, due to transactivation domain and the presence of PKA, GSK3β, and βTrCP. Also, it has been reported to directly interact with androgen receptor (AR), leading to its nuclear translocation (9) and consequently activate target genes, such as *cyclinD1* and *Fgf15* (34).

Due to the latter observations, we decided to evaluate if there was a correlation between the expression of the evaluated molecules. We observed a positive correlation among nuclear and cytoplasmic GPER with pGLI3 in the nuclear localization. Currently, there is no evidence on the regulation that GPER exerts in these compartments, and it needs to be elucidated in PCa disease. GPER is known to modulate several signaling pathways, PI3K/Akt among them, and the crosstalk between this pathway and GLI activation has previously been reported (14). This could stimulate importin-dependent mechanisms and modulate GSK3β, enabling GPER and pGLI3 translocate into the nucleus. Therefore, it would be an important perspective to evaluate the genes activated by GPER and pGLI3 in the PCa disease.

As complementary data, GLI1 and GLI3 had a negative correlation in their cytoplasmic expression in tumoral tissue. Both factors can interact and modulate each other's activity in cancer cells (9). In PCa it is known that GLI factors are upregulated in presence or absence of androgen, western blots showed that in the presence of AR, GLI3 expression increased in LNCaP cells; however, in the absence of AR GLI1 is predominated. This suggests that hormonal factors and crosstalk from oncogenic signaling pathways affects GLI transcriptional activity in PCa disease (9, 13). This fact has been linked to several non-canonical oncogenic growth signals and demonstrates the contribution of GLI1in differentiation during cancer development (35).

5 Conclusion

GPER has been involved in the regulatory mechanisms in prostate cancer cells; however, the mechanisms underlying these effects are still not fully understood. In this work, the presence of GPER in the nucleus was observed, and a positive correlation with pGLI3 transcriptional factor was established. Interestingly this correlation is maintained in the different prognostic groups. Whether GPER regulates pGLI3 or vice versa is still yet to be discovered, and further analysis should be conducted to solve this question. In a future direction, it would be interesting to describe the genes these molecules activate; this would light up the path in understanding the antitumoral GPER actions.

Data availability statement

The raw data supporting the conclusions of this article will be made available by the authors, without undue reservation.

Ethics statement

The studies involving humans were approved by Ethics Committee of the University Center for Health Sciences. The studies were conducted in accordance with the local legislation and institutional requirements. The present investigation was approved by the Ethics Committee of the University Center for Health Sciences (Opinion No. CI-01719), where exemption from informed consent was considered, based on the guidelines stipulated in CIOMS Guideline 10. The following points were taken into consideration: the research could not be conducted without the exemption from informed consent, considering that our retrospective study was based on the collection of remaining samples from pathological diagnosis; there is no risk to the participants in the study, as personal data information was dissociated, and patient identification is not possible. In addition, this research holds significant social and scientific value for the Mexican population under study.

Author contributions

CR-F: Investigation, Writing – original draft. EL-P: Investigation, Writing – review & editing. EP: Formal analysis, Methodology, Writing – review & editing. MG: Formal analysis, Investigation, Methodology, Resources, Supervision, Writing – review & editing. JV-P: Investigation, Methodology, Visualization, Writing – review & editing. MV-P: Methodology, Resources, Writing – review & editing. ES: Resources, Supervision, Visualization, Writing – review & editing. SZ: Methodology, Supervision, Writing – review & editing. AP-S: Conceptualization, Investigation, Resources, Supervision, Visualization, Writing – review & editing. AR-d-A: Conceptualization, Funding acquisition, Investigation, Project administration, Resources, Supervision, Visualization, Writing – review & editing.

Funding

The author(s) declare that no financial support was received for the research, authorship, and/or publication of this article.

Conflict of interest

The authors declare that the research was conducted in the absence of any commercial or financial relationships that could be construed as a potential conflict of interest.

Publisher's note

All claims expressed in this article are solely those of the authors and do not necessarily represent those of their affiliated organizations, or those of the publisher, the editors and the reviewers. Any product that may be evaluated in this article, or claim that may be made by its manufacturer, is not guaranteed or endorsed by the publisher.

References

1. Wang LE, Lu B, He M, Wang Y, Wang Z, Du L. Prostate cancer incidence and mortality: global status and temporal trends in 89 countries from 2000 to 2019. *Front Public Health* (2022) 10:811044/BIBTEX(February). doi: 10.3389/FPUBH.2022.811044/BIBTEX

2. Bonkhoff H. Estrogen receptor signaling in prostate cancer: implications for carcinogenesis and tumor progression. *Prostate* (2018) 78:2-10. doi: 10.1002/pros.23446

3. Yang K. *Mechanism of GPER Promoting Proliferation, Migration and Invasion of Triple-Negative Breast Cancer Cells through CAF - PubMed* (2019). Available at: https://pubmed.ncbi.nlm.nih.gov/31632554/.

4. Lam HM, Ouyang B, Chen J, Ying J, Wang J, Wu CL, et al. Targeting GPR30 with G-1: A new therapeutic target for castration-resistant prostate cancer. *Endocrine-Related Cancer* (2014) 21(6):903–145. doi: 10.1530/ERC-14-0402

5. Chan Q, Lam H-M, Ng C-F, Lee A, Chan E, Ng H-K, et al. Activation of GPR30 Inhibits the Growth of Prostate Cancer Cells through Sustained Activation of Erk1/2, c-Jun/c-Fos-Dependent Upregulation of P21, and Induction of G2 Cell-Cycle Arrest. *Cell Death Differ* (2010) 17:1511–23. doi: 10.1038/cdd.2010.20

6. Lau KM, Ma FMT, Xia JT, Chan QKYI, Ng CF, To KAF. Activation of GPR30 stimulates GTP-binding of Gαi1 protein to sustain activation of erk1/2 in inhibition of prostate cancer cell growth and modulates metastatic properties. *Exp Cell Res* (2017) 350(1):199–2095. doi: 10.1016/j.yexcr.2016.11.022

7. Xie BY, Lv QY, Ning Cc, Yang BY, Shan Ww, Cheng YA, et al. TET1-GPER-PI3K/AKT pathway is involved in insulin-driven endometrial cancer cell proliferation. *Biochem Biophys Res Commun* (2017) 482(4):857–62. doi: 10.1016/j.bbrc.2016.11.124

8. Luchetti G, Sircar R, Kong JH, Nachtergaele S, Sagner A, Byrne EFX, et al. Cholesterol activates the G-protein coupled receptor smoothened to promote hedgehog signaling. *ELife* (2016) 5(OCTOBER2016):1-22. doi: 10.7554/ELIFE.20304

9. Li NA, Truong S, Nouri M, Moore J, Nakouzi NA, Lubik AA, et al. Non-canonical activation of hedgehog in prostate cancer cells mediated by the interaction of transcriptionally active androgen receptor proteins with gli3. *Oncogene* (2018) 37 (17):2313–255. doi: 10.1038/S41388-017-0098-7

10. Matissek SJ, Elsawa. SF. GLI3: A mediator of genetic diseases, development and cancer. *Cell Communication Signaling* (2020) 18(1):1–205. doi: 10.1186/S12964-020-00540-X

11. Niewiadomski P, Niedziółka SM, Markiewicz Ł, Uśpieński T, Baran B, Chojnowska K. Gli proteins: regulation in development and cancer. *Cells* (2019) 8 (2):1475. doi: 10.3390/CELLS8020147

12. Xu T, Ma D, Chen S, Tang R, Yang J, Meng C, et al. High GPER expression in triple-negative breast cancer is linked to pro-metastatic pathways and predicts poor patient outcomes. *NPJ Breast Cancer* (2022) 8(1):1–11. doi: 10.1038/s41523-022-00472-4

13. Pietrobono S, Gagliardi S, Stecca B. Non-canonical hedgehog signaling pathway in cancer: activation of GLI transcription factors beyond smoothened. *Front Genet* (2019) 10:556/BIBTEX(JUN). doi: 10.3389/FGENE.2019.00556/BIBTEX

14. Schnidar H, Eberl M, Klingler S, Mangelberger D, Kasper M, Hauser-Kronberger C, et al. Epidermal growth factor receptor signaling synergizes with hedgehog/GLI in oncogenic transformation via activation of the MEK/ERK/JUN pathway. *Cancer Res* (2009) 69(4):1284–92. doi: 10.1158/0008-5472.CAN-08-2331/654471/P/EPIDERMAL-GROWTH-FACTOR-RECEPTOR-SIGNALING

15. Peng Y-C, Levine CM, Zahid S, Lynette Wilson E, Joyner AL. Sonic hedgehog signals to multiple prostate stromal stem cells that replenish distinct stromal subtypes during regeneration. *Proc Natl Acad Sci* (2013) 110(51):20611–165. doi: 10.1073/PNAS.1315729110

16. Bushman W. Hedgehog signaling in prostate development, regeneration and cancer. *J Dev Biol* (2016) 4(4):2-8. doi: 10.3390/JDB4040030

17. Zhou H, Kim S, Ishii S, Boyer TG. Mediator modulates gli3-dependent sonic hedgehog signaling. *Mol Cell Biol* (2006) 26(23):8667–825. doi: 10.1128/MCB.00443-06/ASSET/476208B7-99C7-43E4-8262-479C5CB99D91/ASSETS/GRAPHIC/ZMB0230664020010.JPEG

18. Burleson M, Deng JJ, Qin T, Duong TM, Yan Y, Gu X, et al. GLI3 is stabilized by SPOP mutations and promotes castration resistance via functional cooperation with

androgen receptor in prostate cancer. *Mol Cancer Research : MCR* (2022) 20(1):62–76. doi: 10.1158/1541-7786.MCR-21-0108

19. Lappano R, De Marco P, De Francesco EM, Chimento A, Pezzi V, Maggiolini M. Cross-talk between GPER and growth factor signaling. *J Steroid Biochem Mol Biol* (2013) 137(September):50–6. doi: 10.1016/j.jsbmb.2013.03.005

20. Wang Y, Ding Q, Yen CJ, Xia W, Izzo JG, Lang JY, et al. The crosstalk of MTOR/S6K1 and hedgehog pathways. *Cancer Cell* (2012) 21(3):374–87. doi: 10.1016/J.CCR.2011.12.028

21. Villegas VE, Rondón-Lagos M, Annaratone L, Castellano I, Grismaldo A, Sapino A, et al. Tamoxifen treatment of breast cancer cells: impact on hedgehog/GLI1 signaling. *Int J Mol Sci* (2016) 17(3):3085. doi: 10.3390/IJMS17030308

22. R Core Team. *Language and environment for statistical computing. R Foundation for Statistical Computing Vienna, Austria.* (2022). Available at: http://www.Rproject.org/, (Accessed January 13 2022).

23. Arang N, Silvio Gutkind. J. G protein-coupled receptors and heterotrimeric G proteins as cancer drivers. *FEBS Lett* (2020) 594(24):4201–325. doi: 10.1002/1873-3468.14017

24. Fuentes N, Silveyra P. Estrogen receptor signaling mechanisms. *Adv Protein Chem Struct Biol* (2019) 116(January):135–70. doi: 10.1016/BS.APCSB.2019.01.001

25. Lappano R, Rigiracciolo D, De Marco P, Avino S, Cappello AR, Rosano C, et al. Recent advances on the role of G protein-coupled receptors in hypoxia-mediated signaling. *AAPS J* (2016) 18(2):305–105. doi: 10.1208/s12248-016-9881-6

26. Rago V, Romeo F, Giordano F, Ferraro A, Carpino A. Identification of the G protein-coupled estrogen receptor (GPER) in human prostate: expression site of the estrogen receptor in the benign and neoplastic gland. *Andrology* (2016) 4(1):121–27. doi: 10.1111/andr.12131

27. *Anti-G-Protein Coupled Receptor 30 Antibody (Ab39742) | Abcam* (n.). Available at: https://www.abcam.com/g-protein-coupled-receptor-30-antibody-ab39742.html (Accessed February 15, 2023).

28. Pupo M, Vivacqua A, Perrotta I, Pisano A, Aquila S, Abonante S, et al. The nuclear localization signal is required for nuclear GPER translocation and function in breast cancer-associated fibroblasts (CAFs). *Mol Cell Endocrinol* (2013) 376(1–2):23–32. doi: 10.1016/J.MCE.2013.05.023

29. Yu T, Yang G, Hou Y, Tang X, Wu C, Wu XA, et al. Cytoplasmic GPER translocation in cancer-associated fibroblasts mediates CAMP/PKA/CREB/glycolytic axis to confer tumor cells with multidrug resistance. *Oncogene* (2017) 36(15):2131–45. doi: 10.1038/ONC.2016.370

30. Trnski D, Sabol M, GojevićA, Martinić M, Ozretić P, Musani V, et al. GSK3β and gli3 play a role in activation of hedgehog-gli pathway in human colon cancer — Targeting GSK3β Downregulates the signaling pathway and reduces cell proliferation. *Biochim Biophys Acta (BBA) - Mol Basis Dis* (2015) 12):2574–84. doi: 10.1016/J.BBADIS.2015.09.005

31. Ramaswamy B, Lu Y, Teng KY, Nuovo G, Li X, Shapiro CL, et al. Hedgehog signaling is a novel therapeutic target in tamoxifen-resistant breast cancer aberrantly activated by PI3K/AKT pathway. *Cancer Res* (2012) 72(19):5048–595. doi: 10.1158/0008-5472.CAN-12-1248

32. Wang C, Pan Y, Wang B. Suppressor of fused and spop regulate the stability, processing and function of gli2 and gli3 full-length activators but not their repressors. *Dev (Cambridge England)* (2010) 137(12):2001–95. doi: 10.1242/DEV.052126

33. Rodrigues MFS, Miguita L, De Andrade NP, Heguedusch D, Rodini CO, Moyses RA, et al. GLI3 knockdown decreases stemness, cell proliferation and invasion in oral squamous cell carcinoma. *Int J Oncol* (2018) 53(6):2458–725. doi: 10.3892/IJO.2018.4572/HTML

34. Wilson SL, Wilson JP, Wang C, Wang B, Mcconnell SK. Primary cilia and gli3 activity regulate cerebral cortical size. *Dev Neurobiol* (2012) 72(9):1196–12125. doi: 10.1002/DNEU.20985

35. Palle K, Mani C, Tripathi K, Athar. M. Aberrant GLI1 activation in DNA damage response, carcinogenesis and chemoresistance. *Cancers* (2015) 7(4):2330–525. doi: 10.3390/CANCERS7040894

frontiers | Frontiers in Endocrinology

TYPE Review
PUBLISHED 07 February 2024
DOI 10.3389/fendo.2024.1338420

OPEN ACCESS

EDITED BY
Anna Perri,
Magna Græcia University of Catanzaro, Italy

REVIEWED BY
Biagio Barone,
Azienda Ospedaliera di Caserta, Italy
Jale Yuzugulen,
Eastern Mediterranean University, Türkiye
Eldar Nadyrov,
Gomel State Medical University, Belarus

*CORRESPONDENCE
Dawei Li
lidaweimd@aliyun.com

†These authors have contributed equally to this work

RECEIVED 14 November 2023
ACCEPTED 18 January 2024
PUBLISHED 07 February 2024

CITATION
Sun J, Tian T, Wang N, Jing X, Qiu L, Cui H, Liu Z, Liu J, Yan L and Li D (2024) Pretreatment level of serum sialic acid predicts both qualitative and quantitative bone metastases of prostate cancer. *Front. Endocrinol.* 15:1338420. doi: 10.3389/fendo.2024.1338420

Pretreatment level of serum sialic acid predicts both qualitative and quantitative bone metastases of prostate cancer

Jingtao Sun[1†], Tian Tian[2†], Naiqiang Wang[1], Xuehui Jing[1,3], Laiyuan Qiu[1], Haochen Cui[1], Zhao Liu[1], Jikai Liu[1], Lei Yan[1] and Dawei Li[1*]

[1]Department of Urology, Qilu Hospital of Shandong University, Jinan, China, [2]Respiratory and Critical Care Medicine Department, Qilu Hospital of Shandong University, Jinan, China, [3]Department of Urology, Yucheng People's Hospital, Dezhou, China

Background: Recently, serum sialic acid (SA) has emerged as a distinct prognostic marker for prostate cancer (PCa) and bone metastases, warranting differential treatment and prognosis for low-volume (LVD) and high-volume disease (HVD). In clinical settings, evaluating bone metastases can prove advantageous.

Objectives: We aimed to establish the correlation between SA and both bone metastasis and HVD in newly diagnosed PCa patients.

Methods: We conducted a retrospective analysis of 1202 patients who received a new diagnosis of PCa between November 2014 and February 2021. We compared pretreatment SA levels across multiple groups and investigated the associations between SA levels and the clinical parameters of patients. Additionally, we compared the differences between HVD and LVD. We utilized several statistical methods, including the non-parametric Mann-Whitney U test, Spearman correlation, receiver operating characteristic (ROC) curve analysis, and logistic regression.

Results: The results indicate that SA may serve as a predictor of bone metastasis in patients with HVD. ROC curve analysis revealed a cut-off value of 56.15 mg/dL with an area under the curve of 0.767 (95% CI: 0.703-0.832, $P < 0.001$) for bone metastasis versus without bone metastasis and a cut-off value of 65.80 mg/dL with an area under the curve of 0.766 (95% CI: 0.644-0.888, $P = 0.003$) for HVD versus LVD. Notably, PCa patients with bone metastases exhibited significantly higher SA levels than those without bone metastases, and HVD patients had higher SA levels than LVD patients. In comparison to the non-metastatic and LVD cohorts, the cohort with HVD exhibited higher levels of alkaline phosphatase (AKP) (median, 122.00 U/L), fibrinogen (FIB) (median, 3.63 g/L), and prostate-specific antigen (PSA) (median, 215.70 ng/mL), as well as higher Gleason scores (> 7). Multivariate logistic regression analysis demonstrated that an SA level of > 56.15 mg/dL was independently associated with the presence of bone metastases in PCa patients (OR =

2.966, P = 0.018), while an SA level of > 65.80 mg/dL was independently associated with HVD (OR = 1.194, P = 0.048).

Conclusion: The pretreatment serum SA level is positively correlated with the presence of bone metastases.

KEYWORDS

serum sialic acid, bone metastases, prostate cancer, low-volume disease, high-volume disease

1 Introduction

Prostate cancer (PCa) is a prevalent malignancy that originates from the male reproductive system. Despite a lower incidence rate among Asians compared to Americans and Europeans (1), the mortality and morbidity rates associated with PCa are on the rise in China due to improvements in living standards, lifestyle changes, and advancements in screening methods (2, 3). The use of prostate-specific antigen (PSA) for population screening, diagnosis, and monitoring of PCa has been a subject of controversy since its purification (4). Although PSA screening has some benefits, such as early detection of PCa, it also has several drawbacks, such as high costs, long waiting times, limited sensitivity, and low specificity. Current evidence suggests that the overall public health impact of PSA screening is not significantly greater than its benefits (5–7). Various treatment options are available for patients diagnosed with early-stage PCa, including surgical removal, chemotherapy, and castration therapy (8). Metastasis is the leading cause of death in PCa, with lymph nodes near the primary tumor being the initial sites of metastasis, followed by bone metastases (9). Currently, there exists no efficacious treatment for patients afflicted with bone metastases (10, 11). Multiple studies have demonstrated that individuals with bone metastases stemming from PCa have a poorer prognosis and a reduced quality of life (12). Consequently, the timely identification of bone metastases in PCa patients is of paramount importance. Although a bone scan is frequently employed for early detection, its specificity is limited, resulting in a high incidence of false-positive results. Given a thorough comprehension of PCa, emission computerized tomography (ECT) is regarded as one of the most effective techniques for detecting bone metastases in patients at present (13–15). Despite the expenses and radioactivity associated with the procedure, it is deemed a valuable investment. Thus, there is an urgent need for novel biomarkers to aid in the identification and long-term monitoring of bone metastases in PCa patients.

Acetylneuraminic acid (sialic acid [SA]), a nine-carbon monosaccharide initially reported in 1957, may serve as a potential candidate. The termination of glycoprotein side chains and glycolipid side chains, which are fundamental constituents of cellular membranes, occurs at this location (16). Furthermore, this agent not only provides cytoprotection but also safeguards cell membranes (17). Multiple studies have established a correlation between elevated levels of SA and cancer, as evidenced in patients (18) with ovarian cancer (19), breast cancer (20), oral cancer (21), and neck cancer (22). Additionally, certain chemical agents have been shown to enhance disease invasion by altering SA levels or impeding SA production, as demonstrated in some studies (23, 24). A noteworthy correlation has been established between SA levels and PCa (25, 26). Notably, patients with PCa who exhibit elevated SA levels are more prone to exhibit heightened levels of PSA, lactate dehydrogenase (LDH), and α-L-fucosidase (AFU), a higher Gleason score, and a higher metastasis incidence rate (26). At present, the primary treatment modalities for PCa include androgen deprivation therapy, radiation therapy, ablative therapy, chemotherapy, and emerging immunotherapies. In clinical settings, it may be necessary to employ multiple approaches simultaneously (27–29). However, this does not diminish the significance of thoroughly assessing the metastatic load of patients prior to treatment in order to determine appropriate treatment options and prognoses (30, 31). Currently, investigations into the correlation between pretreatment SA levels and the metastatic burden of PCa are limited. Therefore, our study was designed to examine this potential association through retrospective data analysis.

2 Materials and methods

2.1 Patients selection

This retrospective analysis was performed on 1202 PCa patients diagnosed by prostate biopsy in our hospital's Urology Department between January 2014 and January 2021. The inclusion criteria encompassed the following: (I) Absence of any prior cancer diagnosis; (II) Absence of hematologic disorders to prevent potential confounding of hematologic markers; (III) Availability of comprehensive postoperative pathology findings; (IV) Availability of comprehensive clinical data; (V) Diagnosed with PCa. Our study excluded patients with any one or more of the following conditions: (I) Patients with hematological diseases (Individuals diagnosed with hematological disorders, or prescribed medications known to potentially alter blood markers), known infections, and other

malignancies; (II) Patients who had undergone prostate surgery (such as transurethral resection) before their biopsies; (III) Pathologically diagnosed patients with prostatic intraepithelial neoplasms and atypical small acinar proliferations; (IV) Patients with incomplete clinical data. Following that, we collected the following information from the medical records of eligible patients: age at the time of diagnosis, AKP, LDH, AFU, FIB, and PSA levels, pathological characteristics (including pathological grade and stage), and ECT results. The data screening process of the study is shown in Figure 1. Our study was approved by the Medical Ethics Committee of Qilu Hospital of Shandong University (KYLL-202208-044-1).

2.2 Data collection

Data were obtained from the database of Qilu Hospital of Shangdong University, including age at the time of diagnosis, AKP, LDH, AFU, FIB, and PSA levels, pathological characteristics (including pathological grade and stage), and ECT results. Pathological grades were evaluated using the Gleason system and pathological stages were evaluated according to TNM 2021. Assessment of bone metastasis was performed using ECT, where a positive test result indicated the presence of metastatic lesions. When an isolated condensed radionuclide spot was observed, this was considered as one metastatic lesion.

2.3 Measurement of hematology indices

Five milliliters of venous blood was drawn from each patient after they had fasted for 12 h in the early morning before any clinical intervention was given. During the experiment, test tubes containing a clot activator and gel were used to store blood samples, which coagulated naturally at room temperature. The samples were centrifuged for 10 min at 2000 rpm. After the serum was obtained, the AKP, LDH, AFU, and SA concentrations were determined using a Roche Cobas 8000 automatic analyzer. The normal concentration range for AKP was 45.00 to 125.00 U/L; the normal concentration range for LDH was 120.00 U/L to 230.00 U/L; the normal concentration range for AFU was < 40.00 U/L; and the normal concentration range for SA was 45.60 to 75.40 mg/dL. Before the prostate biopsy, plasma PSA levels and FIB concentrations were determined as well. To measure PSA and FIB levels, blood samples (about 3.50 mL) were collected. Samples were collected in plastic tubes with coagulant/separating glue for PSA analysis and in plastic tubes containing 3.80% sodium citrate for FIB detection. The normal concentration range for FIB was 2.00 to 4.00 g/L; the normal concentration range for PSA was < 4.00 ng/mL.

2.4 Statistical analysis

In total, 1202 cases of PCa were enrolled. Based on frequency analysis, AKP, LDH, AFU, FIB, and PSA did not have a normal distribution, so medians (percentiles) were used instead. To determine whether SA followed a normal distribution, the Kolmogorov-Smirnov test was employed on the means and standard deviations (SDs) in each group. Normally distributed data were analyzed using Student's *t* test. Non-normally distributed data were analyzed using the Mann-Whitney U test or the Kruskal-Wallis H test. The correlation between two parameters was analyzed using the Spearman method. Categorical variables are presented as numbers (percentages), and the Chi-square test was used to compare the groups. The associations of different parameters with the bone metastasis status and HVD were evaluated

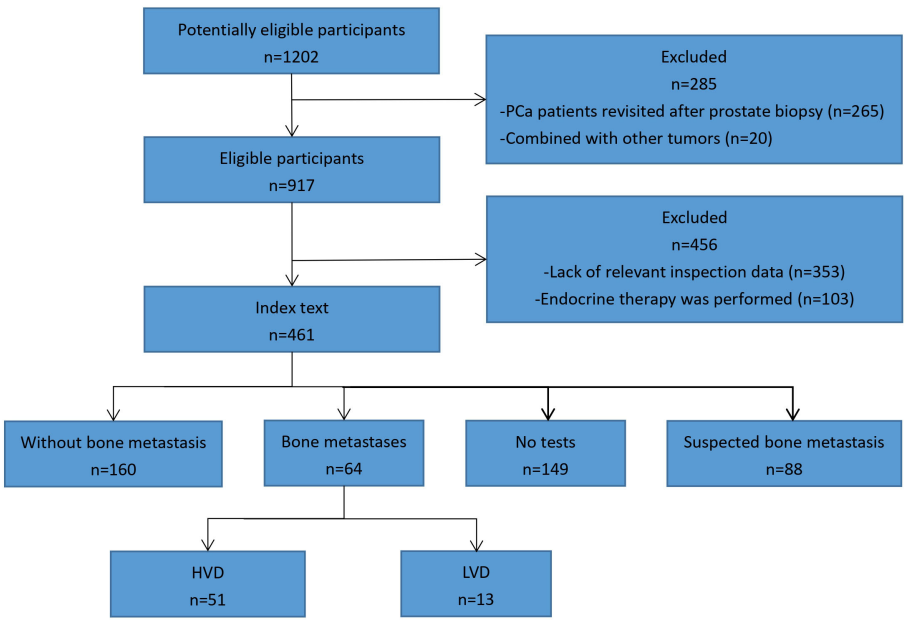

FIGURE 1
The data screening process of the study.

by univariate and multivariate logistic regression analysis. To establish SA cut-off values, a receiver operating characteristic (ROC) curve was plotted and the resulting area under the curve (AUC) was calculated. The value with the largest Youden index (calculated as (sensitivity + specificity) + 1) was defined as the optimal cut-off value. Differences were considered to be statistically significant if $P < 0.05$. Statistical analysis was performed using Statistical Package for Social Sciences (SPSS) version 19.0 (SPSS, Inc., Chicago, IL, USA). The dynamic nomogram is introduced as a model, wherein the summation of individual patient scores on predictive factors enables the computation of their total score and subsequent determination of their risk for the outcome event. Variables exhibiting p values of 0.05 or lower in the logistic regression analysis were incorporated into the nomogram. Calibration curves and receiver operating characteristic (ROC) analysis were utilized to assess the predictive capabilities of the model. Additionally, decision curve analysis (DCA) was employed to evaluate the net benefits of clinical interventions guided by the model (R vision 4.1.3).

3 Results

3.1 Clinical characteristics of PCa patients

The characteristics of the patients are presented in Table 1. The location and quantity of bone metastases in PCa patients were assessed through ECT scanning as reported previously (32). The total number of patients diagnosed with bone metastases was 64.

3.2 The relationship between serum sialic acid and clinical characteristics

The median SA level in the cohort with bone metastases was found to be 62.70 mg/dL, which was observed to be significantly higher than in the non-bone metastasis cohort (53.75 mg/dl) ($P < 0.001$) (Figure 2A). Further examination of the HVD and LVD groups indicated that patients with HVD exhibited elevated SA levels in comparison to patients with LVD (65.70 mg/dL) ($P = 0.003$) (Figure 2B).

ROC curve analysis was conducted to determine the predictive value of pretreatment SA levels for bone metastases. As depicted in Figure 2C, a cut-off level of 56.15 mg/dL SA was obtained, with SA levels above this threshold being associated with a higher risk of bone metastases (AUC = 0.767; 95% CI: 0.703-0.832; $P < 0.001$; sensitivity: 0.813, specificity:0.631). Our assessment of the ROC curve derived from SA levels of patients with LVD or HVD yielded an AUC of 0.766 (95% CI: 0.644-0.888), with an optimal threshold value of 65.80 mg/dL (sensitivity: 0.490, specificity:1.000) (Figure 2D).

As shown in Table 2, subjects in the present study were also divided into two groups based on SA levels (≤ 56.15 mg/dL vs. > 56.15 mg/dL). A significant association was found between pretreatment SA levels and AKP, LDH, FIB, and PSA levels, Gleason score, pT stage, and bone metastasis (all $P < 0.050$). Moreover, we divided the databases into two categories based on their SA levels (≤ 65.80 mg/dL vs. > 65.80 mg/dL) (Table 3). In addition to AKP, LDH, FIB, and PSA levels, Gleason score, pT stage, and HVD, pretreatment SA levels were significantly associated with these parameters (all $P < 0.050$).

TABLE 1 Clinical characteristics of selected PCa patients ($n = 461$).

Parameter	Values
Age (years)	70.00 (64.00, 76.00)
AKP (U/L)	73.00 (59.50, 95.00)
LDH (U/L)	194.00 (174.00, 224.00)
AFU (U/L)	16.00 (13.00, 20.00)
FIB (g/L)	3.13 (2.66, 3.65)
PSA (ng/mL)	34.87 (11.78, 125.30)
SA (mg/dL)	55.90 (50.75, 63.50)
Pathological grade	
Low (GS ≤ 7)	197 (42.73)
High (GS > 7)	242 (52.49)
Missing information	22 (4.77)
Pathological stage	
pT2	340 (73.75)
pT3	5 (1.08)
pT4	98 (21.26)
biopsy	18 (3.91)
ECT (bone metastasis burden)	
Without bone metastases	160 (34.71)
LVD patients	13 (2.82)
HVD patients	51 (11.06)
Suspicion	88 (19.09)
ECT not performed	149 (32.32)

Data are presented as median (P25, P75) or *n* (%). AKP, alkaline phosphatase; LDH, lactate dehydrogenase; AFU, α-L-fucosidase; FIB, fibrinogen; PSA, prostate-specific antigen; SA, serum sialic acid; PCa, prostate cancer; T, tumor; pathological grades are categorized as high grade and low grade using GS; pathological stage is assessed based on postoperative pathology results (not biopsy) in accordance with the 2021 TNM classification system.

3.3 Comparison of serum sialic acid levels between PCa patients with and without bone metastasis

Data were missing for three PCa patients without bone metastases. To determine the parameters that differ between the three groups, we excluded patients with missing data. The first group had no bone metastasis, the second group had LVD, and the third group had HVD. *P*1 denotes the outcome of comparing the group without bone metastasis to the LVD group, whereas *P*2 represents the result of comparing the group without bone metastasis to the HVD group. Lastly, *P*3 signifies the outcome of comparing the LVD group to the HVD group. The three groups are compared in Table 4. Between any two groups, there was no statistically significant

difference in age and AFU levels. In addition, there were statistically significant differences in PSA and AKP levels between any two groups. The HVD group had higher FIB levels compared with the non-metastatic and LVD groups ($P < 0.050$). The HVD group had higher Gleason scores compared with the non-metastatic ($P = 0.000$) and LVD groups ($P = 0.001$). There were no statistically significant differences in FIB levels ($P = 0.417$), and Gleason scores ($P = 0.340$) between the group without metastatic disease and LVD patients. When the LVD group was compared to non-metastatic patients ($P = 0.143$) and the HVD group ($P = 0.409$), there was no statistically significant difference in LDH levels. There was, however, a statistically significant difference in LDH levels between the patients without metastatic disease and the HVD group ($P = 0.000$).

3.4 The relationship between serum sialic acid levels and HVD

To further examine the clinical effects of pretreatment SA levels in the diagnosis of bone metastases and HVD, a logistic regression analysis was conducted. The final model selection was made using a backward stepdown selection process. As shown in Table 5, elevated SA levels significantly predicted poor diagnostic outcomes of bone metastases in the univariate and multivariate analysis (P < 0.050). In addition, elevated AKP levels, high PSA levels, and high Gleason score were significantly associated with the diagnosis of bone metastases based on univariate and multivariate analysis (AKP: univariate analysis: HR = 1.034, P = 0.000 and multivariate analysis: HR = 1.029, P = 0.000; PSA: univariate analysis: HR = 1.007, P = 0.000 and multivariate analysis: HR = 1.005, P = 0.000; Gleason score: univariate analysis: HR = 3.023, P = 0.001 and multivariate analysis: HR = 4.372, P = 0.003) (Table 5). Interestingly, in HVD patients, elevated SA levels were significantly predicted. Both univariate and multivariate logistic regressions showed that elevated SA levels, PSA levels and high Gleason score are independently associated with HVD patients (all P < 0.050) (Table 6). However, HVD was not significantly correlated with AKP based on univariate and multivariate logistic regressions (Table 6).

3.5 Nomogram model of bone metastasis and HVD

As shown in Figure 3, all significant factors for bone metastasis (Figure 3A) and HVD (Figure 3B) occurrence were integrated into the nomogram for predicting the probabilities of bone metastasis

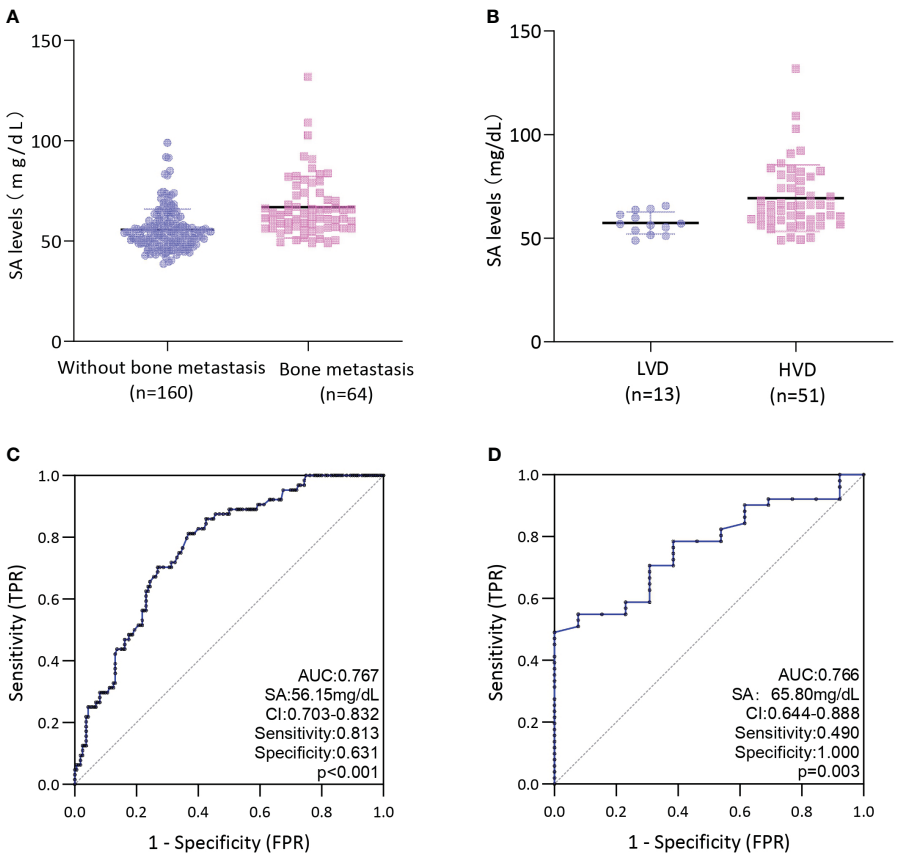

FIGURE 2
(A) Comparison of SA levels between bone metastases and without bone metastases in PCa patients; **(B)** Comparison of SA levels between LVD and HVD in PCa patients with bone metastases; **(C)** ROC curves for determination of cut-off value of SA levels regarding prediction of bone metastases in PCa patients; **(D)** ROC curves for determination of cut-off value of SA levels regarding prediction of HVD in PCa patients; HVD, high volume disease; LVD, low volume disease.

TABLE 2 Comparison of clinical parameters between groups presenting distinct ranges of SA levels (≤56.15 mg/dL vs. >56.15 mg/dL).

Parameter	SA ≤ 56.15 mg/dL (*n* = 237)	SA > 56.15 mg/dL (*n* = 224)	Statistics	*P*
Age (years)	70.00 (64.00, 75.50)	70.00 (64.00, 76.00)	−0.045	0.964*
AKP (U/L)	64.00 (53.00, 77.50)	82.00 (68.25, 118.50)	−9.386	0.000*
LDH (U/L)	187.00 (169.00, 210.00)	198.00 (179.00, 241.50)	−4.519	0.000*
AFU (U/L)	16.00 (13.00, 20.00)	16.00 (13.00, 20.75)	−0.870	0.384*
FIB (g/L)	2.76 (2.53, 3.09)	3.61 (3.17, 4.27)	−12.556	0.000*
PSA (ng/mL)	24.27 (10.50, 66.48)	66.67 (16.19, 216.95)	−5.239	0.000*
Gleason score (≤7 vs. >7)	115/107	82/135	8.712	0.003#
pT stage (T1-2 vs. T3-4)	197/31	143/72	24.536	0.000#
Metastatic patients	12 (10.60)	52 (46.80)	36.010	0.000#

Data are presented as median (P25, P75), *n/n*, or *n* (%). *Z-values; #x2 values; AKP, alkaline phosphatase; LDH, lactate dehydrogenase; AFU: α-L-fucosidase; FIB, fibrinogen; PSA, prostate-specific antigen; SA, serum sialic acid; PCa, prostate cancer; T, tumor; pathological grades are categorized as high grade and low grade using GS; $P < 0.05$ is considered as statistically significant.

TABLE 3 Comparison of clinical parameters between groups presenting distinct ranges of SA levels (≤65.80 mg/dL vs. >65.80 mg/dL).

Parameter	SA ≤ 65.80 mg/dL (*n* = 365)	SA > 65.80 mg/dL (*n* = 96)	Statistics	*P*
Age (years)	71.00 (64.00, 76.00)	69.00 (61.25, 76.00)	−1.453	0.146*
AKP (U/L)	68.00 (57.00, 83.50)	102.00 (73.25, 152.50)	−7.556	0.000*
LDH (U/L)	191.00 (171.00, 214.00)	214.00 (181.25, 263.00)	−4.419	0.000*
AFU (U/L)	16.00 (13.00, 20.00)	16.00 (13.00, 19.75)	−0.392	0.695*
FIB (g/L)	2.94 (2.61, 3.34)	4.25 (3.64, 5.20)	−12.298	0.000*
PSA (ng/mL)	29.07 (10.85, 94.13)	94.12 (21.93, 344.28)	−5.350	0.000*
Gleason score (≤7 vs. >7)	166/182	31/60	5.422	0.020#
pT stage (T1-2 vs. T3-4)	286/67	54/36	17.757	0.000#
HVD patients	26 (66.70)	25 (100.00)	10.458	0.001#

Data are presented as median (P25, P75), n/n, or n (%). *Z-values; #x^2 values; HVD, high-volume disease; AKP, alkaline phosphatase; LDH, lactate dehydrogenase; AFU, α-L-fucosidase; FIB, fibrinogen; PSA, prostate-specific antigen; SA, serum sialic acid; PCa, prostate cancer; T, tumor; pathological grades are categorized as high grade and low grade using GS; $P < 0.05$ is considered as statistically significant.

TABLE 4 Comparison of clinical parameters among non-metastatic (Group 1), LVD (Group 2), and HVD group (Group 3).

Parameter	Group 1 (*n* = 160)	Group 2 (*n* = 13)	Group 3 (*n* = 51)	*P*1 (sta)	*P*2 (sta)	*P*3 (sta)
Age (years)	71.00 (64.00, 75.00)	69.00 (68.00, 75.00)	68.00 (63.00, 76.00)	0.804 (−0.248*)	0.409 (−1.066*)	0.531 (−0.627*)
AKP (U/L)	67.50 (56.00, 78.00)	90.00 (69.00, 96.00)	122.00 (95.00, 276.00)	0.007 (−2.719*)	0.000 (−8.090*)	0.002 (−3.163*)
LDH (U/L)	185.50 (168.00, 211.50)	197.00 (178.00, 222.50)	212.00 (182.00, 273.00)	0.143 (−1.466*)	0.000 (−4.126*)	0.409 (−0.826*)
AFU (U/L)	16.00 (13.00, 20.75)	18.00 (15.50, 27.00)	18.00 (13.00, 23.00)	0.056 (−1.909*)	0.141 (−1.471*)	0.332 (−0.970*)
FIB (g/L)	2.96 (2.62, 3.39)	2.91 (2.75, 3.51)	3.63 (3.01, 4.47)	0.417 (−0.812*)	0.000 (−4.879*)	0.026 (−2.228*)
PSA (ng/mL)	31.01 (11.54, 79.01)	58.23 (28.56, 138.17)	215.70 (104.50, 507.60)	0.092 (−1.687*)	0.000 (−7.090*)	0.002 (−3.062*)
GS (≤7 vs. >7)	82/75	5/8	12/39	0.340 (0.911#)	0.000 (12.801#)	0.001 (10.458#)
SA > 56.15 mg/dL	59.00 (36.88)	8.00 (61.54)	44.00 (86.27)	0.079 (3.082#)	0.000 (37.771#)	0.101 (2.695#)
SA > 65.80 mg/dL	21.00 (13.13)	0.00 (0.00)	25.00 (49.02)	0.341 (0.906#)	0.000 (29.227#)	0.001 (10.458#)

Data are presented as median (P25, P75), n/n, or n (%). *Z-values; #x^2 values; LVD, low-volume disease; HVD, high-volume disease; P1, Group 1 vs. Group 2; P2, Group 1 vs. Group 3; P3, Group 2 vs. Group 3; sta, statistics; PSA, prostate-specific antigen; T, tumor; $P < 0.05$ is considered as statistically significant.

TABLE 5 Univariate and multivariate logistic regression analysis of selected parameters in PCa and its bone metastases.

Variable	Univariate regression			Multivariate regression		
	HR	95% CI of OR	*P*-value	HR	95% CI of OR	*P*-value
Age	0.982	0.947-1.018	0.322	/	/	/
LDH	1.014	1.007-1.022	0.000	/	/	/
AKP	1.034	1.021-1.047	0.000	1.029	1.015-1.044	0.000
AFU	1.042	0.997-1.088	0.066	1.067	1.005-1.132	0.033
FIB	1.409	1.092-1.818	0.008	/	/	/
PSA	1.007	1.004-1.009	0.000	1.005	1.002-1.008	0.000
SA (mg/dL): >56.15 vs. ≤56.15	7.418	3.665-15.014	0.000	2.966	1.203-7.315	0.018
Gleason score	3.023	1.599-5.715	0.001	4.372	1.637-11.673	0.003

PCa, prostate cancer; LDH, lactate dehydrogenase; AKP, alkaline phosphatase; FIB, fibrinogen; PSA, prostate-specific antigen; HR, hazard ratio; P < 0.05 is considered as statistically significant; 95% CI: 95% confidence interval.

and HVD. Among them, age, SA levels, and AKP levels were divided according to their cut-off values. The ROC curve demonstrated good discrimination in predicting PCa (Figure 4A) and in predicting HVD (Figure 4D). In addition, the DCA curves and calibration curves indicated good agreement between the predicted and observed probabilities of bone metastasis (Figures 4B, C) and HVD (Figures 4E, F).

4 Discussion

PCa is a prevalent malignancy among men and is a significant contributor to mortality (33). PCa ranks as the third most frequently detected cancer in males, with an estimated 1.4 million global diagnoses projected for 2021, and it stands as the fifth primary contributor to cancer-related mortality. Various risk factors, encompassing genetic predisposition, advanced age, ethnic background, elevated testosterone levels, and lifestyle choices, significantly influence the initiation of PCa. Moreover, the incidence of PCa exhibits notable variation across diverse geographical regions, with developed and industrialized nations demonstrating a heightened prevalence (34, 35). Furthermore, research suggests that the incidence of PCa is positively correlated with advancing age among patients (34, 36). The overall incidence rate stands at 31 cases per 100,000 males across all age groups, while the lifetime cumulative risk is estimated at 3.9%. Notably, the prevalence of PCa among men aged 75 and above exceeds one in four individuals (37, 38). While the majority of cases are indolent and do not result in death, a substantial number of cases present with intermediate- or high-risk localized, locally advanced, or metastatic cancer despite treatment (39). The primary cause of PCa-related mortality is metastatic disease, which occurs when PCa cells proliferate beyond the prostate and disseminate to other organs, particularly the lungs, liver, bones, and lymph nodes (40). The likelihood of bone metastasis is significantly higher in patients with PCa who present with both osteoblastic and osteolytic lesions (41). The treatment of PCa has become increasingly diverse due to the wide range of available techniques (42). Local therapy is advantageous for many individuals, and patients who undergo radical prostatectomy have a better prognosis than those who receive radiation therapy (43). Presently, androgen deprivation therapy is the standard treatment for metastatic hormone-

TABLE 6 Univariate and multivariate logistic regression analysis of selected parameters in LVD patients and HVD patients.

Variable	Univariate regression			Multivariate regression		
	OR	95% CI of OR	*P*-value	OR	95% CI of OR	*P*-value
Age	0.973	0.901-1.051	0.493	/	/	/
LDH	1.002	0.996-1.008	0.511	/	/	/
AKP	1.018	1.000-1.036	0.046	/	/	/
AFU	0.937	0.857-1.025	0.157	/	/	/
FIB	2.660	1.026-6.891	0.044	/	/	/
PSA	1.008	1.001-1.015	0.021	1.013	1.001-1.025	0.028
SA (mg/dL): >65.80 vs. ≤65.80	1.131	1.026-1.247	0.013	1.194	1.001-1.423	0.048
Gleason score	2.031	0.558-7.388	0.282	31.217	1.985-490.831	0.014

HVD, high-volume disease; LDH, lactate dehydrogenase; AKP, alkaline phosphatase; FIB, fibrinogen; PSA, prostate-specific antigen; HR, hazard ratio; P < 0.05 is considered as statistically significant; 95% CI, 95% confidence interval.

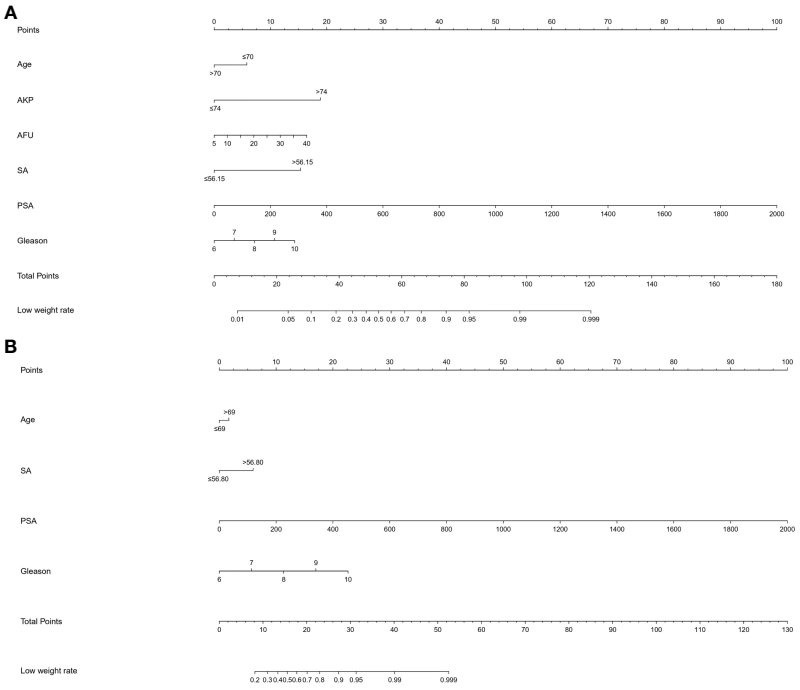

FIGURE 3
(A) A nomogram for predicting bone metastasis of PCa patients. **(B)** A nomogram for predicting HVD patients. The nomogram is used by summing all points identified on the scale for each variable. The total points projected on the bottom scales indicate the probabilities of bone metastasis and HVD. PCa, prostate cancer.

sensitive PCa. Furthermore, the combination of second-generation antiandrogens has been shown to increase the survival rate of men with metastatic castration-resistant PCa (M0 CRPC) (44, 45). However, aggressive treatment methods for PCa can result in significant adverse effects on continence and erectile function (46, 47). Therefore, it is imperative to accurately determine the clinical type and stage of PCa prior to initiating treatment.

Notably, clinically significant disparities between HVD and LVD have been observed in PCa, with LVD often being characterized as oligo-metastatic based on numerous studies (32, 48). Numerous clinical trials have established a correlation between (49–51). Furthermore, a consensus has yet to be reached on the definitions of HVD and LVD. Notably, both CHARTED and LATITUDE scores, which share many similarities, have been identified as significant predictors of survival. Consequently, we have opted to differentiate between HVD and LVD based on the CHARTED experiment's definition (52).

Research has indicated that SA molecules are integral to the process of cancer metastasis. The progression of malignant tumors towards migration, invasion, and metastasis involves alterations in the levels of numerous intracellular and extracellular proteins, as well as modifications to normal cellular behavior, including extracellular matrix degradation, reduced cell adhesion, heightened cell motility, and augmented local microvessel formation, ultimately culminating in metastasis.

Prior research has demonstrated the significant involvement of adhesive glycoproteins in tumor metastasis, whereby the upregulation of 2-6-sialyltransferase and fibronectin expression influences the migratory capacity of mouse liver cancer cells (53). Furthermore, SA has been identified as a mediator of tumor cell adhesion to platelets, white blood cells, and vascular endothelial cells, while also reducing cell adhesion to collagen IV (a constituent of the basement membrane) and intercellular adhesion (54). Moreover, it has been demonstrated that the capacity to interact with nerve cell adhesion molecules can be augmented, thereby promoting the invasion, migration, and metastasis of neoplastic cells (55).

Despite the currently available antitumor pharmacological regimens, bone metastases originating from PCa have yet to be effectively managed. In comparison to antiangiogenic agents and matrix metalloproteinase inhibitors, pharmacotherapy targeting aberrant SA receptors may prove to be a more efficacious strategy in the future for combating tumor metastasis. AL10, a novel sialyltransferase inhibitor, has been shown to impede the adhesion, migration, actin expression, and invasion of malignant cells (56). Furthermore, SA, a molecule exhibiting a strong attraction towards anticancer drugs, presents a promising avenue for the advancement of antitumor therapy. Notably, highly metastatic tumor cells express certain adhesion molecules, including CD22 (57), and exhibit a heightened capacity for binding with SA. Consequently, anticancer drugs bound to SA can accumulate on the surface of tumor or metastatic cells, thereby augmenting the efficacy of the drugs. The development of such drugs has emerged as a prominent area of research.

The present study investigated the levels of SA in 461 patients prior to treatment, in conjunction with other pertinent indices and clinical characteristics. Furthermore, ROC curves were generated to predict bone metastases and HVD in PCa patients based on preoperative SA levels. The optimal diagnostic cut-off value for

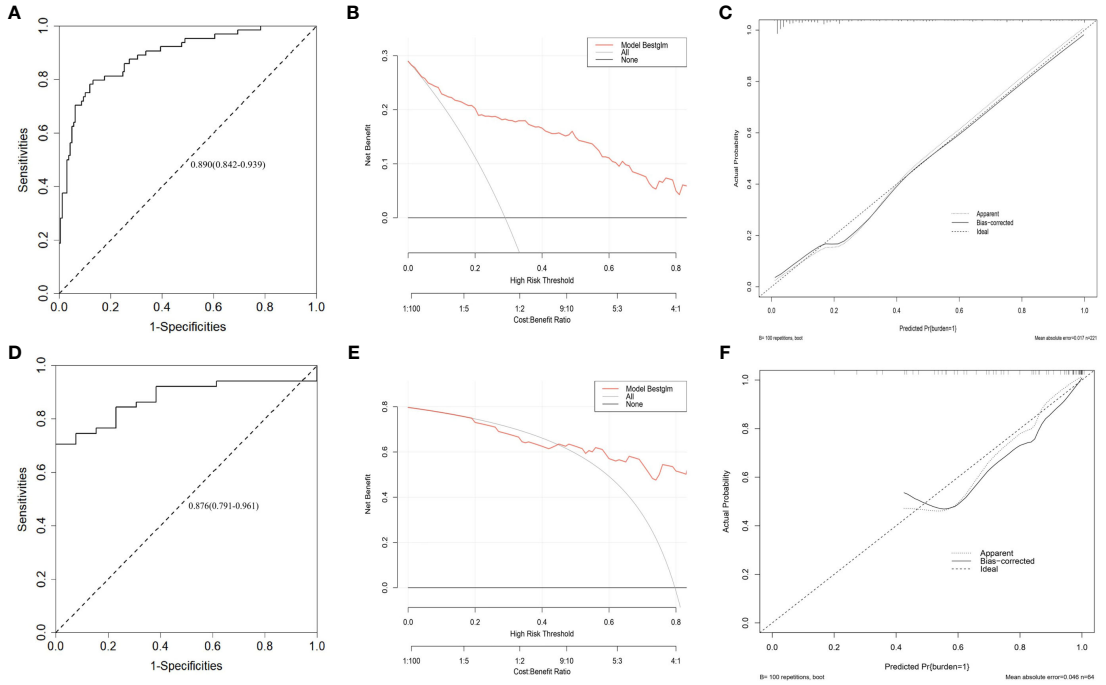

FIGURE 4
ROC curve **(A)**, DCA curve **(B)** and calibration curve **(C)** for assessing the discrimination and calibration of the nomogram in predicting the probabilities of bone metastasis. ROC curve **(D)**, DCA curve **(E)** and calibration curve **(F)** for assessing the discrimination and calibration of the nomogram in predicting the probabilities of HVD.

discriminating between patients with and without bone metastases was determined to be 56.15 mg/dL, while the optimal diagnostic cut-off for distinguishing between LVD and HVD was 65.80 mg/dL. We also presented AUC, sensitivity, and specificity as measures of accuracy. Our findings indicate that an elevated level of SA exhibits high sensitivity and specificity in the diagnosis of bone metastases in patients with PCa. Notably, pretreatment SA levels were significantly higher in patients with HVD compared to non-metastatic patients and patients with LVD. Multivariate regression analysis revealed that SA is independently associated with HVD. Therefore, elevated SA levels may serve as a valuable diagnostic tool for identifying osteometastases and HVD in PCa patients.

In this study, an examination was conducted on pretreatment SA levels in a cohort of 461 patients, alongside other pertinent assay indices and clinical characteristics. Consistent with previous research by Goswami K (58) and Cong Zhang (26) et al., our findings indicate a significant elevation in SA levels among patients with bone metastasis compared to those without, as well as higher SA levels in patients with HVD compared to those with LVD. Subsequently, patients diagnosed with PCa were subsequently stratified based on age, AKP, LDH, FIB, and PSA levels. The findings revealed a strong association between SA levels and LDH, AKP, FIB, and PSA. These results align with the conclusions drawn by Crook MA et al. (59), as no statistically significant correlation was observed between SA levels and age. Furthermore, a notable correlation was observed between SA levels and pathological grade, whereby higher pathological grades were accompanied by elevated SA levels. The patients were categorized into three groups based on the results of ECT: those without bone metastases, those with LVD, and those with HVD. The levels of SA exhibited a gradual increase across the three groups, with SA levels being lowest in the group without bone metastases, followed by the LVD group, and highest in the HVD group. ROC curves were then generated to assess the predictive value of preoperative SA levels for bone metastases and HVD. The optimal diagnostic cut-off points, determined by the maximum Younden index (60), were found to be > 56.15 mg/dL for distinguishing between bone metastases and the absence of bone metastases, and > 65.80 mg/dL for distinguishing between HVD and LVD. The picture also displayed the AUC, sensitivity, and specificity values for determining accuracy. It was evident that elevated SA levels exhibited high sensitivity and specificity in diagnosing bone metastases and HVD in PCa patients. Furthermore, SA levels were included in both univariate and multivariate analyses, which revealed their significance in diagnosing bone metastases and HVD. Consequently, elevated SA levels hold promise in the diagnosis of bone metastases and HVD in PCa patients.

Notwithstanding, there exist several constraints that necessitate consideration in this study. First, a retrospective study was conducted in a single location, which may have led to a statistically significant degree of selection bias. Second, despite the recognition of ECT as the "golden standard" for identifying skeletal metastases, this technique may still yield an erroneous diagnosis for patients with PCa. Third, despite the implementation of rigorous enrollment criteria, it was not

feasible to entirely eliminate conditions that could impact plasma SA levels, such as varicose veins in the lower extremities and atherosclerosis. Finally, certain HVD patients may have had undetected visceral metastases due to inadequate assessment. To validate these findings, it will be imperative to conduct multicenter prospective studies with larger sample sizes.

In summary, pretreatment plasma SA levels exhibit a positive correlation with the number of bone metastases and are independently linked to HVD. These results suggest that SA levels in the bloodstream may serve as a potential marker for more accurate diagnosis and treatment of advanced PCa.

5 Conclusion

The present study established a correlation between SA levels and the clinicopathological characteristics of patients with PCa and HVD. Elevated SA levels prior to surgery could serve as an indicator of increased malignancy risk and advanced cancer stages. The findings of this study suggested that SA levels could serve as a valuable screening and prognostic marker for PCa and HVD.

Author contributions

JS: Data curation, Software, Writing – original draft. TT: Data curation, Writing – review & editing. NW: Software, Writing – original draft. XJ: Software, Writing – original draft. LQ: Writing – review & editing. HC: Methodology, Writing – review & editing. ZL: Methodology, Writing – review & editing. JL: Methodology, Writing – review & editing. LY: Data curation, Writing – review & editing. DL: Methodology, Writing – review & editing.

Funding

The author(s) declare financial support was received for the research, authorship, and/or publication of this article. This study was partly supported by financial grants from the National Nature Science Foundation of China (grant Nos: 82172743, 81502213 and 82102999), the Natural Science Foundation of Shandong Province (grant Nos: ZR2020QH068 and ZR2021MH029).

Acknowledgments

The authors thank Cong Zhang (Fudan University, China) for the critical reading of this manuscript.

Conflict of interest

The authors declare that the research was conducted in the absence of any commercial or financial relationships that could be construed as a potential conflict of interest.

Publisher's note

All claims expressed in this article are solely those of the authors and do not necessarily represent those of their affiliated organizations, or those of the publisher, the editors and the reviewers. Any product that may be evaluated in this article, or claim that may be made by its manufacturer, is not guaranteed or endorsed by the publisher.

References

1. Bernard B, Muralidhar V, Chen Y-H, Sridhar SS, Mitchell EP, Pettaway CA, et al. Impact of ethnicity on the outcome of men with metastatic, hormone-sensitive prostate cancer. *Cancer* (2017) 123:1536–44. doi: 10.1002/cncr.30503

2. Prostate Cancer Working Group of China Anti-Cancer A and Genitourinary Cancer CExpert consensus on genetic testing in Chinese prostate cancer patientedition). *China Oncol* (2018) 28:627–33.

3. Huang Q, Zi H, Luo L, Li X, Zhu C, Zeng X. Secular trends of morbidity and mortality of prostate, bladder, and kidney cancers in Chinto 2019 and their predictions to 2030. *BMC Cancer* (2022) 22. doi: 10.1186/s12885-022-10244-9

4. Chung J-W, Kim HT, Ha Y-S, Lee EH, Chun SY, Lee C-H, et al. Identification of a novel non-invasive biological marker to overcome the shortcomings of PSA in diagnosis and risk stratification for prostate cancer: Initial prospective study of developmental endothelial locus-1 protein. *PloS One* (2021) 16. doi: 10.1371/journal.pone.0250254

5. Scott E, Munkley J. Glycans as biomarkers in prostate cancer. *Int J Mol Sci* (2019) 20. doi: 10.3390/ijms20061389

6. Boerrigter E, Groen LN, Van Erp NP, Verhaegh GW, Schalken JA. Clinical utility of emerging biomarkers in prostate cancer liquid biopsies. *Expert Rev Mol Diagnostics* (2020) 20:219–30. doi: 10.1080/14737159.2019.1675515

7. Wang J, Ni J, Beretov J, Thompson J, Graham P, Li Y. Exosomal microRNAs as liquid biopsy biomarkers in prostate cancer. *Crit Rev Oncol Hematol* (2020) 145. doi: 10.1016/j.critrevonc.2019.102860

8. Nuhn P, De Bono JS, Fizazi K, Freedland SJ, Grilli M, Kantoff PW, et al. Update on systemic prostate cancer therapies: management of metastatic castration-resistant prostate cancer in the era of precision oncology. *Eur Urol* (2019) 75:88–99. doi: 10.1016/j.eururo.2018.03.028

9. Datta K, Muders M, Zhang H, Tindall DJ. Mechanism of lymph node metastasis in prostate cancer. *Future Oncol* (2010) 6:823–36. doi: 10.2217/fon.10.33

10. Norum J, Nieder C. Treatments for metastatic prostate cancer (mPC): A review of costing evidence. *Pharmacoeconomics* (2017) 35:1223–36. doi: 10.1007/s40273-017-0555-8

11. Body J-J, Casimiro S, Costa L. Targeting bone metastases in prostate cancer: improving clinical outcome. *Nat Rev Urol* (2015) 12:340–56. doi: 10.1038/nrurol.2015.90

12. Mollica V, Rizzo A, Rosellini M, Marchetti A, Ricci AD, Cimadamore A, et al. Bone targeting agents in patients with metastatic prostate cancer: state of the art. *Cancers (Basel)* (2021) 13:546. doi: 10.3390/cancers13030546

13. Liu J, Dong Y, Xu D, Zhang C, Lan T, Chang D. Progress in diagnosis of bone metastasis of prostate cancer. *Zhong nan da xue xue bao Yi xue ban = J Cent South Univ Med Sci* (2021) 46:1147–52. doi: 10.11817/j.issn.1672-7347.2021.200999

14. Campana LG, Edhemovic I, Soden D, Perrone AM, Scarpa M, Campanacci L, et al. Electrochemotherapy - Emerging applications technical advances, new indications, combined approaches, and multi-institutional collaboration. *Ejso* (2019) 45:92–102. doi: 10.1016/j.ejso.2018.11.023

15. Kaku H, Saika T, Tsushima T, Nagai A, Yokoyama T, Abarzua F, et al. Combination chemotherapy with estramustine phosphate, ifosfamide and cisplatin for hormone-refractory prostate cancer. *Acta Med Okayama* (2006) 60:43–9. doi: 10.18926/AMO/30759

16. Chittemsetti S, Manchikatla PK, Guttikonda V. Estimation of serum sialic acid in oral submucous fibrosis and oral squamous cell carcinoma. *J Oral Maxillofac Pathol JOMFP* (2019) 23:156–. doi: 10.4103/jomfp.JOMFP_239_18

17. Schauer R, Kamerling JP. Exploration of the sialic acid world. *Adv Carbohydr Chem Biochem* (2018) 75:1–213. doi: 10.1016/bs.accb.2018.09.001

18. Zhang Z, Wuhrer M, Holst S. Serum sialylation changes in cancer. *Glycoconj J* (2018) 35:139–60. doi: 10.1007/s10719-018-9820-0

19. Dedova T, Braicu EI, Sehouli J, Blanchard V. Sialic acid linkage analysis refines the diagnosis of ovarian cancer. *Front Oncol* (2019) 9. doi: 10.3389/fonc.2019.00261

20. Acikgoz E, Duzagac F, Guven U, Yigitturk G, Kose T, Oktem G. "Double hit" strategy: Removal of sialic acid from the dendritic cell surface and loading with CD44 +/CD24-/low cell lysate inhibits tumor growth and metastasis by targeting breast cancer stem cells. *Int Immunopharmacol* (2022) 107. doi: 10.1016/j.intimp.2022.108684

21. Guruaribam VD, Sarumathi T. Relevance of serum and salivary sialic acid in oral cancer diagnostics. *J Cancer Res Ther* (2020) 16:401–4. doi: 10.4103/jcrt.JCRT_512_19

22. Mikkonen JJW, Singh SP, Akhi R, Salo T, Lappalainen R, Gonzalez-Arriagada WA, et al. Potential role of nuclear magnetic resonance spectroscopy to identify salivary metabolite alterations in patients with head and neck cancer. *Oncol Lett* (2018) 16:6795–800. doi: 10.3892/ol.2018.9419

23. Schmidt CQ, Ederveen ALH, Harder MJ, Wuhrer M, Stehle T, Blaum BS. Biophysical analysis of sialic acid recognition by the complement regulator Factor H. *Glycobiology* (2018) 28:765–73. doi: 10.1093/glycob/cwy061

24. Moons SJ, Adema GJ, Derks MTGM, Boltje TJ, Bull C. Sialic acid glycoengineering using N-acetylmannosamine and sialic acid analogs. *Glycobiology* (2019) 29:433–45. doi: 10.1093/glycob/cwz026

25. Pihikova D, Pakanova Z, Nemcovic M, Barath P, Belicky S, Bertok T, et al. Sweet characterisation of prostate specific antigen using electrochemical lectin-based immunosensor assay and MALDI TOF/TOF analysis: Focus on sialic acid. *Proteomics* (2016) 16:3085–95. doi: 10.1002/pmic.201500463

26. Zhang C, Yan L, Song H, Ma Z, Chen D, Yang F, et al. Elevated serum sialic acid levels predict prostate cancer as well as bone metastases. *J Cancer* (2019) 10:449–57. doi: 10.7150/jca.27700

27. Gamat M, McNeel DG. Androgen deprivation and immunotherapy for the treatment of prostate cancer. *Endocr Relat Cancer* (2017) 24:T297–310. doi: 10.1530/ERC-17-0145

28. Evans AJ. Treatment effects in prostate cancer. *Modern Pathol* (2018) 31:110–21. doi: 10.1038/modpathol.2017.158

29. Achard V, Putora PM, Omlin A, Zilli T, Fischer S. Metastatic prostate cancer: treatment options. *Oncology* (2022) 100:48–59. doi: 10.1159/000519861

30. Kyriakopoulos CE, Chen Y-H, Carducci MA, Liu G, Jarrard DF, Hahn NM, et al. Chemohormonal therapy in metastatic hormone-sensitive prostate cancer: long-term survival analysis of the randomized phase III E3805 CHAARTED trial. *J Clin Oncol* (2018) 36:1080. doi: 10.1200/JCO.2017.75.3657

31. Parker CC, James ND, Brawley CD, Clarke NW, Hoyle AP, Ali A, et al. Radiotherapy to the primary tumour for newly diagnosed, metastatic prostate cancer (STAMPEDE): a randomised controlled phase 3 trial. *Lancet* (2018) 392:2353–66. doi: 10.1016/S0140-6736(18)32486-3

32. Xie G-S, Li G, Li Y, Pu J-X, Huang Y-H, Li J-H, et al. Clinical association between pre-treatment levels of plasma fibrinogen and bone metastatic burden in newly diagnosed prostate cancer patients. *Chin Med J* (2019) 132:2684–9. doi: 10.1097/CM9.0000000000000506

33. Sekhoacha M, Riet K, Motloung P, Gumenku L, Adegoke A, Mashele S. Prostate cancer review: genetics, diagnosis, treatment options, and alternative approaches. *Molecules* (2022) 27. doi: 10.3390/molecules27175730

34. Gandaglia G, Leni R, Bray F, Fleshner N, Freedland SJ, Kibel A, et al. Epidemiology and prevention of prostate cancer. *Eur Urol Oncol* (2021) 4:877–92. doi: 10.1016/j.euo.2021.09.006

35. Bray F, Parkin DM, African Canc Registry N. Cancer in sub-Saharan Africa in 2020: a review of current estimates of the national burden, data gaps, and future needs. *Lancet Oncol* (2022) 23:719–28. doi: 10.1016/S1470-2045(22)00270-4

36. Perdana NR, Mochtar CA, Umbas R, Hamid ARA. The risk factors of prostate cancer and its prevention: A literature review. *Acta Med Indonesiana* (2016) 48:228–38.

37. Crocetto F, Barone B, D'Aguanno G, Falcone A, de Vivo R, Rienzo M, et al. Vitamin D, a regulator of androgen levels, is not correlated to PSA serum levels in a cohort of the middle Italy region participating to a prostate cancer screening campaign. *J Clin Med* (2023) 12(5):1831. doi: 10.3390/jcm12051831

38. Giovannucci E. The epidemiology of vitamin D and cancer incidence and mortality: A review (United States). *Cancer Causes Control* (2005) 16:83–95. doi: 10.1007/s10552-004-1661-4

39. Klotz L. Active surveillance in intermediate-risk prostate cancer. *BJU Int* (2020) 125:346–54. doi: 10.1111/bju.14935

40. Pin F, Prideaux M, Bonewald LF, Bonetto A. Osteocytes and cancer. *Curr Osteoporosis Rep* (2021) 19:616–25. doi: 10.1007/s11914-021-00712-9

41. Cui Y-X, Evans BAJ, Jiang WG. New roles of osteocytes in proliferation, migration and invasion of breast and prostate cancer cells. *Anticancer Res* (2016) 36:1193–201.

42. Wallace TJ, Torre T, Grob M, Yu J, Avital I, Bruecher B, et al. Current approaches, challenges and future directions for monitoring treatment response in prostate cancer. *J Cancer* (2014) 5:3–24. doi: 10.7150/jca.7709

43. Sebesta EM, Anderson CB. The surgical management of prostate cancer. *Semin Oncol* (2017) 44:347–57. doi: 10.1053/j.seminoncol.2018.01.003

44. Ritch C, Cookson M. Recent trends in the management of advanced prostate cancer. *F1000Res* (2018) 7. F1000 Faculty Rev-513. doi: 10.12688/f1000research.15382.1

45. Nevedomskaya E, Baumgart SJ, Haendler B. Recent advances in prostate cancer treatment and drug discovery. *Int J Mol Sci* (2018) 19. doi: 10.3390/ijms19051359

46. Fossati N, Willemse P-PM, Van den Broeck T, van den Bergh RCN, Yuan CY, Briers E, et al. The benefits and harms of different extents of lymph node dissection during radical prostatectomy for prostate cancer: A systematic review. *Eur Urol* (2017) 72:84–109. doi: 10.1016/j.eururo.2016.12.003

47. Donovan JL, Hamdy FC, Lane JA, Mason M, Metcalfe C, Walsh E, et al. Patient-reported outcomes after monitoring, surgery, or radiotherapy for prostate cancer. *N Engl J Med* (2016) 375:1425–37. doi: 10.1056/NEJMoa1606221

48. Zhang Y, Ding L, Zheng Y, Wang K, Xia W, Wang J, et al. Retrospective validation of bone risk stratification criteria for men with de novo metastatic hormone-naive prostate cancer in China. *Peerj* (2023) 11. doi: 10.7717/peerj.14500

49. Ibe IK, Sahlstrom A, White A, Henderson SE, Lee FY. Metastatic cancers to bone: an overview and cancer-induced bone loss. *Instructional course lectures* (2019) 68:547–56.

50. Patanaphan V, Salazar OM, Risco R. Breast-cancer - metastatic patterns and their prognosis. *South Med J* (1988) 81:1109–12. doi: 10.1097/00007611-198809000-00011

51. Burlaka AA, Makhmudov DE, Lisnyi II, Paliichuk AV, Zvirych VV, Lukashenko AV. Parenchyma-sparing strategy and oncological prognosis in patients with colorectal cancer liver metastases. *World J Surg Oncol* (2022) 20. doi: 10.1186/s12957-022-02579-1

52. Buelens S, Poelaert F, Dhondt B, Fonteyne V, De Visschere P, Ost P, et al. Metastatic burden in newly diagnosed hormone-naive metastatic prostate cancer: Comparing definitions of CHAARTED and LATITUDE trial. *Urologic Oncology-Seminars Original Investigations* (2018) 36. doi: 10.1016/j.urolonc.2017.12.009

53. Yu S, Fan J, Liu L, Zhang L, Wang S, Zhang J. Caveolin-1 up-regulates integrin α2,6-sialylation to promote integrin α5β1-dependent hepatocarcinoma cell adhesion. *FEBS Lett* (2013) 587:782–7. doi: 10.1016/j.febslet.2013.02.002

54. Rivadeneyra L, Falet H, Hoffmeister KM. Circulating platelet count and glycans. *Curr Opin Hematol* (2021) 28:431–7. doi: 10.1097/MOH.0000000000000682

55. Crespo HJ, Lau JTY, Videira PA. Dendritic cells: a spot on sialic acid. *Front Immunol* (2013) 4. doi: 10.3389/fimmu.2013.00491

56. Chiang C-H, Wang C-H, Chang H-C, More SV, Li W-S, Hung W-C. A novel sialyltransferase inhibitor AL10 suppresses invasion and metastasis of lung cancer cells by inhibiting integrin-mediated signaling. *J Cell Physiol* (2010) 223:492–9. doi: 10.1002/jcp.22068

57. Pluvinage JV, Sun J, Claes C, Flynn RA, Haney MS, Iram T, et al. The CD22-IGF2R interaction is a therapeutic target for microglial lysosome dysfunction in Niemann-Pick type C. *Sci Trans Med* (2021) 13. doi: 10.1126/scitranslmed.abg2919

58. Goswami K, Nandeesha H, Koner BC, Nandakumar DN. A comparative study of serum protein-bound sialic acid in benign and Malignant prostatic growth: possible role of oxidative stress in sialic acid homeostasis. *Prostate Cancer Prostatic Dis* (2007) 10:356–9. doi: 10.1038/sj.pcan.4500965

59. Crook MA, Tutt P, Pickup JC. Elevated serum sialic-acid concentration in niddm and its relationship to blood-pressure and retinopathy. *Diabetes Care* (1993) 16:57–60. doi: 10.2337/diacare.16.1.57

60. Hanley JA, McNeil BJ. The meaning and use of the area under A receiver operating characteristic (Roc) curve. *Radiology* (1982) 143:29–36. doi: 10.1148/radiology.143.1.7063747

frontiers | Frontiers in Endocrinology

TYPE Original Research
PUBLISHED 09 February 2024
DOI 10.3389/fendo.2024.1358416

OPEN ACCESS

EDITED BY
Anna Perri,
Magna Græcia University of Catanzaro, Italy

REVIEWED BY
Xiaoqiang Wang,
City of Hope, United States
Marcos Edgar Herkenhoff,
University of São Paulo, Brazil
Mudasir Rashid,
Howard University Hospital, United States

*CORRESPONDENCE
Xiaoqiang Liu
xiaoqiangliu1@163.com

†These authors have contributed equally to this work

RECEIVED 19 December 2023
ACCEPTED 26 January 2024
PUBLISHED 09 February 2024

CITATION
Hao X, Ren C, Zhou H, Li M, Zhang H and Liu X (2024) Association between circulating immune cells and the risk of prostate cancer: a Mendelian randomization study. *Front. Endocrinol.* 15:1358416. doi: 10.3389/fendo.2024.1358416

Association between circulating immune cells and the risk of prostate cancer: a Mendelian randomization study

Xuexue Hao†, Congzhe Ren†, Hang Zhou†, Muwei Li, Hao Zhang and Xiaoqiang Liu*

Department of Urology, Tianjin Medical University General Hospital, Tianjin, China

Background: There is still limited research on the association between immune cells and the risk of prostate cancer. Further investigations are warranted to comprehend the intricate associations at play.

Methods: We used a bidirectional two-sample Mendelian randomization (MR) analysis to investigate the causal relationship between immune cell phenotypes and prostate cancer. The summary data for immune cell phenotypes was derived from a study cohort, including 3,757 individuals from Sardinia with data on 731 immune cell phenotypes. The summary data for prostate cancer were obtained from the UK Biobank database. Sensitivity analyses were conducted, and the combination of MR-Egger and MR-Presso was used to assess horizontal pleiotropy. Cochran's Q test was employed to evaluate heterogeneity, and the results were subjected to FDR correction.

Results: Our study identified two immune cell phenotypes significantly associated with the risk of prostate cancer, namely CD25 on naive-mature B cells (OR = 0.998, 95% CI, 0.997-0.999, *P* = 2.33E-05, FDR = 0.017) and HLA DR on CD14- CD16- cells (OR = 1.001, 95% CI, 1.000-1.002, *P* = 8.01E-05, FDR = 0.03). When adjusting FDR to 0.2, we additionally found six immune cell phenotypes influencing the incidence of prostate cancer. These include FSC-A on B cells (OR = 1.002, 95% CI, 1.001-1.002, *P* = 7.77E-04, FDR = 0.133), HLA DR on plasmacytoid dendritic cells (OR = 1.001, 95% CI, 1.000-1.001, *P* = 0.001, FDR = 0.133), CD14+ CD16- monocyte % monocytes (OR = 1.002, 95% CI, 1.001-1.003, *P* = 0.001, FDR = 0.133), and HVEM on effector memory CD4+ T cells (OR = 1.001, 95% CI, 1.000-1.002, *P* = 0.002, FDR = 0.169), which are positively correlated with the risk of prostate cancer. Conversely, CD25 on IgD+ B cells (OR = 0.998, 95% CI, 0.997-0.999, *P* = 0.002, FDR = 0.169) and Monocytic Myeloid-Derived Suppressor Cells AC (OR = 0.999, 95% CI, 0.999-1.000, *P* = 0.002, FDR = 0.17) are negatively correlated with the risk of prostate cancer.

Conclusion: This study has revealed causal relationships between immune cell phenotypes and prostate cancer, supplying novel insights that might aid in identifying potential therapeutic targets of prostate cancer.

KEYWORDS

prostate cancer, immune cells, Mendelian randomization study, causality, reverse causality

Introduction

Prostate cancer is the second most common cancer in males, with an incidence rate second only to lung cancer. It is also the most common cancer in the male urinary system (1). The incidence of prostate cancer increases with the age of males (2). Additionally, there are significant differences in the incidence of prostate cancer based on race and geographic location. There is a 40-fold difference in incidence rates between African American males with the highest incidence and native Asian males with the lowest incidence in the United States (3). Western Europe, Northern Europe, North America, and other countries are high-incidence regions for prostate cancer, while regions such as Asia and North Africa have relatively lower incidence rates of prostate cancer (4). In addition to recognized age factors, risk factors for prostate cancer also include genetics, baldness, height, and others. Additionally, there are modifiable risk factors, including diet, smoking, and alcohol consumption (5).

An increasing number of studies have found a complex and close association between the immune system and cancer (6, 7). Many immunotherapies, such as immune checkpoint inhibitors or direct targeting of the tumor immune microenvironment, are used in cancer treatment, focusing on various immune cells within the immune system (8). Under normal circumstances, immune cells exert anti-tumor effects through immune surveillance and immune cytotoxicity. However, under certain conditions, certain immune cells may also promote the progression of tumors (9). This dual effect of immune cells occurs in various cancers. Studies have found a positive correlation between higher levels of FOXP3+ T cells mediating immune tolerance and lower levels of CD8+ T cells mediating cytotoxicity with the risk of breast cancer, colorectal cancer, and lung cancer in normal healthy populations (10). Similarly, research suggests that changes in the composition of immune cell tissues are linked to an elevated or reduced risk of specific cancers (11).. Immune cells also play a crucial role in prostate cancer (12–14). Studying the connection between immune cells and prostate cancer will contribute to exploring the mechanisms of prostate cancer, providing more potential treatment methods, and alleviating the burden on patients and society. Currently, there is still limited research on the association between immune cells and the risk of prostate cancer (15). More studies are needed to understand the complex connections involved.

Mendelian randomization (MR) is a method that utilizes genetic variations as instrumental variables (IVs) to assess observed causal relationships (16). The purpose of this approach is to simulate a randomized controlled trial, mitigating the influence of potential confounding factors in observational studies (17). Traditional observational studies determine disease risk factors by examining the relationship between exposure and outcomes. However, these studies may be limited in drawing valid causal conclusions due to confounding factors or reverse causation (18). Compared to traditional observational studies, MR is valuable for investigating causal relationships between risk factors and clinical diseases because genetic variations are randomly assigned at conception, typically unrelated to confounding factors, and unaffected by reverse causation (19). Our research aims to explore a causal relationship between immune cell traits and prostate cancer through a comprehensive two-sample bidirectional MR analysis.

Methods

Study design

The flowchart of the two-sample bidirectional Mendelian randomization (MR) analysis for immune cell phenotypes and the risk of prostate cancer is depicted in Figure 1. Initially, we employ immune cell phenotypes as the exposure to analyze which immune cell phenotypes may have potential causal relationships with the risk of prostate cancer. Subsequently, we use prostate cancer as the exposure and explore the potential reverse causal relationships with immune cell phenotypes. Single nucleotide polymorphisms (SNPs) are utilized as IVs in the study. The selected IVs satisfy three crucial assumptions: (1) IVs are associated with the risk exposure. (2) IVs are unrelated to any confounding factors influencing the exposure-outcome relationship. (3) IVs can only affect the outcome through the exposure and not through any other pathways (20). Any IVs violating the three major assumptions will be excluded.

Data sources

Immunology-related GWAS data sources

Our research data is derived from open GWAS databases and the UK Biobank database. The studies involved have all been approved by the local ethics committee. This study did not collect new data and does not require new ethical approval.

The summary statistics of immune cell phenotypes are derived from the GWAS database. GWAS data identifier from GCST90001391 to GCST90002121 (https://www.ebi.ac.uk/gwas/studies/GCST90002121). A cohort study involving 3,757 Sardinian individuals reported data on 22 million variants for 731 immune cell phenotypes. The 731 immune cell phenotypes consist of 118 absolute cell counts (AC), 192 relative counts (RC), 389 median fluorescence intensities (MFIs) of surface antigens, and 32 morphological parameters (MP).

This study involved the collection of peripheral blood from blood donors, which was then subjected to flow cytometry analysis following antibody staining. This process allowed for the identification and quantification of different cell subpopulations (21).

GWAS data sources for prostate cancer

Prostate cancer data were obtained from the UK Biobank database, comprising a study population of 462,933 individuals of European descent. The case group consisted of 3,269 individuals, and the control group included 459,664 individuals, involving 9,851,867 SNPs.

Selection of IVs

We set the threshold for SNPs related to immune cell phenotypes at $P < 1 \times 10^{-5}$. Additionally, we conducted a Linkage Disequilibrium (LD) check on these SNPs ($r^2 = 0.001$ and kb = 10,000). The values of r^2 or kb represent the degree of linkage disequilibrium between two loci, indicating that if there is LD between two loci, their allele frequencies are not independent but correlated in some way. For SNPs related to prostate cancer, we

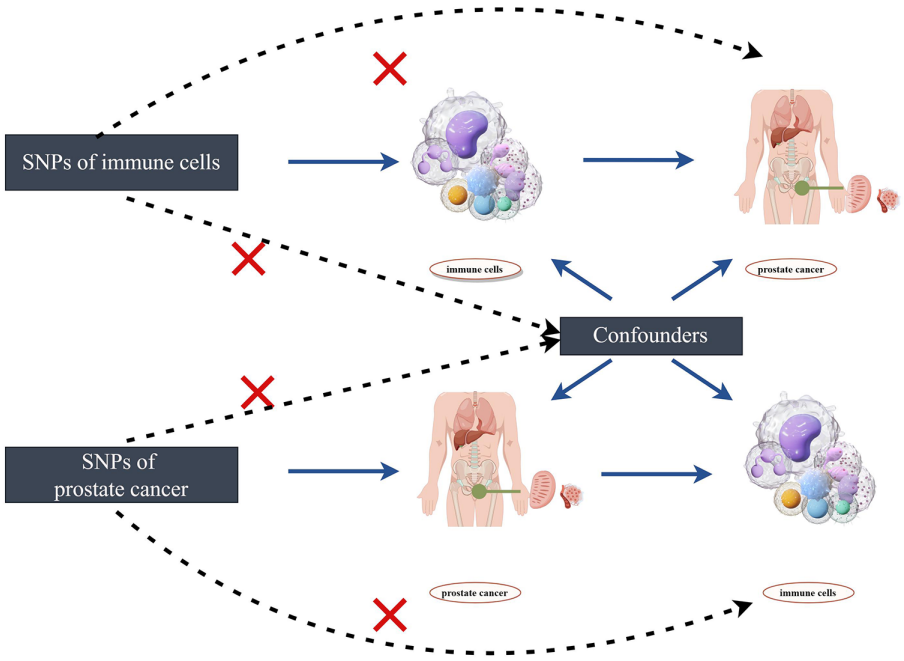

FIGURE 1
The design of bidirectional Mendelian randomization (MR) study by Figdraw.

applied a threshold of $P < 5 \times 10^{-8}$ and similarly performed LD checks ($r^2 = 0.001$ and kb = 10,000). We calculated the F-statistic for each SNP, and SNPs with low F-values (< 10) were removed as IVs to assess IV strength and mitigate weak instrument bias (22). Finally, we utilized the PhenoScanner database to exclude SNPs associated with potential confounding variables.

Statistical analysis

In order to explore the causal relationship between immune cell phenotypes and the risk of prostate cancer, this study primarily utilized the TwoSampleMR and MRPRESSO packages in R (4.2.3). The main conventional MR analysis methods employed included Inverse Variance Weighting (IVW), MR-Egger, Weighted Median, Weighted Mode, and MR-Presso. Depending on the specific situation, choose random or fixed-effect IVW. IVW, as the primary analytical method, aims to estimate the causal relationship between exposure factors and outcomes by combining the effects of various genetic variations, providing a comprehensive causal estimation. However, IVW has limitations as it relies on the three fundamental assumptions mentioned earlier and can only avoid the influence of confounding factors in the absence of horizontal pleiotropy. Therefore, when using the IVW method, the potential for horizontal pleiotropy must be considered (23).

In this study, we employed a combination of MR-Egger and MR-Presso to assess the presence of horizontal pleiotropy ($P < 0.05$ considered to indicate horizontal pleiotropy). Additionally, Cochran's Q test was utilized to assess heterogeneity among the selected SNPs ($P < 0.05$ considered to indicate heterogeneity). Compared to MR-Egger, which detects and quantifies the degree of horizontal pleiotropy through intercept testing, MR-Presso can identify and address outliers beyond horizontal pleiotropy (24).

To explore reverse causality, the same methods were used for reverse MR analysis of immune cell phenotypes and prostate cancer. Moreover, considering the issue of multiple testing, FDR correction was performed using the online tool Bioladder. According to previous studies, FDR < 0.2 is considered suggestive of a causal relationship, while FDR < 0.05 is considered to indicate a significant causal relationship.

Results

The causal effect of immunophenotypes on prostate cancer

We first analyzed the causal effects of 731 immune cell phenotypes as exposure variables on prostate cancer, and the results of the analysis are shown in Figure 2. Our research findings revealed that two immune cell phenotypes are significantly associated with the risk of prostate cancer. Specifically, CD25 on naive-mature B cells (OR = 0.998, 95% CI, 0.997-0.999, P = 2.33E-05, FDR = 0.017) shows a significant negative correlation with the risk of prostate cancer, while HLA DR on CD14- CD16- cells (OR = 1.001, 95% CI, 1.000-1.002, P = 8.01E-05, FDR = 0.03) exhibits a significant positive correlation with the risk of prostate cancer. When adjusting the false discovery rate (FDR) to 0.2, we identified associations between six immune cell phenotypes and the risk of prostate cancer. Among them, FSC-A on B cells (OR = 1.002, 95% CI, 1.001-1.002, P = 7.77E-04, FDR = 0.133), HLA DR on plasmacytoid dendritic cells (OR = 1.001, 95% CI, 1.000-1.001, P = 0.001, FDR = 0.133), CD14+ CD16- monocyte % monocytes (OR = 1.002, 95% CI, 1.001-1.003, P = 0.001, FDR = 0.133), and HVEM on effector memory CD4+ T cells (OR = 1.001, 95% CI, 1.000-

10.3389/fendo.2024.1358416

Traits	method	nsnp	pval	PFDR	OR(95%CI)	Heterogeneity.P	Pleiotropy.P	PRESSO.GlobalTest.P
	MR Egger	10	0.607		0.999(0.994 to 1.004)	0.549		
	Weighted median	10	0.021		0.999(0.997 to 1.000)			
CD25 on naive-mature B cell	Inverse variance weighted	10	2.33e-05	0.017	0.998(0.997 to 0.999)	0.645	0.841	0.717
	Simple mode	10	0.203		0.999(0.997 to 1.001)			
	Weighted mode	10	0.126		0.999(0.997 to 1.000)			
	MR Egger	8	0.008		1.002(1.001 to 1.002)	0.378		
	Weighted median	8	0.006		1.001(1.001 to 1.002)			
HLA DR on CD14- CD16-	Inverse variance weighted	8	8.01e-05	0.03	1.001(1.000 to 1.002)	0.107	0.066	0.222
	Simple mode	8	0.221		1.001(1.000 to 1.002)			
	Weighted mode	8	0.005		1.001(1.001 to 1.002)			
	MR Egger	9	0.293		1.003(0.998 to 1.007)	0.462		
	Weighted median	9	0.138		1.001(1.000 to 1.002)			
FSC-A on B cell	Inverse variance weighted	9	7.77e-04	0.133	1.002(1.001 to 1.002)	0.543	0.634	0.593
	Simple mode	9	0.402		1.001(0.999 to 1.003)			
	Weighted mode	9	0.416		1.001(0.999 to 1.003)			
	MR Egger	7	0.545		0.997(0.989 to 1.005)	0.791		
	Weighted median	7	0.020		0.998(0.997 to 1.000)			
CD25 on IgD+ B cell	Inverse variance weighted	7	7.84e-04	0.133	0.998(0.997 to 0.999)	0.875	0.845	0.891
	Simple mode	7	0.200		0.999(0.996 to 1.001)			
	Weighted mode	7	0.173		0.999(0.997 to 1.000)			
	MR Egger	10	0.019		1.001(1.000 to 1.001)	0.61		
	Weighted median	10	4.09e-04		1.001(1.000 to 1.001)			
HLA DR on plasmacytoid Dendritic Cell	Inverse variance weighted	10	0.001	0.133	1.001(1.000 to 1.001)	0.613	0.37	0.558
	Simple mode	10	0.620		1.000(0.999 to 1.001)			
	Weighted mode	10	0.009		1.001(1.000 to 1.001)			
	MR Egger	9	0.087		1.007(1.000 to 1.015)	0.786		
	Weighted median	9	0.005		1.002(1.001 to 1.003)			
CD14+ CD16- monocyte %monocyte	Inverse variance weighted	9	0.001	0.133	1.002(1.001 to 1.003)	0.604	0.162	0.661
	Simple mode	9	0.114		1.002(1.000 to 1.004)			
	Weighted mode	9	0.076		1.002(1.000 to 1.004)			
	MR Egger	12	0.843		1.000(0.997 to 1.003)	0.113		
	Weighted median	12	0.296		1.000(1.000 to 1.001)			
HVEM on Effector Memory CD4+ T cell	Inverse variance weighted	12	0.002	0.169	1.001(1.000 to 1.002)	0.122	0.443	0.116
	Simple mode	12	0.748		1.000(0.999 to 1.002)			
	Weighted mode	12	0.804		1.000(0.999 to 1.001)			
	MR Egger	11	0.058		0.999(0.998 to 1.000)	0.52		
	Weighted median	11	0.009		0.999(0.999 to 1.000)			
Monocytic Myeloid-Derived Suppressor Cells AC	Inverse variance weighted	11	0.002	0.17	0.999(0.999 to 1.000)	0.515	0.334	0.499
	Simple mode	11	0.200		0.999(0.998 to 1.000)			
	Weighted mode	11	0.031		0.999(0.998 to 1.000)			

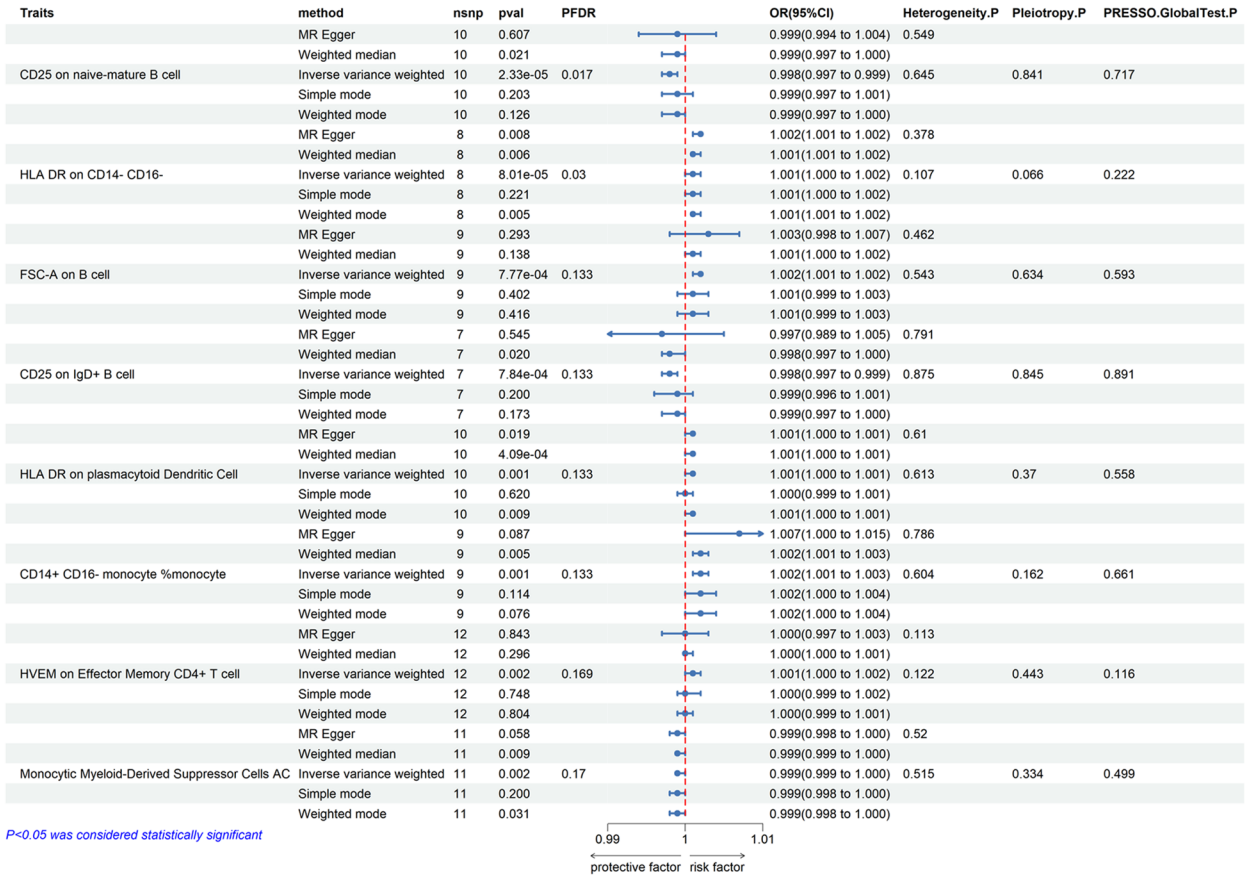

FIGURE 2
Forest plots showed the causal effect of immunophenotypes on prostate cancer. nsnp, nonsynonymous single-nucleotide polymorphism; OR, odds ratio; CI, confidence interval; PFDR, P value corrected by FDR.

1.002, $P = 0.002$, FDR = 0.169) are positively correlated with the risk of prostate cancer, while CD25 on IgD+ B cells (OR = 0.998, 95% CI, 0.997-0.999, $P = 0.002$, FDR = 0.169) and Monocytic Myeloid-Derived Suppressor Cells AC (OR = 0.999, 95% CI, 0.999-1.000, $P = 0.002$, FDR = 0.17) are negatively correlated with the risk of prostate cancer. Subsequently, a horizontal pleiotropy test was conducted using MR-Egger and MR-Presso in combination. No horizontal pleiotropy was detected in the above results, and Cochran's Q test revealed no heterogeneity in all outcomes. Following that, scatter plots and funnel plots also supported these findings (Supplementary Figures 1, 2). We further employed a heatmap for visual analysis of the research results. Initially, we filtered out the IDs of all positive results of immune cell phenotypes based on the p-values from the IVW method. Subsequently, different colors in Figure 3 represent the p-values of sensitivity analysis results for each immune cell phenotype.

The causal effect of I prostate cancer on immunophenotypes

In the reverse MR analysis, we identified some positive results, but after FDR correction (FDR < 0.05), no statistically significant results were observed. Similarly, after adjusting to FDR < 0.2, no meaningful results were detected.

Discussion

Through a two-sample bidirectional MR study, we identified two immune cell phenotypes significantly associated with the risk of prostate cancer (FDR < 0.05). After adjusting for FDR < 0.20, an additional six immune cell phenotypes were found to be related to the risk of prostate cancer. In the reverse MR analysis, we also observed some positive results; however, after FDR correction, no significant correlations were identified.

Our study revealed a significant negative correlation between CD25 on naive-mature B cells and the risk of prostate cancer. Additionally, CD25 on IgD+ B cells also showed a negative correlation with the risk of prostate cancer, while FSC-A on B cells exhibited a positive correlation with the risk of prostate cancer. CD25 constitutes a component of the interleukin-2 (IL-2) receptor and is exhibited on the surface of diverse immune and non-immune cellular entities (25). The role of CD25 may vary significantly depending on its expression on different cell types. Regulatory T cells (Tregs) promote tumor progression, and CD25 is widely expressed on Tregs. Studies have found that depleting Tregs through anti-CD25 antibodies can exert an anti-tumor immune effect (26–28). However, recent research has found that agonists preserving the activity of CD25 can activate tumor-specific CD8 T cells, exerting an anti-tumor immune effect (29). These studies

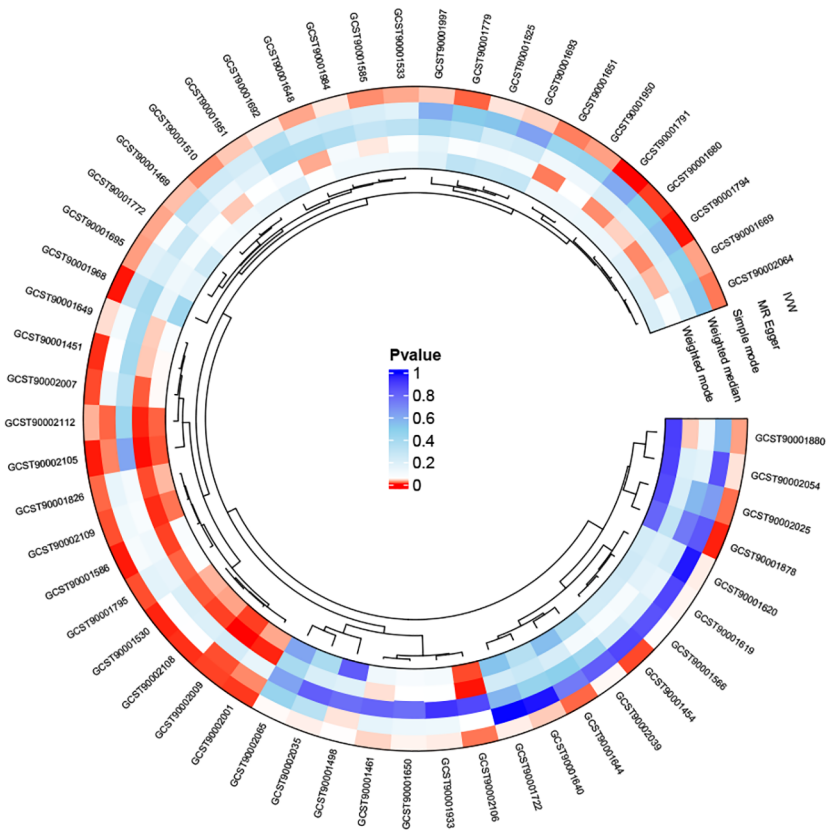

FIGURE 3
The heatmap depicting the IDs of immune cell phenotypes with positive results and the p-values from the sensitivity analysis: The outer circle represents the IDs of immune cell phenotypes, while the inner circle uses different colors to indicate the p-values of different sensitivity analysis results.

highlight the complex and crucial role of CD25 in tumor immunotherapy. Our study found that CD25 on naive-mature B cells and CD25 on IgD+ B cells are protective factors against prostate cancer. This finding aligns with similar conclusions from current research. Naive-mature B cells refer to B cells that have matured but have not been activated. In tumor immunity, naive-mature B cells may play an anti-tumor role by stimulating immune responses and assisting other immune cells (29). IgD+ B cells are a subset of B cells in the immune system, and they engage in immune responses through the surface expression of IgD. On B cells, IgD can coexist with other immunoglobulins, collectively regulating immune reactions (30). Studies have found the expansion of clonal B cells in both the blood and sentinel lymph nodes of prostate cancer patients, with a predominant presence of immature B cells in the blood (12). This reflects the protective role of B cells, including immature B cells, in prostate cancer.

Our study identified HLA DR on CD14- CD16-, CD14+ CD16- monocyte %monocyte, and HLA DR on plasmacytoid Dendritic Cell as risk factors for the incidence of prostate cancer. CD14 and CD16 are surface markers on immune cells, playing crucial roles in signal recognition, signal transduction, and enhancement of immune responses. They exert significant functions in both tumor and non-tumor diseases (31, 32). In the Monocyte panel, they were identified based on HLA-DR positivity. Pavlovic et al. has found reduced expression of the monocyte HLA-DR molecule in prostate cancer (33). A previous study indicated that enhancing monocyte function in the human body can be achieved by upregulating HLA-DR, contributing to anti-prostate cancer effects (34). Monocytes were categorized into classical cells (CD14+CD16−), non-classical cells (CD14−CD16+), and intermediate cells (CD14+CD16+) (21). Although the role of HLA-DR on CD14-CD16- is rarely mentioned, a recent study (35) still highlights its significant involvement in schizophrenia, warranting further attention. Currently, there is no dedicated study on the specific mechanism of HLA DR on CD14- CD16- in the development of prostate cancer. Further research is needed to validate our findings and explore the potential mechanisms involved. Plasmacytoid Dendritic Cells are multifunctional immune cells, and their clinical significance in the tumor microenvironment (TME) remains unclear (36), previous studies have found the immunosuppressive role of plasmacytoid dendritic cells in gastric cancer (37). The mechanisms by which they function in prostate cancer still require further exploration. Our study also found that Monocytic Myeloid-Derived Suppressor Cells (M-MDSCs) may be a potential protective factor in the development of prostate cancer. M-MDSC and polymorphonuclear MDSC (PMN-MDSC) are two

main cellular subtypes of myeloid-derived suppressor cells (MDSCs). Morphologically, M-MDSCs resemble monocytes, while PMN-MDSCs have a multi-lobed nucleus similar to polymorphonuclear (PMN) cells. Moreover, these two subtypes express different surface molecules, and their distribution varies across different tumors (38). Previous studies have found that PMN-MDSCs contribute to the progression and immune evasion of prostate cancer (39, 40). Idorn et al. have identified increased expression of M-MDSCs in patients with castration-resistant prostate cancer, suggesting its involvement in the immune suppressive environment of prostate cancer patients (41). Further specific research is needed to elucidate these findings.

The strengths of our study include the first-time application of MR methods to investigate the relationship between immune cell phenotypes and prostate cancer. Our conclusions were derived under strict examination of horizontal pleiotropy, reducing the interference of confounding factors and the impact of reverse causality on the results. Additionally, our study identified immune cell phenotypes significantly associated with prostate cancer, which have been less explored in previous research. This may provide new insights for exploring potential immunotherapeutic targets in prostate cancer. Our study also has some limitations. Although we included 731 immune cell phenotypes in our research, there are still some immune cell phenotypes that could not be analyzed due to data limitations. Additionally, since the data sources are predominantly of European descent, limited to adults, and do not support stratification by gender and age, this may impact the generalizability and accuracy of the results. This study is based on a cohort study of individuals from Sardinia. The Sardinian population possesses unique genetic characteristics, and the study conclusions may not be applicable to broader populations. Future validation in larger and more diverse patient cohorts is necessary to ensure the robustness and generalizability of our conclusions. Furthermore, the selection of instrumental variables for immune cell phenotypes ($P < 1\times10-5$) and the interpretation of reverse results (FDR < 0.2) are not as stringent. Finally, we hope that future research will involve larger sample sizes and more comprehensive Mendelian randomization studies to further explore the relationship between immune cell phenotypes and prostate cancer.

Conclusions

This study has revealed causal relationships between immune cell phenotypes and prostate cancer, supplying novel insights that might aid in comprehending the pathogenic mechanisms of prostate cancer and identifying potential therapeutic targets.

Data availability statement

The original contributions presented in the study are included in the article/Supplementary Material. Further inquiries can be directed to the corresponding author.

Ethics statement

Ethical approval was not required for the study involving humans in accordance with the local legislation and institutional requirements. Written informed consent to participate in this study was not required from the participants or the participants' legal guardians/next of kin in accordance with the national legislation and the institutional requirements.

Author contributions

XH: Writing – review & editing, Methodology, Software, Writing – original draft. CR: Writing – original draft, Software. HZho: Writing – original draft, Investigation. ML: Data curation, Writing – review & editing. HZha: Data curation, Writing – review & editing. XL: Project administration, Supervision, Writing – review & editing.

Funding

The author(s) declare financial support was received for the research, authorship, and/or publication of this article. The study received funding from the Chinese National Natural Science Funds (82171594).

Acknowledgments

Thanks to GWAS database contributors for sharing the data.

Conflict of interest

The authors declare that the research was conducted in the absence of any commercial or financial relationships that could be construed as a potential conflict of interest.

Publisher's note

Supplementary material

The Supplementary Material for this article can be found online at: https://www.frontiersin.org/articles/10.3389/fendo.2024.1358416/full#supplementary-material

References

1. Rebello RJ, Oing C, Knudsen KE, Loeb S, Johnson DC, Reiter S, et al. Prostate cancer. *Nat Rev Dis Primers* (2021) 7:8. doi: 10.1038/s41572-021-00249-2

2. Belkahla S, Nahvi I, Biswas S, Nahvi I, Ben Amor N. Advances and development of prostate cancer, treatment, and strategies: A systemic review. *Front Cell Dev Biol* (2022) 10:991330. doi: 10.3389/fcell.2022.991330

3. Pernar CH, Ebot EM, Wilson KM, Mucci LA. The epidemiology of prostate cancer. *Cold Spring Harbor Perspect Med* (2018) 8:a030361. doi: 10.1101/cshperspect.a030361

4. Vickers AJ, Elfiky A, Freeman VL, Roach M 3rd. Race, biology, disparities, and prostate cancer. *Eur Urol* (2022) 81:463–5. doi: 10.1016/j.eururo.2022.02.007

5. Bergengren O, Pekala KR, Matsoukas K, Fainberg J, Mungovan SF, Bratt O, et al. 2022 Update on prostate cancer epidemiology and risk factors-A systematic review. *Eur Urol* (2023) 84:191–206. doi: 10.1016/j.eururo.2023.04.021

6. Gonzalez H, Hagerling C, Werb Z. Roles of the immune system in cancer: from tumor initiation to metastatic progression. *Genes Dev* (2018) 32:1267–84. doi: 10.1101/gad.314617.118

7. Hiam-Galvez KJ, Allen BM, Spitzer MH. Systemic immunity in cancer. *Nat Rev Cancer* (2021) 21:345–59. doi: 10.1038/s41568-021-00347-z

8. Tang T, Huang X, Zhang G, Hong Z, Bai X, Liang T. Advantages of targeting the tumor immune microenvironment over blocking immune checkpoint in cancer immunotherapy. *Signal Transduction Targeted Ther* (2021) 6:72. doi: 10.1038/s41392-020-00449-4

9. Peña-Romero AC, Orenes-Piñero E. Dual effect of immune cells within tumour microenvironment: pro- and anti-tumour effects and their triggers. *Cancers* (2022) 14:1681. doi: 10.3390/cancers14071681

10. Song M, Tworoger SS. Systemic immune response and cancer risk: filling the missing piece of immuno-oncology. *Cancer Res* (2020) 80:1801–3. doi: 10.1158/0008-5472.CAN-20-0730

11. Palomero L, Galván-Femenía I, de Cid R, Espín R, Barnes DR, Cimba, et al. Immune cell associations with cancer risk. *iScience* (2020) 23:101296. doi: 10.1016/j.isci.2020.101296

12. Saudi A, Banday V, Zirakzadeh AA, Selinger M, Forsberg J, Holmbom M, et al. Immune-activated B cells are dominant in prostate cancer. *Cancers* (2023) 15:920. doi: 10.3390/cancers15030920

13. Andersen LB, Nørgaard M, Rasmussen M, Fredsøe J, Borre M, Ulhøi BP, et al. Immune cell analyses of the tumor microenvironment in prostate cancer highlight infiltrating regulatory T cells and macrophages as adverse prognostic factors. *J Pathol* (2021) 255:155–65. doi: 10.1002/path.5757

14. Molina OE, LaRue H, Simonyan D, Hovington H, Têtu B, Fradet V, et al. High infiltration of CD209(+) dendritic cells and CD163(+) macrophages in the peritumor area of prostate cancer is predictive of late adverse outcomes. *Front Immunol* (2023) 14:1205266. doi: 10.3389/fimmu.2023.1205266

15. Kwon JTW, Bryant RJ, Parkes EE. The tumor microenvironment and immune responses in prostate cancer patients. *Endocrine-related Cancer* (2021) 28:T95–t107. doi: 10.1530/ERC-21-0149

16. Sekula P, Del Greco MF, Pattaro C, Köttgen A. Mendelian randomization as an approach to assess causality using observational data. *J Am Soc Nephrol: JASN* (2016) 27:3253–65. doi: 10.1681/ASN.2016010098

17. Bowden J, Holmes MV. Meta-analysis and Mendelian randomization: A review. *Res Synthesis Methods* (2019) 10:486–96. doi: 10.1002/jrsm.1346

18. Kim MS, Song M, Shin JI, Won HH. How to interpret studies using Mendelian randomisation. *BMJ Evidence-Based Med* (2023) 28:251–4. doi: 10.1136/bmjebm-2022-112149

19. Weith M, Beyer A. The next step in Mendelian randomization. *eLife* (2023) 12: e86416. doi: 10.7554/eLife.86416

20. Lor GCY, Risch HA, Fung WT, Au Yeung SL, Wong IOL, Zheng W, et al. Reporting and guidelines for mendelian randomization analysis: A systematic review of oncological studies. *Cancer Epidemiol* (2019) 62:101577. doi: 10.1016/j.canep.2019.101577

21. Orrù V, Steri M, Sidore C, Marongiu M, Serra V, Olla S, et al. Complex genetic signatures in immune cells underlie autoimmunity and inform therapy. *Nat Genet* (2020) 52:1036–45. doi: 10.1038/s41588-020-0684-4

22. Wang K, Han S. Effect of selection bias on two sample summary data based Mendelian randomization. *Sci Rep* (2021) 11:7585. doi: 10.1038/s41598-021-87219-6

23. Mbutiwi FIN, Dessy T, Sylvestre MP. Mendelian randomization: A review of methods for the prevention, assessment, and discussion of pleiotropy in studies using the fat mass and obesity-associated gene as an instrument for adiposity. *Front Genet* (2022) 13:803238. doi: 10.3389/fgene.2022.803238

24. Boehm FJ, Zhou X. Statistical methods for Mendelian randomization in genome-wide association studies: A review. *Comput Struct Biotechnol J* (2022) 20:2338–51. doi: 10.1016/j.csbj.2022.05.015

25. Peng Y, Tao Y, Zhang Y, Wang J, Yang J, Wang Y. CD25: A potential tumor therapeutic target. *Int J Cancer* (2023) 152:1290–303. doi: 10.1002/ijc.34281

26. Villanueva MT. Anti-CD25 antibody tips the T cell balance. *Nat Rev Drug Discovery* (2021) 20:18. doi: 10.1038/d41573-020-00206-w

27. Lee JH, Jung KH, Kim M, Lee KH. Cysteine-specific (89)Zr-labeled anti-CD25 IgG allows immuno-PET imaging of interleukin-2 receptor-α on T cell lymphomas. *Front Immunol* (2022) 13:1017132. doi: 10.3389/fimmu.2022.1017132

28. Zhang J, Fu Q, He Y, Lv H, Qian Y, Zhang Y, et al. Differences of circulating CD25(hi) bregs and their correlations with CD4 effector and regulatory T cells in autoantibody-positive T1D compared with age-matched healthy individuals. *J Immunol Res* (2022) 2022:2269237. doi: 10.1155/2022/2269237

29. Fuss P, Bal K, Jerzyńska J, Podlecka D, Stelmach W, Stelmach I. Association between environmental exposure and CD4+CD25+ regulatory T cells. *Allergologia immunopathologia* (2019) 47:43–6. doi: 10.1016/j.aller.2018.04.003

30. Rampoldi F, Donato E, Ullrich L, Deseke M, Janssen A, Demera A, et al. γδ T cells license immature B cells to produce a broad range of polyreactive antibodies. *Cell Rep* (2022) 39:110854. doi: 10.1016/j.celrep.2022.110854

31. Sakakura K, Takahashi H, Motegi SI, Yokobori-Kuwabara Y, Oyama T, Chikamatsu K. Immunological features of circulating monocyte subsets in patients with squamous cell carcinoma of the head and neck. *Clin Immunol (Orlando Fla.)* (2021) 225:108677. doi: 10.1016/j.clim.2021.108677

32. Prat M, Le Naour A, Coulson K, Lemée F, Leray H, Jacquemin G, et al. Circulating CD14 (high) CD16(low) intermediate blood monocytes as a biomarker of ascites immune status and ovarian cancer progression. *J Immunother Cancer* (2020) 8:e000472. doi: 10.1136/jitc-2019-000472

33. Vuk-Pavlović S, Bulur PA, Lin Y, Qin R, Szumlanski CL, Zhao X, et al. Immunosuppressive CD14+HLA-DRlow/- monocytes in prostate cancer. *Prostate* (2010) 70:443–55. doi: 10.1002/pros.21078

34. Santiago KB, Rodrigues JCZ, de Oliveira Cardoso E, Conte FL, Tasca KI, Romagnoli GG, et al. Brazilian red propolis exerts a cytotoxic action against prostate cancer cells and upregulates human monocyte functions. *Phytother Res PTR* (2023) 37:399–409. doi: 10.1002/ptr.7618

35. Wang C, Zhu D, Zhang D, Zuo X, Yao L, Liu T, et al. Causal role of immune cells in schizophrenia: Mendelian randomization (MR) study. *BMC Psychiatry* (2023) 23:590. doi: 10.1186/s12888-023-05081-4

36. Adimora IJ, Wilson NR, Pemmaraju N. Blastic plasmacytoid dendritic cell neoplasm (BPDCN): A promising future in the era of targeted therapeutics. *Cancer* (2022) 128:3019–26. doi: 10.1002/cncr.34345

37. Tussiwand R. Plasmacytoid dendritic cells turn red! *Nat Immunol* (2023) 24:563–4. doi: 10.1038/s41590-023-01472-7

38. Özkan B, Lim H, Park SG. Immunomodulatory function of myeloid-derived suppressor cells during B cell-mediated immune responses. *Int J Mol Sci* (2018) 19:1468. doi: 10.3390/ijms19051468

39. Wen J, Huang G, Liu S, Wan J, Wang X, Zhu Y, et al. Polymorphonuclear MDSCs are enriched in the stroma and expanded in metastases of prostate cancer. *J Pathol Clin Res* (2020) 6:171–7. doi: 10.1002/cjp2.160

40. Li N, Liu Q, Han Y, Pei S, Cheng B, Xu J, et al. ARID1A loss induces polymorphonuclear myeloid-derived suppressor cell chemotaxis and promotes prostate cancer progression. *Nat Commun* (2022) 13:7281. doi: 10.1038/s41467-022-34871-9

41. Idorn M, Køllgaard T, Kongsted P, Sengeløv L, Thor Straten P. Correlation between frequencies of blood monocytic myeloid-derived suppressor cells, regulatory T cells and negative prognostic markers in patients with castration-resistant metastatic prostate cancer. *Cancer Immunol Immunother CII* (2014) 63:1177–87. doi: 10.1007/s00262-014-1591-2

frontiers | Frontiers in Endocrinology

TYPE Original Research
PUBLISHED 21 March 2024
DOI 10.3389/fendo.2024.1293953

OPEN ACCESS

EDITED BY
Guadalupe Maya-Núñez,
Mexican Social Security Institute (IMSS), Mexico

REVIEWED BY
Yupeng Wu,
First Affiliated Hospital of Fujian Medical University, China
Yalbi I. Balderas-Martínez,
National Institute of Respiratory Diseases-Mexico (INER), Mexico

*CORRESPONDENCE
Juan Jiao
kafeidoujiao@126.com
Wei Li
wayne@ccmu.edu.cn
Yuanming Pan
peterfpan2020@mail.ccmu.edu.cn

RECEIVED 14 September 2023
ACCEPTED 12 March 2024
PUBLISHED 21 March 2024

CITATION
Li S, Cai S, Huang J, Li Z, Shi Z, Zhang K, Jiao J, Li W and Pan Y (2024) Develop prediction model to help forecast advanced prostate cancer patients' prognosis after surgery using neural network.
Front. Endocrinol. 15:1293953.
doi: 10.3389/fendo.2024.1293953

Develop prediction model to help forecast advanced prostate cancer patients' prognosis after surgery using neural network

Shanshan Li[1], Siyu Cai[2,3], Jinghong Huang[4], Zongcheng Li[5], Zhengyu Shi[6], Kai Zhang[7], Juan Jiao[1]*, Wei Li[2]* and Yuanming Pan[2]*

[1]Department of Clinical Laboratory, The Seventh Medical Center of Chinese PLA General Hospital, Beijing, China, [2]Cancer Research Center, Beijing Chest Hospital, Capital Medical University/Beijing Tuberculosis and Thoracic Tumor Research Institute, Beijing, China, [3]Dermatology Department, General Hospital of Western Theater Command, Chengdu, Sichuan, China, [4]Department of Biochemistry, School of Medicine/Key Laboratory of Xinjiang Ministry of Education, Shihezi University, Shihezi, Xinjiang, China, [5]Urinary Surgery Department, The First People's Hospital of Ziyang, Ziyang, Sichuan, China, [6]Chengdu Eighth People's Hospital, Chengdu, Sichuan, China, [7]General Department, Beijing Chest Hospital, Capital Medical University/Beijing Tuberculosis and Thoracic Tumor Research Institute, Tongzhou District, Beijing, China

Background: The effect of surgery on advanced prostate cancer (PC) is unclear and predictive model for postoperative survival is lacking yet.

Methods: We investigate the National Cancer Institute's Surveillance, Epidemiology, and End Results (SEER) database, to collect clinical features of advanced PC patients. According to clinical experience, age, race, grade, pathology, T, N, M, stage, size, regional nodes positive, regional nodes examined, surgery, radiotherapy, chemotherapy, history of malignancy, clinical Gleason score (composed of needle core biopsy or transurethral resection of the prostate specimens), pathological Gleason score (composed of prostatectomy specimens) and prostate-specific antigen (PSA) are the potential predictive variables. All samples are divided into train cohort (70% of total, for model training) and test cohort (30% of total, for model validation) by random sampling. We then develop neural network to predict advanced PC patients' overall. Area under receiver operating characteristic curve (AUC) is used to evaluate model's performance.

Results: 6380 patients, diagnosed with advanced (stage III-IV) prostate cancer and receiving surgery, have been included. The model using all collected clinical features as predictors and based on neural network algorithm performs best, which scores 0.7058 AUC (95% CIs, 0.7021-0.7068) in train cohort and 0.6925 AUC (95% CIs, 0.6906-0.6956) in test cohort. We then package it into a Windows 64-bit software.

Conclusion: Patients with advanced prostate cancer may benefit from surgery. In order to forecast their overall survival, we first build a clinical features-based prognostic model. This model is accuracy and may offer some reference on clinical decision making.

KEYWORDS

prediction model, prostate cancer, prognosis, surgery, neural network, deep learning

Background

Prostate cancer (PC) is the second-most common solid organ malignancy globally and the most prevalent solid organ malignancy in males in the United States (1). In Western nations, the second-most prominent cause of men's cancer-related mortality is also PC, and more than 30,000 men die from it in the United States (2). Race, age, family history, obesity, and other conditions are mainly risk factors for PC (3, 4). Usually, PC patients with T3-T4, prostate-specific antigen (PSA) ≥ 20 ng/ml, lymph node or distant site metastasis have the potential for being diagnosed with advanced PC.

Advanced PC is typically regarded as incurable. On one hand, since Charles Huggins initially observed the impact of androgen deprivation therapy (ADT) on metastatic PC patients, inhibition of androgen receptor signaling with ADT has been the basis of therapy for metastatic PC. ADT has involved several types, like surgical castration or pharmacological castration. However, despite the fact that ADT provides about 1-2 years' remissions in the majority of patients, PC can grow resistant, called metastatic castration-resistant PC (5). On the other hand, traditionally, advanced PC is still dominated by ADT treatment, and radical prostatectomy (RP) is rarely the first option. The primary cause may be that the presence of tumor extension into the rhabdosphincter, rectal wall, and seminal vesicles usually implies a poor prognosis and is often accompanied by fatal surgical complications (6, 7). However, with the improvement and refinement of surgical technology, particularly the introduction of robot-assisted radical prostatectomy (RALP), the prognosis of advanced PC is steadily improving, and the rate of surgical complications may also be handled (7, 8). In recent years, cytoreductive prostatectomy (CP) has gradually attracted attention. Some evidence suggests a feasible role for CP in metastatic PC (9–11). Axel Heidenreich et al. observed that advanced PC patients responding well to neoadjuvant androgen deprivation therapy had a better progression-free survival (PFS) (38.6 vs 26.5 months, P = 0.032) after CP than control group (9). These findings imply that surgery might be a novel and effective treatment option for advanced PC. However, there is no consensus on which patients are appropriate or how to predict their outcome.

In this study, we investigate the National Cancer Institute's Surveillance, Epidemiology, and End Results (SEER) database for records regarding PC patients with staged III-IV and undergoing surgery, and create a neural network prediction model to estimate their postoperative survival. We then package the model into a software, which is convenient for clinicians to use and decision-making assistance.

Abbreviations: PC, prostate cancer; PSA, prostate-specific antigen; ADT, androgen deprivation therapy; RP, radical prostatectomy; RALP, robot-assisted radical prostatectomy; CP, cytoreductive prostatectomy; PFS, progression-free survival; SEER, Surveillance, Epidemiology, and End Results; AJCC, American Joint Committee on Cancer; LASSO, least absolute shrinkage and selection operator; OS, overall survival; AUC, area under receiver operating characteristic curve; CIs, confidence interval; GUI, graphical user interface; CPH, Cox proportional hazard; HR, hazard ratio; DeepPC, survival predictive tool for advanced prostate cancer patients after surgery; NPV, negative predictive value; PPV, positive predictive value; ROC, receiver operating characteristic curves; CSS, cancer-specific survival; DSS, disease-specific survival.

Methods

Patients and datasets

Retrieving with SEER*Stat (8.4.0), we utilize the 17 Registries database (2000–2019), which covers approximately 26.5% of the U.S. population, and set "Site and Morphology. Site recode ICD-O-3/WHO 2008" as "Prostate" to get the raw data of prostate cancer. Raw data are filtered to reserve patients diagnosed in 2010-2015 years for they containing the detailed 7th American Joint Committee on Cancer (AJCC) stage and confirmed as stage III-IV with complete surgery records. Samples with missing values are omitted, and 5 samples are taken out due to their contradictory records about lymphatic metastasis. 6380 samples are adopted finally. Then all patients are divided into train cohort (70% of total) and test cohort (30% of total) by random sampling. Train cohort is used to conduct survival models, validated by its own and test cohort. According to SEER's criteria, tumor diameters exceeding 989mm are still recorded as 989mm, and patients over the age of 100 are still documented as 100 (Figure 1).

The SEER program registries routinely collect demographic and clinic data, and the mortality data reported by SEER were provided

10.3389/fendo.2024.1293953

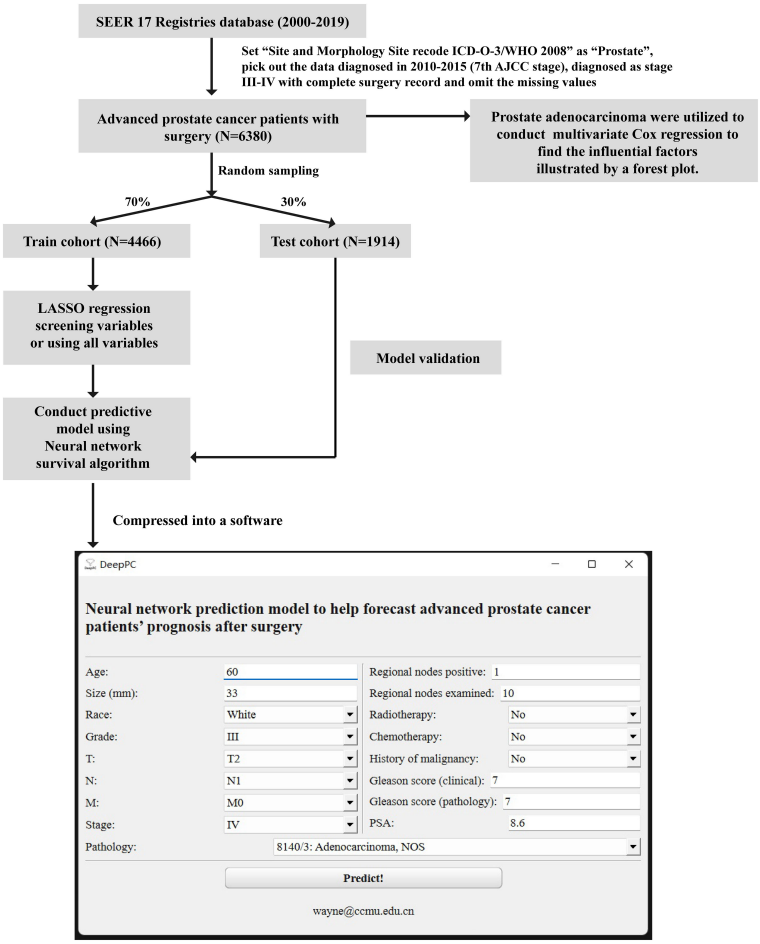

FIGURE 1
Flow chart of this study. SEER, Surveillance, Epidemiology, and End Results database; AJCC, American Joint Committee on Cancer; LASSO, least absolute shrinkage and selection operator; PSA, prostate-specific antigen.

by the National Center for Health Statistics, according to SEER website. The 17 Registries database (2000-2019) is submitted in November 2021, and the follow-up cut-off date is December 31, 2019, according to SEER description manual. We have signed the SEER Research Data Use Agreement to acquire access.

Data cleaning and feature engineering

Usually more predictive variables show a better performance, so we collect them as much as possible. According to clinical experience, age, race, grade, pathology, T, N, M, stage, size, regional nodes positive, regional nodes examined, surgery, radiotherapy, chemotherapy, history of malignancy, clinical Gleason score (composed of needle core biopsy or transurethral resection of the prostate specimens), pathological Gleason score (composed of prostatectomy specimens) and PSA are the potential predictive variables. At first, all clinical features above are used to conduct models, with evaluated fitting and overfitting in both train and test cohorts.

Then, considering the potential multicollinearity among these variables (though sometimes not considered in neural network model), we apply least absolute shrinkage and selection operator (LASSO) regression to screen clinical features mentioned above. The key to LASSO regression is to allocate an appropriate lambda value, which is confirmed by a 5-fold cross validation and the minimum one is adopted. The clinical features with a non-zero coefficient in LASSO regression (short for LASSO variables) are taken out to build prognostic model. Only the train cohort is used in this process, and R package glmnet is used to achieve work above.

Survival model training and evaluation

All data are separated into two parts, train cohort for LASSO regression and conducting models, and test cohort for further validation. Some variables (T and M) are merged, although they are shown specifically on the baseline table.

Using the pytorch platform based on python 3.9.7, we construct a deep learning survival model to predict overall survival (OS) probability of the PC patients. The deep learning survival model contained input layers (the clinical features), activation layers (convert the computing results to nonlinear ones), drop out layers (silence some neurons randomly to avoid overfitting) and batch

normalization layers (ensure that the mean and variance of the input variables are fixed within a certain range to improve model performance). We turn on the early stopping function, which can end training automatically when model's performance gets no improvement after several rounds of trainings (set as 30 rounds here). Batch size training is enabled and 512 samples are used each time. Adam is designated as optimizer with 0.05 learning rate. Numerical clinical features are normalized (subtract the mean and divide by the standard deviation) and categorical clinical features are transformed into number encodings before training. Python package pandas, numpy, pycox, matplotlib, lifelines and scikit-learn assist us with the above process.

The traditional CPH model has been built too, to make a contrast, with the help of python package lifelines. All models are conducted using both all clinical features collected this time or LASSO filtered ones.

The main evaluation indicator is area under receiver operating characteristic curve (AUC). An AUC closer to 1.0 reflects the model perfect in predicting, while a model scoring 0.5 AUC tends to random guess. We evaluate models in both train and test cohorts, reporting the mean AUC and 95% confidence interval (CIs) by Bootstrap.

The neural network is compressed as a graphical user interface (GUI) software for clinicians to use finally.

Survival analysis

All data both train and test cohorts are finally employed to conduct Cox proportional hazard (CPH) regression, revealing the hazard ratio (HR) and 95% CIs to discover influential factors of advanced prostate adenocarcinoma (8140/3) after surgery. A forest plot is drawn to visualize results above with the use of R package ezcox, survival and survminer.

Statistical analysis

This study is analyzed with R software. The comparison between train cohort and test cohort is assessed using Student's t or Mann-Whitney U test for continuous variables, Chi-square test for categorical variables. $P < 0.05$ of two-sided is considered statistically significant.

This research is conducted in accordance with the Declaration of Helsinki. This retrospective cohort study uses data from the publicly available SEER database, patients' information has been anonymized and not traceable. And the data submitters have gotten informed consent from participants and obtained the ethical permission. Given that, this research is exempted from ethical applications and written consent.

Results

Clinical characteristics

A total of 6380 patients, diagnosed with advanced (stage III-IV) PC and receiving surgery, have been included. After random sampling, 4466 (70% of total) in train cohort and 1914 (30% of total) in test cohort. The detailed clinical information is displayed in Table 1. Two cohorts have no significant difference in clinical features. The mean age is 63.28 years old in train cohort and 63.1 years old in test cohort. Most patients are white and diagnosed with grade III in two cohorts. Adenocarcinoma is the most common

TABLE 1 Clinical information of two cohorts.

	Train cohort (N=4466)	Test cohort (N=1914)	Statistical method	P value
	No. (%)			
Age			Student's t	0.3349
Mean (SD)	63.28 (6.84)	63.1 (7.08)		
Race			Chi-square	0.8640
White	3611 (80.86)	1542 (80.56)		
Black	410 (9.18)	173 (9.04)		
Other	445 (9.96)	199 (10.40)		
Grade			Chi-square	0.7252
I	22 (0.49)	13 (0.68)		
II	1079 (24.16)	472 (24.66)		
III	3354 (75.10)	1423 (74.35)		
IV	11 (0.25)	6 (0.31)		

(Continued)

TABLE 1 Continued

	Train cohort (N=4466) No. (%)	Test cohort (N=1914) No. (%)	Statistical method	P value
Pathology			Chi-square	0.3535
8140/3: Adenocarcinoma, NOS	4399 (98.50)	1880 (98.22)		
8201/3: Cribriform carcinoma, NOS	2 (0.04)	0 (0)		
8246/3: Neuroendocrine carcinoma, NOS	2 (0.04)	0 (0)		
8255/3: Adenocarcinoma with mixed subtypes	11 (0.25)	6 (0.31)		
8480/3: Mucinous adenocarcinoma	5 (0.11)	4 (0.21)		
8481/3: Mucin-producing adenocarcinoma	1 (0.02)	1 (0.05)		
8490/3: Signet ring cell carcinoma	0 (0)	2 (0.10)		
8500/3: Infiltrating duct carcinoma, NOS	29 (0.65)	16 (0.84)		
8550/3: Acinar cell carcinoma	14 (0.31)	5 (0.26)		
8574/3: Adenocarcinoma with neuroendocrine differentiation	3 (0.07)	0 (0)		
T			Chi-square	0.9349
T2	11 (0.25)	2 (0.10)		
T2a	7 (0.16)	3 (0.16)		
T2b	6 (0.13)	4 (0.21)		
T2c	90 (2.02)	37 (1.93)		
T3	10 (0.22)	6 (0.31)		
T3a	2774 (62.11)	1181 (61.70)		
T3b	1506 (33.72)	654 (34.17)		
T4	62 (1.39)	27 (1.41)		
N			Chi-square	0.1863
N0	3747 (83.90)	1631 (85.21)		
N1	719 (16.10)	283 (14.79)		
M			Chi-square	0.1256
M0	4431 (99.22)	1905 (99.53)		
M1a	5 (0.11)	2 (0.10)		
M1b	29 (0.65)	5 (0.26)		
M1c	1 (0.02)	2 (0.10)		
Stage			Chi-square	0.0897
III	3686 (82.53)	1613 (84.27)		
IV	780 (17.47)	301 (15.73)		
Size			Wilcoxon signed-rank	0.1028
Median (IQR)	23 (17, 32)	22 (17, 30)		
Regional nodes positive			Wilcoxon signed-rank	0.2139
Median (IQR)	0 (0, 0)	0 (0, 0)		
Regional nodes examined			Wilcoxon signed-rank	0.4381
Median (IQR)	7 (3, 12)	7 (4, 12)		

(Continued)

TABLE 1 Continued

	Train cohort (N=4466)	Test cohort (N=1914)	Statistical method	P value
	No. (%)			
Radiotherapy			Chi-square	0.3138
No	3613 (80.9)	1569 (81.97)		
Yes	853 (19.1)	345 (18.03)		
Chemotherapy			Chi-square	0.1210
No	4423 (99.04)	1903 (99.43)		
Yes	43 (0.96)	11 (0.57)		
History of malignancy			Chi-square	0.7347
No	4164 (93.24)	1789 (93.47)		
Yes	302 (6.76)	125 (6.53)		
Gleason score (clinical)			Wilcoxon signed-rank	0.6437
Median (IQR)	7 (7, 8)	7 (7, 8)		
Gleason score (pathology)			Wilcoxon signed-rank	0.3687
Median (IQR)	7 (7, 8)	7 (7, 8)		
PSA			Wilcoxon signed-rank	0.5917
Median (IQR)	8 (5.6, 13.4)	7.8 (5.6, 13.3)		
Survival time			Wilcoxon signed-rank	0.0592
Median (IQR)	75 (58, 96)	73 (57, 95)		
Dead			Chi-square	0.5402
No	4015 (89.90)	1711 (89.39)		
Yes	451 (10.10)	203 (10.61)		

SD, standard deviation. Grade I, well differentiated; Grade II, moderately differentiated; Grade III, poorly differentiated; Grade IV, undifferentiated, anaplastic. NOS, not otherwise specified. IQR, inter-quartile range. Gleason score (clinical), composed of needle core biopsy or transurethral resection of the prostate specimens. Gleason score (pathology), composed of prostatectomy specimens. PSA, prostate-specific antigen.

pathology type. Most patients are staged T3a, N0, M0 or stage III. The median tumor diameter is 23 mm in train cohort and 22 mm in test cohort. The median regional nodes positive is 0 and median regional nodes examined is 7 in both two cohorts. Most patients got no radiotherapy or chemotherapy, and had no history of malignancy. The median Gleason score is 7 (either clinical or pathology) in two cohorts. The median PSA is 8 ng/ml in train cohort and 7.8 ng/ml in test cohort. The median survival time is 75 months in train cohort and 73 months in test cohort. Most patients survive in both two cohorts.

Predictive variables

We conduct models using all clinical features at first. Then LASSO regression is used to discover non-zero coefficient variables and screen clinical features (Supplementary Figure 1A). Concrete coefficient values are exhibited on Supplementary Table 1. Finally, these clinical features are picked out: age, M, stage, chemotherapy, history of malignancy, clinical Gleason score, pathological Gleason score, which all above are short for LASSO variables. All variables and LASSO variables are both used to conduct models too, by neural network and CPH. Prior to training, numerical clinical features are standardized according to their mean and standard deviation (Supplementary Table 2), and categorical clinical characteristics are converted into number encodings (Supplementary Table 3).

Model performance

LASSO variables are input, then a neural network is finished training after 35 epochs, according to the deep learning custom and tuning. The model has 0.6811 AUC (95% CIs: 0.6799-0.6849) in train cohort and 0.6779 AUC (95% CIs: 0.6740-0.6790) in test cohort (Table 2). The training curve has been saved in (Supplementary Figure 1B).

When it comes to all variables, a neural network is finished training after 36 epochs. And this model scores 0.7058 AUC (95%

TABLE 2 The performance of conducted models.

	Cox proportional hazard model				Neural network survival model			
	Train cohort		Test cohort		Train cohort		Test cohort	
	AUC	95% CI	AUC	95% CI	AUC	95% CI	AUC	95% CI
LASSO vars	0.6657	0.6633-0.6686	0.6719	0.6653-0.6707	0.6811	0.6799-0.6849	0.6779	0.6740-0.6790
All vars	0.6639	0.6604-0.6657	0.6696	0.6678-0.6731	0.7058	0.7021-0.7068	0.6925	0.6906-0.6956

AUC, area under receiver operating characteristic curve. CI, confidence interval. LASSO vars, least absolute shrinkage and selection operator screened out the predictive variables, including age, M, stage, size, chemotherapy, history of malignancy, Gleason score clinical (composed of needle core biopsy or transurethral resection of the prostate specimens) and Gleason score pathology (composed of prostatectomy specimens).
ALL vars, all variables collected this study, including LASSO variables, race, grade, pathology, T, N, regional nodes positive, regional nodes examined, radiotherapy and PSA (prostate-specific antigen).

CIs, 0.7021-0.7068) in train cohort and 0.6925 AUC (95% CIs, 0.6906-0.6956) in test cohort (Table 2). The training curve has been saved in (Supplementary Figure 1C).

We also execute CPH regression to compare, using all variables and LASSO variables. The LASSO variables' AUC is 0.6657 (95% CIs: 0.6633-0.6686) and 0.6719 (95% CIs: 0.6653-0.6707) in train and test cohort respectively. All variables get AUC of 0.6639 (95% CIs: 0.6604-0.6657) and 0.6696 (95% CIs: 0.6678-0.6731) in train and test cohort respectively. Overall speaking, neural network has a better performance than CPH (Table 2).

Model's further evaluation and compression

Then we suggest the model calculating with all variables and based on neural network to serves as the survival predictive tool for advanced PC patients after surgery (DeepPC). The architecture of DeepPC is as follows: it has 10 layers, including a linear layer (17 x 16 nodes), an activation layer (Relu function), a batch normalization layer, a dropout layer (10%), a linear layer (16 x 16 nodes), another activation layer (Relu function), another batch normalization layer, another dropout layer (10%), a linear layer (16 x 1 nodes) and the final activation layer (Sigmoid transformation) (Figure 2A). The detailed parameters of DeepPC are stored in Supplementary Figure 2.

We then validate DeepPC further in its 1-, 3-, 5- and 10-years prediction of PC patients' OS. For 1 year, DeepPC gets 0.6303 AUC (95% CIs, 0.5250-0.7357), 0.5764 specificity, 0.6957 sensitivity, 0.9973 negative predictive value (NPV) and 0.0084 positive predictive value (PPV) in train cohort, and 0.6210 AUC (95% CIs, 0.4381-0.8039), 0.4129 specificity, 0.8750 sensitivity, 0.9987 NPV and 0.0062 PPV in test cohort. For 3 years, DeepPC has 0.6834 AUC (95% CIs: 0.6331-0.7336), 0.7025 specificity, 0.5897 sensitivity, 0.9845 NPV and 0.0506 PPV in train cohort, and 0.6708 AUC (95% CIs: 0.5896-0.7519), 0.6907 specificity, 0.6222 sensitivity, 0.9870 NPV and 0.0462 PPV in test cohort. For 5 years, DeepPC shows 0.7294 AUC (95% CIs: 0.6974-0.7615), 0.6078 specificity, 0.7362 sensitivity, 0.9745 NPV and 0.1017 PPV in train cohort, and 0.6751 AUC (95% CIs: 0.6225-0.7276), 0.7021 specificity, 0.6017 sensitivity, 0.9641 NPV and 0.1172 PPV in test cohort. For 10 years, DeepPC scores 0.6990 AUC (95% CIs: 0.6733-0.7248), 0.6178 specificity, 0.6748 sensitivity, 0.9440 NPV and 0.1659 PPV in train cohort, and 0.7136 AUC (95% CIs: 0.6754-0.7517), 0.7216 specificity, 0.6373 sensitivity, 0.9434 NPV and 0.2145 PPV in test cohort. (Table 3) The receiver operating characteristic curves (ROC) of DeepPC in 1-, 3-, 5- and 10-years' performance are illustrated in Figure 2B.

We then compressed DeepPC into a GUI Windows software (Figure 2C). When age, race, grade, pathology, T, N, M, stage, size, regional nodes positive, regional nodes examined, surgery, radiotherapy, chemotherapy, history of malignancy, clinical Gleason score (composed of needle core biopsy or transurethral resection of the prostate specimens), pathological Gleason score (composed of prostatectomy specimens) and PSA of one prostate cancer patient are inputted, user can click "Predict!" button to launch the pre-trained DeepPC. After calculating, it will automatically open the user's default browser to draw the patient's survival curve (Kaplan-Meier curve) (Figure 2D). The curve is interactive. When the user hovers over, the specific month and survival probability will pop up automatically. We also keep the original python edition for easier processing when we need to predict the survival of PC patients in batches (Supplementary Figure 3).

Survival analysis

Two cohorts are carried in Cox regression to identify the protective and dangerous factors of advanced prostate adenocarcinoma (8140/3) after surgery. The visualization of patients' clinical data is shown in Figure 3. After analysis, age (HR 1.03, 95% CIs 1.02 - 1.04, P < 0.001), history of malignancy (HR 1.53, 95% CIs: 1.18 - 1.98, P = 0.001), clinical Gleason score (HR 1.16, 95% CIs: 1.04 - 1.29, P = 0.005) and pathological Gleason score (HR 1.50, 95% CIs: 1.34 - 1.66, P < 0.001) tend to dangerous factors. And other race (HR 0.74, 95% CIs: 0.55 - 1.00, P = 0.048), regional nodes examined (HR 0.99, 95% CIs: 0.98 - 1.00, P = 0.020) tend to be protective factors (Figure 4).

Discussion

PC is the most common male malignant tumor and the second most fatal tumor, with 20% progressing to potentially lethal illness (12). PC patients with low malignant potential or indolent disease

10.3389/fendo.2024.1293953

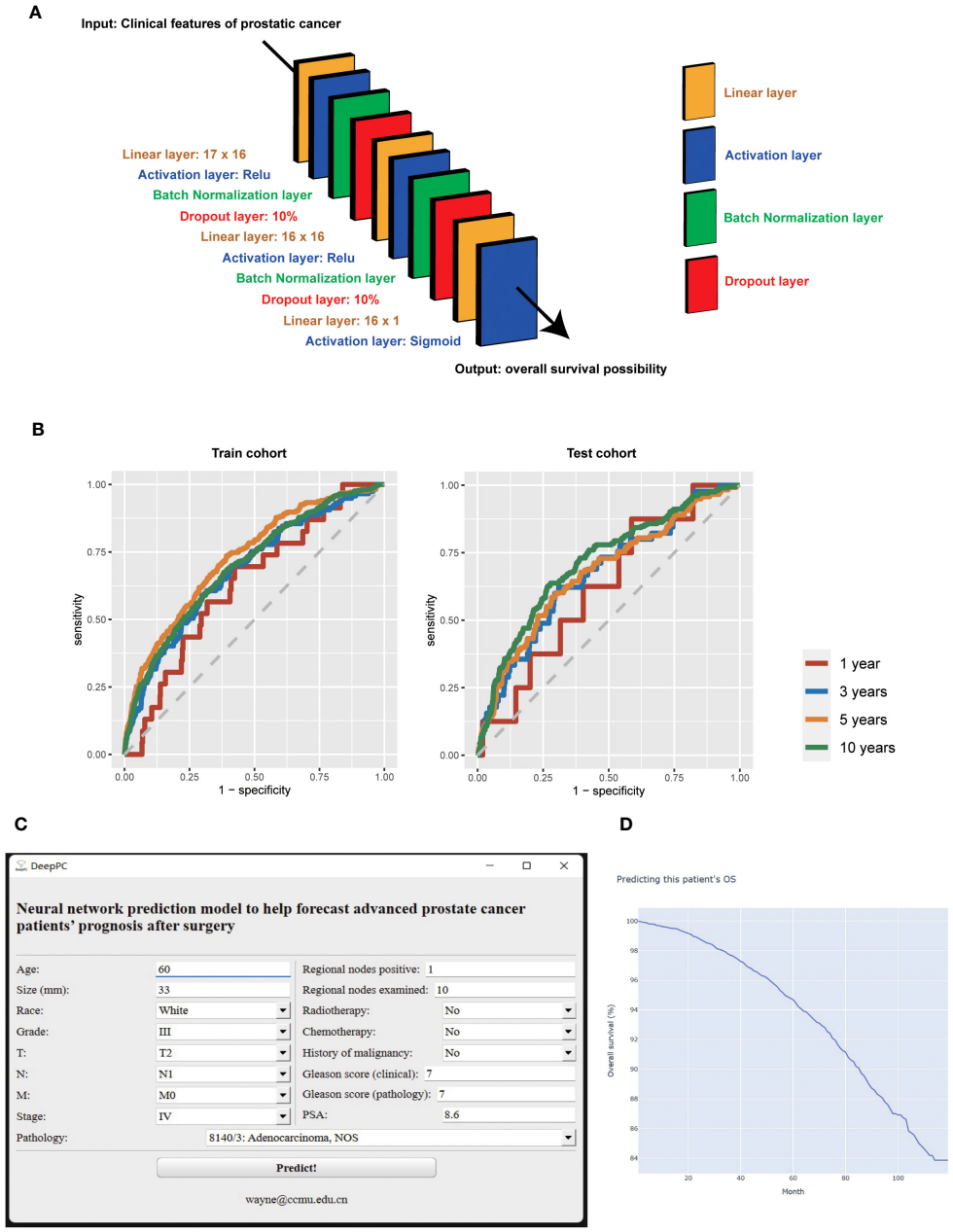

FIGURE 2
The structure **(A)**, receiver operating characteristic curves **(B)**, graphical user interface **(C)**, and computational results **(D)** of survival predictive tool for advanced prostate cancer patients after surgery (DeepPC). PSA, prostate-specific antigen.

typically receive active surveillance regimens, patients with localized disease tend to get radiotherapy and RP surgery, and patients with aggressive or metastatic PC usually undergo a combination of several ADT-based therapies such as hormonal therapy, radiotherapy, chemotherapy, and immunotherapy (12).

Trauma, bleeding, and survival benefit or not, are the main reasons that there has been controversy over whether advanced PC should undergo surgical treatment in the past. However, with the boom of treatment like minimally invasive surgical therapy, individuals with advanced PC are no longer confined to ADT (13). Surgery, and radiation, with or without ADT, are increasingly being used to treat advanced PC patients, particularly locally advanced PC patients (10, 14). John F. Ward et al. found the respective cancer-specific survival (CSS) rates of 5652 T3 advanced PC patients after RP were 95%, 90% and 79%, and the complications and incontinence rate was similar to T2 PC patients (15). Chao-Yu Hsu et al. reported that in 235 T3a PC patients after RP, the OS of 5 and 10 years reached 95.9% and 77.0%, and CSS was 98.7% and 91.6% respectively. They also observed 23.5% cT3a PC patients were clinically over-staged (pT2), which might cause them lose the surgery chance as a result (16). After analyzing 1093 cT4 PC patients, Peter A. S. Johnstone

TABLE 3 The performance of neural network model in 1-, 3-, 5- and 10-years' survival prediction.

	Train cohort				Test cohort			
	1 year	3 years	5 years	10 years	1 year	3 years	5 years	10 years
AUC	0.6303	0.6834	0.7294	0.6990	0.6210	0.6708	0.6751	0.7136
AUC 95% CI	0.5250-0.7357	0.6331-0.7336	0.6974-0.7615	0.6733-0.7248	0.4381-0.8039	0.5896-0.7519	0.6225-0.7276	0.6754-0.7517
Specificity	0.5764	0.7025	0.6078	0.6178	0.4129	0.6907	0.7021	0.7216
Sensitivity	0.6957	0.5897	0.7362	0.6748	0.8750	0.6222	0.6017	0.6373
NPV	0.9973	0.9845	0.9745	0.9440	0.9987	0.9870	0.9641	0.9434
PPV	0.0084	0.0506	0.1017	0.1659	0.0062	0.0462	0.1172	0.2145

AUC, area under receiver operating characteristic curve; CI, confidence interval; NPV, negative predictive value; PPV, positive predictive value.

et al. noticed that T4 PC patients who received RP treatment had the highest 5-year OS and relative survival rate when compared to those who got therapy ADT, radiotherapy or ADT and radiotherapy combination treatment (17). Ryan K Berglund et al. also believed neoadjuvant goserelin acetate and flutamide therapy followed by RP was feasible and might be an alternative to a strategy of combined radiation and ADT (18). RP has also been shown to improve survival in PC individuals with lymph nodes and distant metastases. Thomas Steuber et al. noted that among 158 localized PC patients with lymph node metastasis, patients after RP had longer PFS compared with unoperated patients (P = 0.005) (19). Jutta Engel et al. also held the view that lymph node positive patients with full RP had better survival than patients with abandoned RP, and that RP was a significant independent predictor of survival (P < 0.0001) (20). After identifying 8185 patients, Stephen H. Culp et al. thought metastatic PC patients having RP (67.4% in OS and 75.8% in disease-specific survival, DSS) or brachytherapy (52.6 in OS and 61.3% in DSS) had substantially higher than no surgery or radiation therapy patients (22.5% in OS and 48.7% in DSS, respectively) (P < 0.001) (21). Axel Heidenreich also observed in adequately-chosen males with metastatic PC who react well to neoadjuvant ADT, CP or RP is a viable option (9).

The present quandary is determining which advanced PC patients may benefit from surgery and what their unique prognosis is (10). Accurately estimating an advanced PC patient's prognosis is not only a worry for patient and his families, but it is also a potential reference for clinical decision-making. For example, in the clinical scenario that we imagine, doctors can utilize DeepPC to estimate the difference or benefit in OS probability between performing surgery and not doing, when talking about an advanced prostate cancer patient. Besides, some concerns are heightened by the fact that the existing evidence of advanced PC patients' surgical benefit is still retrospective, with no prospective randomized controlled clinical studies. In light of this condition, we attempt to develop a model to forecast advanced PC patients' survival.

At present, the most often used technique for constructing prediction models is based on CPH, which investigates the relationship between variables and survival time and provides recommendations on their HR based on a linear hypothesis. As a semi-parametric and linear model, it may not be suitable to predict survival for limited precision. Therefore, the DeepSurv algorithm, developed by Eu-Tteum Baek and colleagues, has been taken a good use of completing this study (22, 23). DeepSurv converges deep neural network and CPH regression, and it can find out about the complex and nonlinear relationships between prognostic clinical variables and an individual's probability of mortality in true world, which has shown huge potential on medical field (24–26). Our previous studies have also demonstrated DeepSurv may outperform CPH in predicting tumor patients' survival (27, 28). Therefore, we construct survival models using both CPH and DeepSurv algorithm this time, using all variables collected or LASSO to filter potential predictive clinical features, and chose the better one to serve as the final model.

In this study, we include 6380 diagnosed with advanced (stage III-IV) PC patients who got surgery from SEER database. After random sampling, 4466 samples (70% of total) in train cohort are used to construct prediction model to forecast their prognosis, and 1914 samples (30% of total) in test cohort are utilized to validate this model further. The model using all collected clinical features as predictors and based on neural network algorithm performs best, which scores 0.7058 AUC (95% CIs, 0.7021-0.7068) in train cohort and 0.6925 AUC (95% CIs, 0.6906-0.6956) in test cohort. We then package it into a Windows 64-bit software.

There is currently no predictive model for postoperative survival in patients with advanced PC. We reviewed other postoperative prostate cancer prediction models designed for non-advanced PC. Enchong Zhang et al. developed a PC prognostic model based on six DNA methylation sites, which scored 0.823-0.891 AUC. But their model lacks validation on independent datasets (29). Linda G W Kerkmeijer et al. analyzed 3383 localized PC patients, and built a model to predict their DSS before treatment. The C-statistic of their model was 0.78 (95% CIs: 0.74 - 0.82) (30). Zezhen Liu et al. constructed an immune-related biomarker-based risk model to predict PC prognosis, which got 0.749-0.804 AUC (31). (Supplementary Table 4) These findings suggest that the use of biomarkers such as gene expression may improve the accuracy of PC prognostic prediction.

The AUC of DeepPC is about 0.7, showing predictive value but moderate. On the one hand, it could be due to the large difference in prognosis for advanced prostate cancer, while on the other, it could be due to diverse surgical procedures. Because the SEER database lacks extensive descriptions of surgical procedures and biomarker information, the impacts discussed above are not included in this analysis, which limit model's performance. Besides, models in this

10.3389/fendo.2024.1293953

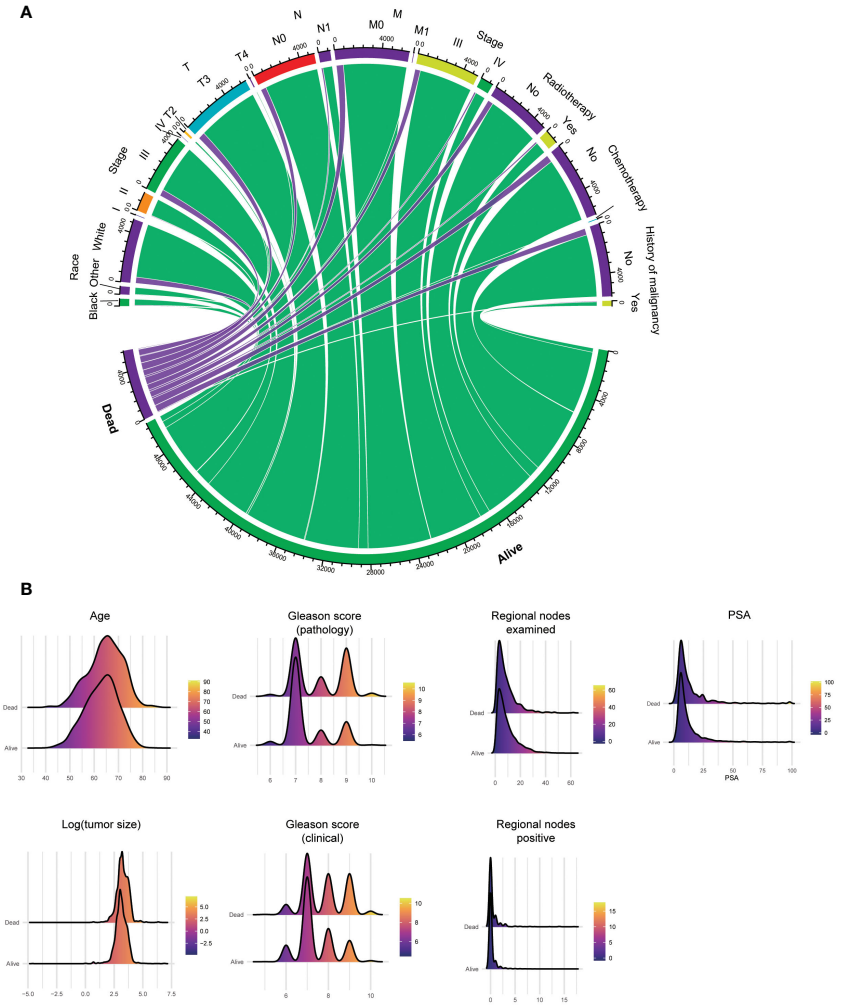

FIGURE 3
Clinical data's visualization of postoperative survival in patients with advanced prostate adenocarcinoma (8140/3) and receiving surgery, including categorical **(A)** and numerical **(B)** clinical features. PSA, prostate-specific antigen.

Variable		N	Hazard Ratio	P
Age		6279	1.03 (1.02, 1.04)	<0.001***
Race	White	5071	Reference	
	Black	575	1.17 (0.90, 1.54)	0.240
	Other	633	0.74 (0.55, 1.00)	0.048*
Grade	I	35	Reference	
	II	1536	0.99 (0.14, 7.17)	0.994
	III	4692	1.05 (0.15, 7.53)	0.961
	IV	16	1.54 (0.18, 13.43)	0.695
T	T2	160	Reference	
	T3	6035	1.86 (1.00, 3.48)	0.050
	T4	84	1.65 (0.64, 4.23)	0.299
N	N0	5293	Reference	
	N1	986	0.99 (0.40, 2.44)	0.976
M	M0	6238	Reference	
	M1	41	1.52 (0.65, 3.52)	0.331
Stage	III	5219	Reference	
	IV	1060	1.37 (0.56, 3.36)	0.488
Size		6279	1.00 (1.00, 1.00)	0.303
Regional nodes positive		6279	1.04 (0.96, 1.11)	0.339
Regional nodes examined		6279	0.99 (0.98, 1.00)	0.020*
Radiotherapy	No	5104	Reference	
	Yes	1175	1.05 (0.87, 1.27)	0.612
Chemotherapy	No	6228	Reference	
	Yes	51	1.55 (0.88, 2.72)	0.129
History of malignancy	No	5859	Reference	
	Yes	420	1.53 (1.18, 1.98)	0.001**
Gleason score (clinical)		6279	1.16 (1.04, 1.29)	0.005**
Gleason score (pathology)		6279	1.50 (1.34, 1.66)	<0.001***
PSA		6279	1.00 (1.00, 1.01)	0.490

FIGURE 4
Multivariate Cox regression to find the influential factors of advanced prostate adenocarcinoma (8140/3) patients' overall survival after surgery. PSA, prostate-specific antigen.

study are established only based on SEER data, and more prospective and multi-center data may better train and validate DeepPC. We and other researchers can investigate upgrading these metrics in future study in order to increase DeepPC performance.

Conclusion

Patients with advanced prostate cancer may benefit from surgery. In order to forecast their overall survival, we first build a clinical features-based prognostic model. This model is accuracy and may offer some reference on clinical decision making.

Data availability statement

The datasets used and analyzed during the current study are available from the corresponding authors on reasonable request.

Ethics statement

Ethical approval was not required for the study involving humans in accordance with the local legislation and institutional requirements. Written informed consent to participate in this study was not required from the participants or the participants' legal guardians/next of kin in accordance with the national legislation and the institutional requirements.

Author contributions

SL: Conceptualization, Data curation, Formal Analysis, Methodology, Writing – original draft, Writing – review & editing. SC: Data curation, Formal Analysis, Methodology, Writing – original draft. JH: Data curation, Methodology, Writing – original draft. ZL: Data curation, Formal Analysis, Methodology, Writing – original draft. ZS: Data curation, Formal Analysis, Methodology, Writing – original draft. KZ: Formal Analysis, Methodology, Writing – original draft. JJ: Conceptualization, Investigation, Writing – original draft, Writing – review & editing. WL: Conceptualization, Data curation, Formal Analysis, Investigation, Methodology, Software, Writing – original draft, Writing – review & editing. YP: Conceptualization, Methodology, Project administration, Supervision, Writing – original draft, Writing – review & editing.

Funding

The author(s) declare financial support was received for the research, authorship, and/or publication of this article. This study was supported by the Capital's Funds for Health Improvement and Research (No. 2018-2-5092) to JJ.

Conflict of interest

The authors declare that the research was conducted in the absence of any commercial or financial relationships that could be construed as a potential conflict of interest.

Publisher's note

All claims expressed in this article are solely those of the authors and do not necessarily represent those of their affiliated organizations, or those of the publisher, the editors and the reviewers. Any product that may be evaluated in this article, or claim that may be made by its manufacturer, is not guaranteed or endorsed by the publisher.

Supplementary material

The Supplementary Material for this article can be found online at: https://www.frontiersin.org/articles/10.3389/fendo.2024.1293953/full#supplementary-material

SUPPLEMENTARY TABLE 1
Coefficients of clinical features in least absolute shrinkage and selection operator (LASSO) regression.

SUPPLEMENTARY TABLE 2
The value of the mean and standard deviation of the variable.

SUPPLEMENTARY TABLE 3
Numerical encodings of categorical variables.

SUPPLEMENTARY TABLE 4
Model performance in predicting prognosis of patients with non-advanced prostate cancer in part previous literature.

SUPPLEMENTARY FIGURE 1
(A) The change of coefficients in least absolute shrinkage and selection operator (LASSO) Cox regression when used to filter clinical features. **(B)** the training curves of neural networks when using variables filtered by LASSO. **(C)** the training curves of neural networks when using all collected clinical features.

SUPPLEMENTARY FIGURE 2
The parameters of survival predictive tool for advanced prostate cancer patients after surgery (DeepPC).

SUPPLEMENTARY FIGURE 3
Python version of survival predictive tool for advanced prostate cancer patients after surgery (DeepPC), which is suitable for batch calculations of large-scale population.

SUPPLEMENTARY FILE 1
Python codes used to train predictive tool for advanced prostate cancer patients after surgery (DeepPC).

SUPPLEMENTARY FILE 2
The predictive tool for advanced prostate cancer patients after surgery (DeepPC) (windows version). Linkage: https://drive.google.com/file/d/1VXp4JKPxniSWe-F0k9tmGW6D8Oe1Agkb/view?usp=sharing

References

1. Sathianathen NJ, Konety BR, Crook J, Saad F, Lawrentschuk N. Landmarks in prostate cancer. *Nat Rev Urol*. (2018) 15:627–42. doi: 10.1038/s41585-018-0060-7

2. Siegel RL, Miller KD, Wagle NS, Jemal A. Cancer statistics, 2023. *CA Cancer J Clin*. (2023) 73:17–48. doi: 10.3322/caac.21763

3. Patel AR, Klein EA. Risk factors for prostate cancer. *Nat Clin Pract Urol*. (2009) 6:87–95. doi: 10.1038/ncpuro1290

4. Sekhoacha M, Riet K, Motloung P, Gumenku L, Adegoke A, Mashele S. Prostate cancer review: genetics, diagnosis, treatment options, and alternative approaches. *Molecules*. (2022) 27(17):5730. doi: 10.3390/molecules27175730

5. Komura K, Sweeney CJ, Inamoto T, Ibuki N, Azuma H, Kantoff PW. Current treatment strategies for advanced prostate cancer. *Int J Urol*. (2018) 25:220–31. doi: 10.1111/iju.13512

6. Stenzl A, Merseburger AS. Radical prostatectomy in advanced-stage and -grade disease: cure, cytoreduction, or cosmetics? *Eur Urol*. (2008) 53:234–6. doi: 10.1016/j.eururo.2007.10.048

7. Veeratterapillay R, Goonewardene SS, Barclay J, Persad R, Bach C. Radical prostatectomy for locally advanced and metastatic prostate cancer. *Ann R Coll Surg Engl*. (2017) 99:259–64. doi: 10.1308/rcsann.2017.0031

8. Jacobs EF, Boris R, Masterson TA. Advances in robotic-assisted radical prostatectomy over time. *Prostate Cancer*. (2013) 2013:902686. doi: 10.1155/2013/902686

9. Heidenreich A, Pfister D, Porres D. Cytoreductive radical prostatectomy in patients with prostate cancer and low volume skeletal metastases: results of a feasibility and case-control study. *J Urol*. (2015) 193:832–8. doi: 10.1016/j.juro.2014.09.089

10. Mathieu R, Korn SM, Bensalah K, Kramer G, Shariat SF. Cytoreductive radical prostatectomy in metastatic prostate cancer: does it really make sense? *World J Urol*. (2017) 35:567–77. doi: 10.1007/s00345-016-1906-3

11. Rajwa P, Zattoni F, Maggi M, Marra G, Kroyer P, Shariat SF, et al. Cytoreductive radical prostatectomy for metastatic hormone-sensitive prostate cancer-evidence from recent prospective reports. *Eur Urol Focus*. (2023) 9:637–41. doi: 10.1016/j.euf.2023.01.011

12. Adamaki M, Zoumpourlis V. Prostate cancer biomarkers: from diagnosis to prognosis and precision-guided therapeutics. *Pharmacol Ther*. (2021) 228:107932. doi: 10.1016/j.pharmthera.2021.107932

13. Hupe MC, Merseburger AS. Advanced prostate cancer. *World J Urol*. (2021) 39:295–6. doi: 10.1007/s00345-021-03618-4

14. Faiena I, Singer EA, Pumill C, Kim IY. Cytoreductive prostatectomy: evidence in support of a new surgical paradigm (Review). *Int J Oncol*. (2014) 45:2193–8. doi: 10.3892/ijo.2014.2656

15. Ward JF, Slezak JM, Blute ML, Bergstralh EJ, Zincke H. Radical prostatectomy for clinically advanced (Ct3) prostate cancer since the advent of prostate-specific antigen testing: 15-year outcome. *BJU Int*. (2005) 95:751–6. doi: 10.1111/j.1464-410X.2005.05394.x

16. Hsu CY, Joniau S, Oyen R, Roskams T, Van Poppel H. Outcome of surgery for clinical unilateral T3a prostate cancer: A single-institution experience. *Eur Urol*. (2007) 51:121–8. doi: 10.1016/j.eururo.2006.05.024

17. Johnstone PA, Ward KC, Goodman M, Assikis V, Petros JA. Radical prostatectomy for clinical T4 prostate cancer. *Cancer*. (2006) 106:2603–9. doi: 10.1002/cncr.21926

18. Berglund RK, Tangen CM, Powell IJ, Lowe BA, Haas GP, Carroll PR, et al. Ten-year follow-up of neoadjuvant therapy with goserelin acetate and flutamide before radical prostatectomy for clinical T3 and T4 prostate cancer: update on southwest oncology group study 9109. *Urology*. (2012) 79:633–7. doi: 10.1016/j.urology.2011.11.019

19. Steuber T, Budaus L, Walz J, Zorn KC, Schlomm T, Chun F, et al. Radical prostatectomy improves progression-free and cancer-specific survival in men with lymph node positive prostate cancer in the prostate-specific antigen era: A confirmatory study. *BJU Int*. (2011) 107:1755–61. doi: 10.1111/j.1464-410X.2010.09730.x

20. Engel J, Bastian PJ, Baur H, Beer V, Chaussy C, Gschwend JE, et al. Survival benefit of radical prostatectomy in lymph node-positive patients with prostate cancer. *Eur Urol*. (2010) 57:754–61. doi: 10.1016/j.eururo.2009.12.034

21. Culp SH, Schellhammer PF, Williams MB. Might men diagnosed with metastatic prostate cancer benefit from definitive treatment of the primary tumor? A seer-based study. *Eur Urol*. (2014) 65:1058–66. doi: 10.1016/j.eururo.2013.11.012

22. Baek ET, Yang HJ, Kim SH, Lee GS, Oh IJ, Kang SR, et al. Survival time prediction by integrating cox proportional hazards network and distribution function network. *BMC Bioinf*. (2021) 22:192. doi: 10.1186/s12859-021-04103-w

23. Kvamme H, Borgan Ø, Scheel I. Time-to-event prediction with neural networks and cox regression. (2019) 20(129):1–30.

24. Hashimoto DA, Rosman G, Rus D, Meireles OR. Artificial intelligence in surgery: promises and perils. *Ann Surg*. (2018) 268:70–6. doi: 10.1097/SLA.0000000000002693

25. Howard FM, Kochanny S, Koshy M, Spiotto M, Pearson AT. Machine learning-guided adjuvant treatment of head and neck cancer. *JAMA Netw Open*. (2020) 3:e2025881. doi: 10.1001/jamanetworkopen.2020.25881

26. Adeoye J, Koohi-Moghadam M, Lo AWI, Tsang RK, Chow VLY, Zheng LW, et al. Deep learning predicts the Malignant-transformation-free survival of oral potentially Malignant disorders. *Cancers (Basel)*. (2021) 13(26):6054. doi: 10.3390/cancers13236054

27. Li W, Lin S, He Y, Wang J, Pan Y. Deep learning survival model for colorectal cancer patients (Deepcrc) with asian clinical data compared with different theories. *Arch Med Sci*. (2023) 19:264–9. doi: 10.5114/aoms/156477

28. Li W, Zhang M, Cai S, Wu L, Li C, He Y, et al. Neural network-based prognostic predictive tool for gastric cardiac cancer: the worldwide retrospective study. *BioData Min*. (2023) 16:21. doi: 10.1186/s13040-023-00335-z

29. Zhang E, Hou X, Hou B, Zhang M, Song Y. A risk prediction model of DNA methylation improves prognosis evaluation and indicates gene targets in prostate cancer. *Epigenomics*. (2020) 12:333–52. doi: 10.2217/epi-2019-0349

30. Kerkmeijer LG, Monninkhof EM, van Oort IM, van der Poel HG, de Meerleer G, van Vulpen M. Predict: model for prediction of survival in localized prostate cancer. *World J Urol*. (2016) 34:789–95. doi: 10.1007/s00345-015-1691-4

31. Liu Z, Zhong J, Cai C, Lu J, Wu W, Zeng G. Immune-related biomarker risk score predicts prognosis in prostate cancer. *Aging (Albany NY)*. (2020) 12:22776–93. doi: 10.18632/aging.103921

frontiers | Frontiers in Pharmacology

TYPE Systematic Review
PUBLISHED 09 May 2024
DOI 10.3389/fphar.2024.1379389

OPEN ACCESS

EDITED BY
Vittoria Rago,
University of Calabria, Italy

REVIEWED BY
Diana Simona Antal,
Victor Babes University of Medicine and Pharmacy, Romania
Prem Prakash Kushwaha,
Case Western Reserve University, United States

*CORRESPONDENCE
Jing Chen,
chenjing010@126.com

RECEIVED 31 January 2024
ACCEPTED 16 April 2024
PUBLISHED 09 May 2024

CITATION
Wang S, Zhang F and Chen J (2024), Application and potential value of curcumin in prostate cancer: a meta-analysis based on animal models.
Front. Pharmacol. 15:1379389.
doi: 10.3389/fphar.2024.1379389

Application and potential value of curcumin in prostate cancer: a meta-analysis based on animal models

Shiheng Wang[1,2], Fengxia Zhang[2] and Jing Chen[1]*

[1]College of Medical Imaging Laboratory and Rehabilitation, Xiangnan University, Chenzhou, China, [2]Institute for History of Medicine and Medical Literature, China Academy of Chinese Medical Sciences, Beijing, China

Introduction: Curcumin is gaining recognition as an agent for cancer chemoprevention and is presently administered to humans. However, the limited number of clinical trials conducted for the treatment of prostate cancer is noteworthy. Animal models serve as valuable tools for enhancing our understanding of disease mechanisms and etiology in humans. The objective of this study was to examine the anti-prostate cancer effects of curcumin *in vivo* for comprehending its current research status and potential clinical applicability.

Methods: Our methodology involved a systematic exploration of animal studies pertaining to curcumin and prostate cancer, as documented in PubMed, Web of Science, Embase, Cochrane Library, CNKI, Wanfang database, Vip database, and SinoMed, up to 03 September 2023. Risk of bias was assessed using the SYRCLE Animal Study Risk of Bias tool. The results were combined using the RevMan 5.3.

Results: A comprehensive analysis was conducted on 17 studies encompassing 263 mouse transplantation tumor models. The findings of this meta-analysis demonstrated that curcumin exhibited a superior inhibitory effect on the volume of prostate cancer tumors in mice compared to the control group (standardized mean difference [SMD]: 1.16, 95% confidence interval [CI]: 0.52, 1.80, $p < 0.001$). Additionally, curcumin displayed a more effective inhibition of mice prostate cancer tumor weight (SMD: −3.27, 95% CI: −4.70, −1.83, $p < 0.001$). Furthermore, in terms of tumor inhibition rate, curcumin exhibited greater efficacy (SMD: 0.25, 95% CI: 0.23, 0.27, $p < 0.001$). Moreover, curcumin more effectively inhibited PCNA mRNA (SMD: −3.11, 95% CI: −4.60, −1.63, $p < 0.001$) and MMP2 mRNA (SMD: −3.19, 95% CI: 5.85, −0.53, $p < 0.001$).

Conclusion: Curcumin exhibited inhibitory properties towards prostate tumor growth and demonstrated a beneficial effect on prostate cancer treatment, thereby offering substantiation for further clinical investigations. It is important to acknowledge that the included animal studies exhibited considerable heterogeneity, primarily because of the limited number of studies included. Consequently, additional randomized controlled trials are required to comprehensively assess the efficacy of curcumin in humans.

Systematic Review Registration: (https://www.crd.york.ac.uk/prospero/display_record.php?ID=CRD42023464661), identifier (CRD42023464661).

KEYWORDS

curcumin, prostate cancer, animal models, systematic review, meta-analysis

1 Introduction

Prostate cancer (PCa) is a malignant neoplasm associated with high morbidity and mortality rates. Statistical data indicate that in 2020, there were a projected total of 1,414,259 newly diagnosed cases of PCa worldwide, constituting approximately 7.3% of all newly diagnosed patients with cancer and positioning it as the second most prevalent cancer type. Additionally, PCa is expected to cause 375,304 deaths by, accounting for approximately 3.8% of all cancer-related fatalities (Sung et al., 2021). The prevalence and fatality rates of PCa have increased substantially within the framework of the progressively aging population. Projections indicate that by 2040, the global incidence of PCa is anticipated to surge to approximately 2.3 million fresh cases, accompanied by 740,000 fatalities (National Health Commission of the People's Republic of China, 2019; Ferlay et al.). PCa has emerged as a significant determinant of wellbeing and mortality in men. The principal therapeutic modalities for PCa include surgery, radiotherapy, and chemotherapy. Nevertheless, these interventions are not without limitations and may adversely affect patients' quality of life; hence, it is imperative to address the constraints of existing therapies by advancing and implementing novel anticancer drugs that exhibit enhanced therapeutic efficacy and minimize adverse effects. In this context, herbal extracts have garnered considerable attention, as substantiated by scientific research indicating their potential to inhibit tumor growth (Singh et al., 2022; Bai et al., 2023). Curcumin, a polyphenol derived from turmeric, is commonly used in culinary applications owing to its antioxidant, antimicrobial, and anti-inflammatory properties (Hewlings and Kalman, 2017). A previous meta-analysis has demonstrated the therapeutic potential of curcumin for the treatment of malignant tumors (de Oliveira et al., 2022). To date, there is a lack of published meta-analyses examining the efficacy of curcumin in PCa treatment. Nonetheless, curcumin has demonstrated a significant effect on various PCa cell types when used as a therapeutic intervention (Termini et al., 2020). Previous studies have demonstrated that curcumin has multiple mechanisms of action in relation to PCa. Primarily, it exerts inhibitory effects on the prostate-specific antigen (PSA) by reducing its function and inhibiting its activity, thereby leading to decreased transcriptional activity of the androgen receptor (AR) and diminished expression of AR protein in LNCaP cells (Hewlings and Kalman, 2017). Furthermore, it has been demonstrated that curcumin can impede the activation of NF-κB induced by tumor necrosis factor and facilitate apoptosis in cells affected by PCa (Yang et al., 2005). Additionally, curcumin can hinder PCa progression by upregulating miR-143 and FOXD3 in DU145 and PC-3 cells and concurrently downregulating PGK1 expression (Cao et al., 2017). Furthermore, the inhibition of metastasis and survival of DU145 and PC-3 cells by curcumin *via* the Notch-1 signaling pathway has garnered significant interest in the medical field, highlighting the potential therapeutic value of curcumin in the management of PCa.

Despite the existence of prospective randomized controlled trials on curcumin for PCa (Ide et al., 2010; Hejazi et al., 2016), the limited number of studies and the lack of uniform outcome indicators prevents the execution of a meta-analysis. Currently, there is a growing body of research focusing on animal testing of curcumin for PCa, as animal models serve as valuable tools to enhance our understanding of human disease mechanisms and etiology (Sena et al., 2014). Understanding the mechanisms underlying the therapeutic effects of curcumin in PCa remains incomplete, indicating the need for further investigation. Consequently, the clinical use of curcumin remains a distant prospect. Moreover, the translation of findings from animal studies into human clinical trials poses significant challenges. In this regard, meta-analyses of animal study data are valuable as they facilitate the identification of disparities between preclinical and clinical trial outcomes and aid in enhancing the design of clinical trials (Vesterinen et al., 2014). The primary and paramount recommendation to enhance reproducibility and translation, as outlined by Spanagel, is to perform preclinical meta-analyses (Spanagel, 2022). Hence, our objective was to investigate the therapeutic effects and potential significance of curcumin in animal models of PCa to offer a point of reference for clinical investigation and pharmaceutical advancement.

2 Data and methods

2.1 Registration

This study adhered to the PRISMA guidelines for reporting systematic reviews and was prospectively registered with PROSPERO (https://www.crd.york.ac.uk/PROSPERO/#myprospero) (ID: CRD42023464661).

2.2 Search strategy

PubMed, Embase, Cochrane Library, Web of Science, CNKI, Wanfang, VIP, and SinoMed databases were systematically searched from their inception until 03 September 2023. In addition, a manual search of the references of the included studies was performed. The search strategy was designed based on the following criteria: (1) study population: animal models of PCa and (2) intervention: curcumin. Table 1 presents the search strategy used for the PubMed database.

2.3 Inclusion criteria

2.3.1 Research object

(1) Animal models were limited to rats and mice; (2) PCa models; (3) complete papers, not abstracts; (5) the resulting data were available and could be extracted; (6) control group; and (7) no restrictions on publication time and language.

2.3.2 Intervention

(1) The experimental group was only administered a certain dose of curcumin, and the source of curcumin was not restricted; (2) the control group was administered equal amounts of placebo (such as normal saline and polyethylene glycol) or other drugs (such as paclitaxel and alpha-tomatine); and (3) there was no restriction on the method of taking the medicine, either orally or by injection.

TABLE 1 PubMed search strategy.

Search number	Query
1	Curcumin [MeSH Terms]
2	(((((((Curcumin [Title/Abstract]) OR (1,6-Heptadiene-3,5-dione, 1,7-bis(4-hydroxy-3-methoxyphenyl)-, (E,E)-[Title/Abstract])) OR (Turmeric Yellow [Title/Abstract])) OR (Yellow, Turmeric [Title/Abstract])) OR (Curcumin Phytosome [Title/Abstract])) OR (Phytosome, Curcumin [Title/Abstract])) OR (Diferuloylmethane [Title/Abstract])) OR (Mervia [Title/Abstract]))
3	1 OR 2
4	Prostatic Neoplasms OR Prostatic Intraepithelial Neoplasia [MeSH Terms]
5	1. ((prostat* [Title/Abstract] AND (cancer* [Title/Abstract] OR malignan* OR carcinom* [Title/Abstract] OR tumo* OR neopla* [Title/Abstract] OR adenocarcinom* OR intraepithelial OR adeno* [Title/Abstract])
6	4 OR 5
7	3 AND 6

2.3.3 Outcome measures

Tumor volume (calculated using the formula: Tumor volume (mm3) = π/6 (long diameter × short diameter)2), tumor weight (g), tumor inhibition rate (calculated as (mean tumor weight of control group - mean tumor weight of experimental group)/mean tumor weight of control group * 100%), proliferating cell nuclear antigen-mRNA (PCNA-mRNA), and matrix metallo peptidase (matrix metallo peptidase2-mRNA, MMP2-mRNA). (5) Type of study: animal experiment (randomized control: intervention and control groups). There were no restrictions on the publication time or language.

2.4 Exclusion criteria

(1) Studies with incomplete or unanalyzable data; (2) cell tests, reviews, abstracts, letters, plans, or *in vitro* studies; (3) curcumin was used in the control group; and (4) curcumin was not the main component of the intervention in the experimental group.

2.5 Literature screening

Two researchers (Wang and Zhang) independently used the literature management software EndnoteX9 to screen literature. First, duplicate literature is excluded by searching for duplicate literature. Titles and abstracts were read according to the inclusion and exclusion criteria. If the PICOS met the inclusion criteria, the study was included. Documents were excluded if the exclusion criteria were met. Finally, we read the full text and judge whether the literature meets the inclusion criteria, and if it does, we include it. After screening was completed, the two participants were compared, and if the results were the same, the included study was finally determined. Otherwise, a third researcher (Jing Chen) was consulted or the decision was discussed.

2.6 Data extraction

Two researchers (Wang and Zhang) designed the data extraction tables based on the information required for the research. After reaching a mutual agreement, the necessary information was filtered. Two studies independently extracted data from articles or graphs. The extracted information included the first author, year, sample size, age, intervention, study duration, dose, and outcome indicators. If the data could not be extracted, the author was contacted via email for missing or additional data. Finally, the extracted data were entered into EXCEL. If the extracted outcome index data were continuous, they were uniformly expressed as means and SD. If the outcome index data were binary, they were expressed as the number of occurrence cases ® and number of samples (n). If not, they were converted. If the information extracted by the two people was inconsistent, it was first discussed upon. On still being unsolved, it was either further discussed upon or a third researcher was consulted to decide (Chen).

2.7 Quality evaluation

Two researchers (Wang and Zhang) used the SYRCLE Animal Studies Bias Risk Tool (Hooijmans et al., 2014a) to conduct bias risk assessment. SYRCLE's Risk of Bias tool is an adapted version of the Cochrane risk-of-bias tool used in animal intervention studies. This was an objective assessment of possible biases or confusion in the tools used for the design, conduct, and measurement of the animal experiments. Its suitability for different types and domains of animal experiments covered six areas of bias: selection, implementation, measurement, loss to follow-up, reporting, and others. In each area, the risk of bias was judged to be low (+), unclear (?), or high risk (−). Two researchers independently assessed the risk of bias in the included studies, and if there was a disagreement, a third researcher (Chen) was consulted for resolution.

2.8 Statistical analysis

The meta-analysis was conducted using Revman5.4 and Stata 16.0 software. Relative risk (RR) was employed for dichotomous data, whereas standardized mean difference (SMD) was used for continuous data. The effect estimates were calculated using 95% confidence intervals (CIs). Initially, a heterogeneity test was conducted to address

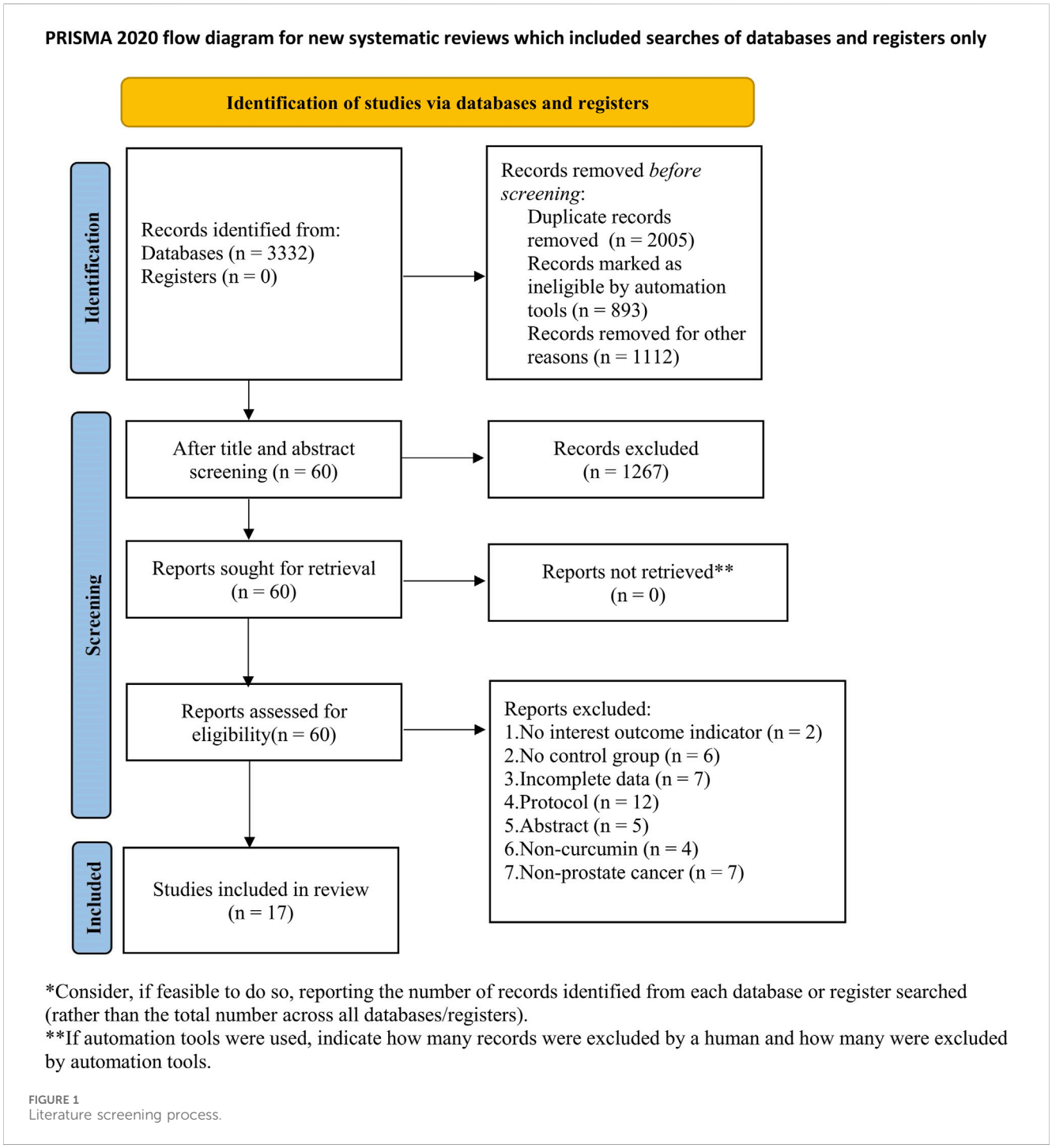

FIGURE 1
Literature screening process.

anticipated heterogeneity, with the I2 statistic (Higgins and Thompson, 2002) being employed for this purpose. In light of the absence of uniformity across animal studies, a random-effects model was chosen, and various statistical techniques, such as meta-regression, subgroup analyses, and sensitivity analyses, were employed to investigate the origins of heterogeneity. Funnel plots were generated to examine publication bias, adhering to the Cochrane Handbook's recommendation to include at least 10 relevant literature sources. Assessment of publication bias involved a visual assessment of funnel plot asymmetry.

3 Results

3.1 Results of literature screening

A comprehensive search was conducted on 3,332 papers, eliminating 2,005 duplicates. Subsequently, 1,267 papers were excluded based on an evaluation of their titles and abstracts. Upon further examination of the full text, an additional 43 papers were excluded for various reasons, such as the absence of endpoint indicators suitable for inclusion, lack of a control group, incomplete data, inadequate trial plan or abstract, intervention not

TABLE 2 Basic characteristics of the included studies.

First author	Country	Year	Age	Cell types	Intervention (I/C)	Administration	Cases (I/C)	Treatment (week)	Outcome indicator
Zhang (2013)	China	2013	4w	PC-3	Curcumin placebo	intraperitoneal injection	6.6	4	Tumor volume, tumor weight
Ye (2015)	China	2015	4-5w	PC-3	Curcumin, Polyethylene glycol	intraperitoneal injection	5.7	2	Tumor volume, PCNAmRNA
QI et al. (2015)	China	2015	4w	PC-3	Curcumin, saline	intraperitoneal injection	6.6	4	MMP2mRNA
Qi (2009)	China	2009	4w	PC-3	Curcumin, Paclitaxel	intraperitoneal injection	6.6	4	Tumor suppressor, PCNAmRNA, MMP2 mRNA
MAO et al. (2019)	China	2019	4-5w	RM-1	Curcumin, DMSO	intraperitoneal injection	10.10	2	Tumor weight, tumor suppression
Limin et al. (2007)	China	2007	4-6w	PC-3	Curcumin, polyethylene glycol	intraperitoneal injection	6.6	4	Tumor volume, tumor weight, tumor inhibition
Roy et al. (2016)	China	2016	4w	PC-3	Curcumin, Polyethylene glycol	intraperitoneal injection	6.6	4	tumor weight
LI et al. (2013)	China	2013	4-6w	PC-3	Curcumin, saline	intraperitoneal injection	12.12	4	Tumor volume, tumor weight, tumor inhibition
ZHAO et al. (2010)	China	2010	4-6w	PC-3	Curcumin, placebo	intraperitoneal injection	6.6	4	Tumor volume, PCNAmRNA,MMP2mRNA
Zhao et al. (2018)	China	2017	-	LNCaP	Curcumin, DMSO	intraperitoneal injection	4.4	7	Tumor volume
Yang et al. (2015)	China	2015	-	PC-3	Curcumin, Polyethylene glycol	intraperitoneal injection	8.8	4	Tumor volume, tumor weight, tumor inhibition
Dorai et al. (2001)	United States of America	2001	6-8w	LNCaP	Curcumin, feed	profess conviction	10.10	6	Tumor volume
Khor et al. (2006)	United States of America	2006	6w	PC-3	Curcumin, PEITC	intraperitoneal injection	12.12	4	Tumor volume, tumor weight
Huang et al. (2015)	China	2015	6-7w	PC-3	Curcumin, α-Tomatine	intraperitoneal injection	9.9	4	Tumor volume, tumor weight
Fernández-Martínez et al. (2009)	Spain	2009	5-6w	PC-3	Curcumin, NS-398	intraperitoneal injection	8.8	4	Tumor volume, tumor weight, MMP2mRNA
Cheng et al. (2020)	China	2020	5-8w	LC540	Curcumin, DMSO	intraperitoneal injection	6.6	1	Tumor volume, tumor weight
Barve et al. (2008)	United States of America	2008	-	PC-3	Curcumin, PEITC	profess conviction	12.9	16	PCNAmRNA

I, test group; C, control group; DMSO, dimethyl sulfoxide; PEITC, phenethyl isothiocyanate.

10.3389/fphar.2024.1379389

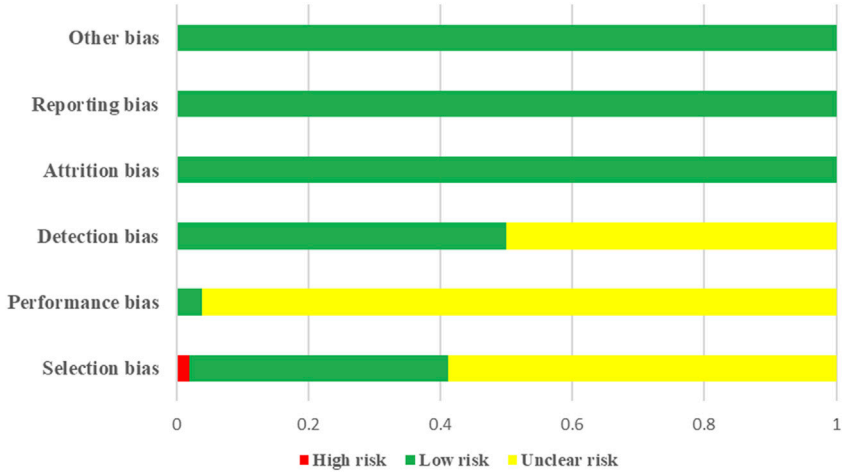

FIGURE 2
Results of risk of bias assessment.

involving curcumin, and absence of PCa. Ultimately, 17 animal trials were deemed eligible for inclusion. Figure 1 shows the results of the literature review.

3.2 Basic characteristics

Seventeen animal experiments involving the use of mouse transplantation tumor models were included in the analysis. The experimental group consisted of 132 mice, whereas the control group consisted of 131 mice, resulting in a total of 263 mice used in the study. Among the included studies, 13 originated in China (Limin et al., 2007; Qi, 2009; ZHAO et al., 2010; LI et al., 2013; Zhang, 2013; Huang et al., 2015; QI et al., 2015; Yang et al., 2015; Ye, 2015; Roy et al., 2016; Zhao et al., 2018; MAO et al., 2019; Cheng et al., 2020). Additionally, three studies were conducted in the United States (Dorai et al., 2001; Khor et al., 2006; Barve et al., 2008), while one study was conducted in Spain (Fernández-Martínez et al., 2009). Curcumin, obtained from Sigma (USA), was administered to the test group predominantly intraperitoneally, with only a few studies utilizing oral administration. The control group, in contrast, received a placebo intervention. Table 2 summarizes the basic characteristics of the included studies.

3.3 Risk of bias assessment

Three studies (QI et al., 2015; Roy et al., 2016; MAO et al., 2019) used the random number table method to address selection bias, whereas one study (Dorai et al., 2001) employed randomization to allocate participants into intervention groups. The remaining studies did not provide sufficient information on their approaches to selection bias. Regarding implementation bias, only one study (ZHAO et al., 2010) reported the use of randomization and blinding, whereas the remaining studies did not explicitly state their methods. Blinding was not described in any of the studies, indicating potential measurement bias. The risks of lost visits, reporting, and other biases were relatively low. Figures 2, 3 show the results of the risk of bias assessment.

3.4 Meta-analysis results

3.4.1 Tumor volume

Twelve studies (Dorai et al., 2001; Higgins and Thompson, 2002; Khor et al., 2006; Limin et al., 2007; Fernández-Martínez et al., 2009; ZHAO et al., 2010; LI et al., 2013; Zhang, 2013; Hooijmans et al., 2014a; Huang et al., 2015; Yang et al., 2015; Ye, 2015; Roy et al., 2016; Zhao et al., 2018; Cheng et al., 2020) included in the analysis provided data on the tumor volume. The findings revealed a noteworthy suppressive effect of curcumin on PCa tumor volume in mice compared to that in the control groups (SMD: 1.16, 95% CI: 0.52, 1.80, $p < 0.001$). A considerable heterogeneity was observed among the included studies (I2 = 89%). Figure 4 shows a forest plot of tumor volume after curcumin treatment of PCa.

3.4.2 Tumor weight

Ten studies (Khor et al., 2006; Limin et al., 2007; Fernández-Martínez et al., 2009; LI et al., 2013; Zhang, 2013; Huang et al., 2015; Yang et al., 2015; Roy et al., 2016; Cheng et al., 2020) provided data on tumor weight, and the findings revealed a significant inhibitory effect of curcumin on the tumor weight of PCa in mice when compared to the control groups (SMD: −3.27, 95% CI: −4.70, −1.83, $p < 0.001$). Notably, substantial heterogeneity was observed among the included studies (I2 = 88%). Figure 5 shows a forest plot of tumor weight after curcumin treatment of PCa.

3.4.3 Tumor suppression rate

Tumor suppression rates were reported in five studies (Limin et al., 2007; Qi, 2009; LI et al., 2013; Yang et al., 2015; MAO et al., 2019). The findings indicated that curcumin exhibited a significantly higher tumor inhibition rate in mouse PCa than in the control group (SMD: 0.90, 95% CI: 0.44, 1.36, $p < 0.001$). Figure 6 shows a forest plot of the tumor inhibition rate of curcumin treatment in PCa.

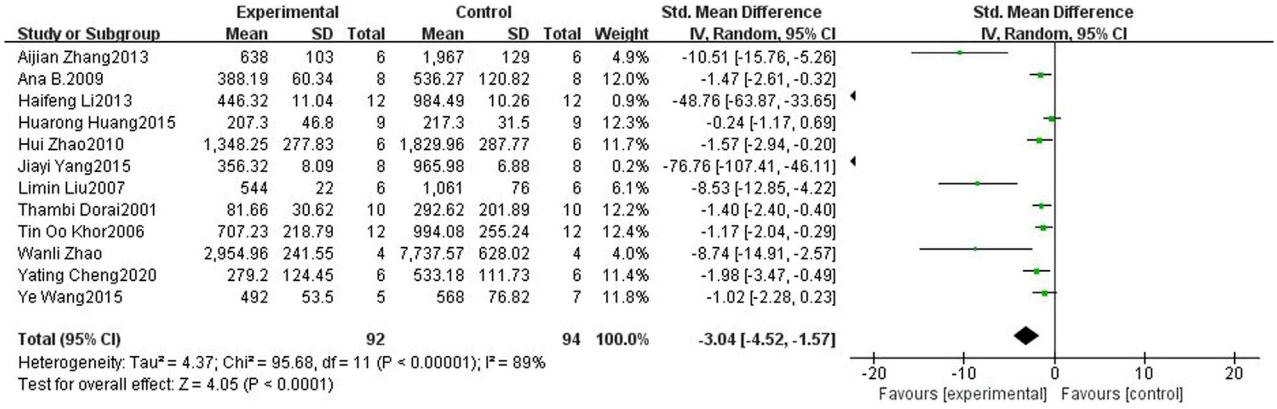

FIGURE 3
Forest plot of tumor volume for curcumin treatment of prostate cancer.

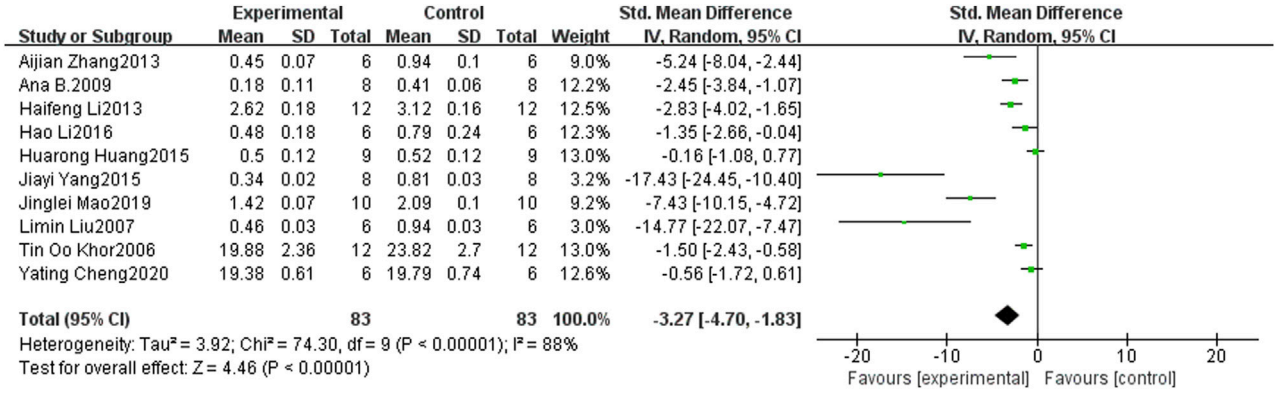

FIGURE 4
Forest plot of tumor weight for curcumin treatment of prostate cancer.

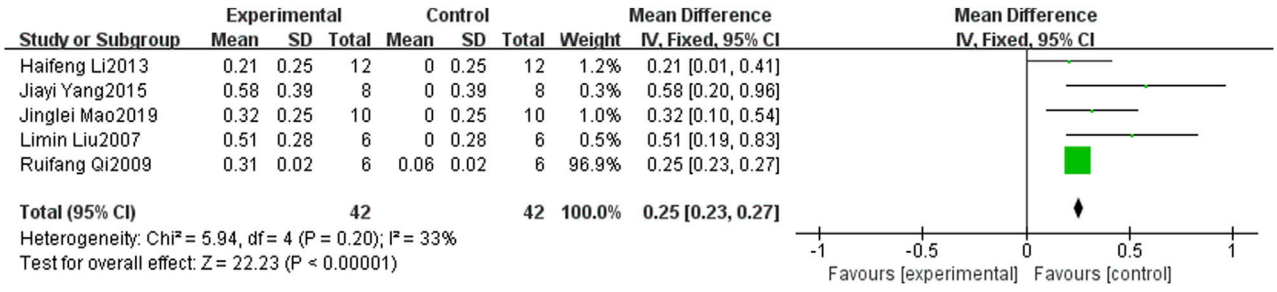

FIGURE 5
Forest plot of tumor inhibition rate for curcumin treatment of prostate cancer.

3.4.4 PCNA mRNA

Four studies (Barve et al., 2008; Qi, 2009; ZHAO et al., 2010; Ye, 2015) documented the presence of PCNA mRNA. The findings indicated that curcumin exhibited superior inhibition of PCNA mRNA in mice PCa tumors when compared to the control group (SMD: −3.11, 95% CI: −4.60, −1.63, $p < 0.001$). Figure 7 shows a forest plot of PCNA mRNA expression after curcumin treatment in PCa.

3.4.5 MMP2 mRNA

Three studies (Qi, 2009; ZHAO et al., 2010; QI et al., 2015) examined the expression of MMP2 mRNA and found that curcumin demonstrated a significantly greater inhibitory effect on MMP2 mRNA in a mice transplant tumor model of PCa when compared to the control group (SMD: −3.19, 95% CI: −5.85, −0.53, $p < 0.001$). Figure 8 shows a forest plot of MMP2 mRNA expression after curcumin treatment in PCa.

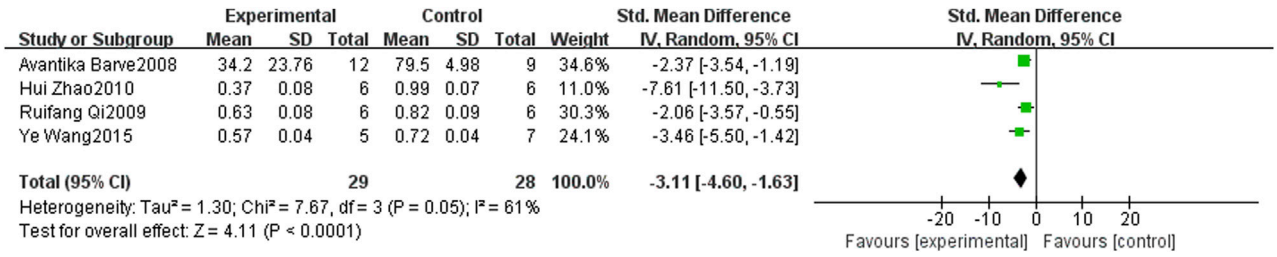

FIGURE 6
Forest plot of PCNA mRNA for curcumin treatment of prostate cancer.

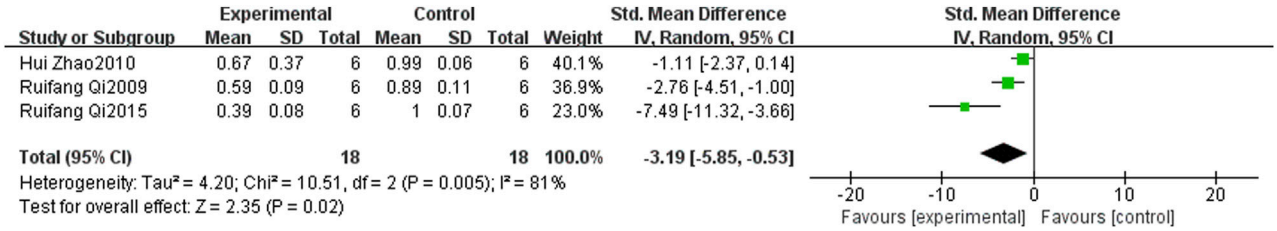

FIGURE 7
Forest plot of MMP2 mRNA for curcumin treatment of prostate cancer.

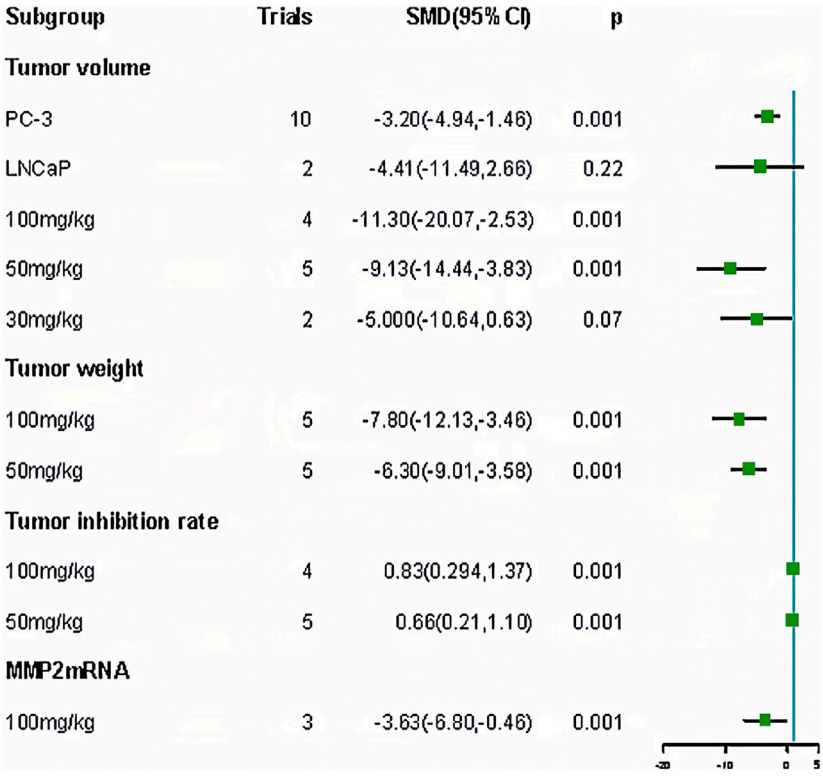

FIGURE 8
Forest plot of subgroup for curcumin treatment of prostate cancer.

TABLE 3 Meta-regression results of curcumin in the treatment of prostate cancer.

Intervention	Trials	Outcome indicator	
		Treatments	Dosages
MMP2 mRNA	3	-	0.603
PCNAmRNA	4	0.557	0.808
Tumor volume	12	0.071	0.509
tumor weight	10	0.658	0.183
Tumor Suppression Rate	5	0.286	0.033

3.5 Meta regression

We performed a meta-analysis of duration and dose. The results showed that the curcumin dose affected the tumor inhibition rate ($p < 0.05$) (Table 3). Subsequently, we performed a subgroup analysis of the doses. Subgroup analysis showed that the effect of 100 mg/kg curcumin (SMD: 0.83, 95% CI: 0.294.1.37) was better than 50 mg/kg curcumin (SMD: 0.66, 95% CI: 0.21.1.10), which proved that the meta regression results were correct (Table 4).

3.6 Subgroup and sensitivity analyses

We performed a subgroup analysis of PCa cell types and doses. The results showed that: (1) ginger had different effects on different PCa cells. The effect of the PC - 3 (SMD: 11.30, 95% CI: 20.07, 2.53) was superior to that of the LNCaP (SMD: 4.41, 95% CI: 11.49, 2.66). The effect of the PC - 3 (SMD: 11.30, 95% CI: 20.07, 2.53) was superior to the LNCaP (SMD: 4.41, 95% CI: 11.49, 2.66). (2) Different doses of curcumin had different effects on outcome indexes. In terms of tumor volume, effect of ranking was 100 mg/kg (SMD: 11.30, 95% CI: 20.07, 2.53) > 50 mg/kg (SMD: 9.13, 95% CI: 14.44, 3.83) > 30 mg/kg (SMD: 5.00, 95% CI: 10.64, 0.63). The effect on tumor weight was 100 mg/kg (SMD: 7.80, 95% CI: 12.13, 3.46) > 50 mg/kg (SMD: 6.30, 95% CI: 9.01, 3.58). The tumor inhibition rate was 100 mg/kg (SMD: 0.83, 95% CI: 0.294, 1.37) to 50 mg/kg (SMD: 0.66, 95% CI: 0.21, 1.10). The results of the subgroup analysis showed a positive correlation between the curcumin dose and results; the higher the dose, the better the effect (Table 4; Figure 9). Contour-weighted funnel plots and cut-and-complement methods showed a low likelihood of publication bias (Figure 9, Table 5).

Sensitivity analysis was performed on the results of the meta-analysis. The following results were obtained: tumor volume (SMD: −3.04, 95% CI: 4.51,-1.57, $p = 0.0001$), tumor weight (SMD: 3.62, 95% CI: 5.14,-2.09, $p = 0.0001$), tumor inhibition rate (SMD: 0.90, 95% CI: 0.44, 1.36, $p = 0.0001$), PCNA mRNA (SMD: 3.45, 95% CI: 5.10, 1.81, $p = 0.0001$), and MMP2 mRNA (SMD: 3.56, 95% CI: 6.46, 0.67, $p = 0.0001$). The results of sensitivity analysis showed that the results of the meta-analysis were stable (Table 6).

4 Discussion

4.1 Summary of evidence

This study included 17 meta-analyses that aimed to examine the evidence derived from animal studies on the therapeutic efficacy of curcumin in the treatment of PCa. The findings indicated that curcumin exhibited inhibitory effects on PCNA and MMP2 mRNA expression and the growth of malignant tumors in PCa cells of animal models when compared to control groups. The stability of the results was confirmed through a sensitivity analysis. Furthermore, the meta-regression analysis demonstrated that the dosage of curcumin had a significant impact on the rate of tumor inhibition in the animal model. Through subgroup analysis, a positive correlation between the dosage of curcumin and the outcomes was determined, indicating that higher doses of curcumin yielded more favorable effects.

4.2 Mechanisms underlying the therapeutic effects of curcumin in PCa management

Curcumin exhibits anticancer properties, as demonstrated in a meta-analysis conducted by de Oliveira et al. (de Oliveira et al., 2022).

TABLE 4 Results of subgroup analysis.

Outcomes	Subgroup	Trials	SMD95% CI	P
Tumor volume	PC-3	10	−3.20 (-4.94,-1.46)	0.0001
	LNCaP	2	−4.41 (−11.49.2.66)	0.22
	100 mg/kg	4	−11.30 (-20.07,-2.53)	0.0001
	50 mg/kg	5	−9.13 (-14.44,-3.83)	0.0001
	30 mg/kg	2	−5.000 (−10.64.0.63)	0.069
Tumor weight	100 mg/kg	5	−7.80 (-12.13,-3.46)	0.0001
	50 mg/kg	5	−6.30 (-9.01,-3.58)	0.0001
Tumor inhibition rate	100 mg/kg	4	0.83 (0.294.1.37)	0.0001
	50 mg/kg	5	0.66 (0.21.1.10)	0.0001
MMP2mRNA	100 mg/kg	3	−3.63 (-6.80,-0.46)	0.0001

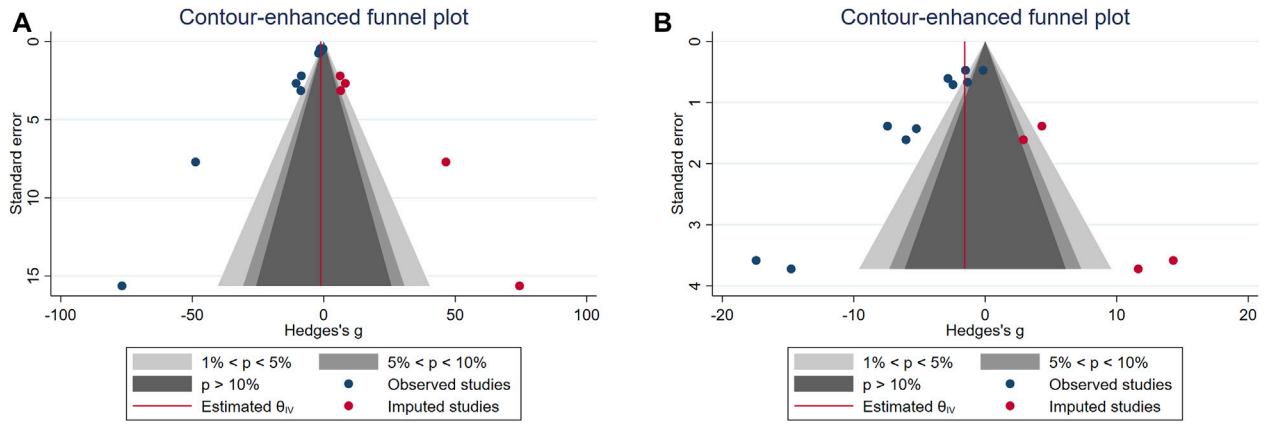

FIGURE 9
(A) Weighted funnel plot of tumor volume. **(B)** Weighted funnel plot of tumor weight.

TABLE 5 Results of publication bias detection.

Outcomes	Trim and fill method outcome	Hedges's g	95% CI
Tumor volume	Observed	−1.34	−1.75,-0.94
	Observed + Imputed	−1.144	−1.54,-0.73
Tumor weight	Observed	−1.96	−2.43,-1.493
	Observed + Imputed	−1.56	−2.018,-1.10

TABLE 6 Sensitivity analysis results.

Outcomes	SMD95% CI	P
Tumor volume	−3.04 (−4.51,-1.57)	0.0001
Tumor weight	−3.62 (-5.14,-2.09)	0.0001
Tumor Suppression Rate	0.90 (0.44.1.36)	0.0001
PCNAmRNA	−3.45 (−5.10,-1.81)	0.0001
MMP2mRNA	−3.56 (-6.46,-0.67)	0.0001

The analysis revealed that curcumin exerts therapeutic effects on various tumor types, including the inhibition of tumor growth (SMD: −3.03; 95% CI: −3.84, −2.21; $p < 0.00001$), reduction in tumor volume (SMD: −7.30; 95% CI: −11.39,-3.21; $p < 0.00001$), and decrease in tumor weight (SMD: −3.96; 95% CI: −6.22, - 1.70; $p = 0.0006$). Furthermore, studies have indicated that curcumin exhibits a greater affinity for PCa cells than for healthy prostate epithelial cells in individuals without the disease, suggesting its potential as a chemopreventive agent against human PCa (Srivastava et al., 2007). However, the existing body of meta-analytical studies on the efficacy of curcumin in PCa remains insufficient. This study, in contrast, revealed significant reductions in both prostate tumor volume and weight, as well as the inhibition of PCa cell growth, following curcumin administration. These effects were attributed to three primary pathways of action. First, curcumin can impede PCa LNCaP cell viability and induce apoptosis (Mukhopadhyay et al., 2001; Nakamura et al., 2002). Curcumin exhibited anti-proliferative properties in LNCaP cells, resulting in a dose-dependent reduction in DNA synthesis efficiency (Mukhopadhyay et al., 2002). Additionally, it downregulated the expression of G1/S-specific cyclin D1, which is frequently overexpressed in various tumor cells and is a crucial target for inhibiting tumor cell proliferation (Bharti et al., 2003; Shankar and Srivastava, 2007; Mahammedi et al., 2016; Yang et al., 2017; Choi et al., 2019; Termini et al., 2020; Ferlay et al.). Curcumin exerted inhibitory effects on the proliferation of PCa cells by downregulating cyclin D1 expression, thereby impeding the transition of tumor cells from the G1 to S phase. Disruption of cell cycle led to apoptosis. In addition, curcumin upregulated Bax, which promotes apoptosis, and downregulated Bcl-2, which inhibits apoptosis in cancer cells. Bcl-2 and Bax expression is closely associated with apoptosis in cancer cells.

In the present study, curcumin exhibited a noteworthy advantage in suppressing PCNA mRNA and MMP2 mRNA in comparison to the control group ($p < 0.05$). PCNA mRNA, a recently discovered probe for assessing the proliferative activity of PCa cells, reflects the extent of cell proliferation (Squires et al., 2003). PCNA mRNA serves as a robust positive marker of the proliferative activity of PCa cells, thereby emerging as a novel determinant for assessing the biological behavior of PCa. Strong positive expression of PCNA mRNA signifies the presence of PCa cells with heightened proliferative activity, elevated malignancy levels, and an unfavorable prognosis, thus establishing a novel criterion for evaluating the biological behavior of PCa (Park et al., 2005; Prusty and Das, 2005). MMP2 mRNA is a member of the matrix metalloproteinases (MMPs), a group of proteins that

have been demonstrated to be associated with tumor metastasis (Dos Reis et al., 2009). Additionally, MMPs play a role in tumor growth regulation by maintaining the integrity of cellular pathways (Dorai et al., 2000a). The expression of MMP2 is minimal in benign prostate hyperplasia tissues, whereas in PCa tissues, its expression level correlates with the degree of proliferation. MMP2 is highly expressed in PCa tissues and plays a crucial role in the metastatic progression of prostate tumors (Dorai et al., 2000b). The findings from the cellular assay demonstrated that curcumin could impede the expression of PCNA and MMP2 in PCa cells, thereby highlighting its distinctive merits in PCa management (Hong et al., 2006; Teiten et al., 2011). However, given the limited number of incorporated studies, further rigorous investigations encompassing both the fundamental and clinical realms are imperative to substantiate the efficacy of curcumin in suppressing PCNA mRNA and MMP2 mRNA.

4.3 Current status of clinical research and future application potential

Currently, the use of curcumin for PCa treatment relies primarily on preliminary investigations and limited clinical studies, resulting in insufficient evidence. However, few published clinical studies have substantiated the efficacy and safety of curcumin in the treatment of PCa. For instance, Mahammedi conducted a study involving 30 patients with desmoplasma-resistant PCa, administering a combination of docetaxel/prednisone and curcumin. The findings of the study conducted by Choi et al. (2019) revealed that a significant reduction in PSA levels was observed in 59% of the participants, with 14% achieving complete normalization. Additionally, 40% of the patients reported experiencing symptom relief. Furthermore, the study demonstrated that the adverse effects were attributable to the administration of docetaxel rather than curcumin, as the latter exhibited no toxic effects. The trial, which was randomized and double-blinded, encompassed a sample of 97 individuals diagnosed with PCa and indicated a statistically significant decrease in the proportion of patients experiencing PSA progression over a 6-month treatment period in the curcumin group compared with that in the placebo group (10.3% vs 30.2%, $p = 0.00259$). Additionally, the incidence of adverse events was lower in the curcumin group (15.56%) than that in the placebo group (34.78%). Notably, the Clinical Trial Registry platform (https://beta.clinicaltrials.gov) currently hosts numerous ongoing clinical studies on curcumin for PCa, with some already completed or in progress (e.g., NCT02064673, NCT04731844, NCT03211104, NCT03769766, etc.). Increasing attention on curcumin treatment for PCa indicates its potential for broad clinical applications. Consequently, our future focus will be directed towards closely monitoring clinical studies on curcumin for PCa, aiming to gather additional clinical evidence.

4.4 Factors affecting curcumin treatment of PCa

Several clinical studies have demonstrated that curcumin dosage plays a significant role in its effectiveness (de Waure et al., 2023). High doses of curcumin, such as 3.6 g/d for 6 months or 8 g/d for 28 days, have been shown to effectively reduce tumor volume and enhance survival rates (Kuriakose et al., 2016; Santosa et al., 2022). These findings are consistent with those of the present study. Furthermore, studies have indicated that the physicochemical properties of curcumin influence its efficacy. Notably, curcumin exhibits poor water solubility and low systemic bioavailability of approximately 0.47% when administered orally (Mirzaei et al., 2017). Encapsulation of curcumin within polymeric nanocarriers has been suggested as a potential solution to improve its physicochemical properties (Klippstein et al., 2015). Polymer nanocapsules, which are characterized by vesicular nanostructures encompassing an oily core encased by a polymer wall, have been extensively studied to enhance curcumin stability, augment its apparent water solubility, improve its bioavailability, and enhance its *in vivo* anti-inflammatory (Asadirad et al., 2022), neuroprotective (Hoppe et al., 2013), and antitumor effects (Zanotto-Filho et al., 2013). This will significantly enhance the advancement of curcumin-based pharmaceuticals and clinical utilization of curcumin. The findings of this study indicate that curcumin has a more pronounced effect on PC-3 cells than on LNCaP cells. Currently, there is a lack of evidence elucidating the underlying reasons, which is potentially attributable to the limited number of LNCaP cells included in this study (only two studies). Given the limited number of included studies, further research is warranted to validate the effects of curcumin dosage, treatment duration, administration method, PCa cell type, and other relevant factors on its efficacy.

4.5 Strengths and limitations of this study

Strengths of this study: This study is the inaugural systematic review of animal studies investigating the effects of curcumin on PCa. The evidence derived from these studies holds immense potential for evaluating the effectiveness and possible clinical applications of curcumin in cancer treatment. Consequently, this evidence can serve as a foundation for the design and implementation of clinical trials as well as the advancement of novel therapeutic interventions.

Limitations of this study: The inability to conduct a meta-analysis of the clinical studies was attributed to the limited number of available trials. This limitation was further compounded by the absence of standardized protocols in the included animal trials, resulting in substantial heterogeneity in terms of study design, disease staging, control group, dose, and regimen. Meta-analysis of animal trials may exhibit even greater heterogeneity than clinical studies (Hooijmans et al., 2014b). Consequently, numerous meta-analyses on animal tests have encountered challenges in addressing this issue (de Oliveira et al., 2022; Luís et al., 2023; Dan et al., 2024). Subgroup analyses have been commonly performed to address heterogeneity. However, owing to the limited number of articles within each subgroup, we conducted a subgroup analysis solely on dosage, precluding the examination of factors, such as the mode of administration, treatment duration, and treatment frequency. The findings from the subgroup analyses indicated that dosage exerted an impact on the results, albeit without a substantial reduction in heterogeneity. The meta-analysis conducted by e Oliveira TV et al. (de Oliveira et al., 2022) examined the impact of curcumin's mode of administration, dose, and treatment duration on the outcomes

reported in various articles. The findings revealed that these factors did not significantly influence the results and there was no substantial reduction in heterogeneity. These findings are consistent with the results of this study. Furthermore, a significant number of experimental studies lack comprehensive reporting of randomization methods, allocation concealment, and randomization of outcome assessments, thereby leading to an indeterminate risk of selection, implementation, and measurement biases. Consequently, there is a pressing need to enhance the methodological rigor of animal testing, given that the findings of such studies frequently inform clinical applications. Petersen et al. (Petersen et al., 2016). Discussed the limitation of interpreting preclinical studies, arguing that this increases the difficulty of evaluating the results of preclinical studies owing to differences in pharmacokinetics and pharmacodynamics between humans and animals. He recommends the creation of consensus guidelines for evaluating the conduct and reporting of preclinical research findings. Meta-analyses of animal experiments should be referenced in the future, which will help improve the quality of evidence in animal experiments.

5 Conclusion

Determining the underlying factors contributing to the heterogeneity in animal studies remains challenging because of the substantial variations observed in experimental settings. Nonetheless, animal studies are imperative to unravel the etiology of these diseases and evaluate the safety and effectiveness of therapeutic interventions. In the present investigation, we examined the effects of curcumin in preclinical trials targeting PCa. The findings revealed a favorable outcome associated with curcumin administration in PCa treatment, with dosage potentially influencing its efficacy. Notwithstanding the limited number of incorporated studies and the substantial variability in the outcomes, this meta-analysis methodically and impartially measured the impact of curcumin in the management of PCa, thereby offering significant insights for clinical investigations. Consequently, additional double-blind, placebo-controlled, randomized clinical trials are required to assess the efficacy of curcumin in humans.

Data availability statement

The raw data supporting the conclusion of this article will be made available by the authors, without undue reservation.

Author contributions

SW: Writing–review and editing, Writing–original draft. FZ: Writing–review and editing. JC: Writing–review and editing, Supervision.

Funding

The author(s) declare that no financial support was received for the research, authorship, and/or publication of this article.

Conflict of interest

The authors declare that the research was conducted in the absence of any commercial or financial relationships that could be construed as a potential conflict of interest.

Publisher's note

References

Asadirad, A., Nashibi, R., Khodadadi, A., Ghadiri, A. A., Sadeghi, M., Aminian, A., et al. (2022). Antiinflammatory potential of nano-curcumin as an alternative therapeutic agent for the treatment of mild-to-moderate hospitalized COVID-19 patients in a placebo-controlled clinical trial. *Phytother. Res.* 36 (2), 1023–1031. doi:10.1002/ptr.7375

Bai, Y., Li, M., Geng, D., Liu, S., Chen, Y., Li, S., et al. (2023). Polyphyllins in cancer therapy: a systematic review and meta-analysis of animal studies. *Phytomedicine* 121, 155096. doi:10.1016/j.phymed.2023.155096

Barve, A., Khor, T. O., Hao, X., Keum, Y. S., Yang, C. S., Reddy, B., et al. (2008). Murine prostate cancer inhibition by dietary phytochemicals--curcumin and phenyethylisothiocyanate. *Pharm. Res.* 25 (9), 2181–2189. doi:10.1007/s11095-008-9574-7

Bharti, A. C., Donato, N., Singh, S., and Aggarwal, B. B. (2003). Curcumin (diferuloylmethane) down-regulates the constitutive activation of nuclear factor-kappa B and IkappaBalpha kinase in human multiple myeloma cells, leading to suppression of proliferation and induction of apoptosis. *Blood* 101 (3), 1053–1062. doi:10.1182/blood-2002-05-1320

Cao, H., Yu, H., Feng, Y., Chen, L., and Liang, F. (2017). Curcumin inhibits prostate cancer by targeting PGK1 in the FOXD3/miR-143 axis. *Cancer Chemother. Pharmacol.* 79 (5), 985–994. doi:10.1007/s00280-017-3301-1

Cheng, Y., Yang, Y., Wu, Y., Wang, W., Xiao, L., Zhang, Y., et al. (2020). The curcumin derivative, H10, suppresses hormone-dependent prostate cancer by inhibiting 17β-hydroxysteroid dehydrogenase type 3. *Front. Pharmacol.* 11, 637. doi:10.3389/fphar.2020.00637

Choi, Y. H., Han, D. H., Kim, S. W., Kim, M. J., Sung, H. H., Jeon, H. G., et al. (2019). A randomized, double-blind, placebo-controlled trial to evaluate the role of curcumin in prostate cancer patients with intermittent androgen deprivation. *Prostate* 79 (6), 614–621. doi:10.1002/pros.23766

Dan, L., Hao, Y., Song, H., Wang, T., Li, J., He, X., et al. (2024). Efficacy and potential mechanisms of the main active ingredients of astragalus mongholicus in animal models of liver fibrosis: a systematic review and meta-analysis. *J. Ethnopharmacol.* 319 (Pt 1), 117198. doi:10.1016/j.jep.2023.117198

de Oliveira, T. V., Stein, R., de Andrade, D. F., and Beck, R. C. R. (2022). Preclinical studies of the antitumor effect of curcumin-loaded polymeric nanocapsules: a systematic review and meta-analysis. *Phytother. Res.* 36 (8), 3202–3214. doi:10.1002/ptr.7538

de Waure, C., Bertola, C., Baccarini, G., Chiavarini, M., and Mancuso, C. (2023). Exploring the contribution of curcumin to cancer therapy: a systematic review of randomized controlled trials. *Pharmaceutics* 15 (4), 1275. doi:10.3390/pharmaceutics15041275

Dorai, T., Cao, Y. C., Dorai, B., Buttyan, R., and Katz, A. E. (2001). Therapeutic potential of curcumin in human prostate cancer. III. Curcumin inhibits proliferation, induces apoptosis, and inhibits angiogenesis of LNCaP prostate cancer cells *in vivo*. *Prostate* 47 (4), 293–303. doi:10.1002/pros.1074

Dorai, T., Gehani, N., and Katz, A. (2000a). Therapeutic potential of curcumin in human prostate cancer-I. curcumin induces apoptosis in both androgen-dependent and androgen-independent prostate cancer cells. *Prostate Cancer Prostatic Dis.* 3 (2), 84–93. doi:10.1038/sj.pcan.4500399

Dorai, T., Gehani, N., and Katz, A. (2000b). Therapeutic potential of curcumin in human prostate cancer. II. Curcumin inhibits tyrosine kinase activity of epidermal growth factor receptor and depletes the protein. *Mol. Urol.* 4 (1), 1–6.

Dos Reis, S. T., Pontes, J., Jr, Villanova, F. E., Borra, P. M. d. A., Antunes, A. A., Dall'oglio, M. F., et al. (2009). Genetic polymorphisms of matrix metalloproteinases: susceptibility and prognostic implications for prostate cancer. *J. Urol.* 181 (5), 2320–2325. doi:10.1016/j.juro.2009.01.012

Ferlay, J., Ervik, M., Lam, F., et al. *Global cancer observatory: cancer today*. France: International Agency for Research on CancerLyon.

Fernández-Martínez, A. B., Bajo, A. M., Valdehita, A., Isabel Arenas, M., Sánchez-Chapado, M., Carmena, M. J., et al. (2009). Multifunctional role of VIP in prostate cancer progression in a xenograft model: suppression by curcumin and COX-2 inhibitor NS-398. *Peptides* 30 (12), 2357–2364. doi:10.1016/j.peptides.2009.09.018

Hejazi, J., Rastmanesh, R., Taleban, F. A., Molana, S. H., Hejazi, E., Ehtejab, G., et al. (2016). Effect of curcumin supplementation during radiotherapy on oxidative status of patients with prostate cancer: a double blinded, randomized, placebo-controlled study. *Nutr. Cancer* 68 (1), 77–85. doi:10.1080/01635581.2016.1115527

Hewlings, S. J., and Kalman, D. S. (2017). Curcumin: a review of its' effects on human Health. *foods* 6, 92. doi:10.3390/foods6100092

Higgins, J. P., and Thompson, S. G. (2002). Quantifying heterogeneity in a meta-analysis. *Stat. Med.* 21 (11), 1539–1558. doi:10.1002/sim.1186

Hong, J. H., Ahn, K. S., Bae, E., Jeon, S. S., and Choi, H. Y. (2006). The effects of curcumin on the invasiveness of prostate cancer *in vitro* and *in vivo*. *Prostate Cancer Prostatic Dis.* 9 (2), 147–152. doi:10.1038/sj.pcan.4500856

Hooijmans, C. R., Rovers, M. M., de Vries, R. B., Leenaars, M., Ritskes-Hoitinga, M., and Langendam, M. W. (2014a). SYRCLE's risk of bias tool for animal studies. *BMC Med. Res. Methodol.* 14, 43. doi:10.1186/1471-2288-14-43

Hooijmans, C. R., Rovers, M. M., de Vries, R. B., Leenaars, M., Ritskes-Hoitinga, M., and Langendam, M. W. (2014b). SYRCLE's risk of bias tool for animal studies. *BMC Med. Res. Methodol.* 14, 43. doi:10.1186/1471-2288-14-43

Hoppe, J. B., Coradini, K., Frozza, R. L., Oliveira, C. M., Meneghetti, A. B., Bernardi, A., et al. (2013). Free and nanoencapsulated curcumin suppress β-amyloid-induced cognitive impairments in rats: involvement of BDNF and Akt/GSK-3β signaling pathway. *Neurobiol. Learn Mem.* 106, 134–144. doi:10.1016/j.nlm.2013.08.001

Huang, H., Chen, X., Li, D., He, Y., Li, Y., Du, Z., et al. (2015). Combination of α-tomatine and curcumin inhibits growth and induces apoptosis in human prostate cancer cells. *PLoS One* 10 (12), e0144293. doi:10.1371/journal.pone.0144293

Ide, H., Tokiwa, S., Sakamaki, K., Nishio, K., Isotani, S., Muto, S., et al. (2010). Combined inhibitory effects of soy isoflavones and curcumin on the production of prostate-specific antigen. *Prostate* 70 (10), 1127–1133. doi:10.1002/pros.21147

Khor, T. O., Keum, Y. S., Lin, W., Kim, J. H., Hu, R., Shen, G., et al. (2006). Combined inhibitory effects of curcumin and phenethyl isothiocyanate on the growth of human PC-3 prostate xenografts in immunodeficient mice. *Cancer Res.* 66 (2), 613–621. doi:10.1158/0008-5472.CAN-05-2708

Klippstein, R., Wang, J. T., El-Gogary, R. I., Bai, J., Mustafa, F., Rubio, N., et al. (2015). Passively targeted curcumin-loaded PEGylated PLGA nanocapsules for colon cancer therapy *in vivo*. *small* 11 (36), 4704–4722. doi:10.1002/smll.201403799

Kuriakose, M. A., Ramdas, K., Dey, B., Iyer, S., Rajan, G., Elango, K. K., et al. (2016). A randomized double-blind placebo-controlled phase IIB trial of curcumin in oral leukoplakia. *Cancer Prev. Res. (Phila)* 9 (8), 683–691. doi:10.1158/1940-6207.CAPR-15-0390

Li, H. F., Chen, F. M., Shi, J. Q., et al. (2013). Tumor-suppressive effects of toughening moiety-curcumin monolipids enhanced on prostate cancer. *Chin. J. Exp. Surg.* 30 (12), 2493–2495. doi:10.3760/cma.j.issn.1001-9030.2013.12.004

Limin, L., Kong, X., Chang, X., et al. (2007). Experimental study on the effect of curcumin on prostate cancer PC-3M graft tumors. *Chin. J. Gerontology* 27 (1), 45–47. doi:10.3969/j.issn.1005-9202.2007.01.019

Luís, Â., Marcelino, H., Domingues, F., Pereira, L., and Cascalheira, J. F. (2023). Therapeutic potential of resveratrol for glioma: a systematic review and meta- analysis of animal model studies. *Int. J. Mol. Sci.* 24 (23), 16597. doi:10.3390/ijms242316597

Mahammedi, H., Planchat, E., Pouget, M., Durando, X., Curé, H., Guy, L., et al. (2016). The new combination docetaxel, prednisone and curcumin in patients with castration-resistant prostate cancer: a pilot phase II study. *Oncology* 90 (2), 69–78. doi:10.1159/000441148

Mao, J., Xiong, X., and Gong, H. (2019). Effects of curcumin on tumor growth and immune function in prostate cancer-bearing mice. *Chin. J. Male Sci.* 25 (7), 590–594. doi:10.13263/j.cnki.nja.2019.07.003

Mirzaei, H., Shakeri, A., Rashidi, B., Jalili, A., Banikazemi, Z., and Sahebkar, A. (2017). Phytosomal curcumin: a review of pharmacokinetic, experimental and clinical studies. *Biomed. Pharmacother.* 85, 102–112. doi:10.1016/j.biopha.2016.11.098

Mukhopadhyay, A., Banerjee, S., Stafford, L. J., Xia, C., Liu, M., and Aggarwal, B. B. (2002). Curcumin-induced suppression of cell proliferation correlates with down-regulation of cyclin D1 expression and CDK4-mediated retinoblastoma protein phosphorylation. *oncogene* 21 (57), 8852–8861. doi:10.1038/sj.onc.1206048

Mukhopadhyay, A., Bueso-Ramos, C., Chatterjee, D., Pantazis, P., and Aggarwal, B. B. (2001). Curcumin downregulates cell survival mechanisms in human prostate cancer cell lines. *Oncogene* 20 (52), 7597–7609. doi:10.1038/sj.onc.1204997

Nakamura, K., Yasunaga, Y., Segawa, T., Ko, D., Moul, J. W., Srivastava, S., et al. (2002). Curcumin down-regulates AR gene expression and activation in prostate cancer cell lines. *Int. J. Oncol.* 21 (4), 825–830. doi:10.3892/ijo.21.4.825

National Health Commission of the People's Republic of China (2019). Chinese guidelines for diagnosis and treatment of prostate cancer 2018 (English version). *Chin. J. Cancer Res.* 31 (1), 67–83. doi:10.21147/j.issn.1000-9604.2019.01.04

Park, C. H., Lee, J. H., and Yang, C. H. (2005). Curcumin derivatives inhibit the formation of Jun-Fos-DNA complex independently of their conserved cysteine residues. *J. Biochem. Mol. Biol.* 38 (4), 474–480. doi:10.5483/bmbrep.2005.38.4.474

Petersen, G. H., Alzghari, S. K., Chee, W., Sankari, S. S., and La-Beck, N. M. (2016). Meta-analysis of clinical and preclinical studies comparing the anticancer efficacy of liposomal versus conventional non-liposomal doxorubicin. *J. Control Release* 232, 255–264. doi:10.1016/j.jconrel.2016.04.028

Prusty, B. K., and Das, B. C. (2005). Constitutive activation of transcription factor AP-1 in cervical cancer and suppression of human papillomavirus (HPV) transcription and AP-1 activity in HeLa cells by curcumin. *Int. J. Cancer* 113 (6), 951–960. doi:10.1002/ijc.20668

Qi, R. (2009). *Effects of curcumin combined with paclitaxel on proliferation and invasion of prostate cancer PC-3 cells* in vitro *and* in vivo. Shandong: Qingdao University. doi:10.7666/d.y1469102

Qi, R., Yu, X., and Zhao, H. (2015). Inhibitory effect of curcumin on the migration of PC-3 cells in prostate cancer and its effect on the expression of MMP2 *in vivo* and *in vitro*. *China J. Basic Chin. Med.* 21 (11), 1398–1400.

Roy, L., Zhang, A., Zhang, J., et al. (2016). *Study on the effect of curcumin on prostate cancer PC-3 nude mice transplanted tumors*, 353–354.

Santosa, D., Suharti, C., Riwanto, I., Dharmana, E., Pangarsa, E. A., Setiawan, B., et al. (2022). Curcumin as adjuvant therapy to improve remission in myeloma patients: a pilot randomized clinical trial. *Casp. J. Intern Med.* 13 (2), 375–384. doi:10.22088/cjim.13.2.9

Sena, E. S., Currie, G. L., McCann, S. K., Macleod, M. R., and Howells, D. W. (2014). Systematic reviews and meta-analysis of preclinical studies: why perform them and how to appraise them critically. *J. Cereb. Blood Flow. Metab.* 34 (5), 737–742. doi:10.1038/jcbfm.2014.28

Shankar, S., and Srivastava, R. K. (2007). Involvement of Bcl-2 family members, phosphatidylinositol 3'-kinase/AKT and mitochondrial p53 in curcumin (diferulolylmethane)-induced apoptosis in prostate cancer. *Int. J. Oncol.* 30 (4), 905–918. doi:10.3892/ijo.30.4.905

Singh, D., Gupta, M., Sarwat, M., and Siddique, H. R. (2022). Apigenin in cancer prevention and therapy: a systematic review and meta-analysis of animal models. *Crit. Rev. Oncol. Hematol.* 176, 103751. doi:10.1016/j.critrevonc.2022.103751

Spanagel, R. . (2022). Ten points to improve reproducibility and translation of animal research. *Front. Behav. Neurosci.* 16, 869511. doi:10.3389/fnbeh.2022.869511

Squires, M. S., Hudson, E. A., Howells, L., Sale, S., Houghton, C. E., Jones, J. L., et al. (2003). Relevance of mitogen activated protein kinase (MAPK) and phosphotidylinositol-3-kinase/protein kinase B (PI3K/PKB) pathways to induction of apoptosis by curcumin in breast cells. *Biochem. Pharmacol.* 65 (3), 361–376. doi:10.1016/s0006-2952(02)01517-4

Srivastava, R. K., Chen, Q., Siddiqui, I., Sarva, K., and Shankar, S. (2007). Linkage of curcumin-induced cell cycle arrest and apoptosis by cyclin-dependent kinase inhibitor p21(/WAF1/CIP1). *Cell Cycle* 6 (23), 2953–2961. doi:10.4161/cc.6.23.4951

Sung, H., Ferlay, J., Siegel, R. L., Laversanne, M., Soerjomataram, I., Jemal, A., et al. (2021). Global cancer statistics 2020: GLOBOCAN estimates of incidence and mortality worldwide for 36 cancers in 185 countries. *CA Cancer J. Clin.* 71 (3), 209–249. doi:10.3322/caac.21660

Teiten, M. H., Gaascht, F., Cronauer, M., Henry, E., Dicato, M., and Diederich, M. (2011). Anti-proliferative potential of curcumin in androgen-dependent prostate cancer cells occurs through modulation of the Wingless signaling pathway. *Int. J. Oncol.* 38 (3), 603–611. doi:10.3892/ijo.2011.905

Termini, D., Den Hartogh, D. J., Jaglanian, A., and Tsiani, E. (2020). Curcumin against prostate cancer: current evidence. *Biomolecules* 10 (11), 1536. doi:10.3390/biom10111536

Vesterinen, H. M., Sena, E. S., Egan, K. J., Hirst, T. C., Churolov, L., Currie, G. L., et al. (2014). Meta-analysis of data from animal studies: a practical guide. *J. Neurosci. Methods* 221, 92–102. doi:10.1016/j.jneumeth.2013.09.010

Yang, J., Ning, J., Peng, L., and He, D. (2015). Effect of curcumin on Bcl-2 and Bax expression in nude mice prostate cancer. *Int. J. Clin. Exp. Pathol.* 8 (8), 9272–9278.

Yang, J., Wang, C., Zhang, Z., Chen, X., Jia, Y., Wang, B., et al. (2017). Curcumin inhibits the survival and metastasis of prostate cancer cells via the Notch-1 signaling pathway. *apmis* 125 (2), 134–140. doi:10.1111/apm.12650

Yang, L., Zhang, L. Y., Chen, W. W., Kong, F., Zhang, P. J., Hu, X. Y., et al. (2005). Inhibition of the expression of prostate specific antigen by curcumin. *Yao Xue Xue Bao* 40 (9), 800–803.

Ye, W. (2015). *Inhibitory effect of curcumin combined with TfRmAb on human prostate cancer PC-3 cells transplanted tumor in nude mice*. Hubei: Huazhong University of Science and Technology. doi:10.7666/d.D735214

Zanotto-Filho, A., Coradini, K., Braganhol, E., Schröder, R., de Oliveira, C. M., Simões-Pires, A., et al. (2013). Curcumin-loaded lipid-core nanocapsules as a strategy to improve pharmacological efficacy of curcumin in glioma treatment. *Eur. J. Pharm. Biopharm.* 83 (2), 156–167. doi:10.1016/j.ejpb.2012.10.019

Zhang, A. (2013). *Inhibitory effect and mechanism of curcumin on prostate cancer PC-3 cell line transplanted tumor in nude mice*. Kunming Medical University.

Zhao, W., Zhou, X., Qi, G., and Guo, Y. (2018). Curcumin suppressed the prostate cancer by inhibiting JNK pathways via epigenetic regulation. *J. Biochem. Mol. Toxicol.* 32 (5), e22049. doi:10.1002/jbt.22049

Zhao, H., Yu, X., Qi, R., et al. (2010). Study on the effect of curcumin and paclitaxel combination on prostate cancer PC-3 transplantation tumor in nude mice. *Mod. Biomed. Prog.* 10 (5), 823–827.

frontiers | Frontiers in Endocrinology

TYPE Review
PUBLISHED 30 May 2024
DOI 10.3389/fendo.2024.1396192

OPEN ACCESS

EDITED BY
Vittoria Rago,
University of Calabria, Italy

REVIEWED BY
Xiaoqiang Wang,
City of Hope, United States
Jagpreet Singh Nanda,
Cedars Sinai Medical Center, United States

*CORRESPONDENCE
Iman M. Talaat
italaat@sharjah.ac.ae
Waseem El-Huneidi
welhuneidi@sharjah.ac.ae

RECEIVED 05 March 2024
ACCEPTED 14 May 2024
PUBLISHED 30 May 2024

CITATION
Elemam NM, Hotait HY, Saleh MA, El-Huneidi W and Talaat IM (2024) Insulin-like growth factor family and prostate cancer: new insights and emerging opportunities. *Front. Endocrinol.* 15:1396192. doi: 10.3389/fendo.2024.1396192

Insulin-like growth factor family and prostate cancer: new insights and emerging opportunities

Noha M. Elemam[1,2], Hassan Youssef Hotait[3], Mohamed A. Saleh[1,2,4], Waseem El-Huneidi[2,5]* and Iman M. Talaat[1,2,6]*

[1]Clinical Sciences Department, College of Medicine, University of Sharjah, Sharjah, United Arab Emirates, [2]Research Institute for Medical and Health Sciences, University of Sharjah, Sharjah, United Arab Emirates, [3]Pathology & Genetics Department, Dubai Hospital, Dubai, United Arab Emirates, [4]Department of Pharmacology and Toxicology, Faculty of Pharmacy, Mansoura University, Mansoura, Egypt, [5]Basic Medical Sciences Department, College of Medicine, University of Sharjah, Sharjah, United Arab Emirates, [6]Pathology Department, Faculty of Medicine, Alexandria University, Alexandria, Egypt

Prostate cancer is the second most commonly diagnosed cancer in men. The mammalian insulin-like growth factor (IGF) family is made up of three ligands (IGF-I, IGF-II, and insulin), three receptors (IGF-I receptor (IGF-1R), insulin receptor (IR), and IGF-II receptor (IGF-2R)), and six IGF-binding proteins (IGFBPs). IGF-I and IGF-II were identified as potent mitogens and were previously associated with an increased risk of cancer development including prostate cancer. Several reports showed controversy about the expression of the IGF family and their connection to prostate cancer risk due to the high degree of heterogeneity among prostate tumors, sampling bias, and evaluation techniques. Despite that, it is clear that several IGF family members play a role in prostate cancer development, metastasis, and androgen-independent progression. In this review, we aim to expand our understanding of prostate tumorigenesis and regulation through the IGF system. Further understanding of the role of IGF signaling in PCa shows promise and needs to be considered in the context of a comprehensive treatment strategy.

KEYWORDS

prostate cancer, IGF-I, IGF-II, IGF-1 receptor, IGF-2 receptor

1 Introduction

Prostate cancer (PCa) is the fifth leading cause of cancer-related mortality in men worldwide, as well as being the second most commonly diagnosed solid-organ cancer, after lung cancer, in men (1, 2). PCa happens at a rate of 11.3 per 100,000 in developing countries and 37.5 per 100,000 in industrialized countries (3). Similarly, mortality rates in

developed and developing nations are 8.1 and 5.9 per 100,000, respectively. According to current estimates, approximately 10 million males are presently diagnosed with PCa, with approximately 400,000 deaths per year, and this figure is expected to rise to over 800,000 by 2040 (3, 4). Although PCa is generally diagnosed at an early stage, the risk-benefit ratio of the treatment remains uncertain. It still represents a global challenge because of the significant morbidity from the current form of therapy and the long disease history and uncertainty in individual patients' clinical progress (5–7). Approximately 5% of men diagnosed with PCa are diagnosed with distant metastases (often in multiple sites), and 15% are diagnosed with locoregional metastases (8). Such cases have a poor overall survival rate of only 30% for five years (8).

2 The insulin-like growth factor family

The mammalian insulin-like growth factor (IGF) family is made up of three ligands (IGF-I, IGF-II, and insulin) and three receptors (IGF-I receptor (IGF-1R), insulin receptor (IR), and IGF-II receptor (IGF-2R)) (9). IGF-1R and IR are receptor tyrosine kinases (RTKs) that are structurally similar hetero-tetramers. IR has two alternatively spliced isoforms, IRA and IRB, whose functions are currently unknown. IGF-II, which binds to IRA and IGF-1R and is a more potent mitogen than IGF-I, has recently been demonstrated to control IR isoforms rather than insulin-binding affinities (10). IRB governs metabolic processes in adults, whereas IRA controls prenatal growth and development and mediates the mitogenic effects of insulin. A family of six IGF-binding proteins (IGFBPs) tightly controls the amounts of IGF-I and IGF-II as well as their bioavailability in the circulation and cells (11). IGFBPs are distinct from ligands and receptors and have a greater affinity (pM) for IGFs than their corresponding receptors (nM) (10). IGF-I and IGF-II are produced by a variety of cells, including the liver and muscles, among others. They are secreted constitutively as opposed to being retained in the cells of origin, where they serve as paracrine/autocrine factors (12).

2.1 IGFs

In mammalian cells, the production of IGF-I is mainly induced by growth hormones and transcriptional factors. Then it was shown that IGF-II (67 amino acids) has comparable growth-promoting properties but growth hormone does not regulate its expression (13–15). Additionally, IGF-I and IGF-II are quite similar to insulin in terms of amino acid sequence (16). The three disulfide connections that are shared by these three peptides, allow them to preserve the proper peptide shape. IGFs differ structurally from insulin as they are composed of single chains with a connecting domain (C domain) between the N-terminal B chain and the C-terminal A chain. They result from the elimination of the N- and C-terminal signal peptides from pre-pro-IGF peptides during post-translational processing. The chaperone GRP94 aids in the folding and maturation of the IGF peptides (17, 18).

Studies using knock-out and transgenic mice have revealed additional details about the biological actions of mammalian IGFs. *Igf1-null* mice had a high postnatal mortality rate and were 30% smaller and lighter than wild-type mice (19). The postnatal growth retardation was also present in those who survived, and it was particularly noticeable during both growth stages (pubertal and post-pubertal). Their bones grew more slowly, and their organs were proportionately smaller. *Igf-1r* knockout also caused a serious growth deficit and was embryonically fatal in mice (19).

Despite the findings that unraveled the potential role of IGF-I and IGF-II in development, it is still reported that the expression of both IGF-I and IGF-II is tissue-dependent and time-dependent (20). On the other hand, the role of IGF-II in physiology and disease has been the subject of far fewer investigations than that of IGF-I. However, like IGF-I, most tissues in adults produce IGF-II, with the liver producing the majority of the circulating levels. Notably, IGF-II levels in adults are roughly three times higher than IGF-I. Despite this, IGF-II is thought to play crucial roles in fetal growth and development, and it is abundant in the fetal skeletal muscle (12, 21). The stimulation of the IRA to promote stem cell self-renewal is another unique action of IGF-II. Moreover, the expansion of neural progenitor cells and neural stem cell maintenance is supported by IGF-II/IRA signaling (22).

2.2 IGFBPs

It was evident that the preponderance of circulatory IGFs was much larger than the concentration of peptides in the bloodstream because IGFs were not bound to binding proteins (23). In humans and other mammals, six highly similar high-affinity IGF-binding proteins (IGFBP-1 to IGFBP-6) were identified (24). IGFBPs are pluripotent and used in a variety of metabolic processes. All IGFBPs have conserved three subdomains, including high-affinity IGF-binding terminal domains. Contrarily, one other unstructured domain (known as the central linker domain), is thought to be responsible for the various functions that are unique for each IGFBP (25). Furthermore, it has been reported that the specific function of IGFBP is affected by many post-translational modifications (such as proteolytic cleavage, glycosylation, and phosphorylation). Although this division may not be rigorous, it is possible to roughly divide the functions of IGFBPs into those that rely on their ability to bind and control the activity of IGFs and those that appear to be independent of direct IGF binding (26, 27).

Due to the higher affinity of IGFBPs for IGF-I and IGF-II, the availability of free IGFs decreases and this inhibits them from binding and activation of their receptors. IGFBPs have two key functions that are both critical to the metabolism of IGFs (28). IGFs are produced and swiftly secreted via the constitutive secretory route, as tissues do not contain any intracellular storage of IGFs despite their widespread distribution throughout the body. As soon as they are secreted, IGFs bind to high-affinity IGFBPs, creating binary complexes of about 30–40 kDa. IGFs bound to two IGFBPs, IGFBP-3 and IGFBP-5, can join with the acid-labile subunit (ALS), a third glycoprotein, to form a ternary complex that is about 150 kDa in size (29). Without the ability to store them in tissues, the body can build up enormous IGF reservoirs due to IGFBPs. In humans, the total amount of IGFs in circulation is about 100 nM,

with 80–90% of that amount being found in the ternary complex with IGFBP-3 (30). The second important function of IGFBPs is the creation of new pathways for giving IGFs specificity. IGFs are made in most tissues and can regulate the bulk of cell processes. IGFBPs are synthesized in numerous tissues, at different times, in various amounts, and in several combinations to add some specificity to the IGF activity (12).

Furthermore, at the cellular level, IGFBPs can boost IGF activity in several different ways. This can happen by altering the kinetics of IGF ligand/receptor interactions and preventing receptor downregulation, or by changing the interactions between IGFBPs and ECM or cell surfaces thus localizing and increasing the IGF concentrations near to cell receptors (31).

2.3 IGF receptors

Both IGF-1R and IR are synthesized as polypeptide precursors, which are then modified post-translationally, where α and β subunits are formed upon the cleavage of the precursor molecule. The heterotetramer receptor is made up of two α and two β subunits that are joined together by disulfide bridges. 627 amino acids make up the IGF-1R -subunit, 196 of which are found in the extracellular domain. The intracellular and extracellular domains are joined by a brief transmembrane domain (TM). The juxtamembrane domain (JM), enzymatic tyrosine kinase (TK) domain, and C-terminal domain are the three subdomains of the β-subunit's intracellular domain. Positions 976 to 981 are occupied by the TK ATP-binding motif (GXGXXG), while position 1003 contains a catalytic lysine that is essential for Mg-ATP binding. The activation loop of the TK domain contains a trio of tyrosines at positions 1131, 1135, and 1136 that are crucial for receptor autophosphorylation. The JM region contains an NPEY motif that, after being phosphorylated, serves as a docking site for Shc and the insulin receptor substrates (IRS), whose recruitment signifies the start of the downstream signaling process. The internalization of receptors, which controls signaling, depends on the NPEY motif (32, 33).

Generally, the IGF-1R, which is expressed on most cells, plays specialized roles in well-differentiated cells such as neurons as well as being involved in cellular proliferation and anti-apoptosis during growth and development. The IGF-pluripotent IR's roles, however, are still being defined; for instance, a novel function for the IGF-IR in viral entry into cells has just been identified (34).

Several tissue-growth-related transcription factors, including androgen and estrogen receptors, high-mobility group A1 (HMBA1), Krüppel-like factor 6 (KLF6), eukaryotic translation initiation factor 2 (E2F1), and c-Jun, upregulate IGF-IR expression (12, 35). In contrast, several tumor-suppressor genes, including p53, WT1, and BRCA1 downregulate it (36–38).

3 Post-receptor signaling

The binding of IGF-I, IGF-II, or insulin ligand to the IGF-1R initiates a series of events. The binding of IGFs to their receptors activates both MAPK and PI3K-AKT pathways, which results in downstream cellular effects (such as cellular proliferation, anti-apoptosis, and differentiation actions) through other downstream molecules (39). Furthermore, IGF-1R signaling could be mediated through several proteins such as JNK, Jak1, Jak2, focal adhesion kinase, and TIMP2 (40). Moreover, crosstalk between IGF-1R and G-protein coupled receptors (GPCRs) has been reported which may indicate a potential role of IGF-1R in cancer.

IRS 1-4 and other signaling proteins, such as Shc, bind to the IGF-1R at the extracellular subunit as a result of the binding of IGF-I and IGF-II (41). This autophosphorylation of the subunit residues prepares it to serve as a docking site for these proteins. PI3(p110) kinase's subunit catalyzes the recruitment of protein kinase B (Akt) to the cell membrane (42), causing its phosphorylation and activation, then PI3 regulatory kinase's component, p85, is recruited by IRS-1. Bcl2 antagonist of cell death (Bad), glycogen synthase kinase 3 (GSK3), forkhead transcription factors (FOXO1), and Akt substrate of 160 kDa are only a few of the many substrates for activated Akt (AS160). These elements have a major role in controlling cell metabolism and apoptosis (42, 43). By phosphorylating the protein Tuberous Sclerosis Protein (TSC2), Akt controls protein synthesis by loosening its inhibition on Rheb and activating the mammalian target of rapamycin (mTORC1). A set of mitogen-activated protein kinase (MAPKKK, MAPKK, and MAPK) pathways can be initiated by the phosphorylation of IRS-1 and Shc, which can also result in the recruitment of Grb2, SOS, and Ras. These pathways can then be activated, which promotes cell growth, migration, and survival (44, 45).

Recent research has shown that the IGF-1R (and IR) can migrate to the nucleus in both healthy and cancerous cells through mechanisms that are still being fully elucidated, although sumoylation is thought to be one method. The IGF-1R can bind to DNA and control the transcription of its own receptor gene as well as genes involved in apoptosis and the cell cycle. A more thorough analysis of the whole range of IGF-1R effects within the cell was completed (46).

The internalization of the IGF-1R is a complicated process that includes subcellular transport, intracellular signaling, and recycling of the receptor to the surface in addition to partial destruction of the receptor. The ligand binding process starts with the IGF-increased IR's internalization (endocytosis). Through substrates that specifically bind to tyrosine residues 1250 and 1251 in the C-terminus, internalization, and degradation play a part. Internalization separates the ligand from the receptor via the acidic endosomal route, where caveolin- or clathrin-dependent mechanisms may be used for internalization (47). The lysosomal or proteasomal routes are both options for the receptor's degradation. The process of receptor ubiquitination, which is brought on by ligand interaction, results in the receptor's destruction by the proteasome. The receptor concentration on the surface may therefore be downregulated as a result of ligand binding and internalization, even though the levels may be adjusted by increased IGF-1R gene expression. A collection of proteins called adhesion-associated proteins may regulate subcellular transport. These include the discoidin domain receptor 1 (DDR1), non-receptor tyrosine adhesion kinase FES-related (FER), and non-

integrin collagen RTK. The IGF-1R can translocate to the nucleus or the Golgi apparatus' internal membrane compartments for destruction (28, 47). Intracellular signaling, which appears to be important in the migratory behavior of cancer cells, can be started by the IGF-1R in the Golgi. IGF-I induces the translocation of IGF-1R to the nucleus, where it may bind with DNA to increase transcription, with consequences that seem to support an aggressive cancer phenotype (28, 47).

4 The role of the IGF family in carcinogenesis

The IGF family plays a critical role in various cellular processes such as proliferation, differentiation, and apoptosis (Figure 1). In particular, IGFBPs protect IGFs from degradation and regulate their interactions with the receptors. High circulating levels of the potent mitogen, IGF-I, were previously associated with an increased risk for breast, prostate, lung and colorectal cancers (48–51). Both mitogens, IGF-I and IGF-II, were identified to be overexpressed in various cancer types such as sarcoma, leukemia, breast, lung, colon, stomach, esophagus, liver, pancreas, kidney, thyroid, brain, ovary, cervical, endometrial and prostate cancers (52–57). High IGF-IR expression was positively associated with worse disease outcomes for several cancer types, including prostate and gastric cancer, as well as renal cell carcinoma (58–60).

IGF-I, the crucial peptide hormone involved in controlling human growth and development, functions by promoting cell growth and preventing apoptosis (54, 61, 62). Such actions have a significant impact on the tumor development (63). Other members of the IGF family directly affect cancer-related cellular activities and interact with a wide range of molecules that are crucial for cancer initiation and progression. IGF-I has been associated with the activation of the MAPK and PI3K signaling pathways (64). Additionally, diet and exercise have an impact on the expression and production of IGF-I (65). IGF-I overexpression was previously identified to induce tumor development (66, 67), while high expression of IGF-1R and IGF-II triggered cancer metastasis (68). Additionally, IGF-1R was reported to be essential for cell transformation triggered by oncogenes and tumor-virus proteins (53). Several approaches were implemented to inhibit the mitogenic effect of IGF signaling including eliminating IGF-1R from the cell membrane, blocking the interaction of IGFs with IGF-1R, or interrupting the signal transduction pathway (53, 69–71). On the other hand, IGF-2R is known to antagonize the effect of IGF-II, where tumors that had low expression of IGF-2R or possessed IGF-2R mutations and could not hence degrade IGF-II, had much higher growth rates (72, 73). Thus, restoring IGF-2R expression induced apoptosis and reduced the growth of cancer cells (74).

IGFBPs regulate the interaction between IGF-I and IGF-1R and affect the mitogenic activity of IGF-I (75–84). One of the most studied IGFBPs is IGFBP-3 which prolongs the half-life of the IGFs and regulates their availability to the cell surface receptors (85, 86). Besides, IGFBP-3 has anti-proliferative actions affecting cancer growth (87, 88). It was previously reported that serum levels of IGFBP-3 were inversely associated with cancer risk in those patients. Also, IGFBP-3 was found to inhibit breast and prostate cancer growth and induce apoptosis (89–91). Moreover, vitamin D and its synthetic analogs could increase the expression of IGFBPs and reduce IGF-1R and IGF-II in breast and prostate cancer (92–95). Another factor affecting the expression of IGF family members is the expression of tumor suppressor genes. For example, wild-type p53 protein induces IGFBP-3 expression, represses the transcription of IGF-II, and suppresses IGF-1R expression (96–101).

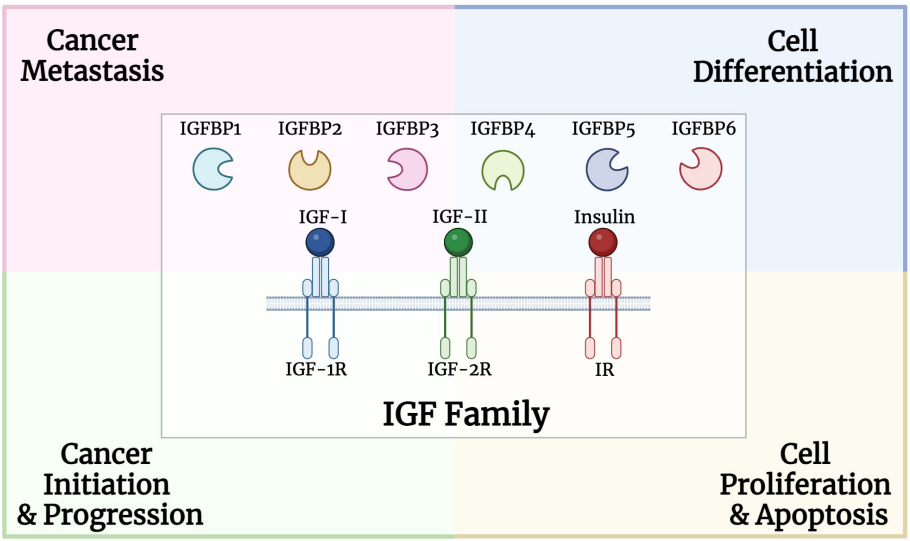

FIGURE 1
Structure and role of insulin growth factor (IGF) family, including binding proteins, ligands, and receptors, in multiple processes involved in carcinogenesis.

5 The impact and expression of the IGF family in neoplastic prostate cells and tissues

During the transition from benign to malignant state in prostate cancer, several IGF family members change. For instance, IGF-I, IGFBP-2 and IGFBP-5 levels rise, while IGF-IR and IGFBP-3 levels lessen (82, 102–104). The controversial reports about the expression of the IGF family and its connection to prostate cancer risk and development may be the result of the high degree of heterogeneity among prostate tumors, sampling bias, evaluation techniques, or the experimental design (105).

Some proteases produced in the prostate cancer microenvironment were previously identified to enhance IGF-I/IGF-1R signaling. These include prostate-specific antigen (PSA), human kallikrein 2, trypsin, and cathepsin D, which were identified to degrade IGFBPs, thus releasing free mitogenic IGF-I (106, 107). High IGF-I expression and low IGFBP-3 in prostate cancer were identified as contributors to cancer initiation and progression by affecting cellular transformation, apoptosis, and metastasis (108). IGF-I and IGFBP-3 expression in prostate cancer patients was strongly associated with more advanced or aggressive disease, indicating a critical role in cancer progression (49). Further studies highlighted the potential of IGF-I as a strong predictor of advanced rather than early-stage prostate cancer (109). On the contrary, a study by Ma et al. reported no significant associations between free IGF-I and other IGF-I biomarkers with lethal and non-lethal prostate cancer (110). However, blood levels of IGFBP-3 showed contradictory results in prostate cancer (111). Serum levels of IGF-I, IGF-II, IGFBP-2, IGFBP-4, and IGFBP-5 were found to be higher in prostate cancer patients (82, 103, 112–116). Moreover, IGFBP-2 expression was found to be higher in the prostate cancer tissue compared to the normal tissue counterpart (102). Neither IGF-II nor IGFBP-2 concentrations were associated with prostate cancer risk (117). On the other hand, low levels of IGFBP-3 were reported in the serum and prostate tumor tissue of cancer patients (102). Moreover, IGF-I was found to be significantly elevated while IGFBP-3 was reported to be reduced in prostate cancer tissues (118). Also, such an expression was found to be linked to tumor size and hyperplasia (118, 119). IGF-I and IGFBP-3 plasma levels were suggested to be indicators of prostate cancer risk (112). Moreover, the lower IGFBP-3 levels could lead to enhanced IGF-I bioavailability (85). In addition, the plasma levels of IGFBP-3 were considerably lower in African-American men compared to white men (120, 121). This could support the findings that African-American men have a higher incidence of prostate cancer than white men (122). Additionally, high IGF-I levels in the blood/serum of healthy men were associated with a high risk of developing prostate cancer (123, 124). This suggests that prolonged exposure to high concentrations of IGF-I could trigger carcinogenesis of prostate epithelial cells (125). Therefore, targeting IGF-I could be a potential therapeutic approach in prostate cancer.

When compared to the benign prostate epithelium, primary prostate cancer had higher levels of IGF-1R expression, which is further escalated in metastasis (126). This was further supported by studies using human prostate xenografts where higher IGF-1R expression was found in metastatic and androgen-independent tumors (127, 128). Also, transgenic mice with a prostate-specific deletion of IGF-1R and the tumor suppressor gene p53 had more aggressive prostate cancer than their wild-type counterparts (129).

In vitro, studies indicated that IGF-I stimulated the proliferation of various prostate cancer cell lines (22Rv1 and DU145) by the activation of the AKT/ERK/MAPK pathway (130). Also, IGF-I regulated the invasion potential of DU145 prostate cancer cells by controlling the activity of MMP-2 and MMP-9 as well as secreted TIMP-2 levels, that are transduced via the PI3K and MAPK pathways (131). Further, IGF-I was described to regulate the expression of miR-143, leading to an increase in IGFR expression in PC-3 and DU145 prostate cancer cell lines. Such an effect was found to lead to resistance to docetaxel treatment (132). Additionally, it has been demonstrated that IGF-I activated androgen receptor signaling in prostate cancer cells via the IGF-1R-forkhead box protein O1 (FOXO1) signaling axis, which is also implicated in castration-resistant prostate cancer (133–135). *In vivo*, PC-3 tumors proliferate at a considerably slower rate in IGF-I-deficient hosts than in IGF-I-expressing hosts (136). Mice injected with the androgen-sensitive and PSA-producing LNCaP cell line were found to develop tumors and their serum PSA levels were correlated with tumor volume (137). Also, mice fed a low-fat diet with xenografts of LAPC-4 showed a decrease in tumor size along with a reduction in the IGF-I expression (138). Other *in vivo* studies reported that the blocking of IGF-1R in combination with castration inhibited prostate cancer growth (139, 140). However, the most thoroughly studied IGF-1R inhibitor, limsitinib, was explored in a phase II study, where it did not significantly alleviate prostate-specific antigen levels after 12 weeks of treatment or increase the overall survival in men with metastatic castrate-resistant prostate cancer (141).

IGFBP-3 is the most prevalent form of the IGFBPs, which has been linked with prostatic growth. The majority of serum and prostatic IGF-I binds to IGFBP-3, thus regulating its concentrations (142). IGFBP-3 was identified to have anti-tumor effects by regulating multiple processes such as adhesion, motility, proliferation, and invasion of prostate cancer cells (143). Additionally, *in vitro* studies using PC3 or DU145 cell lines showed that IGF-I regulates cell adhesion and motility that is needed for the formation of a pre-metastatic niche (144). This was reported to be mediated through integrin expression especially α3, α5, and β1 expression pattern and distribution (145).

The second most prevalent IGFBP is IGFBP-2, which has a growth inhibitory effect on healthy prostate epithelial cells but a strong stimulatory effect on prostate cancer cells via the activation of MAPK and PI3K pathways (146). Also, high IGFBP-2 levels in prostate cancer patients not receiving neoadjuvant hormonal therapy had worse survival compared to patients with low IGFBP-2 levels, thus indicating an androgen effect on the IGFBP-2 action (147).

Proteases targeting IGFBPs are known to degrade IGFBPs into small fragments, thus reducing the affinity of IGFBPs to IGFs. Prostate-specific antigen (PSA) is known to be an IGFBP protease while γ-nerve growth factor (NGF) is also known to degrade

IGFBPs 3, 4, 5, and 6, thereby boosting IGF action (11). Furthermore, other proteases such as human kallikrein 2 (hK2), trypsin, MMPs, and cathepsin D, present in the prostate tumor microenvironment were identified to affect IGFBP-3 and release free IGF-I (107). Protease-resistant IGFBPs could be a potential therapeutic agent in cancer therapy by preventing the mitogenic activity of IGF. Also, it was interesting to find that inhibiting the signaling pathway of epidermal growth factor (EGF), had a suppression effect on IGF-I in prostate cancer cells (148). The protease PAPP-A is responsible for the cleavage of IGFBPs 2, 4, and 5 (149), which was previously linked to cancer development in various types including prostate cancer (150–155). A possible explanation for the role of PAPP-A is through increasing the levels of IGFs and their downstream signaling pathway (156). Studies have reported that PAPP-A levels were elevated in prostate cancer patients, especially those with metastasis (157). On the other hand, several studies reported that the protease-resistant IGFBP-4 led to an inhibition of cell growth and angiogenesis (155, 158). Other *in vitro* and *in vivo* studies indicated that the mutant IGFBP-2 was able to inhibit tumor growth possibly by inhibition of angiogenesis (159).

A subgroup of IGFBPs is called IGFBP-related proteins (IGFBPs-rP) also termed the CNN family (124). These IGFBP-rPs could be critical for the regulation of stromal and epithelial cell growth in the prostate. An interesting protein is insulin-like growth factor binding protein-related protein 1 (IGFBP-rP1)/IGFBP-7. It was found to possess tumor suppressor effects through inhibiting cell growth, and triggering apoptosis and senescence (160). In contrast, another study indicated that it could promote glioma cell growth and migration (161). IGFBP-7 resulted in the activation of the translational repressor 4E-binding protein 1 (4E-BP1) and triggered apoptosis in IGF-1R$^+$ cells. It suppressed IGF-1R downstream signaling, hence hindering protein synthesis, cell growth, and survival (162). *In vitro* and *in vivo* studies revealed a downregulation of IGFBP-5 in prostate cancer cells that inhibited IGF cell growth. In benign prostatic hyperplasia (BPH), IGF-II and IGF-1R were found to be overexpressed by stromal prostate cells. Also, these cells expressed IGFBP-5 which is identified to potentiate the IGF actions (163). Reduced expression of IGFBP-rP1 is associated with carcinogenesis, especially in highly tumorigenic and metastatic prostatic cells (164). IGFBP-rP1 functions as a tumor suppressor in prostate cancer cells, as its overexpression slowed down growth and proliferation rates (165). Also, prostatic cell growth is regulated by IGFBP-rP2 and IGFBP-rP3. Several factors can affect the expression of IGFBP-rP2. For instance, TGF-β boosts the expression of IGFBP-rP2 in both normal and cancerous prostate cells while IGF-I could decrease its expression. IGFBP-rP3 may act as a growth stimulator for prostate cancer cells given that it is preferentially expressed in malignant cells (166). CyrH61/IGFBPs-rP4 is localized in the mesenchyme of the benign prostatic tissue and is downregulated in prostate cancer tissues as well as in cancer cell lines (124, 167).

Our understanding of prostate tumorigenesis and regulation has been expanded especially due to our understanding of the IGF system. A high IGF-I to IGFBP-3 ratio was linked with an increased risk of prostate cancer and could be used as a predictor for prostate cancer development (168). On the other hand, another study by Saleh SAK et al. reported that changes in the serum levels of IGF-I and IGFBP-3 were not considered pre-diagnostic risk factors for prostate cancer development (142). Besides, serum levels of total PSA and free/total PSA ratio were found to be higher in prostate cancer patients (142). Also, PSA and IGF-II showed the power of prognosis and differentiation between prostate cancer and BPH (169).

6 The link between IGF and prostate cancer metastasis

Bones are the most frequent metastatic site for prostate cancer, with 70–80% of patients experiencing skeletal metastases. Prostate cancer can metastasize to numerous organs, including the liver, lymph nodes, lung, and bone. The vertebral column, ribs, skull, and proximal ends of the long bones are among the well-vascularized parts of the skeleton where prostate cancer cells spread frequently. IGF-I and IGF-II, as well as type I and type II IGF receptors, are expressed by bone cells (170). High levels of IGF-I in the primary tumor environment seem to encourage cancer cells to spread to the bone *in vivo*. Moreover, prostate cancer cell lines that highly expressed IGF-1R were likely to develop larger bone mass (171–173). Notably, IGFs influence cell-cell adhesion and motility of cancer cells through the integrin system such as E-cadherin (174–176). The likelihood of metastasis is influenced by such interactions (177–179). Prostate cancer cells can release mediators that change the balance between osteoblast and osteoclast activities, leading to osteoblastic metastases. IGF-I plays a critical role in bone formation and bone resorption through the receptor activator of the nuclear factor-B ligand (RANKL) system in bone (180). IGF-I upregulates the expression of RANKL by bone marrow stromal cells, and osteoblasts, which can bind to RANK on the surface of osteoclast precursors. This ligand-receptor interaction activates NF-κB, which stimulates the differentiation of osteoclast precursors to osteoclasts (180–183). Also, metastatic prostate cancer cells release a urokinase-type plasminogen activator that binds to the corresponding receptor on the surface of osteoblasts. This could trigger the proteolysis of IGFBPs and increase in the bioavailability of IGFs, thus stimulating the proliferation of osteoblasts and cancer cells (Figure 2). A study by Goya M. et al. reported the potential of KM1468, a monoclonal antibody against IGF-I and IGF-II that inhibited the development of new bone formation and the progression of existing bone tumors (184). Also, IGF-I is secreted by the liver, which attracts circulating cancer cells drain and promotes colonization, proliferation, and the establishment of metastasis (185).

IGF-1R was found to control lymphatic metastasis of cancer by inducing the production of VEGF, thus promoting angiogenesis and lymphangiogenesis (186). This was supported by high levels of VEGF in prostate cancer patients with lymph node metastases (187). Androgen deprivation activated FOXO-1 and upregulated VEGF production by inhibiting the IGF-1R pathway (188). By activation of the IGF-1R/Akt/NF-κB pathway, bone-derived IGF-I is the link between metastasized cancer cells during bone metastasis (189).

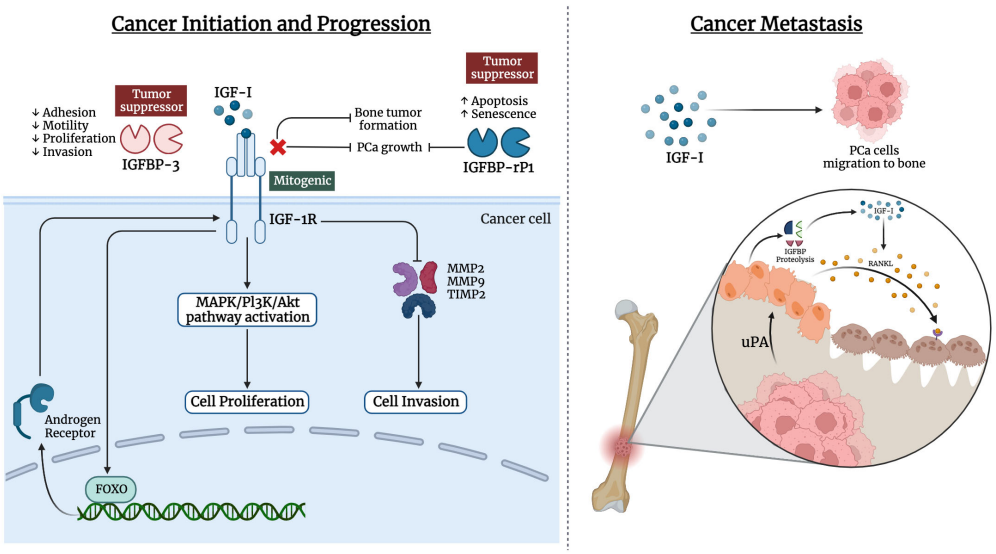

FIGURE 2
Involvement of IGF ligands, receptors, and binding proteins in prostate cancer. The left panel illustrates the interplay of IGF-I in cancer initiation and progression of prostate cancer, while the right panel highlights the IGF-I effect in metastasis of prostate cancer cells to bone tissue.

7 The relation between IGF family and androgen-independent progression

Prostate cancer could progress to be castration-resistant. Several mechanisms have been put forth to explain the progression including: 1) constitutive activation of the androgen receptor due to alternative splicing of the androgen receptor; 2) epigenetic mutations of the androgen receptor; 3) transactivation of the androgen receptor by growth factors and cytokines; and 4) intracrine steroidogenic pathways within the prostate tumor (190–193).

Another critical aspect of the IGF family is that they play a role in the progression of androgen-independent prostate cancer by promoting the growth and survival of prostate tumor cells. Alternative stimulatory pathways that were activated after androgen withdrawal, were found to trigger intracellular signal transduction pathways by completely avoiding or activating the androgen receptor. For example, non-ligand activation of androgen receptors could be initiated by IGF-I, MAPK, and AKT contributing to cell proliferation in an androgen-depleted environment (194). Also, prostate cancer mouse models showed progression from androgen-dependence to androgen-independence to be associated with an increase in IGF-I and decrease in IGFBP-3, further suggesting their role in cancer aggressiveness (128). In mice, castration induced upregulation of IGFBP-5 that enhanced the development of androgen independence (195).

The effective treatment for patients with advanced prostate cancer is androgen ablation, leading to tumor regression (195). This is because proliferation of prostate cancer cells is dependent on androgens. The androgen receptor is known to bind to testosterone and dihydrotestosterone, after which a conformational change and interaction with specific DNA elements occur. The development of androgen-independent prostate cancer takes place as a consequence of the lack of apoptosis that triggers tumor cell survival (196). Furthermore, other mechanisms are associated with the development of androgen-independent prostate cancer including an increase in the sensitivity of the androgen receptor by coactivators as well as enhancement of the signaling pathways by other growth factors (197, 198). Unlike androgens, IGF-I activates tyrosine kinase-associated surface receptors, leading to the proliferation of prostate cancer cells. This is besides the effect of IGF-I on enhancing the androgen receptor transcriptional activity and its sensitivity to suboptimal stimulation by low androgen levels (199). Metastatic and androgen-independent prostate cancer specimens exhibited an increase in IGF-1R expression (126–128). On the other hand, other studies indicated that reduced IGF-1R expression is required to induce androgen independence, proliferation, and metastasis (200, 201). It was suggested that dysregulation of IGF-1R expression through KLF6 loss-of-function may be an intrinsic mechanism for prostate cancer progression to hormone independence. Also, the tumor suppressor BRCA1 was identified to interact with the androgen receptor in prostate cancer cells and regulate IGF-1R production (202). Furthermore, BRCA1 can suppress IGF-1R promoter activity in androgen receptor-negative prostate cancer cell lines but enhance IGF-1R expression at the transcriptional level in androgen receptor-positive prostate cancer cell lines (203).

Also, long-term androgen suppression may boost the resistance of prostate cancer cells to apoptosis through the inhibition of PI3K/AKT pathway (204). IGF-1R expression can be enhanced by androgens via the activation of the ERK pathway (205). Neuropeptides, including endothelin-1, vasoactive intestinal peptide, and neurotensin, were previously identified to boost IGF signaling and stimulate androgen-independent prostate cancer (111, 206–208). Moreover, castration or anti-androgen treatment induces the expression of IGFBP-2,3,4 and 5 (209, 210). This could

be due to an adaptative mechanism to enhance IGF-I mediated mitogenesis, thus leading to androgen independence progression (195, 195, 211). Also, prostate cancer samples and cell lines exhibited growth inhibition when treated with diethylstilbestrol (DES) (212). The expression of the growth-promoting IGFBP-6 was reported to be induced by DES treatment, thus, highlighting its contribution to the effect of DES in androgen-independent prostate cancer (213). Pre-clinical evidence supported the utilization of insulin/IGF-targeting agents in combination with androgen deprivation therapy for prostate cancer. This is attributed to the effect of insulin on the production of androgens by prostate cancer cells, which accelerated the emergence of castration-resistant prostate cancer (214).

8 New drugs targeting the IGF family

For many years now, the gold standard of treatment for advanced or metastatic prostatic cancer has been androgen deprivation therapy (ADT) and second-generation androgen receptors signaling inhibitors (41). Unexpected resistance to castration and recurrence in the form of castration-resistant prostate cancer, for which there are few therapy choices, are regrettably major events contributing to the poor longevity of patients with prostatic cancer, even though these therapies initially demonstrated several pros (105). A lot of research has been done to design agents that target the IGF family and its signaling pathway. For instance, some studies aimed at reducing IGF-I levels or inhibiting the activity of IGF-IR and the downstream signaling pathways. Some of these drugs exhibited an anti-neoplastic activity (184, 215, 216). Antagonists of the growth hormone-releasing hormone, or growth hormone receptor (e.g., pegvisomant), and analogs of somatostatin (e.g. octreotide) resulted in a reduction of IGF-I levels (217). For instance, combinatorial therapy using octreotide and complete androgen blockage had beneficial results in patients with prostate cancer (218). Also, pegvisomant treatment halted the proliferation of prostatic cancer cells (219). As such, anti-IGF-1R monoclonal antibodies (mAbs), human neutralizing IGF antibodies, and tyrosine kinase inhibitors (ligand-gated IGF-R) have been developed. Part of these drugs have been evaluated in clinical studies regarding prostatic cancer either alone or in conjunction with traditional therapy (220).

8.1 Monoclonal anti-IGF-1R antibodies

The primary approach entails employing anti-IGF-1R mAbs to impede ligand-receptor interactions, thereby inducing the internalization and subsequent degradation of IGF-1R. For the treatment of malignant tumors, a number of therapeutic mAbs targeting IGF-1R have been developed, including ganitumab (IgG1) (139), cixutumumab (IgG1) (221–223), and figitumumab (IgG2) (222, 224, 225). The antibodies that have undergone evaluation in clinical trials have demonstrated anti-tumor growth effects to a certain degree and have been well tolerated by the majority of participants.

Cixutumumab and figitumumab have shown mixed results in clinical trials, with some benefits in PSA levels but inconsistent overall survival improvements (221, 226, 227). A12, another mAb, demonstrated promise in preclinical studies by inhibiting cancer cell growth, but requires further research (228, 229). Ganitumab, a unique mAb that avoids interfering with insulin signaling, showed good tolerability but lacks clinical trials in prostate cancer patients (139, 222). Other mAbs like BIIB022 are being explored in other cancers with positive safety profiles (230). Overall, IGF-1R mAbs hold promise for prostatic cancer treatment, but further research is needed to optimize their efficacy and safety, particularly in combination therapies, while exploring new mAbs with improved targeting strategies.

8.2 Neutralizing antibodies for IGF

Monoclonal antibodies that neutralize IGF ligands inhibit proliferative and pro-survival signaling, which are initiated by IGF ligands. IGF-I/II neutralizing monoclonal antibodies simultaneously inhibit multiple IGF signaling pathways but do not affect insulin receptor-β (INSR), which regulates glucose homeostasis (231). As a result, they do not increase the risk of hyperglycemia compared to IGF-1R/INSR tyrosine kinase inhibitors. Few neutralizing antibodies for IGF have been developed, including xentuzumab (IgG1) and dusigitumab (IgG2). Human antibody xentuzumab (BI 836845) specifically targeted IGF-I and IGF-II. It exhibited potential in the treatment of breast cancer and in the mitigation of resistance in prostate cancer. It mainly functions by inhibiting IGF-I levels and impeding its effects. The initial trials were met with acclaim (232–234). Dusigitumab (MEDI-573) is an additional IGF signaling-targeting antibody, whose metabolic impact appeared to be comparatively lesser in nature when compared to alternative IGF-targeting therapies. Although it exhibited anti-tumor properties, its efficacy might be constrained by its relatively low binding affinity (235).

8.3 Tyrosine kinase inhibitors of IGF-1R

Linsitinib targets the insulin and IGF-1R receptors and demonstrated promise in preclinical research but had poor efficacy in clinical trials for prostate cancer among other malignancies. Though it was well tolerated, neither the tumor response nor PSA levels were improved. Though further research is needed, linsitinib may be helpful in breaking through chemotherapy resistance (141, 236, 237). An alternative tyrosine kinase inhibitor, BMS-754807, has shown promise in preclinical research by reducing the proliferation and causing cell death in cancer cells (238). It also affected insulin receptors, though, which could have an effect on blood sugar regulation (239). Its safety and effectiveness in prostate cancer patients have not yet been evaluated in clinical trials.

9 Conclusions

PCa remains a public health burden. The relationship between the IGF family and prostate cancer is intricate as IGF signaling plays

a significant role in the development and progression of prostate cancer. The activation of its downstream signaling pathways promotes cell proliferation, migration, and invasion. Targeting IGF signaling has been considered as a potential therapeutic strategy for PCa. Researchers have explored various approaches to inhibit IGF signaling using antibodies or small molecule inhibitors against various components of the IGF signaling pathway. Therefore, further understanding of the role of IGF signaling in PCa shows promise and needs to be considered in the context of a comprehensive treatment strategy.

Author contributions

NE: Writing – original draft, Writing – review & editing. HH: Writing – original draft, Writing – review & editing. MS: Writing – original draft, Writing – review & editing. WE: Writing – original draft, Writing – review & editing. IT: Writing – original draft, Writing – review & editing.

Funding

The author(s) declare that no financial support was received for the research, authorship, and/or publication of this article.

Conflict of interest

The authors declare that the research was conducted in the absence of any commercial or financial relationships that could be construed as a potential conflict of interest.

Publisher's note

References

1. Bray F, Ferlay J, Soerjomataram I, Siegel RL, Torre LA, Jemal A. Global cancer statistics 2018: GLOBOCAN estimates of incidence and mortality worldwide for 36 cancers in 185 countries. *CA: Cancer J Clin*. (2018) 68:394–424. doi: 10.3322/caac.21492

2. Ferlay J, Soerjomataram I, Dikshit R, Eser S, Mathers C, Rebelo M, et al. Cancer incidence and mortality worldwide: sources, methods and major patterns in GLOBOCAN 2012. *Int J Cancer*. (2015) 136:E359–86. doi: 10.1002/ijc.29210

3. Sung H, Ferlay J, Siegel RL, Laversanne M, Soerjomataram I, Jemal A, et al. Global cancer statistics 2020: GLOBOCAN estimates of incidence and mortality worldwide for 36 cancers in 185 countries. *CA: Cancer J Clin*. (2021) 71:209–49. doi: 10.3322/caac.21660

4. He Y, Xu W, Xiao Y-T, Huang H, Gu D, Ren S. Targeting signaling pathways in prostate cancer: mechanisms and clinical trials. *Signal Transduction Targeted Ther*. (2022) 7:198. doi: 10.1038/s41392-022-01042-7

5. Cuzick J, Thorat MA, Andriole G, Brawley OW, Brown PH, Culig Z, et al. Prevention and early detection of prostate cancer. *Lancet Oncol*. (2014) 15:e484–92. doi: 10.1016/s1470-2045(14)70211-6

6. Desai MM, Cacciamani GE, Gill K, Zhang J, Liu L, Abreu A, et al. Trends in incidence of metastatic prostate cancer in the US. *JAMA Netw Open*. (2022) 5:e222246. doi: 10.1001/jamanetworkopen.2022.2246

7. Prostate cancer: a tale of two sides. *Nat Rev Urol*. (2019) 16:141. doi: 10.1038/s41585-019-0152-z

8. Siegel RL, Miller KD, Jemal A. Cancer statistics, 2018. *CA: Cancer J Clin*. (2018) 68:7–30. doi: 10.3322/caac.21442

9. Simpson A, Petnga W, Macaulay VM, Weyer-Czernilofsky U, Bogenrieder T. Insulin-like growth factor (IGF) pathway targeting in cancer: role of the IGF axis and opportunities for future combination studies. *Targeted Oncol*. (2017) 12:571–97. doi: 10.1007/s11523-017-0514-5

10. Rosenzweig SA. The continuing evolution of insulin-like growth factor signaling. *F1000Research*. (2020) 9(F1000 Faculty Rev):205. doi: 10.12688/f1000research.22198.1

11. Brahmkhatri VP, Prasanna C, Atreya HS. Insulin-like growth factor system in cancer: novel targeted therapies. *BioMed Res Int*. (2015) 2015:538019. doi: 10.1155/2015/538019

12. LeRoith D, Holly JMP, Forbes BE. Insulin-like growth factors: Ligands, binding proteins, and receptors. *Mol Metab*. (2021) 52:101245. doi: 10.1016/j.molmet.2021.101245

13. Yoshida T, Delafontaine P. Mechanisms of IGF-1-mediated regulation of skeletal muscle hypertrophy and atrophy. *Cells*. (2020) 9:1970. doi: 10.3390/cells9091970

14. Cohick WS, Clemmons DR. The insulin-like growth factors. *Annu Rev Physiol*. (1993) 55:131–53. doi: 10.1146/annurev.ph.55.030193.001023

15. Bach LA. The insulin-like growth factor system: towards clinical applications. *Clin Biochemist Rev*. (2004) 25:155.

16. Miller BS, Rogol AD, Rosenfeld RG. The history of the insulin-like growth factor system. *Hormone Res Paediatrics*. (2022) 95:619–30. doi: 10.1159/000527123

17. Denley A, Cosgrove LJ, Booker GW, Wallace JC, Forbes BE. Molecular interactions of the IGF system. *Cytokine Growth factor Rev*. (2005) 16:421–39. doi: 10.1016/j.cytogfr.2005.04.004

18. Vigneri R, Squatrito S, Sciacca L. Insulin and its analogs: actions via insulin and IGF receptors. *Acta diabetologica*. (2010) 47:271–8. doi: 10.1007/s00592-010-0215-3

19. Stratikopoulos E, Szabolcs M, Dragatsis I, Klinakis A, Efstratiadis A. The hormonal action of IGF1 in postnatal mouse growth. *Proc Natl Acad Sci*. (2008) 105:19378–83. doi: 10.1073/pnas.0809223105

20. Frasca F, Pandini G, Scalia P, Sciacca L, Mineo R, Costantino A, et al. Insulin receptor isoform A, a newly recognized, high-affinity insulin-like growth factor II receptor in fetal and cancer cells. *Mol Cell Biol*. (1999) 19:3278–88. doi: 10.1128/MCB.19.5.3278

21. Puche JE, Castilla-Cortázar I. Human conditions of insulin-like growth factor-I (IGF-I) deficiency. *J Trans Med*. (2012) 10:1–29. doi: 10.1186/1479-5876-10-224

22. Blyth AJ, Kirk NS, Forbes BE. Understanding IGF-II action through insights into receptor binding and activation. *Cells*. (2020) 9:2276. doi: 10.3390/cells9102276

23. Allard JB, Duan C. IGF-binding proteins: why do they exist and why are there so many? *Front Endocrinol*. (2018) 9:117. doi: 10.3389/fendo.2018.00117

24. Daza DO, Sundström G, Bergqvist CA, Duan C, Larhammar D. Evolution of the insulin-like growth factor binding protein (IGFBP) family. *Endocrinology*. (2011) 152:2278–89. doi: 10.1210/en.2011-0047

25. Hwa V, Oh Y, Rosenfeld RG. The insulin-like growth factor-binding protein (IGFBP) superfamily. *Endocrine Rev*. (1999) 20:761–87. doi: 10.1210/edrv.20.6.0382

26. Clemmons DR. Role of post translational modifications in modifying the biologic activity of insulin like growth factor binding proteins. *Curr Dir insulin-like Growth factor Res*. (1993) 343:245–53. doi: 10.1007/978-1-4615-2988-0_24

27. Weinzimer SA, Cohen P. Biological significance of insulin-like growth factor binding proteins. *NeuroImmune Biol*. (2002) 2:37–65. doi: 10.1016/S1567-7443(02)80007-2

28. Baxter RC. Signaling pathways of the insulin-like growth factor binding proteins. *Endocrine Rev*. (2023) 44:bnad008. doi: 10.1210/endrev/bnad008

29. Poreba E, Durzynska J. Nuclear localization and actions of the insulin-like growth factor 1 (IGF-1) system components: Transcriptional regulation and DNA damage response. *Mutat Research/Reviews Mutat Res*. (2020) 784:108307. doi: 10.1016/j.mrrev.2020.108307

30. Scharf J, Ramadori G, Braulke T, Hartmann H. Synthesis of insulinlike growth factor binding proteins and of the acid-labile subunit in primary cultures of rat hepatocytes, of Kupffer cells, and in cocultures: Regulation by insulin, insulinlike growth factor, and growth hormone. *Hepatology*. (1996) 23:818–27. doi: 10.1002/(ISSN)1527-3350

31. Firth SM, Baxter RC. Cellular actions of the insulin-like growth factor binding proteins. *Endocrine Rev*. (2002) 23:824–54. doi: 10.1210/er.2001-0033

32. Weis F, Menting JG, Margetts MB, Chan SJ, Xu Y, Tennagels N, et al. The signalling conformation of the insulin receptor ectodomain. *Nat Commun*. (2018) 9:4420. doi: 10.1038/s41467-018-06826-6

33. De Meyts P. Insulin/receptor binding: the last piece of the puzzle? What recent progress on the structure of the insulin/receptor complex tells us (or not) about negative cooperativity and activation. *Bioessays*. (2015) 37:389–97. doi: 10.1002/bies.201400190

34. Ngo M-HT, Jeng H-Y, Kuo Y-C, Nanda JD, Brahmadhi A, Ling T-Y, et al. The role of IGF/IGF-1R signaling in hepatocellular carcinomas: stemness-related properties and drug resistance. *Int J Mol Sci*. (2021) 22:1931. doi: 10.3390/ijms22041931

35. Wu JD, Haugk K, Woodke L, Nelson P, Coleman I, Plymate SR. Interaction of IGF signaling and the androgen receptor in prostate cancer progression. *J Cell Biochem*. (2006) 99:392–401. doi: 10.1002/jcb.20929

36. Werner H. Tumor suppressors govern insulin-like growth factor signaling pathways: implications in metabolism and cancer. *Oncogene*. (2012) 31:2703–14. doi: 10.1038/onc.2011.447

37. Wang P, Mak VCY, Cheung LWT. Drugging IGF-1R in cancer: New insights and emerging opportunities. *Genes Dis*. (2023) 10:199–211. doi: 10.1016/j.gendis.2022.03.002

38. Mancarella C, Morrione A, Scotlandi K. Unraveling the IGF system interactome in sarcomas exploits novel therapeutic options. *Cells*. (2021) 10:2075. doi: 10.3390/cells10082075

39. Moonesi M, Zaka Khosravi S, Molaei Ramshe S, Allahbakhshian Farsani M, Solali S, Mohammadi MH, et al. IGF family effects on development, stability, and treatment of hematological Malignancies. *J Cell Physiol*. (2021) 236:4097–105. doi: 10.1002/jcp.30156

40. Novosyadlyy R, Kurshan N, Lann D, Vijayakumar A, Yakar S, LeRoith D. Insulin-like growth factor-I protects cells from ER stress-induced apoptosis via enhancement of the adaptive capacity of endoplasmic reticulum. *Cell Death Differentiation*. (2008) 15:1304–17. doi: 10.1038/cdd.2008.52

41. Liu G, Zhu M, Zhang M, Pan F. Emerging role of IGF-1 in prostate cancer: A promising biomarker and therapeutic target. *Cancers*. (2023) 15:1287. doi: 10.3390/cancers15041287

42. Hua H, Kong Q, Yin J, Zhang J, Jiang Y. Insulin-like growth factor receptor signaling in tumorigenesis and drug resistance: a challenge for cancer therapy. *J Hematol Oncol*. (2020) 13:1–17. doi: 10.1186/s13045-020-00904-3

43. Nitulescu GM, Van De Venter M, Nitulescu G, Ungurianu A, Juzenas P, Peng Q, et al. The Akt pathway in oncology therapy and beyond. *Int J Oncol*. (2018) 53:2319–31. doi: 10.3892/ijo

44. Revathidevi S, Munirajan AK. Akt in cancer: mediator and more. *Semin Cancer Biol*. (2019) 59:80–91. doi: 10.1016/j.semcancer.2019.06.002

45. Janssen JA. New insights from IGF-IR stimulating activity analyses: Pathological considerations. *Cells*. (2020) 9:862. doi: 10.3390/cells9040862

46. Chughtai S. The nuclear translocation of insulin-like growth factor receptor and its significance in cancer cell survival. *Cell Biochem Funct*. (2020) 38:347–51. doi: 10.1002/cbf.3479

47. Rieger L, O'Connor R. Controlled signaling—insulin-like growth factor receptor endocytosis and presence at intracellular compartments. *Front Endocrinol*. (2021) 11:620013. doi: 10.3389/fendo.2020.620013

48. Hankinson SE, Willett WC, Colditz GA, Hunter DJ, Michaud DS, Deroo B, et al. Circulating concentrations of insulin-like growth factor-I and risk of breast cancer. *Lancet (London England)*. (1998) 351:1393–6. doi: 10.1016/s0140-6736(97)10384-1

49. Chan JM, Stampfer MJ, Giovannucci E, Gann PH, Ma J, Wilkinson P, et al. Plasma insulin-like growth factor-I and prostate cancer risk: a prospective study. *Sci (New York NY)*. (1998) 279:563–6. doi: 10.1126/science.279.5350.563

50. Yu H, Spitz MR, Mistry J, Gu J, Hong WK, Wu X. Plasma levels of insulin-like growth factor-I and lung cancer risk: a case-control analysis. *J Natl Cancer Institute*. (1999) 91:151–6. doi: 10.1093/jnci/91.2.151

51. Ma J, Pollak MN, Giovannucci E, Chan JM, Tao Y, Hennekens CH, et al. Prospective study of colorectal cancer risk in men and plasma levels of insulin-like growth factor (IGF)-I and IGF-binding protein-3. *J Natl Cancer Institute*. (1999) 91:620–5. doi: 10.1093/jnci/91.7.620

52. Frostad S, Bruserud O. *In vitro* effects of insulin-like growth factor-1 (IGF-1) on proliferation and constitutive cytokine secretion by acute myelogenous leukemia blasts. *Eur J Haematol*. (1999) 62:191–8. doi: 10.1111/j.1600-0609.1999.tb01743.x

53. LeRoith D, Baserga R, Helman L, Roberts CT Jr. Insulin-like growth factors and cancer. *Ann Intern Med*. (1995) 122:54–9. doi: 10.7326/0003-4819-122-1-199501010-00009

54. Macaulay VM. Insulin-like growth factors and cancer. *Br J Cancer*. (1992) 65:311–20. doi: 10.1038/bjc.1992.65

55. Oku K, Tanaka A, Yamanishi H, Nishizawa Y, Matsumoto K, Shiozaki H, et al. Effects of various growth factors on growth of a cloned human esophageal squamous cancer cell line in a protein-free medium. *Anticancer Res*. (1991) 11:1591–5.

56. Singh P, Dai B, Yallampalli U, Lu X, Schroy PC. Proliferation and differentiation of a human colon cancer cell line (CaCo2) is associated with significant changes in the expression and secretion of insulin-like growth factor (IGF) IGF-II and IGF binding protein-4: role of IGF-II. *Endocrinology*. (1996) 137:1764–74. doi: 10.1210/endo.137.5.8612513

57. Yaginuma Y, Nishiwaki K, Kitamura S, Hayashi H, Sengoku K, Ishikawa M. Relaxation of insulin-like growth factor-II gene imprinting in human gynecologic tumors. *Oncology*. (1997) 54:502–7. doi: 10.1159/000227610

58. Zu K, Martin NE, Fiorentino M, Flavin R, Lis RT, Sinnott JA, et al. Protein expression of PTEN, insulin-like growth factor I receptor (IGF-IR), and lethal prostate cancer: A prospective study. *Cancer Epidemiology Biomarkers Prev*. (2013) 22:1984–93. doi: 10.1158/1055-9965.EPI-13-0349

59. Sichani MM, Yazdi FS, Moghaddam NA, Chehrei A, Kabiri M, Naeimi A, et al. Prognostic value of insulin- like growth factor-I receptor expression in renal cell carcinoma. *Saudi J Kidney Dis Transplant*. (2010) 21:69–74.

60. Matsubara J, Yamada Y, Hirashima Y, Takahari D, Okita NT, Kato K, et al. Impact of insulin-like growth factor type 1 receptor, epidermal growth factor receptor, and HER2 expressions on outcomes of patients with gastric cancer. *Clin Cancer Res*. (2008) 14:3022–9. doi: 10.1158/1078-0432.CCR-07-1898

61. Qu BH, Karas M, Koval A, LeRoith D. Insulin receptor substrate-4 enhances insulin-like growth factor-I-induced cell proliferation. *J Biol Chem*. (1999) 274:31179–84. doi: 10.1074/jbc.274.44.31179

62. Párrizas M, Saltiel AR, LeRoith D. Insulin-like growth factor 1 inhibits apoptosis using the phosphatidylinositol 3'-kinase and mitogen-activated protein kinase pathways. *J Biol Chem*. (1997) 272:154–61. doi: 10.1074/jbc.272.1.154

63. Cory S, Vaux DL, Strasser A, Harris AW, Adams JM. Insights from Bcl-2 and Myc: Malignancy involves abrogation of apoptosis as well as sustained proliferation. *Cancer Res*. (1999) 59:1685s–92s.

64. Hakuno F, Takahashi S-I. 40 YEARS OF IGF1: IGF1 receptor signaling pathways. *J Mol Endocrinol*. (2018) 61:T69–86. doi: 10.1530/JME-17-0311

65. Yu H, Rohan T. Role of the insulin-like growth factor family in cancer development and progression. *J Natl Cancer Institute*. (2000) 92:1472–89. doi: 10.1093/jnci/92.18.1472

66. Rogler CE, Yang D, Rossetti L, Donohoe J, Alt E, Chang CJ, et al. Altered body composition and increased frequency of diverse Malignancies in insulin-like growth factor-II transgenic mice. *J Biol Chem*. (1994) 269:13779–84. doi: 10.1016/S0021-9258(17)36715-7

67. Bates P, Fisher R, Ward A, Richardson L, Hill DJ, Graham CF. Mammary cancer in transgenic mice expressing insulin-like growth factor II (IGF-II). *Br J Cancer*. (1995) 72:1189–93. doi: 10.1038/bjc.1995.484

68. Guerra FK, Eijan AM, Puricelli L, Alonso DF, de Kier Joffé EB, Kornblihtt AR, et al. Varying patterns of expression of insulin-like growth factors I and II and their receptors in murine mammary adenocarcinomas of different metastasizing ability. *Int J Cancer*. (1996) 65:812–20. doi: 10.1002/(ISSN)1097-0215

69. Pietrzkowski Z, Mulholland G, Gomella L, Jameson BA, Wernicke D, Baserga R. Inhibition of growth of prostatic cancer cell lines by peptide analogues of insulin-like growth factor 1. *Cancer Res*. (1993) 53:1102–6.

70. Neuenschwander S, Roberts CT Jr., LeRoith D. Growth inhibition of MCF-7 breast cancer cells by stable expression of an insulin-like growth factor I receptor antisense ribonucleic acid. *Endocrinology*. (1995) 136:4298–303. doi: 10.1210/endo.136.10.7664648

71. Jiang Y, Rom WN, Yie TA, Chi CX, Tchou-Wong KM. Induction of tumor suppression and glandular differentiation of A549 lung carcinoma cells by dominant-negative IGF-I receptor. *Oncogene*. (1999) 18:6071–7. doi: 10.1038/sj.onc.1202984

72. Byrd JC, Devi GR, de Souza AT, Jirtle RL, MacDonald RG. Disruption of ligand binding to the insulin-like growth factor II/mannose 6-phosphate receptor by cancer-associated missense mutations. *J Biol Chem*. (1999) 274:24408–16. doi: 10.1074/jbc.274.34.24408

73. O'Gorman DB, Costello M, Weiss J, Firth SM, Scott CD. Decreased insulin-like growth factor-II/mannose 6-phosphate receptor expression enhances tumorigenicity in JEG-3 cells. *Cancer Res*. (1999) 59:5692–4.

74. Souza RF, Wang S, Thakar M, Smolinski KN, Yin J, Zou TT, et al. Expression of the wild-type insulin-like growth factor II receptor gene suppresses growth and causes death in colorectal carcinoma cells. *Oncogene*. (1999) 18:4063–8. doi: 10.1038/sj.onc.1202768

75. Pollak M. Insulin and insulin-like growth factor signalling in neoplasia. *Nat Rev Cancer*. (2008) 8:915–28. doi: 10.1038/nrc2536

76. Bachrach LK, Nanto-Salonen K, Tapanainen P, Rosenfeld RG, Gargosky SE. Insulin-like growth factor binding protein production in human follicular thyroid carcinoma cells. *Growth Regul*. (1995) 5:109–18.

77. Kimura G, Kasuya J, Giannini S, Honda Y, Mohan S, Kawachi M, et al. Insulin-like growth factor (IGF) system components in human prostatic cancer cell-lines: LNCaP, DU145, and PC-3 cells. *Int J Urol*. (1996) 3:39–46. doi: 10.1111/j.1442-2042.1996.tb00628.x

78. Pekonen F, Nyman T, Ilvesmaki V, Partanen S. Insulin-like growth factor binding proteins in human breast cancer tissue. *Cancer Res*. (1992) 52:5204–7.

79. Perks CM, Bowen S, Gill ZP, Newcomb PV, Holly JM. Differential IGF-independent effects of insulin-like growth factor binding proteins (1-6) on apoptosis of breast epithelial cells. *J Cell Biochem*. (1999) 75:652–64. doi: 10.1002/(ISSN)1097-4644

80. Reeve JG, Morgan J, Schwander J, Bleehen NM. Role for membrane and secreted insulin-like growth factor-binding protein-2 in the regulation of insulin-like growth factor action in lung tumors. *Cancer Res*. (1993) 53:4680–5.

81. Sheikh MS, Shao ZM, Clemmons DR, LeRoith D, Roberts CT Jr., Fontana JA. Identification of the insulin-like growth factor binding proteins 5 and 6 (IGFBP-5 and 6) in human breast cancer cells. *Biochem Biophys Res Commun*. (1992) 183:1003–10. doi: 10.1016/s0006-291x(05)80290-6

82. Tennant MK, Thrasher JB, Twomey PA, Birnbaum RS, Plymate SR. Insulin-like growth factor-binding proteins (IGFBP)-4, -5, and -6 in the benign and Malignant human prostate: IGFBP-5 messenger ribonucleic acid localization differs from IGFBP-5 protein localization. *J Clin Endocrinol Metab*. (1996) 81:3783–92. doi: 10.1210/jcem.81.10.8855838

83. Yee D, Favoni RE, Lippman ME, Powell DR. Identification of insulin-like growth factor binding proteins in breast cancer cells. *Breast Cancer Res Treat*. (1991) 18:3–10. doi: 10.1007/BF01975437

84. Yee D, Jackson JG, Kozelsky TW, Figueroa JA. Insulin-like growth factor binding protein 1 expression inhibits insulin-like growth factor I action in MCF-7 breast cancer cells. *Cell Growth Differ*. (1994) 5:73–7.

85. Jones JI, Clemmons DR. Insulin-like growth factors and their binding proteins: biological actions. *Endocrine Rev*. (1995) 16:3–34. doi: 10.1210/edrv-16-1-3

86. Baxter RC, Butt AJ, Schedlich LJ, Martin JL. Antiproliferative and pro-apoptotic activities of insulin-like growth factor-binding protein-3. *Growth hormone IGF research: Off J Growth Hormone Res Soc Int IGF Res Soc*. (2000) 10 Suppl A:S10–1. doi: 10.1016/s1096-6374(00)90004-2

87. Butt AJ, Firth SM, Baxter RC. The IGF axis and programmed cell death. *Immunol Cell Biol*. (1999) 77:256–62. doi: 10.1046/j.1440-1711.1999.00822.x

88. Hong J, Zhang G, Dong F, Rechler MM. Insulin-like growth factor (IGF)-binding protein-3 mutants that do not bind IGF-I or IGF-II stimulate apoptosis in human prostate cancer cells. *J Biol Chem*. (2002) 277:10489–97. doi: 10.1074/jbc.M109604200

89. Oh Y, Müller HL, Lamson G, Rosenfeld RG. Insulin-like growth factor (IGF)-independent action of IGF-binding protein-3 in Hs578T human breast cancer cells. Cell surface binding and growth inhibition. *J Biol Chem*. (1993) 268:14964–71. doi: 10.1016/S0021-9258(18)82426-7

90. Gill ZP, Perks CM, Newcomb PV, Holly JM. Insulin-like growth factor-binding protein (IGFBP-3) predisposes breast cancer cells to programmed cell death in a non-IGF-dependent manner. *J Biol Chem*. (1997) 272:25602–7. doi: 10.1074/jbc.272.41.25602

91. Rajah R, Valentinis B, Cohen P. Insulin-like growth factor (IGF)-binding protein-3 induces apoptosis and mediates the effects of transforming growth factor-beta1 on programmed cell death through a p53- and IGF-independent mechanism. *J Biol Chem*. (1997) 272:12181–8. doi: 10.1074/jbc.272.18.12181

92. Rozen F, Yang XF, Huynh H, Pollak M. Antiproliferative action of vitamin D-related compounds and insulin-like growth factor-binding protein 5 accumulation. *J Natl Cancer Institute*. (1997) 89:652–6. doi: 10.1093/jnci/89.9.652

93. Colston KW, Perks CM, Xie SP, Holly JM. Growth inhibition of both MCF-7 and Hs578T human breast cancer cell lines by vitamin D analogues is associated with increased expression of insulin-like growth factor binding protein-3. *J Mol Endocrinol*. (1998) 20:157–62. doi: 10.1677/jme.0.0200157

94. Xie SP, James SY, Colston KW. Vitamin D derivatives inhibit the mitogenic effects of IGF-I on MCF-7 human breast cancer cells. *J Endocrinol*. (1997) 154:495–504. doi: 10.1677/joe.0.1540495

95. Huynh H, Pollak M, Zhang JC. Regulation of insulin-like growth factor (IGF) II and IGF binding protein 3 autocrine loop in human PC-3 prostate cancer cells by vitamin D metabolite 1,25(OH)2D3 and its analog EB1089. *Int J Oncol*. (1998) 13:137–43. doi: 10.3892/ijo.13.1.137

96. Ohlsson C, Kley N, Werner H, LeRoith D. p53 regulates insulin-like growth factor-I (IGF-I) receptor expression and IGF-I-induced tyrosine phosphorylation in an osteosarcoma cell line: interaction between p53 and Sp1. *Endocrinology*. (1998) 139:1101–7. doi: 10.1210/endo.139.3.5832

97. Webster NJ, Resnik JL, Reichart DB, Strauss B, Haas M, Seely BL. Repression of the insulin receptor promoter by the tumor suppressor gene product p53: a possible mechanism for receptor overexpression in breast cancer. *Cancer Res*. (1996) 56:2781–8.

98. Werner H, Karnieli E, Rauscher FJ, LeRoith D. Wild-type and mutant p53 differentially regulate transcription of the insulin-like growth factor I receptor gene. *Proc Natl Acad Sci U.S.A*. (1996) 93:8318–23. doi: 10.1073/pnas.93.16.8318

99. Zhang L, Kashanchi F, Zhan Q, Zhan S, Brady JN, Fornace AJ, et al. Regulation of insulin-like growth factor II P3 promotor by p53: a potential mechanism for tumorigenesis. *Cancer Res*. (1996) 56:1367–73.

100. Zhang L, Zhan Q, Zhan S, Kashanchi F, Fornace AJ Jr., Seth P, et al. p53 regulates human insulin-like growth factor II gene expression through active P4 promoter in rhabdomyosarcoma cells. *DNA Cell Biol*. (1998) 17:125–31. doi: 10.1089/dna.1998.17.125

101. Buckbinder L, Talbott R, Velasco-Miguel S, Takenaka I, Faha B, Seizinger BR, et al. Induction of the growth inhibitor IGF-binding protein 3 by p53. *Nature*. (1995) 377:646–9. doi: 10.1038/377646a0

102. Tennant MK, Thrasher JB, Twomey PA, Birnbaum RS, Plymate SR. Insulin-like growth factor-binding protein-2 and -3 expression in benign human prostate epithelium, prostate intraepithelial neoplasia, and adenocarcinoma of the prostate. *J Clin Endocrinol Metab*. (1996) 81:411–20. doi: 10.1210/jcem.81.1.8550786

103. Tennant MK, Thrasher JB, Twomey PA, Drivdahl RH, Birnbaum RS, Plymate SR. Protein and messenger ribonucleic acid (mRNA) for the type 1 insulin-like growth factor (IGF) receptor is decreased and IGF-II mRNA is increased in human prostate carcinoma compared to benign prostate epithelium. *J Clin Endocrinol Metab*. (1996) 81:3774–82. doi: 10.1210/jcem.81.10.8855837

104. Plymate SR, Tennant M, Birnbaum RS, Thrasher JB, Chatta G, Ware JL. The effect on the insulin-like growth factor system in human prostate epithelial cells of immortalization and transformation by simian virus-40 T antigen. *J Clin Endocrinol Metab*. (1996) 81:3709–16. doi: 10.1210/jcem.81.10.8855827

105. Wu J, Yu E. Insulin-like growth factor receptor-1 (IGF-IR) as a target for prostate cancer therapy. *Cancer metastasis Rev*. (2014) 33:607–17. doi: 10.1007/s10555-013-9482-0

106. Cohen P, Graves HC, Peehl DM, Kamarei M, Giudice LC, Rosenfeld RG. Prostate-specific antigen (PSA) is an insulin-like growth factor binding protein-3 protease found in seminal plasma. *J Clin Endocrinol Metab*. (1992) 75:1046–53. doi: 10.1210/jcem.75.4.1383255

107. Koistinen H, Paju A, Koistinen R, Finne P, Lövgren J, Wu P, et al. Prostate-specific antigen and other prostate-derived proteases cleave IGFBP-3, but prostate cancer is not associated with proteolytically cleaved circulating IGFBP-3. *Prostate*. (2002) 50:112–8. doi: 10.1002/pros.10039

108. Pollak M. Insulin-like growth factors and prostate cancer. *Epidemiologic Rev*. (2001) 23:59–66. doi: 10.1093/oxfordjournals.epirev.a000796

109. Chan JM, Stampfer MJ, Ma J, Gann P, Gaziano JM, Pollak M, et al. Insulin-like growth factor-I (IGF-I) and IGF binding protein-3 as predictors of advanced-stage prostate cancer. *J Natl Cancer Institute*. (2002) 94:1099–106. doi: 10.1093/jnci/94.14.1099

110. Ma C, Wang Y, Wilson KM, Mucci LA, Stampfer MJ, Pollak M, et al. Circulating insulin-like growth factor 1-related biomarkers and risk of lethal prostate cancer. *JNCI Cancer Spectr*. (2022) 6:pkab091. doi: 10.1093/jncics/pkab091

111. Renehan AG, Zwahlen M, Minder C, O'Dwyer ST, Shalet SM, Egger M. Insulin-like growth factor (IGF)-I, IGF binding protein-3, and cancer risk: systematic review and meta-regression analysis. *Lancet (London England)*. (2004) 363:1346–53. doi: 10.1016/s0140-6736(04)16044-3

112. Mantzoros CS, Tzonou A, Signorello LB, Stampfer M, Trichopoulos D, Adami HO. Insulin-like growth factor 1 in relation to prostate cancer and benign prostatic hyperplasia. *Br J Cancer*. (1997) 76:1115–8. doi: 10.1038/bjc.1997.520

113. Djavan B, Bursa B, Seitz C, Soeregi G, Remzi M, Basharkhah A, et al. Insulin-like growth factor 1 (IGF-1), IGF-1 density, and IGF-1/PSA ratio for prostate cancer detection. *Urology*. (1999) 54:603–6. doi: 10.1016/s0090-4295(99)00280-0

114. Ho PJ, Baxter RC. Insulin-like growth factor-binding protein-2 in patients with prostate carcinoma and benign prostatic hyperplasia. *Clin Endocrinol*. (1997) 46:333–42.

115. Cohen P, Peehl DM, Stamey TA, Wilson KF, Clemmons DR, Rosenfeld RG. Elevated levels of insulin-like growth factor-binding protein-2 in the serum of prostate cancer patients. *J Clin Endocrinol Metab*. (1993) 76:1031–5. doi: 10.1210/jcem.76.4.7682560

116. Kanety H, Madjar Y, Dagan Y, Levi J, Papa MZ, Pariente C, et al. Serum insulin-like growth factor-binding protein-2 (IGFBP-2) is increased and IGFBP-3 is decreased in patients with prostate cancer: correlation with serum prostate-specific antigen. *J Clin Endocrinol Metab*. (1993) 77:229–33. doi: 10.1210/jcem.77.1.7686915

117. Roddam AW, Allen NE, Appleby P, Key TJ, Ferrucci L, Carter HB, et al. Insulin-like growth factors, their binding proteins, and prostate cancer risk: analysis of individual patient data from 12 prospective studies. *Ann Intern Med*. (2008) 149:461–71. doi: 10.7326/0003-4819-149-7-200810070-00006

118. Sreenivasulu K, Nandeesha H, Dorairajan LN, Rajappa M, Vinayagam V, Cherupanakkal C. Gene expression of insulin receptor, insulin-like growth factor increases and insulin-like growth factor-binding protein-3 reduces with increase in prostate size in benign prostatic hyperplasia. *Aging Male*. (2018) 21:138–44. doi: 10.1080/13685538.2017.1401994

119. Qian Q, He W, Liu D, Yin J, Ye L, Chen P, et al. M2a macrophage can rescue proliferation and gene expression of benign prostate hyperplasia epithelial and stroma cells from insulin-like growth factor 1 knockdown. *Prostate*. (2021) 81:530–42. doi: 10.1002/pros.24131

120. Tricoli JV, Winter DL, Hanlon AL, Raysor SL, Watkins-Bruner D, Pinover WH, et al. Racial differences in insulin-like growth factor binding protein-3 in men at increased risk of prostate cancer. *Urology*. (1999) 54:178–82. doi: 10.1016/s0090-4295(99)00129-6

121. Platz EA, Pollak MN, Rimm EB, Majeed N, Tao Y, Willett WC, et al. Racial variation in insulin-like growth factor-1 and binding protein-3 concentrations in middle-aged men. *Cancer epidemiology Biomarkers prevention: Publ Am Assoc Cancer Research cosponsored by Am Soc Prev Oncol*. (1999) 8:1107–10.

122. Greenlee RT, Murray T, Bolden S, Wingo PA. Cancer statistics, 2000. *CA: Cancer J Clin*. (2000) 50:7–33. doi: 10.3322/canjclin.50.1.7

123. Qian F, Huo D. Circulating insulin-like growth factor-1 and risk of total and 19 site-specific cancers: cohort study analyses from the UK biobank. *Cancer Epidemiology Biomarkers Prev*. (2020) 29:2332–42. doi: 10.1158/1055-9965.EPI-20-0743

124. Tatoud R. Insulin-like growth factor (IGF) network and prostate pathologies. *Prostate Cancer prostatic Dis.* (1999) 2:66–9. doi: 10.1038/sj.pcan.4500295

125. Matsushita M, Fujita K, Hatano K, De Velasco MA, Uemura H, Nonomura N. Connecting the dots between the gut–IGF-1–prostate axis: A role of IGF-1 in prostate carcinogenesis. *Front Endocrinol.* (2022) 13. doi: 10.3389/fendo.2022.852382

126. Hellawell GO, Turner GD, Davies DR, Poulsom R, Brewster SF, Macaulay VM. Expression of the type 1 insulin-like growth factor receptor is up-regulated in primary prostate cancer and commonly persists in metastatic disease. *Cancer Res.* (2002) 62:2942–50. doi: 10.1016/S1569-9056(02)80120-8

127. Krueckl SL, Sikes RA, Edlund NM, Bell RH, Hurtado-Coll A, Fazli L, et al. Increased insulin-like growth factor I receptor expression and signaling are components of androgen-independent progression in a lineage-derived prostate cancer progression model. *Cancer Res.* (2004) 64:8620–9. doi: 10.1158/0008-5472.Can-04-2446

128. Nickerson T, Chang F, Lorimer D, Smeekens SP, Sawyers CL, Pollak M. *In vivo* progression of LAPC-9 and LNCaP prostate cancer models to androgen independence is associated with increased expression of insulin-like growth factor I (IGF-I) and IGF-I receptor (IGF-IR). *Cancer Res.* (2001) 61:6276–80.

129. Sutherland BW, Knoblaugh SE, Kaplan-Lefko PJ, Wang F, Holzenberger M, Greenberg NM. Conditional deletion of insulin-like growth factor-I receptor in prostate epithelium. *Cancer Res.* (2008) 68:3495–504. doi: 10.1158/0008-5472.Can-07-6531

130. Matsushita M, Fujita K, Hayashi T, Kayama H, Motooka D, Hase H, et al. Gut microbiota–derived short-chain fatty acids promote prostate cancer growth via IGF1 signaling. *Cancer Res.* (2021) 81:4014–26. doi: 10.1158/0008-5472.CAN-20-4090

131. Saikali Z, Setya H, Singh G, Persad S. Role of IGF-1/IGF-1R in regulation of invasion in DU145 prostate cancer cells. *Cancer Cell Int.* (2008) 8:10. doi: 10.1186/1475-2867-8-10

132. Niu X-B, Fu G-B, Wang L, Ge X, Liu W-T, Wen Y-Y, et al. Insulin-like growth factor-I induces chemoresistence to docetaxel by inhibiting miR-143 in human prostate cancer. *Oncotarget;*. (2017) 8:107157. doi: 10.18632/oncotarget.v8i63

133. Plymate SR, Haugk K, Coleman I, Woodke L, Vessella R, Nelson P, et al. An antibody targeting the type I insulin-like growth factor receptor enhances the castration-induced response in androgen-dependent prostate cancer. *Clin Cancer Res.* (2007) 13:6429–39. doi: 10.1158/1078-0432.CCR-07-0648

134. Fan W, Yanase T, Morinaga H, Okabe T, Nomura M, Daitoku H, et al. Insulin-like growth factor 1/insulin signaling activates androgen signaling through direct interactions of foxo1 with androgen receptor *. *J Biol Chem.* (2007) 282:7329–38. doi: 10.1074/jbc.M610447200

135. Weyer-Czernilofsky U, Hofmann MH, Friedbichler K, Baumgartinger R, Adam PJ, Solca F, et al. Antitumor activity of the IGF-1/IGF-2–neutralizing antibody xentuzumab (BI 836845) in combination with enzalutamide in prostate cancer models. *Mol Cancer Ther.* (2020) 19:1059–69. doi: 10.1158/1535-7163.MCT-19-0378

136. Stattin P, Bylund A, Rinaldi S, Biessy C, Déchaud H, Stenman UH, et al. Plasma insulin-like growth factor-I, insulin-like growth factor-binding proteins, and prostate cancer risk: a prospective study. *J Natl Cancer Institute.* (2000) 92:1910–7. doi: 10.1093/jnci/92.23.1910

137. Horoszewicz JS, Leong SS, Kawinski E, Karr JP, Rosenthal H, Chu TM, et al. LNCaP model of human prostatic carcinoma. *Cancer Res.* (1983) 43:1809–18.

138. Ngo TH, Barnard RJ, Cohen P, Freedland S, Tran C, deGregorio F, et al. Effect of isocaloric low-fat diet on human LAPC-4 prostate cancer xenografts in severe combined immunodeficient mice and the insulin-like growth factor axis1. *Clin Cancer Res.* (2003) 9:2734–43.

139. Fahrenholtz CD, Beltran PJ, Burnstein KL. Targeting IGF-IR with ganitumab inhibits tumorigenesis and increases durability of response to androgen-deprivation therapy in VCaP prostate cancer xenografts. *Mol Cancer Ther.* (2013) 12:394–404. doi: 10.1158/1535-7163.MCT-12-0648

140. Nordstrand A, Bergstrom SH, Thysell E, Bovinder-Ylitalo E, Lerner UH, Widmark A, et al. Inhibition of the insulin-like growth factor-1 receptor potentiates acute effects of castration in a rat model for prostate cancer growth in bone. *Clin Exp Metastasis.* (2017) 34:261–71. doi: 10.1007/s10585-017-9848-8

141. Barata P, Cooney M, Tyler A, Wright J, Dreicer R, Garcia JA. A phase 2 study of OSI-906 (linsitinib, an insulin-like growth factor receptor-1 inhibitor) in patients with asymptomatic or mildly symptomatic (non-opioid requiring) metastatic castrate resistant prostate cancer (CRPC). *Investigational New Drugs.* (2018) 36:451–7. doi: 10.1007/s10637-018-0574-0

142. Saleh SAK, Adly HM, Nassir AM. Combination of insulin-like growth factor-1, IGF binding protein-3, chromogranin A and prostate specific antigen can improve the detection of prostate cancer. *J Cancer Metastasis Treat.* (2017) 3:82–9. doi: 10.20517/2394-4722.2017.20

143. Massoner P, Colleselli D, Matscheski A, Pircher H, Geley S, Jansen Dürr P, et al. Novel mechanism of IGF-binding protein-3 action on prostate cancer cells: inhibition of proliferation, adhesion, and motility. *Endocrine-Related Cancer.* (2009) 16:795–808. doi: 10.1677/ERC-08-0175

144. Kolb AD, Bussard KM. The bone extracellular matrix as an ideal milieu for cancer cell metastases. *Cancers.* (2019) 11:1020. doi: 10.3390/cancers11071020

145. Siech C, Rutz J, Maxeiner S, Grein T, Sonnenburg M, Tsaur I, et al. Insulin-like growth factor-1 influences prostate cancer cell growth and invasion through an integrin α3, α5, αV, and β1 dependent mechanism. *Cancers.* (2022) 14:363. doi: 10.3390/cancers14020363

146. Moore MG, Wetterau LA, Francis MJ, Peehl DM, Cohen P. Novel stimulatory role for insulin-like growth factor binding protein-2 in prostate cancer cells. *Int J Cancer.* (2003) 105:14–9. doi: 10.1002/ijc.11015

147. Inman BA, Harel F, Audet JF, Meyer F, Douville P, Fradet Y, et al. Insulin-like growth factor binding protein 2: an androgen-dependent predictor of prostate cancer survival. *Eur Urol.* (2005) 47:695–702. doi: 10.1016/j.eururo.2004.12.015

148. Putz T, Culig Z, Eder IE, Nessler-Menardi C, Bartsch G, Grunicke H, et al. Epidermal growth factor (EGF) receptor blockade inhibits the action of EGF, insulin-like growth factor I, and a protein kinase A activator on the mitogen-activated protein kinase pathway in prostate cancer cell lines. *Cancer Res.* (1999) 59:227–33.

149. Monget P, Oxvig C. PAPP-A and the IGF system. *Annales d'endocrinologie.* (2016) 77:90–6. doi: 10.1016/j.ando.2016.04.015

150. Bischof P, Megevand M. Pregnancy-associated plasma protein-A concentrations in men with testicular and prostatic tumors. *Arch Androl.* (1986) 16:155–60. doi: 10.3109/01485018608986936

151. Boldt HB, Conover CA. Overexpression of pregnancy-associated plasma protein-A in ovarian cancer cells promotes tumor growth in *vivo*. *Endocrinology.* (2011) 152:1470–8. doi: 10.1210/en.2010-1095

152. Bulut I, Coskun A, Ciftci A, Cetinkaya E, Altiay G, Caglar T, et al. Relationship between pregnancy-associated plasma protein-A and lung cancer. *Am J Med Sci.* (2009) 337:241–4. doi: 10.1097/MAJ.0b013e31818967a3

153. Heitzeneder S, Sotillo E, Shern JF, Sindiri S, Xu P, Jones R, et al. Pregnancy-associated plasma protein-A (PAPP-A) in ewing sarcoma: role in tumor growth and immune evasion. *J Natl Cancer Institute.* (2019) 111:970–82. doi: 10.1093/jnci/djy209

154. Prithviraj P, Anaka M, McKeown SJ, Permezel M, Walkiewicz M, Cebon J, et al. Pregnancy associated plasma protein-A links pregnancy and melanoma progression by promoting cellular migration and invasion. *Oncotarget.* (2015) 6:15953–65. doi: 10.18632/oncotarget.3643

155. Ryan AJ, Napoletano S, Fitzpatrick PA, Currid CA, O'Sullivan NC, Harmey JH. Expression of a protease-resistant insulin-like growth factor-binding protein-4 inhibits tumour growth in a murine model of breast cancer. *Br J Cancer.* (2009) 101:278–86. doi: 10.1038/sj.bjc.6605141

156. Pollak M. The insulin and insulin-like growth factor receptor family in neoplasia: an update. *Nat Rev Cancer.* (2012) 12:159–69. doi: 10.1038/nrc3215

157. Tomlins SA, Mehra R, Rhodes DR, Cao X, Wang L, Dhanasekaran SM, et al. Integrative molecular concept modeling of prostate cancer progression. *Nat Genet.* (2007) 39:41–51. doi: 10.1038/ng1935

158. Zhang M, Smith EP, Kuroda H, Banach W, Chernausek SD, Fagin JA. Targeted expression of a protease-resistant IGFBP-4 mutant in smooth muscle of transgenic mice results in IGFBP-4 stabilization and smooth muscle hypotrophy*. *J Biol Chem.* (2002) 277:21285–90. doi: 10.1074/jbc.M112082200

159. Soh CL, McNeil K, Owczarek CM, Hardy MP, Fabri LJ, Pearse M, et al. Exogenous administration of protease-resistant, non-matrix-binding IGFBP-2 inhibits tumour growth in a murine model of breast cancer. *Br J Cancer.* (2014) 110:2855–64. doi: 10.1038/bjc.2014.232

160. Zhu S, Xu F, Zhang J, Ruan W, Lai M. Insulin-like growth factor binding protein-related protein 1 and cancer. *Clinica Chimica Acta.* (2014) 431:23–32. doi: 10.1016/j.cca.2014.01.037

161. Jiang W, Xiang C, Cazacu S, Brodie C, Mikkelsen T. Insulin-like growth factor binding protein 7 mediates glioma cell growth and migration. *Neoplasia.* (2008) 10:1335–42. doi: 10.1593/neo.08694

162. Evdokimova V, Tognon CE, Benatar T, Yang W, Krutikov K, Pollak M, et al. IGFBP7 binds to the IGF-1 receptor and blocks its activation by insulin-like growth factors. *Sci Signaling.* (2012) 5:ra92–ra. doi: 10.1126/scisignal.2003184

163. Cohen P, Peehl DM, Baker B, Liu F, Hintz RL, Rosenfeld RG. Insulin-like growth factor axis abnormalities in prostatic stromal cells from patients with benign prostatic hyperplasia. *J Clin Endocrinol Metab.* (1994) 79:1410–5. doi: 10.1210/jcem.79.5.7525636

164. Hwa V, Tomasini-Sprenger C, Bermejo AL, Rosenfeld RG, Plymate SR. Characterization of insulin-like growth factor-binding protein-related protein-1 in prostate cells. *J Clin Endocrinol Metab.* (1998) 83:4355–62. doi: 10.1210/jcem.83.12.5341

165. Mutaguchi K, Yasumoto H, Mita K, Matsubara A, Shiina H, Igawa M, et al. Restoration of insulin-like growth factor binding protein-related protein 1 has a tumor-suppressive activity through induction of apoptosis in human prostate cancer. *Cancer Res.* (2003) 63:7717–23.

166. López-Bermejo A, Buckway CK, Devi GR, Hwa V, Plymate SR, Oh Y, et al. Characterization of insulin-like growth factor-binding protein-related proteins (IGFBP-rPs) 1, 2, and 3 in human prostate epithelial cells: potential roles for IGFBP-rP1 and 2 in senescence of the prostatic epithelium. *Endocrinology.* (2000) 141:4072–80. doi: 10.1210/endo.141.11.7783

167. Pilarsky CP, Schmidt U, Eissrich C, Stade J, Froschermaier SE, Haase M, et al. Expression of the extracellular matrix signaling molecule Cyr61 is downregulated in prostate cancer. *Prostate.* (1998) 36:85–91. doi: 10.1002/(SICI)1097-0045(19980701)36:2<85::AID-PROS3>3.3.CO;2-X

168. Li L, Yu H, Schumacher F, Casey G, Witte JS. Relation of serum insulin-like growth factor-I (IGF-I) and IGF binding protein-3 to risk of prostate cancer (United States). *Cancer Causes Control.* (2003) 14:721–6. doi: 10.1023/A:1026383824791

169. Trojan L, Bode C, Weiss C, Mayer D, Grobholz R, Alken P, et al. IGF-II serum levels increase discrimination between benign prostatic hyperplasia and prostate cancer and improve the predictive value of PSA in clinical staging. *Eur Urol*. (2006) 49:286–92; discussion 92. doi: 10.1016/j.eururo.2005.08.022

170. Gori F, Hofbauer LC, Conover CA, Khosla S. Effects of androgens on the insulin-like growth factor system in an androgen-responsive human osteoblastic cell line. *Endocrinology*. (1999) 140:5579–86. doi: 10.1210/endo.140.12.7213

171. Zhang XH, Jin X, Malladi S, Zou Y, Wen YH, Brogi E, et al. Selection of bone metastasis seeds by mesenchymal signals in the primary tumor stroma. *Cell*. (2013) 154:1060–73. doi: 10.1016/j.cell.2013.07.036

172. van Golen CM, Schwab TS, Kim B, Soules ME, Su Oh S, Fung K, et al. Insulin-like growth factor-I receptor expression regulates neuroblastoma metastasis to bone. *Cancer Res*. (2006) 66:6570–8. doi: 10.1158/0008-5472.Can-05-1448

173. Heidegger I, Massoner P, Sampson N, Klocker H. The insulin-like growth factor (IGF) axis as an anticancer target in prostate cancer. *Cancer Lett*. (2015) 367:113–21. doi: 10.1016/j.canlet.2015.07.026

174. Goel HL, Fornaro M, Moro L, Teider N, Rhim JS, King M, et al. Selective modulation of type 1 insulin-like growth factor receptor signaling and functions by beta1 integrins. *J Cell Biol*. (2004) 166:407–18. doi: 10.1083/jcb.200403003

175. Damsky CH, Ilić D. Integrin signaling: it's where the action is. *Curr Opin Cell Biol*. (2002) 14:594–602. doi: 10.1016/S0955-0674(02)00368-X

176. Fornaro M, Manes T, Languino LR. Integrins and prostate cancer metastases. *Cancer metastasis Rev*. (2001) 20:321–31. doi: 10.1023/a:1015547830323

177. Mauro L, Surmacz E. IGF-I receptor, cell-cell adhesion, tumour development and progression. *J Mol Histol*. (2004) 35:247–53. doi: 10.1023/b:hijo.0000032356.98363.a2

178. Maile LA, Badley-Clarke J, Clemmons DR. Structural analysis of the role of the beta 3 subunit of the alpha V beta 3 integrin in IGF-I signaling. *J Cell Sci*. (2001) 114:1417–25. doi: 10.1242/jcs.114.7.1417

179. Playford MP, Bicknell D, Bodmer WF, Macaulay VM. Insulin-like growth factor 1 regulates the location, stability, and transcriptional activity of beta-catenin. *Proc Natl Acad Sci U.S.A*. (2000) 97:12103–8. doi: 10.1073/pnas.210394297

180. Rubin J, Ackert-Bicknell CL, Zhu L, Fan X, Murphy TC, Nanes MS, et al. IGF-I regulates osteoprotegerin (OPG) and receptor activator of nuclear factor-kappaB ligand in *vitro* and OPG in *vivo*. *J Clin Endocrinol Metab*. (2002) 87:4273–9. doi: 10.1210/jc.2002-020656

181. Fizazi K, Yang J, Peleg S, Sikes CR, Kreimann EL, Daliani D, et al. Prostate cancer cells-osteoblast interaction shifts expression of growth/survival-related genes in prostate cancer and reduces expression of osteoprotegerin in osteoblasts. *Clin Cancer research: an Off J Am Assoc Cancer Res*. (2003) 9:2587–97.

182. Rubin J, Chung LW, Fan X, Zhu L, Murphy TC, Nanes MS, et al. Prostate carcinoma cells that have resided in bone have an upregulated IGF-I axis. *Prostate*. (2004) 58:41–9. doi: 10.1002/pros.10299

183. Simonet WS, Lacey DL, Dunstan CR, Kelley M, Chang MS, Lüthy R, et al. Osteoprotegerin: a novel secreted protein involved in the regulation of bone density. *Cell*. (1997) 89:309–19. doi: 10.1016/s0092-8674(00)80209-3

184. Goya M, Miyamoto S, Nagai K, Ohki Y, Nakamura K, Shitara K, et al. Growth inhibition of human prostate cancer cells in human adult bone implanted into nonobese diabetic/severe combined immunodeficient mice by a ligand-specific antibody to human insulin-like growth factors. *Cancer Res*. (2004) 64:6252–8. doi: 10.1158/0008-5472.Can-04-0919

185. Li S, Wang N, Brodt P. Metastatic cells can escape the proapoptotic effects of TNF-α through increased autocrine IL-6/STAT3 signaling. *Cancer Res*. (2012) 72:865–75. doi: 10.1158/0008-5472.Can-11-1357

186. Tang Y, Zhang D, Fallavollita L, Brodt P. Vascular endothelial growth factor C expression and lymph node metastasis are regulated by the type I insulin-like growth factor receptor. *Cancer Res*. (2003) 63:1166–71.

187. Tsurusaki T, Kanda S, Sakai H, Kanetake H, Saito Y, Alitalo K, et al. Vascular endothelial growth factor-C expression in human prostatic carcinoma and its relationship to lymph node metastasis. *Br J Cancer*. (1999) 80:309–13. doi: 10.1038/sj.bjc.6690356

188. Li J, Wang E, Rinaldo F, Datta K. Upregulation of VEGF-C by androgen depletion: the involvement of IGF-IR-FOXO pathway. *Oncogene*. (2005) 24:5510–20. doi: 10.1038/sj.onc.1208693

189. Hiraga T, Myoui A, Hashimoto N, Sasaki A, Hata K, Morita Y, et al. Bone-derived IGF mediates crosstalk between bone and breast cancer cells in bony metastases. *Cancer Res*. (2012) 72:4238–49. doi: 10.1158/0008-5472.Can-11-3061

190. Shafi AA, Yen AE, Weigel NL. Androgen receptors in hormone-dependent and castration-resistant prostate cancer. *Pharmacol Ther*. (2013) 140:223–38. doi: 10.1016/j.pharmthera.2013.07.003

191. Yuan X, Cai C, Chen S, Chen S, Yu Z, Balk SP. Androgen receptor functions in castration-resistant prostate cancer and mechanisms of resistance to new agents targeting the androgen axis. *Oncogene*. (2014) 33:2815–25. doi: 10.1038/onc.2013.235

192. Titus MA, Schell MJ, Lih FB, Tomer KB, Mohler JL. Testosterone and dihydrotestosterone tissue levels in recurrent prostate cancer. *Clin Cancer research: an Off J Am Assoc Cancer Res*. (2005) 11:4653–7. doi: 10.1158/1078-0432.Ccr-05-0525

193. Montgomery RB, Mostaghel EA, Vessella R, Hess DL, Kalhorn TF, Higano CS, et al. Maintenance of intratumoral androgens in metastatic prostate cancer: a mechanism for castration-resistant tumor growth. *Cancer Res*. (2008) 68:4447–54. doi: 10.1158/0008-5472.Can-08-0249

194. So A, Gleave M, Hurtado-Col A, Nelson C. Mechanisms of the development of androgen independence in prostate cancer. *World J Urol*. (2005) 23:1–9. doi: 10.1007/s00345-004-0473-1

195. Miyake H, Pollak M, Gleave ME. Castration-induced up-regulation of insulin-like growth factor binding protein-5 potentiates insulin-like growth factor-I activity and accelerates progression to androgen independence in prostate cancer models. *Cancer Res*. (2000) 60:3058–64.

196. Gurumurthy S, Vasudevan KM, Rangnekar VM. Regulation of apoptosis in prostate cancer. *Cancer metastasis Rev*. (2001) 20:225–43. doi: 10.1023/a:1015583310759

197. Grossmann ME, Huang H, Tindall DJ. Androgen receptor signaling in androgen-refractory prostate cancer. *J Natl Cancer Institute*. (2001) 93:1687–97. doi: 10.1093/jnci/93.22.1687

198. Feldman BJ, Feldman D. The development of androgen-independent prostate cancer. *Nat Rev Cancer*. (2001) 1:34–45. doi: 10.1038/35094009

199. Orio F Jr., Térouanne B, Georget V, Lumbroso S, Avances C, Siatka C, et al. Potential action of IGF-1 and EGF on androgen receptor nuclear transfer and transactivation in normal and cancer human prostate cell lines. *Mol Cell Endocrinol*. (2002) 198:105–14. doi: 10.1016/S0303-7207(02)00374-X

200. Plymate SR, Bae VL, Maddison L, Quinn LS, Ware JL. Reexpression of the type 1 insulin-like growth factor receptor inhibits the Malignant phenotype of simian virus 40 T antigen immortalized human prostate epithelial cells. *Endocrinology*. (1997) 138:1728–35. doi: 10.1210/endo.138.4.5071

201. Kaplan PJ, Mohan S, Cohen P, Foster BA, Greenberg NM. The insulin-like growth factor axis and prostate cancer: lessons from the transgenic adenocarcinoma of mouse prostate (TRAMP) model. *Cancer Res*. (1999) 59:2203–9.

202. Cooke DW, Bankert LA, Roberts CT Jr., LeRoith D, Casella SJ. Analysis of the human type I insulin-like growth factor receptor promoter region. *Biochem Biophys Res Commun*. (1991) 177:1113–20. doi: 10.1016/0006-291X(91)90654-P

203. Schayek H, Haugk K, Sun S, True LD, Plymate SR, Werner H. Tumor suppressor BRCA1 is expressed in prostate cancer and controls insulin-like growth factor I receptor (IGF-IR) gene transcription in an androgen receptor-dependent manner. *Clin Cancer research: an Off J Am Assoc Cancer Res*. (2009) 15:1558–65. doi: 10.1158/1078-0432.Ccr-08-1440

204. Moretti RM, Marelli MM, Dondi D, Poletti A, Martini L, Motta M, et al. Luteinizing hormone-releasing hormone agonists interfere with the stimulatory actions of epidermal growth factor in human prostatic cancer cell lines, LNCaP and DU 145. *J Clin Endocrinol Metab*. (1996) 81:3930–7. doi: 10.1210/jcem.81.11.8923840

205. Pandini G, Mineo R, Frasca F, Roberts CT Jr., Marcelli M, Vigneri R, et al. Androgens up-regulate the insulin-like growth factor-I receptor in prostate cancer cells. *Cancer Res*. (2005) 65:1849–57. doi: 10.1158/0008-5472.Can-04-1837

206. Nelson JB, Chan-Tack K, Hedican SP, Magnuson SR, Opgenorth TJ, Bova GS, et al. Endothelin-1 production and decreased endothelin B receptor expression in advanced prostate cancer. *Cancer Res*. (1996) 56:663–8.

207. Sehgal I, Powers S, Huntley B, Powis G, Pittelkow M, Maihle NJ. Neurotensin is an autocrine trophic factor stimulated by androgen withdrawal in human prostate cancer. *Proc Natl Acad Sci U.S.A*. (1994) 91:4673–7. doi: 10.1073/pnas.91.11.4673

208. Markwalder R, Reubi JC. Gastrin-releasing peptide receptors in the human prostate: relation to neoplastic transformation. *Cancer Res*. (1999) 59:1152–9.

209. Nickerson T, Pollak M, Huynh H. Castration-induced apoptosis in the rat ventral prostate is associated with increased expression of genes encoding insulin-like growth factor binding proteins 2,3,4 and 5. *Endocrinology*. (1998) 139:807–10. doi: 10.1210/endo.139.2.5912

210. Thomas LN, Cohen P, Douglas RC, Lazier C, Rittmaster RS. Insulin-like growth factor binding protein 5 is associated with involution of the ventral prostate in castrated and finasteride-treated rats. *Prostate*. (1998) 35:273–8. doi: 10.1002/(SICI)1097-0045(19980601)35:4<273::AID-PROS6>3.3.CO;2-J

211. Kiyama S, Morrison K, Zellweger T, Akbari M, Cox M, Yu D, et al. Castration-induced increases in insulin-like growth factor-binding protein 2 promotes proliferation of androgen-independent human prostate LNCaP tumors. *Cancer Res*. (2003) 63:3575–84.

212. Schulz P, Link TA, Chaudhuri L, Fittler F. Role of the mitochondrial bc1-complex in the cytotoxic action of diethylstilbestrol-diphosphate toward prostatic carcinoma cells. *Cancer Res*. (1990) 50:5008–12.

213. Koike H, Ito K, Takezawa Y, Oyama T, Yamanaka H, Suzuki K. Insulin-like growth factor binding protein-6 inhibits prostate cancer cell proliferation: implication for anticancer effect of diethylstilbestrol in hormone refractory prostate cancer. *Br J Cancer*. (2005) 92:1538–44. doi: 10.1038/sj.bjc.6602520

214. Lubik AA, Gunter JH, Hendy SC, Locke JA, Adomat HH, Thompson V, et al. Insulin increases *de novo* steroidogenesis in prostate cancer cells. *Cancer Res*. (2011) 71:5754–64. doi: 10.1158/0008-5472.CAN-10-2470

215. Haluska P, Carboni JM, Loegering DA, Lee FY, Wittman M, Saulnier MG, et al. *In vitro* and in *vivo* antitumor effects of the dual insulin-like growth factor-I/insulin receptor inhibitor, BMS-554417. *Cancer Res*. (2006) 66:362–71. doi: 10.1158/0008-5472.Can-05-1107

216. Ji QS, Mulvihill MJ, Rosenfeld-Franklin M, Cooke A, Feng L, Mak G, et al. A novel, potent, and selective insulin-like growth factor-I receptor kinase inhibitor blocks insulin-like growth factor-I receptor signaling in *vitro* and inhibits insulin-like growth factor-I receptor dependent tumor growth in *vivo*. *Mol Cancer Ther*. (2007) 6:2158–67. doi: 10.1158/1535-7163.Mct-07-0070

217. Lima GA, Corrêa LL, Gabrich R, Miranda LC, Gadelha MR. IGF-I, insulin and prostate cancer. *Arquivos brasileiros endocrinologia e metabologia*. (2009) 53:969–75. doi: 10.1590/s0004-27302009000800010

218. Sciarra A, Panebianco V, Ciccariello M, Salciccia S, Lisi D, Osimani M, et al. Magnetic resonance spectroscopic imaging (1H-MRSI) and dynamic contrast-enhanced magnetic resonance (DCE-MRI): pattern changes from inflammation to prostate cancer. *Cancer Invest*. (2010) 28:424–32. doi: 10.3109/07357900903287048

219. Schally AV, Varga JL. Antagonistic analogs of growth hormone-releasing hormone: new potential antitumor agents. *Trends Endocrinol metabolism: TEM*. (1999) 10:383–91. doi: 10.1016/S1043-2760(99)00209-X

220. Lin SL, Lin CY, Lee W, Teng CF, Shyu WC, Jeng LB. Mini review: molecular interpretation of the IGF/IGF-1R axis in cancer treatment and stem cells-based therapy in regenerative medicine. *Int J Mol Sci*. (2022) 23:11781. doi: 10.3390/ijms231911781

221. McHugh DJ, Chudow J, DeNunzio M, Slovin SF, Danila DC, Morris MJ, et al. A phase I trial of IGF-1R inhibitor cixutumumab and mTOR inhibitor temsirolimus in metastatic castration-resistant prostate cancer. *Clin Genitourin Cancer*. (2020) 18:171–8.e2. doi: 10.1016/j.clgc.2019.10.013

222. Qu X, Wu Z, Dong W, Zhang T, Wang L, Pang Z, et al. Update of IGF-1 receptor inhibitor (ganitumab, dalotuzumab, cixutumumab, teprotumumab and figitumumab) effects on cancer therapy. *Oncotarget*. (2017) 8:29501–18. doi: 10.18632/oncotarget.15704

223. Dean JP, Sprenger CC, Wan J, Haugk K, Ellis WJ, Lin DW, et al. Response of the insulin-like growth factor (IGF) system to IGF-IR inhibition and androgen deprivation in a neoadjuvant prostate cancer trial: effects of obesity and androgen deprivation. *J Clin Endocrinol Metab*. (2013) 98:E820–8. doi: 10.1210/jc.2012-3856

224. de Bono JS, Piulats JM, Pandha HS, Petrylak DP, Saad F, Aparicio LM, et al. Phase II randomized study of figitumumab plus docetaxel and docetaxel alone with crossover for metastatic castration-resistant prostate cancer. *Clin Cancer research: an Off J Am Assoc Cancer Res*. (2014) 20:1925–34. doi: 10.1158/1078-0432.CCR-13-1869

225. Molife LR, Fong PC, Paccagnella L, Reid AH, Shaw HM, Vidal L, et al. The insulin-like growth factor-I receptor inhibitor figitumumab (CP-751,871) in combination with docetaxel in patients with advanced solid tumours: results of a phase Ib dose-escalation, open-label study. *Br J Cancer*. (2010) 103:332–9. doi: 10.1038/sj.bjc.6605767

226. Wong RL, Duong MT, Tangen CM, Agarwal N, Cheng HH, Vogelzang NJ, et al. Survival outcomes and risk group validation from SWOG S0925: a randomized phase II study of cixutumumab in new metastatic hormone-sensitive prostate cancer. *Prostate Cancer prostatic Dis*. (2020) 23:486–93. doi: 10.1038/s41391-020-0210-x

227. Yu EY, Li H, Higano CS, Agarwal N, Pal SK, Alva A, et al. SWOG S0925: A randomized phase II study of androgen deprivation combined with cixutumumab versus androgen deprivation alone in patients with new metastatic hormone-sensitive prostate cancer. *J Clin Oncol*. (2015) 33:1601–8. doi: 10.1200/JCO.2014.59.4127

228. Hussain M, Rathkopf D, Liu G, Armstrong A, Kelly WK, Ferrari A, et al. A randomised non-comparative phase II trial of cixutumumab (IMC-A12) or ramucirumab (IMC-1121B) plus mitoxantrone and prednisone in men with metastatic docetaxel-pretreated castration-resistant prostate cancer. *Eur J Cancer*. (2015) 51:1714–24. doi: 10.1016/j.ejca.2015.05.019

229. Wu JD, Haugk K, Coleman I, Woodke L, Vessella R, Nelson P, et al. Combined in vivo effect of A12, a type 1 insulin-like growth factor receptor antibody, and docetaxel against prostate cancer tumors. *Clin Cancer research: an Off J Am Assoc Cancer Res*. (2006) 12:6153–60. doi: 10.1158/1078-0432.CCR-06-0443

230. Hewish M, Chau I, Cunningham D. Insulin-like growth factor 1 receptor targeted therapeutics: novel compounds and novel treatment strategies for cancer medicine. *Recent patents anti-cancer Drug Discovery*. (2009) 4:54–72. doi: 10.2174/157489209787002515

231. de Bono J, Lin CC, Chen LT, Corral J, Michalarea V, Rihawi K, et al. Two first-in-human studies of xentuzumab, a humanised insulin-like growth factor (IGF)-neutralising antibody, in patients with advanced solid tumours. *Br J Cancer*. (2020) 122:1324–32. doi: 10.1038/s41416-020-0774-1

232. Macaulay VM, Lord S, Hussain S, Maroto JP, Jones RH, Climent MA, et al. A Phase Ib/II study of IGF-neutralising antibody xentuzumab with enzalutamide in metastatic castration-resistant prostate cancer. *Br J Cancer*. (2023) 129:965–73. doi: 10.1038/s41416-023-02380-1

233. Weyer-Czernilofsky U, Hofmann MH, Friedbichler K, Baumgartinger R, Adam PJ, Solca F, et al. Antitumor activity of the IGF-1/IGF-2-neutralizing antibody xentuzumab (BI 836845) in combination with enzalutamide in prostate cancer models. *Mol Cancer Ther*. (2020) 19:1059–69. doi: 10.1158/1535-7163.MCT-19-0378

234. Aleksic T, Gray N, Wu X, Rieunier G, Osher E, Mills J, et al. Nuclear IGF1R interacts with regulatory regions of chromatin to promote RNA polymerase II recruitment and gene expression associated with advanced tumor stage. *Cancer Res*. (2018) 78:3497–509. doi: 10.1158/0008-5472.CAN-17-3498

235. Zhong H, Fazenbaker C, Breen S, Chen C, Huang J, Morehouse C, et al. MEDI-573, alone or in combination with mammalian target of rapamycin inhibitors, targets the insulin-like growth factor pathway in sarcomas. *Mol Cancer Ther*. (2014) 13:2662–73. doi: 10.1158/1535-7163.MCT-14-0144

236. Lyles RDZ, Martinez MJ, Sherman B, Schurer S, Burnstein KL. Automation, live-cell imaging, and endpoint cell viability for prostate cancer drug screens. *PloS One*. (2023) 18:e0287126. doi: 10.1371/journal.pone.0287126

237. Li W, Wang Z, Wang L, He X, Wang G, Liu H, et al. Effectiveness of inhibitor rapamycin, saracatinib, linsitinib and JNJ-38877605 against human prostate cancer cells. *Int J Clin Exp Med*. (2015) 8:6563–7.

238. Kubat Oktem E, Demir U, Yazar M, Arga KY. Three candidate anticancer drugs were repositioned by integrative analysis of the transcriptomes of species with different regenerative abilities after injury. *Comput Biol Chem*. (2023) 106:107934. doi: 10.1016/j.compbiolchem.2023.107934

239. Franks SE, Jones RA, Briah R, Murray P, Moorehead RA. BMS-754807 is cytotoxic to non-small cell lung cancer cells and enhances the effects of platinum chemotherapeutics in the human lung cancer cell line A549. *BMC Res Notes*. (2016) 9:134. doi: 10.1186/s13104-016-1919-4

frontiers | Frontiers in Endocrinology

TYPE Original Research
PUBLISHED 05 June 2024
DOI 10.3389/fendo.2024.1348310

OPEN ACCESS

EDITED BY
Vittoria Rago,
University of Calabria, Italy

REVIEWED BY
Mohammeed Aufy,
University of Vienna, Austria
Yong Zhang,
The Second Affiliated Hospital of Xi'an Jiaotong University, China

*CORRESPONDENCE
Honglan Zhou
hlzhou@jlu.edu.cn
Song Wang
w_s@jlu.edu.cn

RECEIVED 05 December 2023
ACCEPTED 20 May 2024
PUBLISHED 05 June 2024

CITATION
Cao H, Liu B, Gong K, Wu H, Wang Y, Zhang H, Shi C, Wang P, Du H, Zhou H and Wang S (2024) Association between cathepsins and benign prostate diseases: a bidirectional two-sample Mendelian randomization study.
Front. Endocrinol. 15:1348310.
doi: 10.3389/fendo.2024.1348310

Association between cathepsins and benign prostate diseases: a bidirectional two-sample Mendelian randomization study

Hongliang Cao[1], Bin Liu[1], Kejian Gong[2], Hao Wu[1], Yishu Wang[3], Haiyang Zhang[4], Chengdong Shi[1], Pengyu Wang[1], Hao Du[1], Honglan Zhou[1*] and Song Wang[1*]

[1]Department of Urology II, The First Hospital of Jilin University, Changchun, China, [2]Department of Thoracic Surgery, The First Hospital of Jilin University, Changchun, China, [3]Key Laboratory of Pathobiology, Ministry of Education, Jilin University, Changchun, China, [4]Department of Prosthodontics, Hospital of Stomatology, Jilin University, Changchun, China

Objectives: The relationship between cathepsins and prostate cancer (PCa) has been reported. However, there is a lack of research on cathepsins and benign prostate diseases (BPDs). This study investigated the potential genetic link between cathepsins and BPDs through the utilization of Mendelian randomization (MR) analysis to determine if a causal relationship exists.

Methods: Publicly accessible summary statistics on BPDs were obtained from FinnGen Biobank. The data comprised 149,363 individuals, with 30,066 cases and 119,297 controls for BPH, and 123,057 individuals, with 3,760 cases and 119,297 controls for prostatitis. The IEU OpenGWAS provided the Genome-wide association data on ten cathepsins. To evaluate the causal relationship between BPDs and cathepsins, five distinct MR analyses were employed, with the primary method being the inverse variance weighted (IVW) approach. Additionally, sensitivity analyses were conducted to examine the horizontal pleiotropy and heterogeneity of the findings.

Results: The examination of IVW MR findings showed that cathepsin O had a beneficial effect on BPH (IVW OR=0.94, 95% CI 0.89–0.98, P=0.0055), while cathepsin X posed a threat to prostatitis (IVW OR=1.08, 95% CI 1.00–1.16, P=0.047). Through reverse MR analysis, it was revealed that prostatitis had an adverse impact on cathepsin V (IVW OR=0.89, 95% CI 0.80–0.99, P=0.035), while no favorable association was observed between BPH and cathepsins. The results obtained from MR-Egger, weighted median, simple mode, and weighted mode methods were consistent with the findings of the IVW approach. Based on sensitivity analyses, heterogeneity, and horizontal pleiotropy are unlikely to distort the results.

Conclusion: This study offers the initial evidence of a genetic causal link between cathepsins and BPDs. Our findings revealed that cathepsin O was beneficial in preventing BPH, whereas cathepsin X posed a potential threat to prostatitis. Additionally, prostatitis negatively affected cathepsin V level. These three cathepsins could be targets of diagnosis and treatment for BPDs, which need further research.

KEYWORDS

cathepsins, benign prostate diseases, Mendelian randomization, bi-directional causal effects, benign prostatic hyperplasia (BPH)

Introduction

Benign prostatic diseases (BPDs), mainly including benign prostatic hyperplasia (BPH) and prostatitis, are prevalent urological ailments affecting males globally (1, 2). Compression of the urethra caused by BPH results in clinical symptoms that impact the quality of life for individuals with BPH, including lower urinary tract symptoms (LUTS), episodes of acute urinary retention, and recurring urinary infections (3). Numerous investigations have been carried out regarding the development of BPH; nevertheless, the factors responsible for its occurrence and advancement are still poorly understood (4). Prostatitis is classified into types I–IV by the National Institutes of Health (NIH) in the United States. Chronic prostatitis/chronic pelvic pain syndrome (CP/CPPS) of Type III is categorized into inflammatory CPPS (IIIa) and noninflammatory CPPS (IIIb), making up approximately 90%–95% of cases related to prostatitis (5). Individuals diagnosed with CP/CPPS typically encounter discomfort in the pelvic region, such as pain in the pubic region or perineum, discomfort during sexual activity or ejaculation, painful urination, frequent urination at night and/or a sense of urgency, sexual difficulties, impotence, mental health disorders, and reduced sperm quality (6, 7). Exploring the etiology, diagnosis, and treatment of BPDs in public health has significant practical implications by identifying the causal association of risk factors that can be modified.

The group of lysosomal proteolytic enzymes known as cathepsins plays a crucial role in preserving cellular homeostasis, which are classified into multiple families, including serine proteases (cathepsins A and G), cysteine proteases (cathepsins B, C, F, H, K, L, O, S, V, W, and X), and aspartyl proteases (cathepsins D and E) (8, 9). They are associated with many cellular activities including protein and lipid metabolism, autophagy, antigen presentation, growth factor receptor recycling, cellular stress signaling, extracellular matrix degradation, and lysosome-mediated cell death (10). Various cathepsins have significant roles in various diseases due to their participation in these essential processes (11). The association between cathepsins and prostate cancer (PCa) has been reported, such as cathepsin B. Nalle et al. found that the inhibition of invasion and migration and the activation of apoptosis in PC3 and DU145 prostate cancer cell lines can be achieved by targeting cathepsin B (12). Moreover, the rise in serum levels of cathepsin B and the density of cathepsin B may serve as innovative indicators for the progression of the disease. However, they do not impact the survival of individuals diagnosed with PCa (13). Furthermore, the generation of sphingosine 1-phosphate through acid ceramidase facilitates the invasion of PCa by increasing the expression of cathepsin B (14). Despite several studies suggesting potential applications of cathepsins in PCa disease, there is a lack of studies exploring cathepsins in relation to BPDs. Based on this, we will use Mendelian randomization (MR) to do such a thing.

MR designs utilize genetic diversity as instrumental variables (IVs) to explore the causal association between potential factors and the specific disease, offering several advantages absent in conventional epidemiology (15). In addition, using MR designs can decrease the likelihood of reverse causality and minimize the impact of confounding variables (16). The objective of this study was to examine the causal connection between cathepsins and BPDs, potentially identifying novel avenues for diagnosing and treating BPDs.

Materials and methods

Study design

To establish the bidirectional causal connection between BPDs and cathepsins, a Mendelian randomization (MR) study using two samples was conducted. To investigate the causal relationship between exposure and outcome, the research on MR utilizes instrumental variables (IVs) and examines Single Nucleotide Polymorphisms (SNPs). To acquire valid IVs, three essential assumptions must be met: i) relevance assumption: the IVs must be strongly linked to the exposure (cathepsins); ii) independence assumption: the IVs should not be correlated with any confounding factors; and iii) exclusion assumption: the IVs must solely impact the outcome (BPDs) through the exposure (cathepsins) (17, 18). Figure 1 shows the planned layout of bidirectional two-sample MR between cathepsins and BPDs.

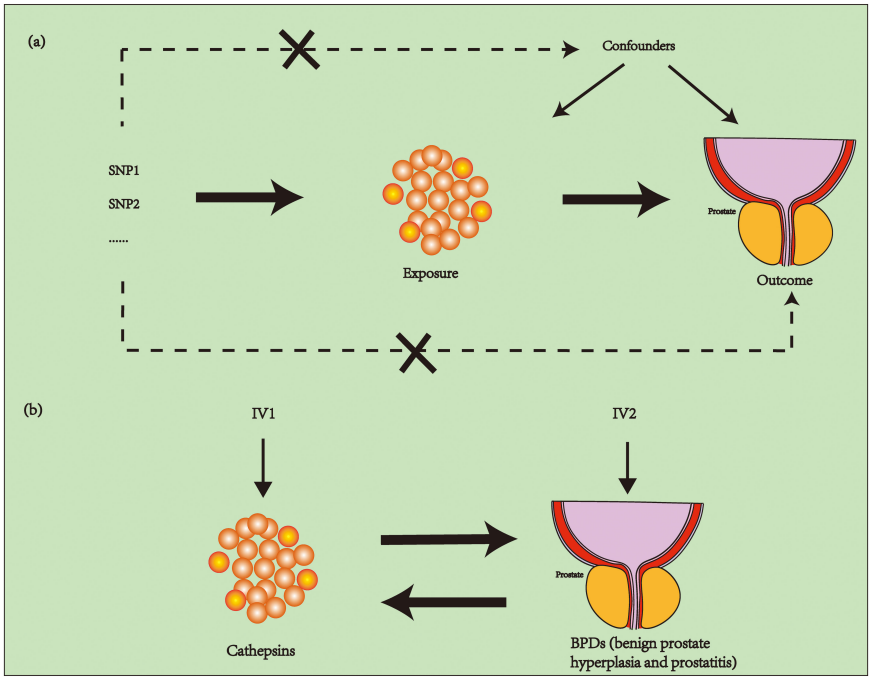

FIGURE 1
The schematic of an MR study involving cathepsins and BPDs (BPH and prostatitis) using two samples. **(A)** In order for the MR study to be valid, three essential assumptions must be met: i) relevance assumption: the IVs must be linked to the exposure; ii) independence assumption: the IVs should not be correlated with any confounding factors; and iii) exclusion assumption: the IVs must solely impact the outcome through the exposure. **(B)** We explore the bidirectional two-sample MR between cathepsins and BPDs. MR, Mendelian randomization; BPDs, benign prostatic diseases; BPH, benign prostatic hyperplasia; IVs, instrumental variables.

GWAS statistics source

Summary statistics on BPDs obtained from FinnGen Biobank (website: https://www.finngen.fi/en) were utilized. The dataset included 149,363 (30,066 cases and 119,297 controls) and 123,057 (3,760 cases and 119,297 controls) separately for BPH and prostatitis. BPH cases are defined in the database based on the N40 criteria in the International Classification of Diseases 10 (ICD-10) Revision codes, as well as the codes 600 in ICD-8 and ICD-9. Prostatitis is a condition that causes inflammation in the prostate gland, which can be caused by infection or non-infectious factors. The objective of FinnGen Biobank, a collaboration between the public and private sectors, is to gather and examine genetic and medical information from 500,000 individuals involved in the Finnish biobank (19). The IEU OpenGWAS (https://gwas.mrcieu.ac.uk) provided the ten Genome-wide association studies (GWAS) of cathepsins (20, 21). The details of GWAS included in MR analyses are described in Table 1.

Selection of genetic instrumental variables

In order to obtain effective IVs, we selected SNPs that were highly correlated with exposure. A conventional threshold was considered, with significant genome-wide importance ($P<5\times 10^{-8}$), linkage disequilibrium (LD), and an r^2 less than 0.001 within a 10,000 kb range. Consequently, the number of SNPs is insufficient to perform MR, thus the following criteria were adopted. We identified SNPs that showed genome-wide significance ($P<5\times10^{-6}$, and $P<5\times10^{-8}$ for BPH in reverse MR), LD, and an $r^2<0.001$ threshold within a 10,000 kb range. We removed palindromic variants for incompatible alleles. The F-statistics were calculated utilizing the following equation:

$$F = \frac{R^2(N-1-K)}{(1-R^2)K}$$

R^2 represents the proportion of variance in exposure that can be accounted for by the IVs, N is the sample size, and K is the number of IVs. SNPs were considered for inclusion if the F-statistic was more significant than or equal to 10, indicating a strong potential to predict exposure (22). The Steiger test posits that the correlation between SNPS and exposure should be greater than the outcome, otherwise reverse causality will occur, and SNPS that fail the test may be unrelated to exposure and excluded (23). MR-PRESSO is capable of detecting horizontal pleiotropy and correcting it by removing outliers. Furthermore, it is able to test the significance of causal inference both before and after the aforementioned correction (24). The chosen SNPs were the final instrumental variables (IVs) for the following MR study.

MR analyses and sensitivity analyses

For MR analyses, five MR methods were employed, namely MR Egger, weighted median, inverse-variance weighted (IVW), simple

TABLE 1 Details of GWAS included in MR analyses.

Trait	IEU GWAS ID	Consortium	Ethnicity	Sample size
BPH	–	FinnGen Biobank	European	149363
Prostatitis	–	FinnGen Biobank	European	123057
Cathepsin S	prot-a-727	NA	European	3301
Cathepsin F	prot-a-722	NA	European	3301
Cathepsin G	prot-a-723	NA	European	3301
Cathepsin H	prot-a-725	NA	European	3301
Cathepsin B	prot-a-718	NA	European	3301
Cathepsin O	prot-a-726	NA	European	3301
Cathepsin E	prot-a-720	NA	European	3301
Cathepsin X	prot-a-729	NA	European	3301
Cathepsin V	prot-a-728	NA	European	3301
Cathepsin D	prot-b-51	NA	European	3394

BPH, benign prostate hyperplasia. NA, Not acquired. "-" indicates not applicable.

mode, and weighted mode. The IVW estimates were selected as the primary method, and four additional methods were used to improve their robustness in a broader range of scenarios (25). Cochran's Q test of IVW and MR Egger (26) also identified heterogeneity. Additionally, the Pleiotropy Residual Sum and Outlier methods (MR-PRESSO) were employed to evaluate and rectify horizontal pleiotropy (24). Moreover, a Leave-one-out analysis was conducted to assess if a solitary SNP influenced or skewed the MR estimate. A funnel plot was employed to assess the likely directional pleiotropy. A statistical significance was determined when the significance level was below 0.05. Figure 2 displays the described workflow of MR and sensitivity analyses. The statistical analyses were conducted in R software 4.3.1 using the TwoSampleMR R package (version 0.5.7) and MR-PRESSO (version 1.0).

Results

Table 2 displays the results of bidirectional two-sample MR between cathepsins and BPDs, and we found three statistically significant positive results. By utilizing the 12 SNPs associated with cathepsin O, we discovered that elevated levels of cathepsin O can decrease the risk of BPH (OR=0.94, 95%CI=0.89–0.98, p-value=0.00553) through the implementation of IVW techniques (Table 2; Supplementary Table 1; Supplementary Figure 1). Moreover, the absence of significant heterogeneity (P-value > 0.05) was confirmed by the MR-Egger and IVW heterogeneity tests. The absence of any impact was shown when using P-values obtained from MR-Pleiotropy Residual Sum and Outlier methods (MR-PRESSO) to evaluate horizontal pleiotropy (Table 3; Supplementary Table 2). In the Leave-one-out sensitivity analysis (Supplementary Figure 2A), there was no individual SNP that significantly undermined the overall impact of cathepsin O on BPH. The symmetrical funnel plot also suggests the absence of pleiotropy (Supplementary Figure 2B). Furthermore, by employing 12SNPs, we discovered a correlation between elevated cathepsin X levels and heightened susceptibility to prostatitis (OR=1.08, 95% CI=1.00–1.16, p-value=0.0477) through the implementation of IVW techniques (Table 2; Supplementary Table 3; Supplementary Figure 3). Comparable to the findings mentioned above, there was an absence of heterogeneity or horizontal pleiotropy in the outcomes (P-value > 0.05) (Table 3; Supplementary Table 4; Supplementary Figure 4).

In reverse MR, we found an association between genetically predicted prostatitis and cathepsin V levels by utilizing 15 prostatitis-related SNPs (Supplementary Table 5). Using IVW methods (Supplementary Figure 5), there is a decrease in the expression of cathepsin V in prostatitis cases (OR=0.89, 95% CI=0.80–0.99, p-value=0.0349). Similar to the analysis mentioned earlier, no signs of pleiotropy and heterogeneity were detected in the findings (P-value > 0.05) (Table 3; Supplementary Table 6; Supplementary Figure 6).

Discussion

This study used MR to examine the reciprocal causal connections between cathepsins and BPDs. The results indicate that cathepsin O protected BPH, cathepsin X posed a risk for prostatitis, and prostatitis had a negative impact on cathepsin V. The findings provide valuable insights into the role of cathepsins in developing BPDs, potentially influencing the development of diagnostic and therapeutic strategies for cathepsins in patients with BPDs.

Previous research has indicated an association between cathepsins and PCa, which shows the possibility of clinical application value. Incorporating 474 males who had a prostate-specific antigen (PSA) concentration ranging from 2.0 to 10 ng/mL, a negative digital rectal examination, and an enlarged prostate

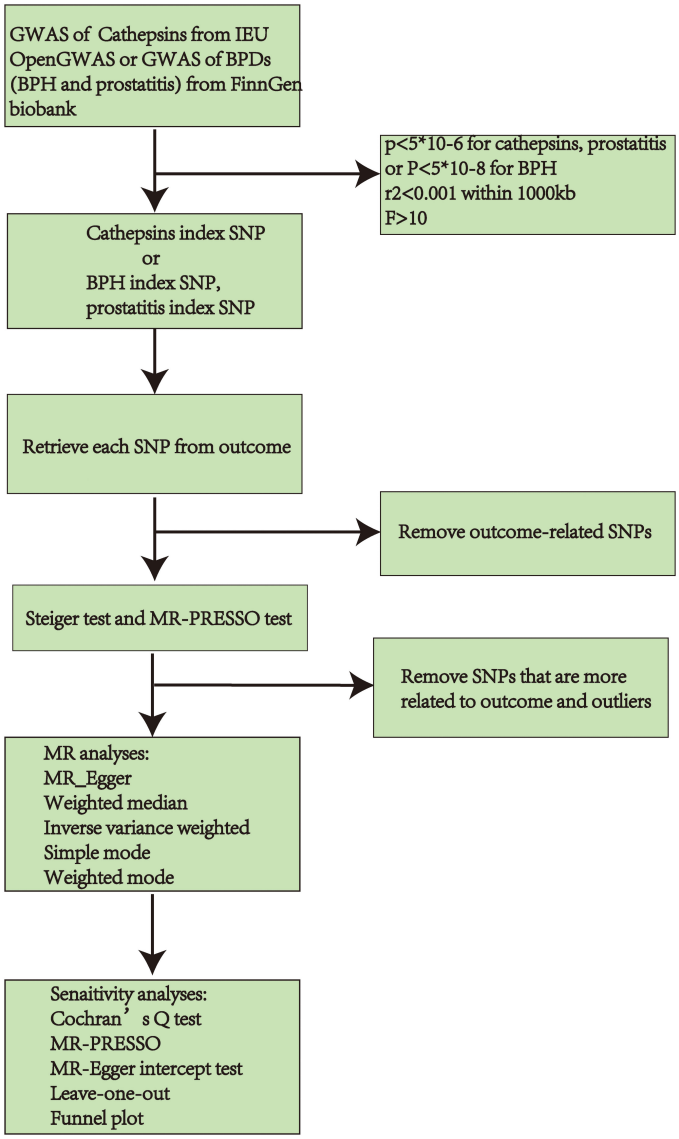

FIGURE 2
Workflow chart of MR discovering causality between cathepsins and BPDs (BPH and prostatitis). GWAS, Genome-Wide Association Study; BPDs, benign prostate diseases; BPH, benign prostate hyperplasia; SNP, Single Nucleotide Polymorphisms; MR, Mendelian randomization.

(volume of at least 35 mL), a retrospective study revealed that combining thrombospondin 1, cathepsin D with %fPSA in a model could enhance the diagnosis of PCa and potentially decrease the need for unnecessary prostate biopsies. This model demonstrated improved specificity for PCa compared to using %fPSA alone (27). In PCa patients, a different protein expression test showed elevated levels of cathepsin S secreted by macrophages, indicating the progression of PCa. Another research by Jennica found that cathepsin H could regulate the migration of PCa cells (PC3) (28). Moreover, cathepsin E amplifies the effectiveness of doxorubicin against PCa cells in humans, which exhibit resistance to apoptosis induced by TRAIL. The up-regulation of cathepsin B promotes the invasion of PCa by producing sphingosine 1-phosphate by acid ceramidase (29). PCa is linked to the heightened presence of cathepsin B in plasma membrane/endosomal fractions, whereas BPH or normal prostate are not (30). Despite several studies suggesting potential applications of cathepsins in PCa disease, more studies need to explore cathepsins for BPDs. Importantly, this study is the initial MR to explore the correlation between cathepsins and BPDs, which warrants additional experimental and clinical investigation for validation.

There are multiple advantages to the current research. Initially, it was the primary study to investigate the impact of cathepsins on BPDs by utilizing extensive GWAS data from Finngen Biobank and the IEU OpenGWAS. Furthermore, since the chosen IVs were situated on a distinct chromosome, it is plausible that any potential gene-gene interaction would have minimal impact on the projected outcome. Furthermore, we employed various reliable

10.3389/fendo.2024.1348310

TABLE 2 Results of bidirectional two-sample MR between cathepsins and BPDs.

	MR			Reverse MR		
Cathepsin	SNPs	Inverse variance weighted		SNPs	Inverse variance weighted	
		OR (95%CI)	p_value		OR (95%CI)	p_value
Cathepsin S						
BPH	20	1.00 (0.97–1.03)	0.983	35	0.92 (0.82–1.04)	0.174
Prostatitis	20	0.99 (0.92–1.06)	0.773	15	0.94 (0.84–1.05)	0.281
Cathepsin F						
BPH	11	1.00 (0.97–1.04)	0.829	35	0.96 (0.86–1.09)	0.539
Prostatitis	11	0.99 (0.91–1.08)	0.815	15	1.00 (0.89–1.12)	0.937
Cathepsin G						
BPH	9	1.01 (0.94–1.08)	0.881	35	1.02 (0.91–1.15)	0.719
Prostatitis	9	1.09 (0.93–1.28)	0.295	15	1.01 (0.91–1.12)	0.879
Cathepsin H						
BPH	7	1.00 (0.97–1.02)	0.826	35	1.02 (0.91–1.15)	0.725
Prostatitis	7	1.03 (0.97–1.09)	0.315	15	0.94 (0.85–1.04)	0.217
Cathepsin B						
BPH	17	1.02 (0.99–1.06)	0.238	35	0.98 (0.86–1.11)	0.713
Prostatitis	17	1.03 (0.95–1.12)	0.433	15	0.98 (0.88–1.08)	0.661
Cathepsin O						
BPH	12	0.94 (0.89–0.98)	0.00553	35	1.01 (0.90–1.14)	0.840
Prostatitis	12	1.05 (0.94–1.17)	0.405	15	0.93 (0.82–1.06)	0.278
Cathepsin E						
BPH	8	0.98 (0.93–1.05)	0.608	35	1.07 (0.93–1.24)	0.345
Prostatitis	8	0.99 (0.89–1.11)	0.895	15	1.04 (0.94–1.15)	0.488
Cathepsin X						
BPH	12	1.00 (0.96–1.03)	0.773	35	0.97 (0.86–1.10)	0.641
Prostatitis	12	1.08 (1.00–1.16)	0.0477	15	0.92 (0.83–1.03)	0.158
Cathepsin V						
BPH	7	0.94 (0.87–1.02)	0.160	35	0.97 (0.86–1.09)	0.615
Prostatitis	7	0.92 (0.75–1.13)	0.449	15	0.89 (0.80–0.99)	0.0349
Cathepsin D						
BPH	7	1.01 (0.97–1.06)	0.574	27	0.96 (0.83–1.12)	0.635
Prostatitis	7	0.97 (0.87–1.07)	0.526	7	1.03 (0.83–1.28)	0.755

The red font represents statistically significant positive results. MR, Mendelian randomization; BPDs, benign prostatic diseases; BPH, benign prostatic hyperplasia.

TABLE 3 Sensitivity analyses of MR analyses with a positive outcome.

Exposure	Outcome	P-value from Cochran's Q test (IVW)	P-value from Cochran's Q test (MR egger)	P value of pleiotropy test	P value of MR-PRESSO
Cathepsin O	BPH	0.535	0.452	0.785	0.579
Cathepsin X	Prostatitis	0.456	0.626	0.124	0.431
Prostatitis	Cathepsin V	0.290	0.238	0.707	0.335

techniques to acquire the MR effects, including MR-PRESSO and the Steiger test. Additionally, we assessed the existence of horizontal pleiotropy. By employing the two-step MR analysis, we successfully pinpointed the association between cathepsins and BPDs.

There are certain constraints in the current investigation. Initially, while three cathepsins were found to be associated with BPDs in our study, the effect was marginal and, probably, of limited clinical relevance. At present, there is a paucity of studies investigating the mechanism between cathepsins and BPDs. Previous studies have demonstrated that cathepsins are involved in all aspects of cellular activity and are strongly linked to the development of various diseases. Further research may yet reveal cathepsins to be a new diagnostic and therapeutic target for BPDs. Nevertheless, this hypothesis requires further experimental verification. Furthermore, the GWAS data may give rise to potential nonlinear relationships or stratification effects. Additionally, the findings might have restricted applicability to individuals of non-European origin because only participants with European heritage were included exclusively. This implies that the causal relationship postulated in this paper is applicable solely to European populations. The emergence of future GWAS data from other ethnic groups will be useful to further explore this causal inference. A comprehensive assessment of mixed populations will be more useful to explore the causal relationship between Cathepsins and BPDs at the genetic level. Lastly, given the complexity of genetic and environmental factors influencing BPDs and levels of cathepsins, we did not include possible confounding factors in our analysis. It is very difficult to identify confounding factors that affect both, and future studies should further identify confounding factors that can affect both to further improve the accuracy of results.

Conclusion

To summarize, our findings indicate that cathepsin O played a beneficial role in BPH, cathepsin X posed a potential risk for prostatitis, and prostatitis had an adverse impact on the expression of cathepsin V. These cathepsins may become new targets for future BPDs diagnosis and treatment, but further validation is needed.

Data availability statement

The original contributions presented in the study are included in the article/Supplementary Material. Further inquiries can be directed to the corresponding authors.

Author contributions

HC: Writing – original draft, Supervision, Software, Formal analysis, Conceptualization. BL: Writing – review & editing, Software, Formal analysis, Data curation. KG: Writing – original draft, Software, Formal analysis, Data curation. HW: Writing – review & editing, Software, Formal analysis, Data curation. YW: Writing – review & editing, Software, Data curation. HZ: Writing – original draft, Software, Data curation. CS: Writing – original draft, Supervision. PW: Writing – review & editing, Supervision. HD: Writing – review & editing, Supervision. HZ: Writing – original draft, Investigation, Conceptualization. SW: Writing – review & editing, Investigation, Conceptualization.

Funding

The author(s) declare financial support was received for the research, authorship, and/or publication of this article. This research was funded by grants from the Jilin Provincial Department of Finance (No: JLSWSRCZX2020-058), Jilin Provincial Department of Science and Technology (No: 20210401154), WU JIEPING Medical Foundation (No: 320.6750.2020-06-37), WU JIEPING Medical Foundation (No: 320.6750.2020-06-36), and Jilin Provincial Department of Science and Technology (No: 20230204011YY).

Conflict of interest

The authors declare that the research was conducted in the absence of any commercial or financial relationships that could be construed as a potential conflict of interest.

Publisher's note

Supplementary material

The Supplementary Material for this article can be found online at: https://www.frontiersin.org/articles/10.3389/fendo.2024.1348310/full#supplementary-material

References

1. The global, regional, and national burden of benign prostatic hyperplasia in 204 countries and territories from 2000 to 2019: a systematic analysis for the Global Burden of Disease Study 2019. *Lancet Healthy Longev.* (2022) 3:e754–e76.

2. Krieger JN, Lee SW, Jeon J, Cheah PY, Liong ML, Riley DE. Epidemiology of prostatitis. *Int J Antimicrob Agents.* (2008) 31 Suppl 1:S85–90. doi: 10.1016/j.ijantimicag.2007.08.028

3. Kim EH, Larson JA, Andriole GL. Management of benign prostatic hyperplasia. *Annu Rev Med*. (2016) 67:137–51. doi: 10.1146/annurev-med-063014-123902

4. Devlin CM, Simms MS, Maitland NJ. Benign prostatic hyperplasia - what do we know? *BJU Int*. (2021) 127:389–99. doi: 10.1111/bju.15229

5. Krieger JN, Nyberg L Jr., Nickel JC. NIH consensus definition and classification of prostatitis. *Jama*. (1999) 282:236–7. doi: 10.1001/jama.282.3.236

6. Polackwich AS, Shoskes DA. Chronic prostatitis/chronic pelvic pain syndrome: a review of evaluation and therapy. *Prostate Cancer Prostatic Dis*. (2016) 19:132–8. doi: 10.1038/pcan.2016.8

7. Wagenlehner FM, Naber KG, Bschleipfer T, Brähler E, Weidner W. Prostatitis and male pelvic pain syndrome: diagnosis and treatment. *Dtsch Arztebl Int*. (2009) 106:175–83. doi: 10.3238/arztebl.2009.0175

8. Reiser J, Adair B, Reinheckel T. Specialized roles for cysteine cathepsins in health and disease. *J Clin Invest*. (2010) 120:3421–31. doi: 10.1172/JCI42918

9. Patel S, Homaei A, El-Seedi HR, Akhtar N. Cathepsins: Proteases that are vital for survival but can also be fatal. *BioMed Pharmacother*. (2018) 105:526–32. doi: 10.1016/j.biopha.2018.05.148

10. Conus S, Simon HU. Cathepsins: key modulators of cell death and inflammatory responses. *Biochem Pharmacol*. (2008) 76:1374–82. doi: 10.1016/j.bcp.2008.07.041

11. Yadati T, Houben T, Bitorina A, Shiri-Sverdlov R. The ins and outs of cathepsins: physiological function and role in disease management. *Cells*. (2020) 9. doi: 10.3390/cells9071679

12. Nalla AK, Gorantla B, Gondi CS, Lakka SS, Rao JS. Targeting MMP-9, uPAR, and cathepsin B inhibits invasion, migration and activates apoptosis in prostate cancer cells. *Cancer Gene Ther*. (2010) 17:599–613. doi: 10.1038/cgt.2010.16

13. Miyake H, Hara I, Eto H. Serum level of cathepsin B and its density in men with prostate cancer as novel markers of disease progression. *Anticancer Res*. (2004) 24:2573–7.

14. Beckham TH, Lu P, Cheng JC, Zhao D, Turner LS, Zhang X, et al. Acid ceramidase-mediated production of sphingosine 1-phosphate promotes prostate cancer invasion through upregulation of cathepsin B. *Int J Cancer*. (2012) 131:2034–43. doi: 10.1002/ijc.27480

15. Birney E. Mendelian randomization. *Cold Spring Harb Perspect Med*. (2022) 12. doi: 10.1101/cshperspect.a041302

16. Sekula P, Del Greco MF, Pattaro C, Köttgen A. Mendelian randomization as an approach to assess causality using observational data. *J Am Soc Nephrol*. (2016) 27:3253–65. doi: 10.1681/ASN.2016010098

17. Boef AG, Dekkers OM, le Cessie S. Mendelian randomization studies: a review of the approaches used and the quality of reporting. *Int J Epidemiol*. (2015) 44:496–511. doi: 10.1093/ije/dyv071

18. Burgess S, Labrecque JA. Mendelian randomization with a binary exposure variable: interpretation and presentation of causal estimates. *Eur J Epidemiol*. (2018) 33:947–52. doi: 10.1007/s10654-018-0424-6

19. Kurki MI, Karjalainen J, Palta P, Sipilä TP, Kristiansson K, Donner KM, et al. FinnGen provides genetic insights from a well-phenotyped isolated population. *Nature*. (2023) 613:508–18.

20. Sun BB, Maranville JC, Peters JE, Stacey D, Staley JR, Blackshaw J, et al. Genomic atlas of the human plasma proteome. *Nature*. (2018) 558:73–9. doi: 10.1038/s41586-018-0175-2

21. Folkersen L, Fauman E, Sabater-Lleal M, Strawbridge RJ, Frånberg M, Sennblad B, et al. Mapping of 79 loci for 83 plasma protein biomarkers in cardiovascular disease. *PloS Genet*. (2017) 13:e1006706. doi: 10.1371/journal.pgen.1006706

22. Pierce BL, Ahsan H, Vanderweele TJ. Power and instrument strength requirements for Mendelian randomization studies using multiple genetic variants. *Int J Epidemiol*. (2011) 40:740–52. doi: 10.1093/ije/dyq151

23. Hemani G, Tilling K, Davey Smith G. Orienting the causal relationship between imprecisely measured traits using GWAS summary data. *PloS Genet*. (2017) 13:e1007081. doi: 10.1371/journal.pgen.1007081

24. Verbanck M, Chen CY, Neale B, Do R. Detection of widespread horizontal pleiotropy in causal relationships inferred from Mendelian randomization between complex traits and diseases. *Nat Genet*. (2018) 50:693–8. doi: 10.1038/s41588-018-0099-7

25. Burgess S, Scott RA, Timpson NJ, Davey Smith G, Thompson SG. Using published data in Mendelian randomization: a blueprint for efficient identification of causal risk factors. *Eur J Epidemiol*. (2015) 30:543–52. doi: 10.1007/s10654-015-0011-z

26. Burgess S, Butterworth A, Thompson SG. Mendelian randomization analysis with multiple genetic variants using summarized data. *Genet Epidemiol*. (2013) 37:658–65. doi: 10.1002/gepi.21758

27. Steuber T, Tennstedt P, Macagno A, Athanasiou A, Wittig A, Huber R, et al. Thrombospondin 1 and cathepsin D improve prostate cancer diagnosis by avoiding potentially unnecessary prostate biopsies. *BJU Int*. (2019) 123:826–33. doi: 10.1111/bju.14540

28. Jevnikar Z, Rojnik M, Jamnik P, Doljak B, Fonovic UP, Kos J. Cathepsin H mediates the processing of talin and regulates migration of prostate cancer cells. *J Biol Chem*. (2013) 288:2201–9. doi: 10.1074/jbc.M112.436394

29. Yasukochi A, Kawakubo T, Nakamura S, Yamamoto K. Cathepsin E enhances anticancer activity of doxorubicin on human prostate cancer cells showing resistance to TRAIL-mediated apoptosis. *Biol Chem*. (2010) 391:947–58. doi: 10.1515/bc.2010.087

30. Sinha AA, Jamuar MP, Wilson MJ, Rozhin J, Sloane BF. Plasma membrane association of cathepsin B in human prostate cancer: biochemical and immunogold electron microscopic analysis. *Prostate*. (2001) 49:172–84. doi: 10.1002/pros.1132

frontiers | Frontiers in Pharmacology

TYPE Original Research
PUBLISHED 18 June 2024
DOI 10.3389/fphar.2024.1383304

OPEN ACCESS

EDITED BY
Anna Perri,
Magna Græcia University of Catanzaro, Italy

REVIEWED BY
Yupeng Wu,
First Affiliated Hospital of Fujian Medical University, China
Xiaolong Cao,
The State University of New Jersey, United States
Xiaopin Duan,
Southern Medical University, China

*CORRESPONDENCE
Yuan Gao,
yuan_gao@fudan.edu.cn
Zhuo Wang,
wztgyx223@163.com

†These authors have contributed equally to this work

RECEIVED 07 February 2024
ACCEPTED 27 May 2024
PUBLISHED 18 June 2024

CITATION
Kang W, Ye C, Yang Y, Lou Y-R, Zhao M, Wang Z and Gao Y (2024), Identification of anoikis-related gene signatures and construction of the prognosis model in prostate cancer. *Front. Pharmacol.* 15:1383304. doi: 10.3389/fphar.2024.1383304

Identification of anoikis-related gene signatures and construction of the prognosis model in prostate cancer

Wanying Kang[1,2†], Chen Ye[3†], Yunyun Yang[3], Yan-Ru Lou[1], Mingyi Zhao[2], Zhuo Wang[3*] and Yuan Gao[1*]

[1]School of Pharmacy, Fudan University, Shanghai, China, [2]Life Science and Biopharmaceutical College, Shenyang Pharmaceutical University, Shenyang, China, [3]Changhai Hospital, Second Military Medical University, Shanghai, China

Background: One of the primary reasons for tumor invasion and metastasis is anoikis resistance. Biochemical recurrence (BCR) of prostate cancer (PCa) serves as a harbinger of its distant metastasis. However, the role of anoikis in PCa biochemical recurrence has not been fully elucidated.

Methods: Differential expression analysis was used to identify anoikis-related genes based on the TCGA and GeneCards databases. Prognostic models were constructed utilizing LASSO regression, univariate and multivariate Cox regression analyses. Moreover, Gene Expression Omnibus datasets (GSE70770 and GSE46602) were applied as validation cohorts. Gene Ontology, KEGG and GSVA were utilized to explore biological pathways and molecular mechanisms. Further, immune profiles were assessed using CIBERSORT, ssGSEA, and TIDE, while anti-cancer drugs sensitivity was analyzed by GDSC database. In addition, gene expressions in the model were examined using online databases (Human Protein Atlas and Tumor Immune Single-Cell Hub).

Results: 113 differentially expressed anoikis-related genes were found. Four genes (EEF1A2, RET, FOSL1, PCA3) were selected for constructing a prognostic model. Using the findings from the Cox regression analysis, we grouped patients into groups of high and low risk. The high-risk group exhibited a poorer prognosis, with a maximum AUC of 0.897. Moreover, larger percentage of immune infiltration of memory B cells, CD8 Tcells, neutrophils, and M1 macrophages were observed in the high-risk group than those in the low-risk group, whereas the percentage of activated mast cells and dendritic cells in the high-risk group were lower. An increased TIDE score was founded in the high-risk group, suggesting reduced effectiveness of ICI therapy. Additionally, the IC50 results for chemotherapy drugs indicated that the low-risk group was more sensitive to most of the drugs. Finally, the genes EEF1A2, RET, and FOSL1 were expressed in PCa cases based on HPA website. The TISCH database suggested that these four ARGs might contribute to the tumor microenvironment of PCa.

Conclusion: We created a risk model utilizing four ARGs that effectively predicts the risk of BCR in PCa patients. This study lays the groundwork for risk stratification and predicting survival outcomes in PCa patients with BCR.

KEYWORDS

prostate cancer, anoikis-related genes, biochemical recurrence, immune infiltration, prognosis

1 Introduction

Prostate cancer (PCa) is ranked as the most common cancer among men worldwide, representing a considerable percentage of cancer-related deaths in the male demographic (Sung et al., 2021). According to estimations, PCa account for 29% of newly diagnosed male malignancies in the United States in 2023. In China, the occurrence of PCa has been on the rise with the aging population and increased screening rates (He et al., 2022; Siegel et al., 2023). Despite advancements in diagnostic and treatment options, around 30% of PCa patients who have radical prostatectomy developed biochemical recurrence (BCR) within a decade, with two-thirds of these recurrences manifesting within the first 2 years after surgery (Lin et al., 2019). A rise in serum prostate-specific antigen (PSA) levels after radical prostatectomy or radical radiotherapy signals biochemical recurrence. This increase was typically an early indicator of PCa progression, which could lead to PCa specific mortality or distant metastasis (Pound et al., 1999; Dess et al., 2017). For patients with BCR requiring salvage therapy, treatment options were limited (Wang M. et al., 2022). Therefore, identifying reliable prognostic biomarkers and understanding the underlying molecular mechanisms involved in BCR were crucial for better risk stratification and personalized treatment strategies in PCa.

Past studies have shown that some molecular prognostic biomarkers other than anoikis may also predict the risk of BCR of PCa. MiRNA such as miR-320a, miR-125A, and miR-196a were reported to be used for predicting the recurrence of PCa after radical prostatectomy (Pashaei et al., 2017; Zhan et al., 2020; Konoshenko and Laktionov, 2021). Moreover, the expression levels of mRNAs such as SAMD5 (Li et al., 2019) and ZNF154 (Zhang et al., 2018) served as prognostic biomarkers for predicting the risk of BCR in PCa. Furthermore, seven immune-related genes including (PPARGC1A、AKR1C2、COMP、EEF1A2、IRF5、NTM and TPX2) were identified as prognostic markers, showing an association with BCR-free survival in PCa patients (Lv et al., 2021). In addition, Prognostic subtypes established using senescence-associated lncRNAs were also closely associated with BCR-free survival in PCa (Feng et al., 2023). However, these molecular prognostic biomarkers above have not been validated in clinical application. In addition, there were some clinicopathological markers such as the Gleason score, clinical stage and PSA levels which were also applied to predict BCR following local PCa treatment (Cornford et al., 2017; D'Andrea et al., 2018). Nevertheless, various clinical outcomes were observed in these patients with the same biomarker (Li et al., 2019). Therefore, more sensitive BCR-related biomarkers for prediction should be developed.

Anoikis is a distinct type of programmed cell death that occurs when cells detach from the extracellular matrix or neighboring cells (Sattari Fard et al., 2023). This process is primarily initiated through the interplay of intrinsic and extrinsic pathways (Paoli et al., 2013). Anoikis is also a critical mechanism in maintaining tissue homeostasis by eliminating cells that have lost their anchorage, preventing their abnormal accumulation, and preventing metastasis (Taddei et al., 2012). Dysfunctions in anoikis can facilitate tumor invasion and migration, the establishment of metastasis in distant tissues, and the development of drug resistance (Kim et al., 2021). Moreover, tumor cells are able to resist anoikis and survive by utilizing a variety of ways, including EMT (Cao et al., 2016), oxidative stress (Giannoni et al., 2008), and adjusting their integrin levels (Hynes, 1992). Lots of research demonstrates that anoikis is essential in the development of a multiple cancers, like renal cancer (Wang et al., 2022), lung cancer (Jin et al., 2018), and gastric cancer (Ye et al., 2020) as well as PCa (Nepali and Kyprianou, 2023). Prior studies reported that several anoikis-related genes (ARGs) were closely correlated to the metastasis and invasion of PCa (Rennebeck et al., 2005; Lee et al., 2021). For example, FLIP, an inhibitor of anoikis, was found upregulated in a mouse model of PCa metastasis (Mawji et al., 2007). Inhibiting the synthesis of FLIP protein reduces the formation of distant tumors (Mawji et al., 2007). Moreover, focal adhesion complex protein Talin1 was a prognostic biomarker, which promote the migration and invasion of PCa through focal adhesion signaling and resistance to anoikis (Sakamoto et al., 2010). Furthermore, the expression of CENPF gene was upregulated in human PC3 cells, and silencing CENPF increases sensitivity to anoikis-induced apoptosis (Shahid et al., 2018). In addition, AR may suppress cell deaths via anoikis and entosis, potentially leading increased PCa metastasis (Wen et al., 2014). There is still a necessity to identify new genetic markers related to anoikis, which could serve as a foundation for risk stratification in patients with BCR of PCa.

In this study, we tried to explore the association between ARGs and the risk of biochemical recurrence in PCa. For this purpose, we employed differentially expressed ARGs from TCGA and the GeneCards databases, establishing an ARG-based signature to forecast biochemical recurrence outcomes in PCa. Moreover, the predictive capacity of ARGs in assessing patient prognosis using Gene Expression Omnibus (GEO) datasets (GSE70770 and GSE46602) were validated. Furthermore, the molecular and immune characteristics, sensitivity to antineoplastic agents, and the effectiveness of immunotherapy associated with the model in PCa were assessed. Finally, the protein expression of prognostic genes was confirmed based on the Tumor Immune Single-Cell Hub (TISCH) and the Human Protein Atlas (HPA). The workflow of this research was illustrated in Figure 1.

2 Materials and methods

2.1 Data collection

The clinical information and transcriptome matrix, encompassing 497 prostate tumor samples and 52 adjacent-normal samples, were acquired from TCGA database (https://portal.gdc.cancer.g-ov/). The expressed genes (DEGs) were differentially detected using the "limma" R package, employing thresholds of $|\log2FC| > 1.0$ and FDR <0.05. Furthermore, we obtained two external validation cohorts, GSE70770 and GSE46602, from the Gene Expression Omnibus (GEO) datasets available at https://www.ncbi.nlm.nih.gov/geo/. In addition, a sum of 912 genes related to anoikis (ANOIKIS-related genes or ARGs) was procured from the GeneCards database (https://www.

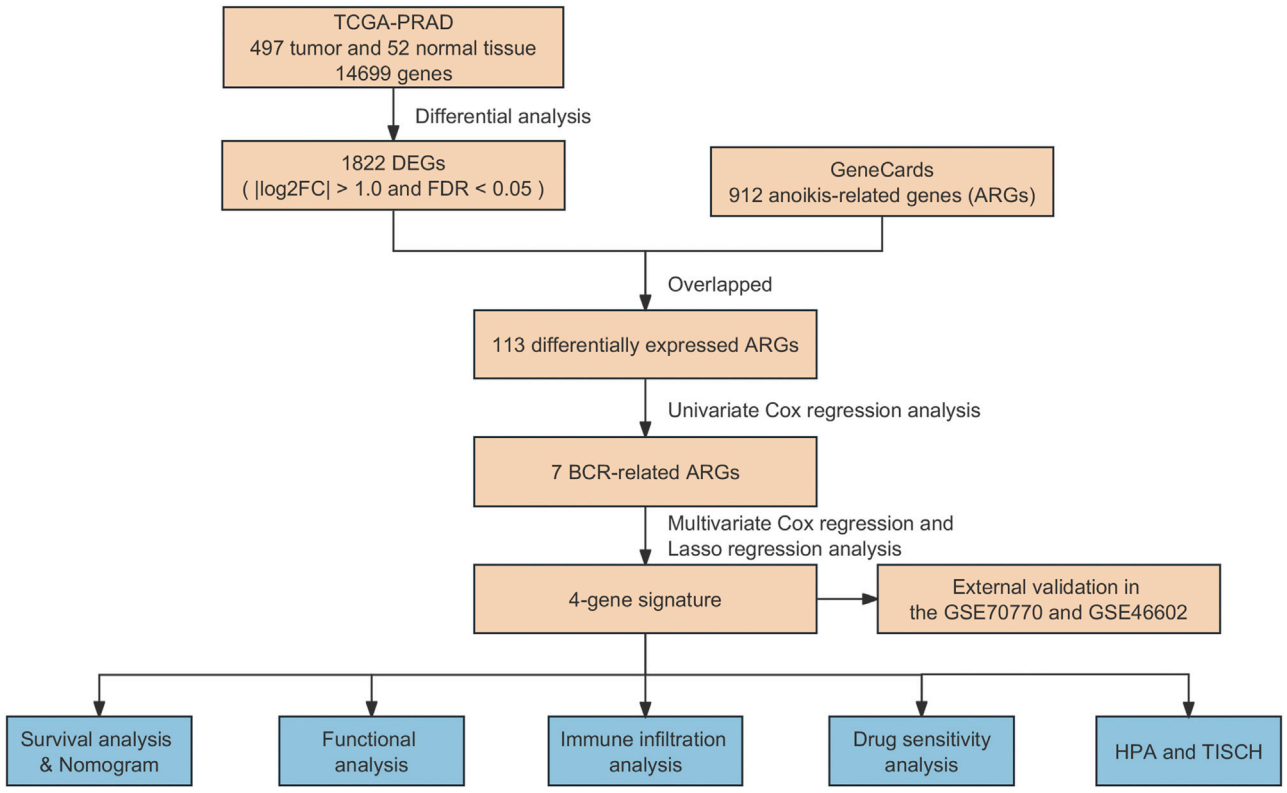

FIGURE 1
Flowchart of data collection and study design.

genecards.org/). The ARGs that were differentially expressed were then retrieved by overlapping with the DEGs.

2.2 Construction of risk score model

In this study, 429 PCa patients were randomly allocated into training and testing sets at a 1:1 ratio, and the training set was employed to develop a risk score model based on ARGs. Univariate Cox analysis, employing the R package "survival", was conducted to identify ARGs significantly associated with BCR of PCa at a significance criterion of $p < 0.05$. Subsequently, to mitigate the risk of overfitting the model, the least absolute shrinkage and selection operator (LASSO) regression algorithm along with 10-fold cross-validation were employed to narrow down the candidate ARGs. Finally, multivariate Cox analysis was performed to select ARGs independently predicting the prognosis of PCa. A risk model was then constructed based on the prognostic ARGs, with the formula: (coefficient × the expression of EEF1A2) + (coefficient × the expression of RET) + (coefficient × the expression of FOSL1) + (coefficient × the expression of PCA3).

Additionally, to stratify all qualified individuals into high- and low-risk groups, the median risk score was used as the threshold. To illustrate the survival discrepancies between individuals in high- and low-risk categories, Kaplan-Meier survival analysis was conducted, utilizing the "survival" and "survminer" packages in R. The model's performance to predict was assessed by conducting the time-dependent receiver operating characteristic (ROC) curve analysis, executed with the "timeROC" package in R. Validation of the model was also carried out in the independent validation set.

2.3 Validation of risk model

To confirm the effectiveness of the prognostic model based on ARGs, the GSE70770 and GSE46602 cohorts were selected as external validation sets. Using the pre-established formula, the risk score of each sample in these two cohorts was calculated. Subsequently, based on the median risk score, all samples from the two datasets were grouped as either low- or high-risk group.

2.4 Construction of ARGs-based nomogram

The clinical and pathological features, encompassing aspects like age, T stage, N stage, and risk score, were compiled and utilized to develop a nomogram model through the use of the "rms" package in R. This model aimed to estimate the possibility of BCR-free survival in PCa patients at 3, 5, and 8 years. Furthermore, univariate and multivariate Cox regression analyses were employed to identify independent prognostic factors from the risk score and various Clinicopathological features.

2.5 Functional enrichment analysis

To analyze the differentially expressed genes (DEGs), "clusterProfiler" R package and the "ggplot2" R package were used to identified the biological processes and signaling pathways based on Gene Ontology (GO), and Kyoto Encyclopedia of Genes and Genomes (KEGG) dataset. Additionally, the "c2.cp.reactome.v7.4.symbols.gmt" was obtained from the MSigDE database, and the reactome pathway-based analysis was carried out using the "GSVA" R package and the "pheatmap" R package.

2.6 Analysis of immune infiltration landscape

The CIBERSORT algorithm utilizes the principle of linear support vector regression to deconvolve the expression matrix of immune cell subtypes to estimate the abundance of immune cells (Newman et al., 2015). To examine the prevalence of diverse immune cell types in the low- and high-risk groups, the CIBERSORT and CIBERSORTx (https://cibersortx.stanford.edu/) were applied to estimate the level and proportion of infiltration of different immune cells. Additionally, a single-sample gene set enrichment analysis (ssGSEA) algorithm was also used to evaluate the differences in immune cell infiltration levels between the different risk groups, utilizing the "GSVA" package in R. The disparities between the low-risk and high-risk groups were visualized using the "ggplot2" package in R. In addition, the correlation between the risk score values with the presence of immune infiltrating cells was also investigated using CIBERSORT method.

2.7 Immunotherapy response and drug sensitivity analysis

The immune evasion potential in PCa patient samples was evaluated using the Tumor Immune Dysfunction and Exclusion (TIDE) algorithm based on data from the TIDE database (http://tide.dfci.harvard.edu/login/). The half maximal inhibitory concentration (IC50) and the expected response of PCa patients to anticancer drugs were calculated with the "oncoPredict" package in R utilizing data from the Genomics of Drug Sensitivity in Cancer (GDSC) database. In addition, the outcomes were visually represented with the "ggplot2" package in the R programming language.

2.8 Validation of prognostic genes

The Tumor Immune Single-Cell Hub (TISCH; http://tisch.comp-genomics.org) was utilized for a comprehensive investigation of the tumor microenvironment (TME) heterogeneity, encompassing a wide range of datasets and cell types. Therefore, we exploited the single-cell RNA sequencing dataset PRAD_GSE141445 (Chen et al., 2021) from the TISCH database for the analysis of the expression of identified ARGs in the TME. To confirm the protein expression of prognostic genes specifically in PCa tissues, immunohistochemistry data were cross-referenced with the Human Protein Atlas (HPA; https://www.proteinatlas.org/).

2.9 Statistical analysis

Continuous variables were evaluated using either the Wilcoxon test or the t-test, depending on their suitability for the data. Spearman correlation analysis was employed for correlational analyses. Kaplan-Meier survival analysis was utilized for the generation of survival curves, and comparisons between these curves were conducted employing the log-rank test. A significance level of $p < 0.05$ was considered suitable for all statistical assessments. All statistical analysis were performed using R software (version 4.3.0).

3 Results

3.1 Identification of differentially expressed ARGs

Gene expression data from both PCa samples and normal tissues in the TCGA-PCa database were subjected to analysis, with 1822 DEGs identified, comprising 1,052 downregulated and 770 upregulated genes (Figure 2A). Subsequently, these DEGs overlapped with the 912 ARGs extracted from GeneCards. Finally, a total of 113 differentially expressed ARGs was applied for further analysis. (Figure 2B).

3.2 Risk model construction based on the ARGs prognostic signatures

To create a predictive signature for the biochemical recurrence status in PCa patients, 429 individuals were randomly divided in equal proportions into a training group (comprising 214 patients) and a testing set (consisting of 215 patients). As shown in Figures 3A–C, univariate Cox regression analysis and LASSO analysis were conducted in the training set, identifying 7 ARGs associated with the BCR rate. Moreover, the multivariate Cox regression analysis found that 4 ARGs independently predictive of PCa prognosis, which were selected to develop a risk prediction model (Supplementary Figure S1A). The risk score was computed utilizing the following formula: (0.261×EEF1A2 expression) + (−0.142×RET expression) + (−0.196×FOSL1 expression) + (−0.184×PCA3 expression). Following this, individuals with PCa were stratified according to the median risk score, and then categorized into high- and low-risk groups. In the training set, analysis of Kaplan-Meier survival curves implied that individuals with elevated risk scores experienced a notably reduced rate of BCR-free survival (Supplementary Figure S1B). The AUC were 0.709, 0.765, and 0.808 for 3-, 5-, and 8-year BCR-free rates, respectively (Supplementary Figure S1C). Risk plots revealed a favorable relation between rising risk scores and the prevalence of BCR in PCa (Supplementary Figure S1D). Furthermore, the expression profiles of the four prognostic ARGs in both the high-risk and low-risk groups were graphically depicted using box plots and a risk heatmap. These findings revealed that individuals with an elevated risk score demonstrated increased expression of EEF1A2. In contrast, PCA3, RET, and FOSL1 showed higher expression levels in the low-risk group, as illustrated in Supplementary Figure S1E. The testing set was then utilized for verification of the predictive accuracy of the risk model. In Figures 3D,E, it is shown that there are significant

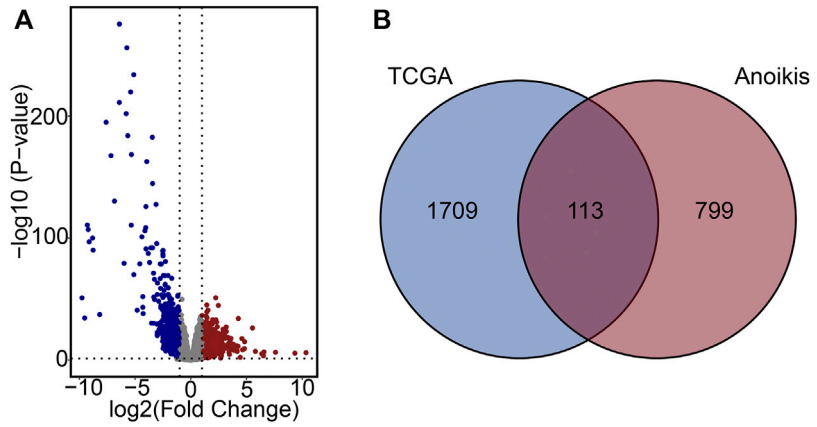

FIGURE 2
Characterization of differentially expressed ARGs. **(A)** Volcano plot of DEGs in PCa. **(B)** Venn diagram of DEGs and ARGs.

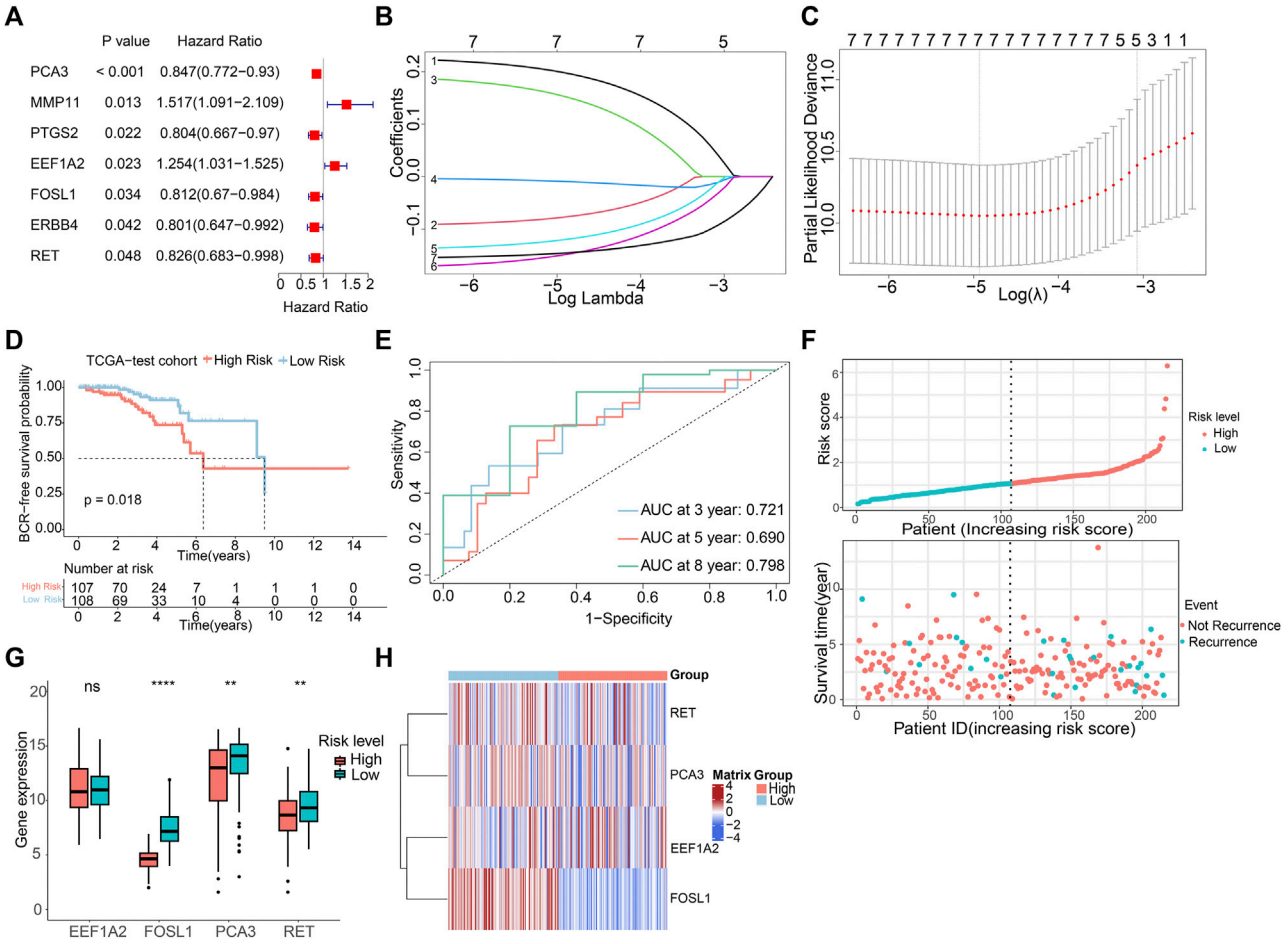

FIGURE 3
Construction of risk model risk model based on the prognostic ARGs in PCa. **(A)** Univariate Cox regression analysis of the ARGs. **(B,C)** LASSO (least absolute shrinkage and selection operator) regression. **(D)** K-M curves of BCR outcome between high- and low-risk score groups in the testing set. **(E)** ROC curves for BCR-free predictive performance at 3-, 5-, and 8-year in the testing set. **(F)** The risk score distribution and BCR status of PCa patients in the testing. **(G,H)** The boxplot and risk heatmap of the prognostic ARGs in the testing set.

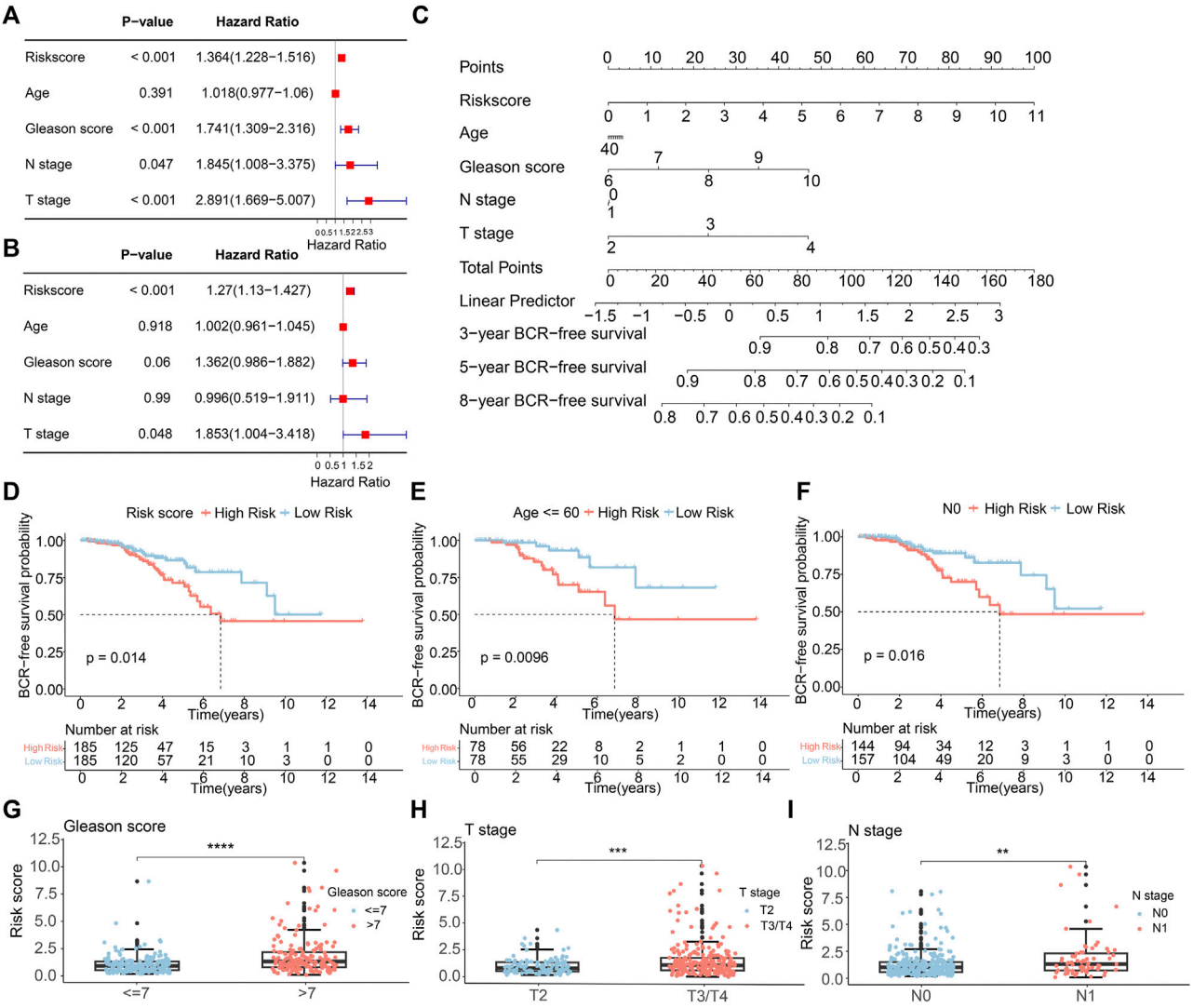

FIGURE 4
The independence of the ARGs prognostic signatures for PCa. **(A)** Univariate Cox analysis and **(B)** multivariate Cox analysis shows the correlation of the BCR-free occurrence and risk score, and clinicopathological factors. **(C)** A nomogram based on the ARGs and clinicopathological factors. **(D)** The K-M survival analysis in the different risk groups of PCa patients in the entire TCGA sets. The BCR-free rate of patients with PCa in the low- and high-risk group among the **(E)** Age≤60; **(F)** N0. The box plots of correlation between risk scores and clinicopathological characteristics, including **(G)** Gleason score; **(H)** T stage; **(I)** N stage.

differences in the BCR-free survival rates among different risk groups in the testing set. The AUC values for the BCR-free survival rates at 3, 5, and 8 years are 0.721, 0.690, and 0.798, respectively, indicating that the risk model based on ARGs has a good predictive performance. Figures 3F–H display the risk distribution plots, gene expression box plots, and risk heatmap of different risk groups in the testing set.

3.3 Independent prognosis analysis of the ARGs prognostic signature

We conducted both multivariate and univariate Cox regression analyses on the comprehensive TCGA-PCa dataset to evaluate the independence of the ARGs prognostic signatures for PCa. The univariate Cox regression analysis unveiled a notable connection between the BCR rate in PCa and factors such as risk score (HR = 1.364, $p < 0.001$), Gleason score (HR = 1.741, $p < 0.001$), N stage (HR = 1.845, $p = 0.047$), and T stage (HR = 2.891, $p < 0.001$) (Figure 4A). The multivariate Cox regression analysis showed that the risk score (HR = 1.27, $p < 0.001$) and T stage (HR = 1.853, $p = 0.048$) were independent prognostic indicators for PCa (Figure 4B). Subsequently, we developed a new nomogram based on clinical pathological features and risk score to predict the 3-, 5-, and 8-year BCR-free survival probabilities of PCa patients (Figure 4C). To explore the prognostic value of the risk score based on ARGs in different clinicopathological factors, we conducted stratified subgroup analyses. As illustrated in Figure 4D, risk stratification of the entire TCGA cohort showed that patients in the high-risk group had notably poorer outcomes. Moreover, PCa patients with different clinical pathological characteristics were divided into

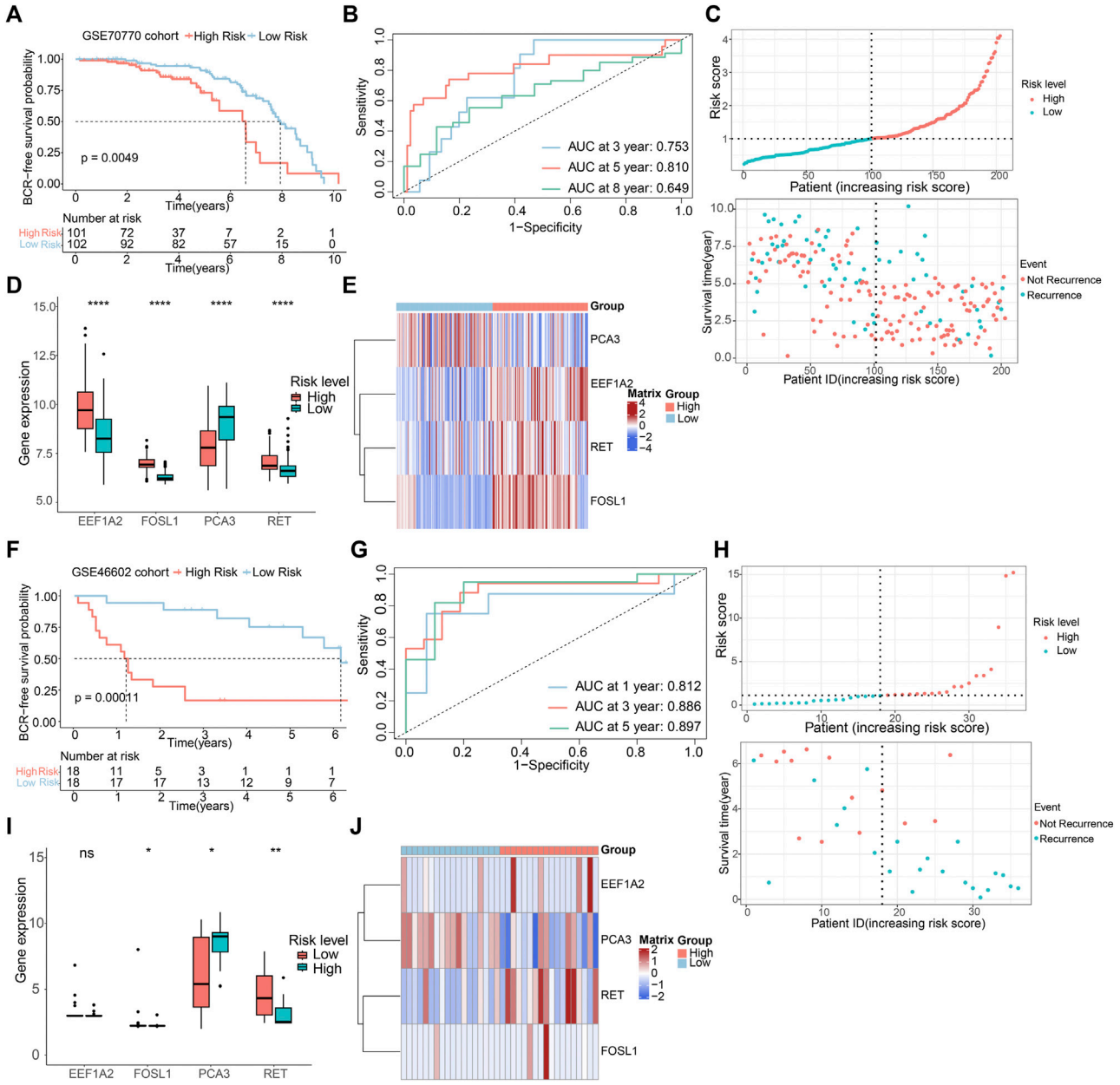

FIGURE 5
Validation of risk model based on GEO cohorts. K-M curves of BCR-free rate between high- and low-risk score groups in the **(A)** GSE70770, **(F)** GSE46602. The AUC of the risk model in the **(B)** GSE70770, **(G)** GSE46602. The risk score distribution and BCR status of PCa patients in the **(C)** GSE70770, **(H)** GSE46602. The boxplots of the prognostic ARGs in the **(D)** GSE70770, **(I)** GSE46602. The risk heatmap of the prognostic ARGs in the **(E)** GSE70770, **(J)** GSE46602.

high-risk and low-risk groups based on the prognostic signature of ARGs. Kaplan-Meier analysis displayed that the occurrence of BCR showed a notably higher level in individuals with a high-risk score in contrast to those in the low-risk group, particularly among individuals aged ≤60 years and those with N0 status (Figures 4E,F). However, due to small sample size or uneven distribution, in patients aged >60, with different Gleason scores, and varying N and T stages, there was no significant difference in BCR incidence (Supplementary Figure S2). Furthermore, Figures 4G–I illustrated that higher risk scores are indeed positively correlated with various adverse clinicopathological characteristics, including higher Gleason scores, higher T stages, and lymph node metastasis. These results indicated that the risk score derived from ARGs can act as a prognostic factor that acts independently in individuals with PCa. It could be effectively used to predict the likelihood of BCR-free survival in PCa patients.

3.4 Validation of risk model based on GEO cohorts

To assess the predictive precision of the risk model, we applied the same methodologies to the GSE70770 and GSE46602 cohorts, utilizing

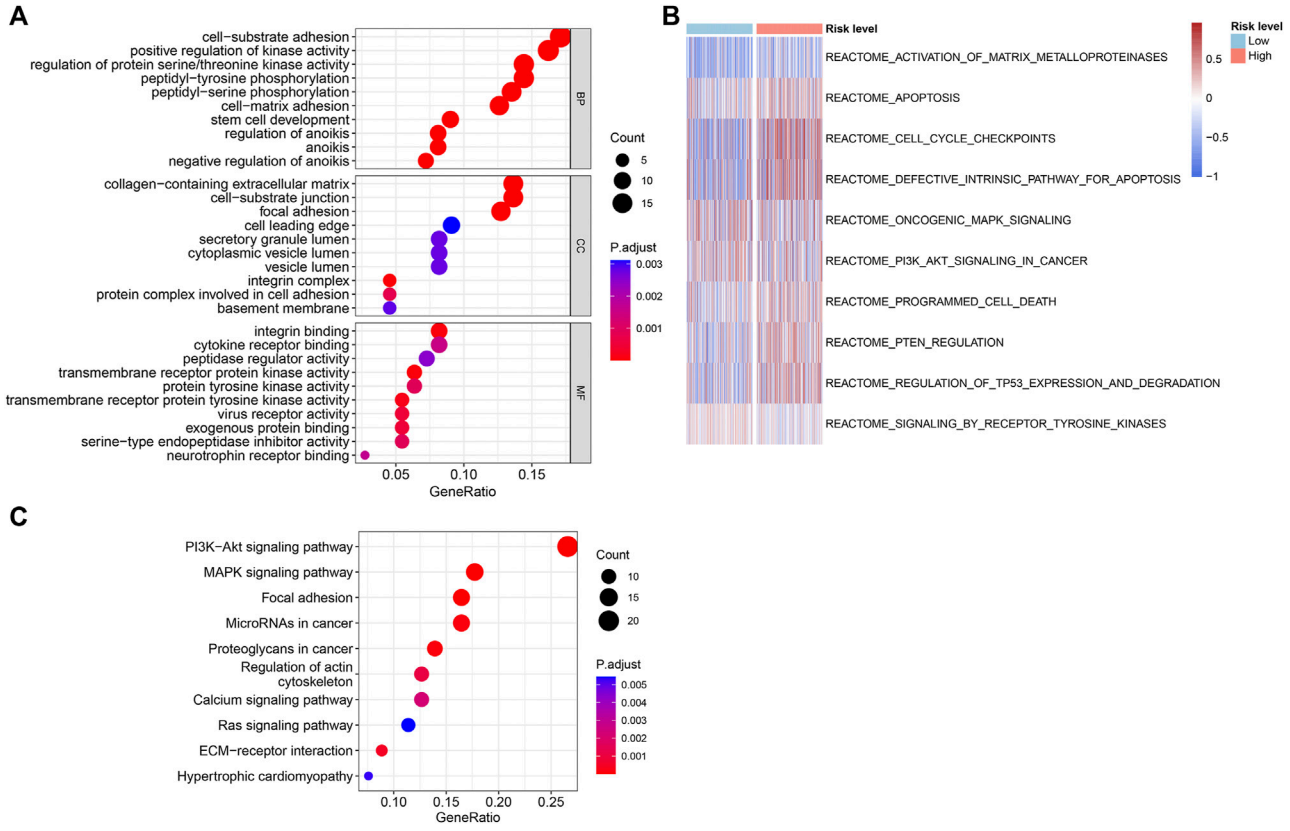

FIGURE 6
Functional enrichment analysis of the differentially expressed ARGs in the different risk groups. **(A)** The results of GO enrichment analysis. **(B)** GSVA analysis shows the REACTOME term of PCa patients in the different risk groups. **(C)** KEGG enrichment analysis of the differentially expressed ARGs.

them as external validation sets. Multivariate Cox regression analysis in both cohorts exhibited the independence of the ARGs prognostic signatures (Supplementary Figure S3). Survival analysis unveiled that patient with low-risk scores displayed notably higher rates of BCR-free survival in comparison to those with high-risk scores (Figures 5A,F), aligning with the observations from the TCGA dataset. The AUC values in the GSE70770 dataset were 0.753, 0.810, and 0.649 for 3-, 5-, and 8-year BCR-free survival predictions, respectively. The AUC values for 1-, 3-, and 5-year BCR-free occurrence in the GSE46602 dataset were 0.812, 0.886, and 0.897, respectively (Figures 5B,G). Figures 5C–E,H–J visually represents the distribution of risk scores, the expression levels of the four prognostic ARGs, and the BCR status of individuals within the two external validation sets. These data implied that the risk model performs well in terms of prognosis.

3.5 Functional enrichment analysis of the differentially expressed ARGs

The underlying biological functions and molecular mechanisms of ARGs were revealed using functional enrichment analysis. ARGs in PCa were shown to be significantly abundant in processes such as cell-substrate adhesion, peptidyl-tyrosine phosphorylation, control of protein serine/threonine kinase activity, cell-matrix adhesion, and anoikis regulation (Figure 6A). The findings of the GSVA enrichment analysis revealed the signature signaling pathways of ARGs for PCa patient in the high- and low-risk groups (Figure 6B). According to KEGG analysis, ARGs in PCa were largely implicated in the PI3K-Akt signaling pathway, the MAPK signaling pathway, and focal adhesion (Figure 6C). The outcomes implied that ARGs might have a substantial role in the migration and metastasis of PCa.

3.6 Immune infiltration analysis

For assessing the pattern of immune cell infiltration in patients with PCa, the CIBERSORT, CIBERSORTx and ssGSEA algorithms were applied, focusing on two risk subgroups. The CIBERSORT analysis showed that the high-risk group displayed a considerably greater proportion of most immune cells. In contrast, the low-risk group had a larger percentage of resting dendritic cells, activated dendritic cells, activated mast cells, and eosinophils, as depicted in Figure 7A. CIBERSORTx is an updated version of CIBERSORT, and the results of both analyses were relatively consistent. Notably, CIBERSORTx identified more cell types, such as plasma cells and CD8 T cells, which showed higher infiltration levels in the high-risk group (Figure 7B). The ssGSEA algorithm demonstrated that individuals with a low-risk score showed a larger portion of mast cells, T cells, T follicular helper cells (TFH), T helper two cells (Th2), and myeloid-derived suppressor cells (MDSC). Conversely, the fraction of effector memory CD4 cells and memory B cells was greater in the high-risk group (Figure 7C). A correlation analysis was

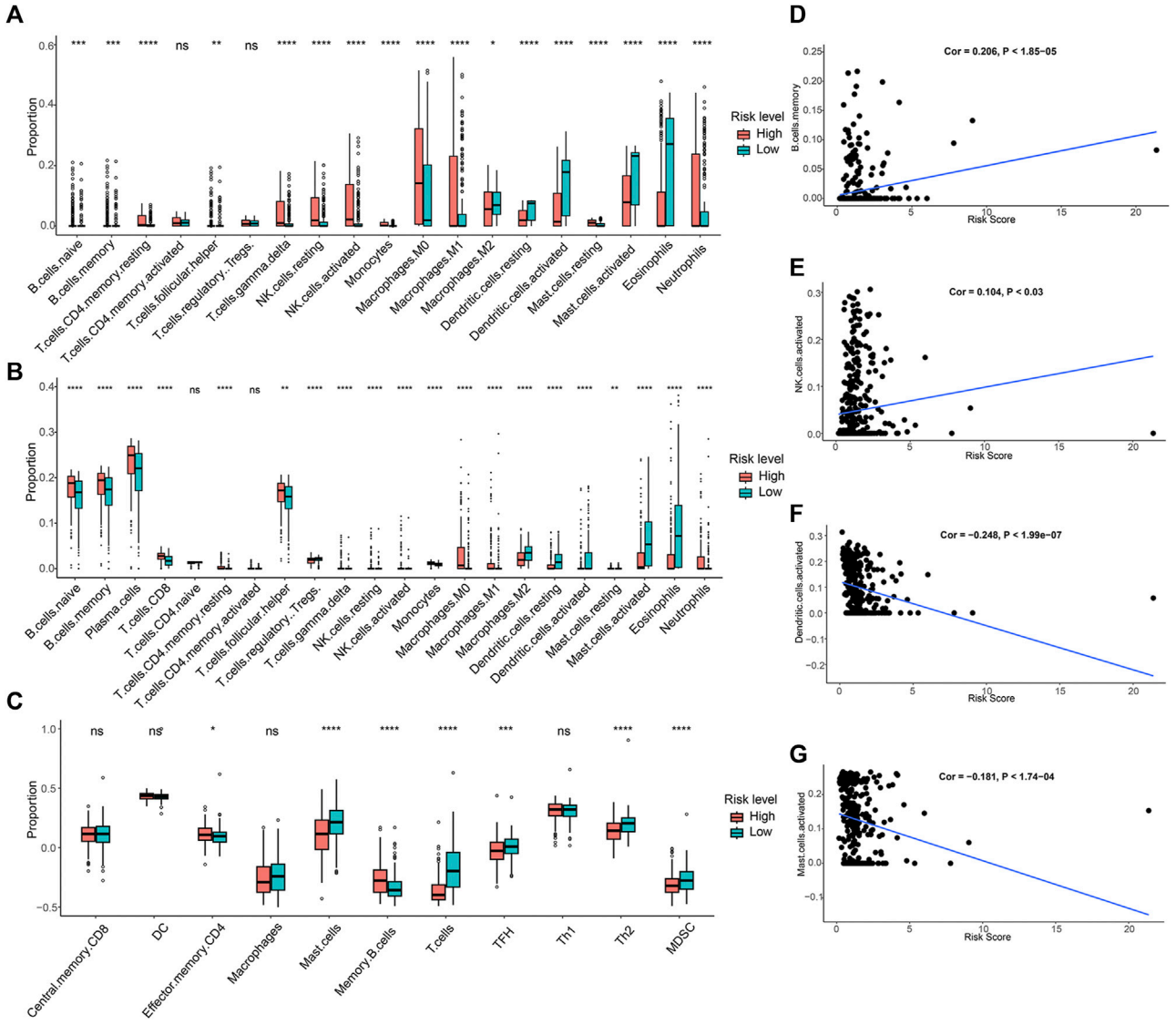

FIGURE 7
Immune infiltration analysis of PCa patients in risk groups. **(A)** The fraction of 19-type immune cells in different risk groups. **(B)** Differences in immune infiltration of 22-type immune cells. **(C)** The proportion of 11-type immune cells in different risk groups. **(D–G)** The correlations between the four immune cells abundance and risk scores.

conducted to investigate the relationship between the abundance of immune cells and the risk score. This analysis revealed that the risk score was in a positive relationship with the presence of memory B cells and activated NK cells, while it showed a negative association with activated dendritic cells and mast cells (Figures 7D–G). Overall, our data suggested a correlation between ARGs risk model and the immune infiltration landscape in patients with PCa.

3.7 Immunotherapy response analysis

Given the wide range of immune infiltration among PCa patients, we investigated the response to immunotherapy in distinct risk groups. The TIDE analysis indicated that high-risk PCa patients exhibited notably higher TIDE scores in contrast to individuals in the low-risk group (Figure 8A). This suggested that individuals with a high-risk score might have a diminished reaction to immune checkpoint therapy. Additionally, the high-risk group demonstrated elevated scores for MDSC, TAM.M2, and exclusion, while showing a lower dysfunction score (Figures 8B–E).

3.8 Drug sensitivity analysis

To evaluate the response to chemotherapeutic drugs in the two subgroups, we carried out a drug sensitivity analysis. The outcomes indicated that the IC50 values of sabutoclax, vinblastine, rapamycin, sepantronium bromide (YM155), docetaxel, mitoxantrone, and paclitaxel were notably greater in the low-risk group. However, it was observed that the high-risk group had a higher IC50 for AZD8055, as indicated in Figures 9A–H. The findings

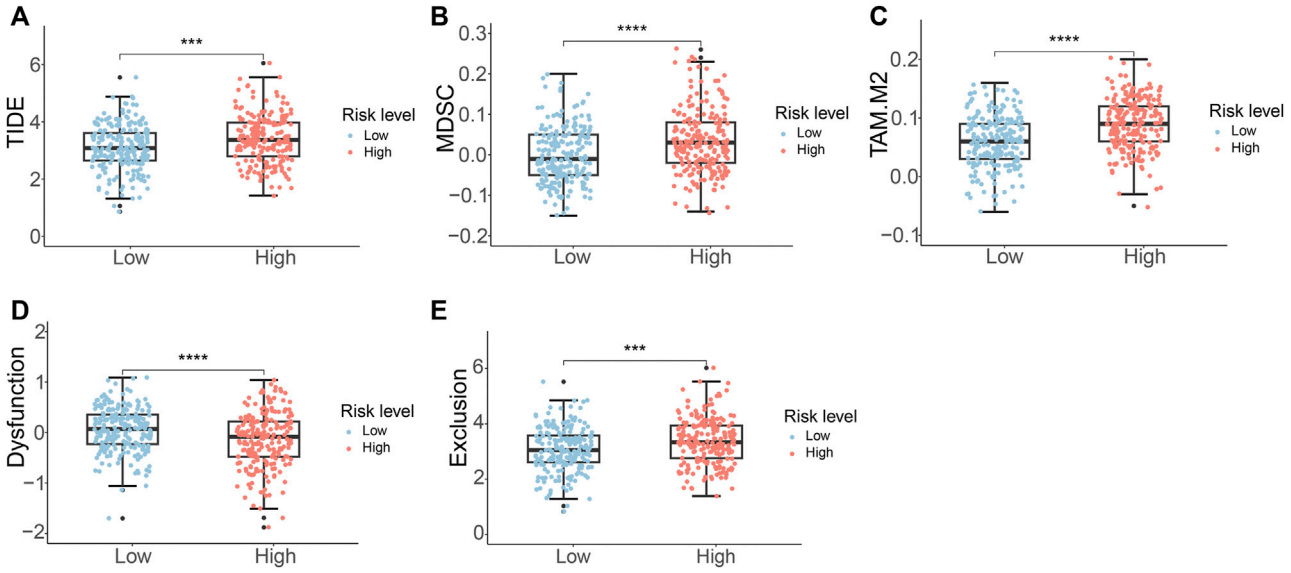

FIGURE 8
Immunotherapy response analysis of PCa patients. **(A)** TIDE score **(B)** MDSC score **(C)** TAM.M2 score **(D)** T-cell dysfunction score **(E)** T-cell exclusion score.

highlighted the diverse efficacy benefits of the selected chemotherapeutic drugs on individuals with PCa in various risk groups and could offer guidance for the selection of chemotherapy for PCa patients.

3.9 Validation of prognostic genes

Based on the information available on the HPA website, we observed that the EEF1A2 gene in the risk model exhibited high expression in PCa cases, while the RET and FOSL1 genes showed moderate or weak expression (Figure 10A). Furthermore, we leveraged the single-cell RNA sequencing dataset GSE141445 from the TISCH database to investigate the expression of four ARGs within the TME. The GSE141445 dataset comprise 18 cell clusters and eight intermediate cell types, the distribution and quantity of these clusters were depicted (Figure 10B). Figures 10C,D showed the expression levels of the genes EEF1A2, RET, FOSL1, and PCA3 in each cell type within the dataset. These data indicated that these four ARGs may contribute in the tumor microenvironment of PCa.

4 Discussion

Early recurrence is associated with a heightened risk of metastasis in PCa, with 24%–34% of patients with BCR progressing to metastatic disease (Pound et al., 1999; Boorjian et al., 2011). Anoikis pertains to a distinctive form of programmed cell death that is initiated when cells disconnect from the extracellular matrix and become isolated from neighboring cells. This mechanism significantly contributes to inhibiting tumor invasion and metastasis. Consequently, evaluating BCR risk based on the anoikis signature is essential for improving the accuracy of PCa prognosis.

In this research, we identified four ARGs that are associated with the risk of BCR in PCa. Utilizing these genes, we constructed a risk model to forecast BCR in PCa using the TCGA dataset, and subsequently, we verified the model in two GEO datasets. Kaplan-Meier survival analysis exhibited a significantly higher risk of BCR in the high-risk group in comparison to the low-risk group. ROC analysis confirmed the effectiveness of the prognostic model in predicting BCR events at 3-, 5-, and 8-year intervals. It was worth noting that the majority of BCR times for patient samples in the GSE46602 dataset were less than 8 years. Consequently, we conducted ROC analysis to validate the prognostic model's performance in predicting 1-, 3-, and 5-year BCR events. The multivariate and univariate Cox regression analyses showed that the risk score derived from ARGs could serve as a standalone prognostic indicator for forecasting BCR-free survival in individuals with PCa. Additionally, we carried out a nomogram to visually represent the influence of the risk score and various clinicopathological characteristics on 3-, 5-, and 8-year BCR-free survival. Taken together, the risk model, based on 4 ARGs, demonstrated accurate assessment capabilities for predicting the BCR risk in PCa patients.

In this study, we identified 4 ARGs for the construction of a BCR risk model in PCa. Among these ARGs, patients with a high-risk score reported greater EEF1A2, RET, and FOSL1 levels, but PCA3 expression was reduced. Previous investigations elucidated some correlations between these genes and the tumorigenesis and pathophysiology of cancer. EEF1A2, a coding gene crucial for protein translation elongation, has been demonstrated to exhibit altered expression in numerous cancers (Cristiano, 2022), which actively participate in the initiation and progression of various cancer types during carcinogenesis (Anand et al., 2002; Hassan et al., 2020; Jia et al., 2021). EEF1A2 was reported to facilitate the

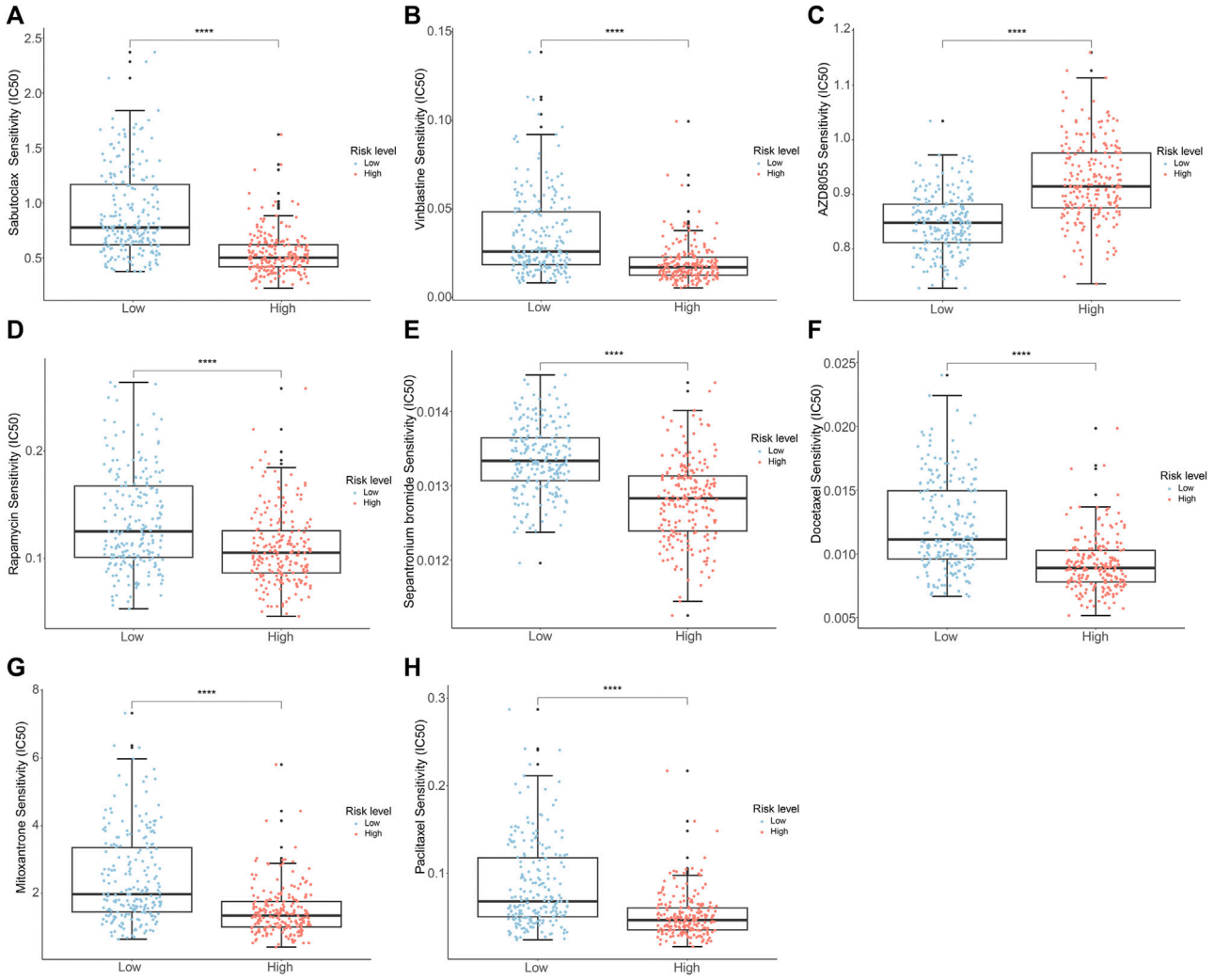

FIGURE 9
Analysis of drug sensitivity of PCa patients in the different risk groups. **(A)** Sabutoclax **(B)** Vinblastine **(C)** AZD8055 **(D)** Rapamycin **(E)** Sepantronium Bromide (YM155) **(F)** Docetaxel **(G)** Mitoxantrone **(H)** Paclitaxel.

migration, invasion, and metastasis of pancreatic cancer cells by activating Akt and upregulating MMP-9 expression (Xu et al., 2013). Inhibiting EEF1A2 leaded to a significant upregulation of apoptotic pathway proteins (caspase3, BAD, BAX, PUMA), while elevated levels of EEF1A2 promoted the proliferation and suppress apoptosis of PCa cells (Sun et al., 2014). Worst et al. observed that EEF1A2 was overexpressed in PCa with higher Gleason scores, and patients with increased EEF1A2 expression had markedly shortened BCR-free survival (Worst et al., 2017). These findings implied that EEF1A2 played a role in the transformation and progression of PCa, which was consistent with our observations of elevated EEF1A2 expression in high-risk populations. RET is a receptor tyrosine kinase, which can mediate cell proliferation, survival, migration, and is associated with the progression of various tumors (Hu et al., 2023). Our data indicated that high expression of RET was linked to poor prognosis in PCa patients. It was reported that RET expression played a crucial role in the survival, proliferation, and anoikis resistance of medullary thyroid carcinoma cells (Lian et al., 2017). In PCa, RET is expressed in all PCa cell lines, and RET signaling can activate the AKT or ERK pathways, promoting PCa transformation-related phenotypes by activating the p70S6 kinase (Ban et al., 2017). Knocking down or pharmacologically inhibiting the RET kinase in various mouse and human neuroendocrine PCa models significantly diminished PCa tumor growth and cellular vitality (VanDeusen et al., 2020). These results suggested that RET was conducive to the development of malignant characteristics in PCa cells, and further investigation of the clinical potential of RET gene was warranted. The FOSL1 gene is responsible for encoding Fos-related antigen 1 (FRA1), which is elevated in breast cancer, colorectal cancer, lung cancer, and various other malignancies (Jiang et al., 2020). Our data also indicated FOSL1 gene was biomarker high expressed in PCa patients. It was reported that the oncogene K-Ras elevated the expression of ITGA6 through FOSL1 inducing resistance to anoikis (Zhang et al., 2017). High expression of FOSL1 in PCa could enhance the proliferation and metastasis of PCa cells by modulating the EMT pathway (Luo et al., 2018). Therefore, as a promoter of EMT, FOSL1 may have a significant impact on PCa carcinogenesis.

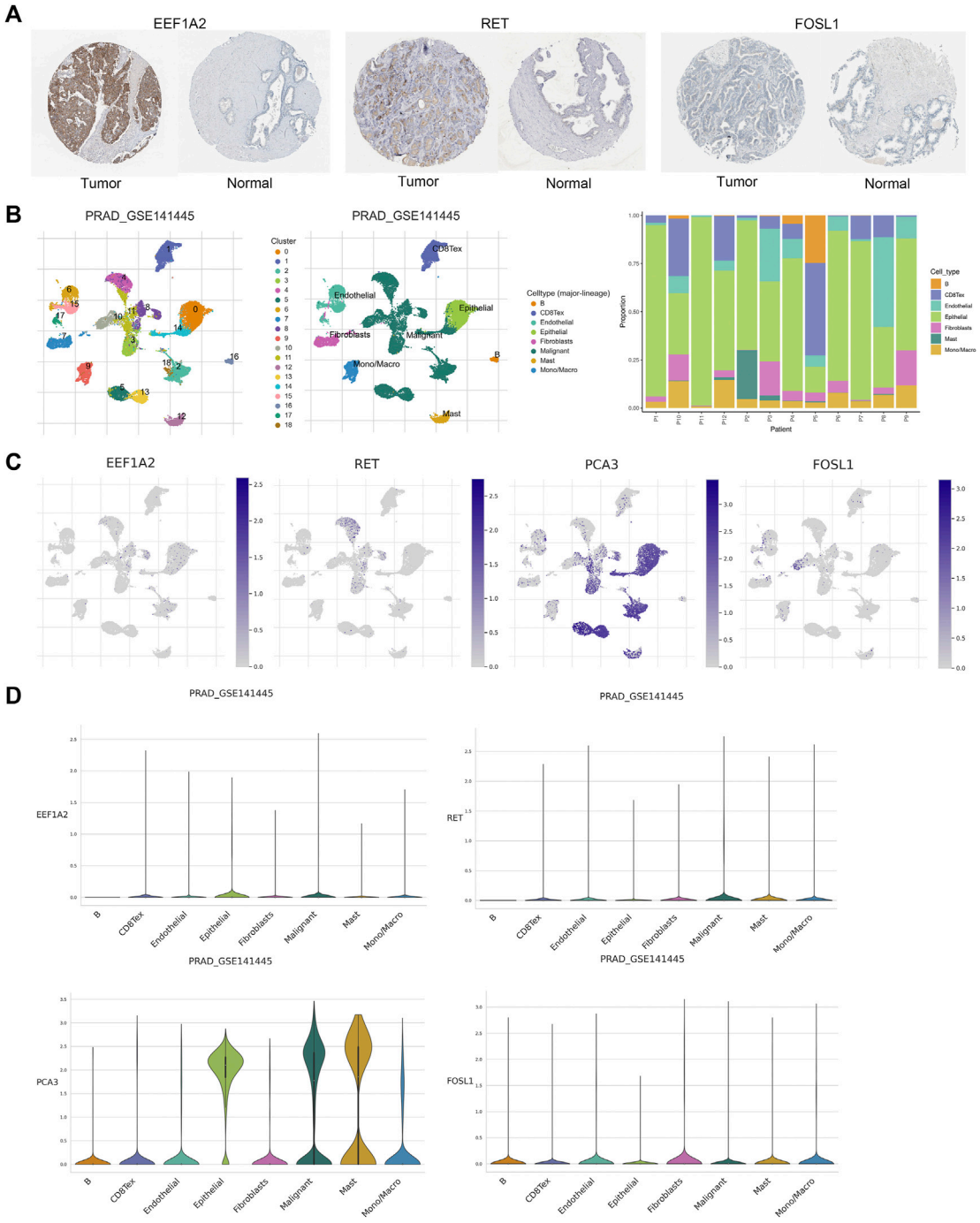

FIGURE 10
Validation of prognostic genes of ARGs. **(A)** Based on the HPA database, the immunohistochemical results for EEF1A2, RET and FOSL1. **(B)** Annotations for all cell types in GSE141445 and the proportion of each cell type. **(C, D)** Proportions and expressions of FOSL1, EEF1A2, PCA3 and RET.

Prostate Cancer Antigen 3 (PCA3) is a specific type of long non-coding RNA (lncRNA) found in the prostate. The levels of PCA3 in urine were commonly used as diagnostic biomarkers for PCa (Lemos et al., 2019). Lauer et al. found that the upregulation of lncRNA PCA3 and the downregulation of PRUNE2 might be early (rather than late) molecular events in the progression of prostate tumors, but were unrelated to BCR (Lauer et al., 2023). Another study also suggested that PCA3 appeared to be an important marker for early-stage or less invasive tumors of PCa, however, the gene expression levels of PCA3 and PRUNE2, as well as the PCA3/PRUNE2 ratio, could differentiate whether patients experience BCR events (Dias-Neto et al., 2017). The differences in BCR outcomes between these two studies might be attributed to the cohorts included. Our findings were in line with the latter results, indicating that PCA3 expression was higher in the group of individuals with low risk of BCR compared to that in the high-

risk group. In summary, EEF1A2, RET, and FOSL1 could serve as prognostic risk factors for PCa. Conversely, PCA3 was negatively correlated with PCa prognosis. The risk model based on these four ARGs not only could be a prognostic marker for BCR in PCa but also had the potential to be a novel prospective target gene for PCa treatment.

We also conducted GO, KEGG, and GSEA enrichment studies on the ARGs to better understand their putative biological roles and molecular processes. As anticipated, these genes exhibited close associations with the biological processes involving the regulation of anoikis and were also linked to the signaling pathways of PI3K-Akt and MAPK. According to current research reports, silencing eEF1A2 significantly reduced the occurrence of hepatocellular carcinoma by inhibiting the PI3K/Akt/NF-κB signaling transduction (Qiu et al., 2016). Activating RET alterations have been shown to enhance the activity of the PI3K/AKT and MAPK pathways, thereby promoting the proliferation and development of various types of tumor cells (Brzezianska and Pastuszak-Lewandoska, 2011; Regua et al., 2022). In melanoma, sustained expression of FOSL1 was associated with continuous overactivation of the MAPK pathway (Maurus et al., 2017). Further, the process of anoikis resistance reported in several studies is indeed related to the pathways we identified. Anoikis resistance has been reported to induce alterations in the Ras/ERK and PI3K/Akt signaling pathways, as well as matrix remodeling, in endothelial cells (de Sousa Mesquita et al., 2017). Depleting mitochondrial DNA in prostate epithelial cells induces the cell to develop anoikis resistance and enhances its invasive ability by activating the PI3K/Akt2 signalling pathway (Moro et al., 2009). Activation of the Src kinase-mediated MAPK pathway was associated with angiogenesis in osteosarcoma cells anoikis resistance (Gao et al., 2019). These studies suggested that ARGs may play a role in the anoikis process of PCa by regulating the PI3K-Akt and MAPK signaling pathways, further investigation is necessary to validate this hypothesis.

Infiltrating immune cells serves a complex biological function in PCa development. Studies have shown that low levels of mast cells in cancer tissue are associated with poor outcomes such as BCR and metastasis in PCa (Hempel et al., 2017; Sfanos, 2022). This is consistent with our results of less mast cell infiltration in the high-risk group. Our study found that the BCR high-risk group had a higher proportion of M1 macrophages, which is consistent with previous research, indicating that infiltrating M1 macrophages are an important adverse prognostic factor for BCR in PCa (Andersen et al., 2021). Moreover, this study also showed that the infiltration level of neutrophils significantly increases in the high-risk group. A study has shown that enhancing the cytotoxicity of neutrophils in the bone might be beneficial for the treatment of patients with bone metastatic PCa (Costanzo-Garvey et al., 2020). Therefore, neutrophils may have important therapeutic implications for bone metastasis patients in the high-risk group. Furthermore, previous studies have reported high levels of tumor-infiltrating CD8 T cells associated with BCR in PCa (Ness et al., 2014), as well as specimens from patients in the high-risk group and those with recurrence or progression of PCa showing more B-cell infiltration (Woo et al., 2014). These findings are consistent with our results, indicating a higher level of infiltration of CD8 T cells and B cells in the high-risk group for BCR. It is worth noting that although the samples in the single-cell RNA sequencing dataset were not risk stratified, the proportions of B cells and $CD8^+$ T cells in them were similar to those in the high-risk group in immune infiltration, and these immune cells may play a similar role in TME of PCa.

TIDE analysis was used to evaluate the potential clinical efficacy of immunotherapy in different risk groups. An elevated TIDE score implied an increased possibility of tumor immune escape, indicating lower benefits from immune checkpoint inhibitor (ICI) therapy for patients (Jiang et al., 2018). Our findings indicated a higher TIDE score in the high-risk group, which suggested that immunotherapy might be less effective in this group of patients. In addition, we calculated the sensitivity of different risk groups to PCa chemotherapeutic agents using drug sensitivity analysis. Clinical trials of commonly used chemotherapy drugs for PCa have shown that using vinblastine or paclitaxel in combination with estramustine can treat patients with locally advanced or hormone-refractory PCa (Hudes et al., 1992; Zelefsky et al., 2000; Kelly et al., 2001; Urakami et al., 2002). The combination of docetaxel with androgen deprivation therapy (ADT) increased survival for those with metastatic hormone-sensitive PCa (Kyriakopoulos et al., 2018). Extensive clinical trials were established the therapeutic efficacy of agents such as rapamycin (Armstrong et al., 2010), sepantronium bromide (YM155) (Tolcher et al., 2012), and mitoxantrone (de Bono et al., 2010) in the treatment of PCa. In summary, the analysis of chemotherapeutic drug sensitivity offered new theoretical support for the clinical pharmacological management of PCa potentially.

There are limitations for this study. Firstly, the clinical cohort of all PCa cases in this study was obtained from public databases, and the sample size was limited. Future work will include larger clinical samples to enhance the accuracy of the results. Secondly, the outcomes of this study lacked validation through *in vitro* experiments. We will verify the expression patterns of these four key genes in the clinical samples using qPCR and immunohistochemistry, thereby increasing the reliability of the conclusions. Lastly, the potential mechanisms by which the four anoikis-related genes regulated the prognosis of PCa patients are required further investigation.

5 Conclusion

In conclusion, we developed a novel model incorporating four ARGs for predicting the risk of BCR in PCa. Our results offered a glimpse into the molecular and immunological characteristics of ARGs in PCa. In addition, we did a preliminary assessment of immunotherapy response and chemotherapeutic drug sensitivity in PCa patients from various risk groups. Collectively, this study potentially offered vital guidance for predicting BCR events in PCa.

Data availability statement

The original contributions presented in the study are included in the article/Supplementary Material, further inquiries can be directed to the corresponding authors.

Author contributions

WK: Conceptualization, Data curation, Investigation, Methodology, Writing–original draft, Writing–review and editing. CY: Conceptualization, Data curation, Investigation, Methodology, Writing–review and editing. YY: Formal Analysis, Software, Validation, Visualization, Writing–review and editing. Y-RL: Formal Analysis, Software, Validation, Visualization, Writing–review and editing. MZ: Conceptualization, Data curation, Formal Analysis, Supervision, Writing–review and editing. ZW: Conceptualization, Project administration, Resources, Supervision, Writing–review and editing. YG: Conceptualization, Funding acquisition, Project administration, Supervision, Writing–review and editing.

Funding

The author(s) declare that financial support was received for the research, authorship, and/or publication of this article. This work was supported by the National Natural Science Foundation of China (No. 82272769, 81972392 and 82203168).

Conflict of interest

The authors declare that the research was conducted in the absence of any commercial or financial relationships that could be construed as a potential conflict of interest.

Publisher's note

Supplementary material

The Supplementary Material for this article can be found online at: https://www.frontiersin.org/articles/10.3389/fphar.2024.1383304/full#supplementary-material

SUPPLEMENTARY FIGURE S1
Construction and validation of risk model risk model. **(A)** Multivariate Cox regression analysis of the ARGs. **(B)** The risk score distribution and BCR status of PCa patients in the training set. **(C)** K-M curves of BCR outcome between high- and low-risk score groups in the training set. **(D)** ROC curves for BCR-free predictive performance at 3-, 5-, and 8-years in the training set. **(E-F)** The boxplot and risk heatmap of the prognostic ARGsin the training set.

SUPPLEMENTARY FIGURE S2
The BCR-free rate of patients with PCa in the low- and high-risk group among the **(A)** Age > 60 ; **(B)** Gleason score > 7; **(C)** Gleason score <= 7 ; **(D)** N1; **(E)** T2; **(F)** T3/T4 .

SUPPLEMENTARY FIGURE S3
Validation of risk model based on GEO cohorts. The multivariate Cox regression analysis in two cohorts **(A)** GSE70770 **(B)** GSE46602.

References

Anand, N., Murthy, S., Amann, G., Wernick, M., Porter, L. A., Cukier, I. H., et al. (2002). Protein elongation factor EEF1A2 is a putative oncogene in ovarian cancer. *Nat. Genet.* 31, 301–305. doi:10.1038/ng904

Andersen, L. B., Nørgaard, M., Rasmussen, M., Fredsøe, J., Borre, M., Ulhøi, B. P., et al. (2021). Immune cell analyses of the tumor microenvironment in prostate cancer highlight infiltrating regulatory T cells and macrophages as adverse prognostic factors. *J. Pathol.* 255, 155–165. doi:10.1002/path.5757

Armstrong, A. J., Netto, G. J., Rudek, M. A., Halabi, S., Wood, D. P., Creel, P. A., et al. (2010). A pharmacodynamic study of rapamycin in men with intermediate-to high-risk localized prostate cancer. *Clin. Cancer Res.* 16, 3057–3066. doi:10.1158/1078-0432.CCR-10-0124

Ban, K., Feng, S., Shao, L., and Ittmann, M. (2017). RET signaling in prostate cancer. *Clin. Cancer Res.* 23, 4885–4896. doi:10.1158/1078-0432.CCR-17-0528

Boorjian, S. A., Thompson, R. H., Tollefson, M. K., Rangel, L. J., Bergstralh, E. J., Blute, M. L., et al. (2011). Long-term risk of clinical progression after biochemical recurrence following radical prostatectomy: the impact of time from surgery to recurrence. *Eur. Urol.* 59, 893–899. doi:10.1016/j.eururo.2011.02.026

Brzezianska, E., and Pastuszak-Lewandoska, D. (2011). A minireview: the role of MAPK/ERK and PI3K/Akt pathways in thyroid follicular cell-derived neoplasm. *Front. Biosci. Landmark Ed.* 16, 422–439. doi:10.2741/3696

Cao, Z., Livas, T., and Kyprianou, N. (2016). Anoikis and EMT: lethal "liaisons" during cancer progression. *Crit. Rev. Oncog.* 21, 155–168. doi:10.1615/CritRevOncog.2016016955

Chen, S., Zhu, G., Yang, Y., Wang, F., Xiao, Y.-T., Zhang, N., et al. (2021). Single-cell analysis reveals transcriptomic remodellings in distinct cell types that contribute to human prostate cancer progression. *Nat. Cell Biol.* 23, 87–98. doi:10.1038/s41556-020-00613-6

Cornford, P., Bellmunt, J., Bolla, M., Briers, E., De Santis, M., Gross, T., et al. (2017). EAU-ESTRO-SIOG guidelines on prostate cancer. Part II: treatment of relapsing, metastatic, and castration-resistant prostate cancer. *Eur. Urol.* 71, 630–642. doi:10.1016/j.eururo.2016.08.002

Costanzo-Garvey, D. L., Keeley, T., Case, A. J., Watson, G. F., Alsamraae, M., Yu, Y., et al. (2020). Neutrophils are mediators of metastatic prostate cancer progression in bone. *Cancer Immunol. Immunother.* 69, 1113–1130. doi:10.1007/s00262-020-02527-6

Cristiano, L. (2022). The pseudogenes of eukaryotic translation elongation factors (EEFs): role in cancer and other human diseases. *Genes & Dis.* 9, 941–958. doi:10.1016/j.gendis.2021.03.009

D'Andrea, D., Soria, F., Abufaraj, M., Gust, K., Foerster, B., Vartolomei, M. D., et al. (2018). Clinical value of cholinesterase in the prediction of biochemical recurrence after radical prostatectomy. *Urol. Oncol.* 36, 528.e7–528. doi:10.1016/j.urolonc.2018.09.015

de Bono, J. S., Oudard, S., Ozguroglu, M., Hansen, S., Machiels, J.-P., Kocak, I., et al. (2010). Prednisone plus cabazitaxel or mitoxantrone for metastatic castration-resistant prostate cancer progressing after docetaxel treatment: a randomised open-label trial. *Lancet* 376, 1147–1154. doi:10.1016/S0140-6736(10)61389-X

de Sousa Mesquita, A. P., de Araújo Lopes, S., Pernambuco Filho, P. C. A., Nader, H. B., and Lopes, C. C. (2017). Acquisition of anoikis resistance promotes alterations in the Ras/ERK and PI3K/Akt signaling pathways and matrix remodeling in endothelial cells. *Apoptosis* 22, 1116–1137. doi:10.1007/s10495-017-1392-0

Dess, R. T., Morgan, T. M., Nguyen, P. L., Mehra, R., Sandler, H. M., Feng, F. Y., et al. (2017). Adjuvant versus early salvage radiation therapy following radical prostatectomy for men with localized prostate cancer. *Curr. Urol. Rep.* 18, 55. doi:10.1007/s11934-017-0700-0

Dias-Neto, E., Nunes, D. N., Thomas, A. M., Smith, T. L., Rao, A., Lauer, R. C., et al. (2017). PCA3 upregulation in prostate cancer: analysis in a cohort of 497 subjects from TCGA. *J. Clin. Oncol.* 35, e16578. doi:10.1200/JCO.2017.35.15_suppl.e16578

Feng, D., Li, D., Wang, J., Wu, R., and Zhang, C. (2023). Senescence-associated lncRNAs indicate distinct molecular subtypes associated with prognosis and androgen response in patients with prostate cancer. *Acta Mater. Medica* 2. doi:10.15212/AMM-2023-0025

Gao, Z., Zhao, G.-S., Lv, Y., Peng, D., Tang, X., Song, H., et al. (2019). Anoikis-resistant human osteosarcoma cells display significant angiogenesis by activating the Src kinase-mediated MAPK pathway. *Oncol. Rep.* 41, 235–245. doi:10.3892/or.2018.6827

Giannoni, E., Buricchi, F., Grimaldi, G., Parri, M., Cialdai, F., Taddei, M. L., et al. (2008). Redox regulation of anoikis: reactive oxygen species as essential mediators of cell survival. *Cell Death Differ.* 15, 867–878. doi:10.1038/cdd.2008.3

Hassan, Md. K., Kumar, D., Patel, S. A., and Dixit, M. (2020). EEF1A2 triggers stronger ERK mediated metastatic program in ER negative breast cancer cells than in ER positive cells. *Life Sci.* 262, 118553. doi:10.1016/j.lfs.2020.118553

He, H., Liang, L., Han, D., Xu, F., and Lyu, J. (2022). Different trends in the incidence and mortality rates of prostate cancer between China and the USA: a joinpoint and age-period-cohort analysis. *Front. Med.* 9, 824464. doi:10.3389/fmed.2022.824464

Hempel, H. A., Cuka, N. S., Kulac, I., Barber, J. R., Cornish, T. C., Platz, E. A., et al. (2017). Low intratumoral mast cells are associated with a higher risk of prostate cancer recurrence: mast cells and prostate cancer recurrence. *Prostate* 77, 412–424. doi:10.1002/pros.23280

Hu, X., Khatri, U., Shen, T., and Wu, J. (2023). Progress and challenges in RET-targeted cancer therapy. *Front. Med.* 17, 207–219. doi:10.1007/s11684-023-0985-y

Hudes, G. R., Greenberg, R., Krigel, R. L., Fox, S., Scher, R., Litwin, S., et al. (1992). Phase II study of estramustine and vinblastine, two microtubule inhibitors, in hormone-refractory prostate cancer. *J. Clin. Oncol.* 10, 1754–1761. doi:10.1200/JCO.1992.10.11.1754

Hynes, R. O. (1992). Integrins: versatility, modulation, and signaling in cell adhesion. *Cell* 69, 11–25. doi:10.1016/0092-8674(92)90115-s

Jia, L., Ge, X., Du, C., Chen, L., Zhou, Y., Xiong, W., et al. (2021). EEF1A2 interacts with HSP90AB1 to promote lung adenocarcinoma metastasis via enhancing TGF-β/SMAD signalling. *Br. J. Cancer* 124, 1301–1311. doi:10.1038/s41416-020-01250-4

Jiang, P., Gu, S., Pan, D., Fu, J., Sahu, A., Hu, X., et al. (2018). Signatures of T cell dysfunction and exclusion predict cancer immunotherapy response. *Nat. Med.* 24, 1550–1558. doi:10.1038/s41591-018-0136-1

Jiang, X., Xie, H., Dou, Y., Yuan, J., Zeng, D., and Xiao, S. (2020). Expression and function of FRA1 protein in tumors. *Mol. Biol. Rep.* 47, 737–752. doi:10.1007/s11033-019-05123-9

Jin, L., Chun, J., Pan, C., Kumar, A., Zhang, G., Ha, Y., et al. (2018). The PLAG1-GDH1 Axis promotes anoikis resistance and tumor metastasis through CamKK2-AMPK signaling in LKB1-deficient lung cancer. *Mol. Cell* 69, 87–99. doi:10.1016/j.molcel.2017.11.025

Kelly, W. K., Curley, T., Slovin, S., Heller, G., McCaffrey, J., Bajorin, D., et al. (2001). Paclitaxel, estramustine phosphate, and carboplatin in patients with advanced prostate cancer. *J. Clin. Oncol. official J. Am. Soc. Clin. Oncol.* 19, 44–53. doi:10.1200/JCO.2001.19.1.44

Kim, H., Choi, P., Kim, T., Kim, Y., Song, B. G., Park, Y.-T., et al. (2021). Ginsenosides Rk1 and Rg5 inhibit transforming growth factor-β1-induced epithelial-mesenchymal transition and suppress migration, invasion, anoikis resistance, and development of stem-like features in lung cancer. *J. Ginseng Res.* 45, 134–148. doi:10.1016/j.jgr.2020.02.005

Konoshenko, M.Yu., and Laktionov, P. P. (2021). MiRNAs and radical prostatectomy: current data, bioinformatic analysis and utility as predictors of tumour relapse. *Andrology* 9, 1092–1107. doi:10.1111/andr.12994

Kyriakopoulos, C. E., Chen, Y.-H., Carducci, M. A., Liu, G., Jarrard, D. F., Hahn, N. M., et al. (2018). Chemohormonal therapy in metastatic hormone-sensitive prostate cancer: long-term survival analysis of the randomized phase III E3805 CHAARTED trial. *J. Clin. Oncol.* 36, 1080–1087. doi:10.1200/JCO.2017.75.3657

Lauer, R. C., Barry, M., Smith, T. L., Thomas, A. M., Wu, J., Du, R., et al. (2023). Dysregulation of the PRUNE2/PCA3 genetic axis in human prostate cancer: from experimental discovery to validation in two independent patient cohorts. *eLife* 12, e81929. doi:10.7554/eLife.81929

Lee, Y., Yoon, J., Ko, D., Yu, M., Lee, S., and Kim, S. (2021). TMPRSS4 promotes cancer stem-like properties in prostate cancer cells through upregulation of SOX2 by SLUG and TWIST1. *J. Exp. Clin. Cancer Res.* 40, 372. doi:10.1186/s13046-021-02147-7

Lemos, A. E. G., Matos, A. da R., Ferreira, L. B., and Gimba, E. R. P. (2019). The long non-coding RNA PCA3: an update of its functions and clinical applications as a biomarker in prostate cancer. *Oncotarget* 10, 6589–6603. doi:10.18632/oncotarget.27284

Li, F., Xu, Y., and Liu, R.-L. (2019). SAMD5 mRNA was overexpressed in prostate cancer and can predict biochemical recurrence after radical prostatectomy. *Int. Urol. Nephrol.* 51, 443–451. doi:10.1007/s11255-019-02096-3

Lian, E. Y., Maritan, S. M., Cockburn, J. G., Kasaian, K., Crupi, M. J. F., Hurlbut, D., et al. (2017). Differential roles of RET isoforms in medullary and papillary thyroid carcinomas. *Endocrine-Related Cancer* 24, 53–69. doi:10.1530/ERC-16-0393

Lin, X., Kapoor, A., Gu, Y., Chow, M. J., Xu, H., Major, P., et al. (2019). Assessment of biochemical recurrence of prostate cancer (Review). *Int. J. Oncol.* 55, 1194–1212. doi:10.3892/ijo.2019.4893

Luo, Y.-Z., He, P., and Qiu, M.-X. (2018). FOSL1 enhances growth and metastasis of human prostate cancer cells through epithelial mesenchymal transition pathway. *Eur. Rev. Med. Pharmacol. Sci.* 22, 8609–8615. doi:10.26355/eurrev_201812_16624

Lv, D., Wu, X., Chen, X., Yang, S., Chen, W., Wang, M., et al. (2021). A novel immune-related gene-based prognostic signature to predict biochemical recurrence in patients with prostate cancer after radical prostatectomy. *Cancer Immunol. Immunother.* 70, 3587–3602. doi:10.1007/s00262-021-02923-6

Maurus, K., Hufnagel, A., Geiger, F., Graf, S., Berking, C., Heinemann, A., et al. (2017). The AP-1 transcription factor FOSL1 causes melanocyte reprogramming and transformation. *Oncogene* 36, 5110–5121. doi:10.1038/onc.2017.135

Mawji, I. A., Simpson, C. D., Gronda, M., Williams, M. A., Hurren, R., Henderson, C. J., et al. (2007). A chemical screen identifies anisomycin as an anoikis sensitizer that functions by decreasing FLIP protein synthesis. *Cancer Res.* 67, 8307–8315. doi:10.1158/0008-5472.CAN-07-1687

Moro, L., Arbini, A. A., Yao, J. L., di Sant'Agnese, P. A., Marra, E., and Greco, M. (2009). Mitochondrial DNA depletion in prostate epithelial cells promotes anoikis resistance and invasion through activation of PI3K/Akt2. *Cell Death Differ.* 16, 571–583. doi:10.1038/cdd.2008.178

Nepali, P. R., and Kyprianou, N. (2023). Anoikis in phenotypic reprogramming of the prostate tumor microenvironment. *Front. Endocrinol. (Lausanne)* 14, 1160267. doi:10.3389/fendo.2023.1160267

Ness, N., Andersen, S., Valkov, A., Nordby, Y., Donnem, T., Al-Saad, S., et al. (2014). Infiltration of CD8+ lymphocytes is an independent prognostic factor of biochemical failure-free survival in prostate cancer: CD8+ Lymphocytes in Prostate Cancer. *Prostate* 74, 1452–1461. doi:10.1002/pros.22862

Newman, A. M., Liu, C. L., Green, M. R., Gentles, A. J., Feng, W., Xu, Y., et al. (2015). Robust enumeration of cell subsets from tissue expression profiles. *Nat. Methods* 12, 453–457. doi:10.1038/nmeth.3337

Paoli, P., Giannoni, E., and Chiarugi, P. (2013). Anoikis molecular pathways and its role in cancer progression. *Biochimica Biophysica Acta (BBA) - Mol. Cell Res.* 1833, 3481–3498. doi:10.1016/j.bbamcr.2013.06.026

Pashaei, E., Pashaei, E., Ahmady, M., Ozen, M., and Aydin, N. (2017). Meta-analysis of miRNA expression profiles for prostate cancer recurrence following radical prostatectomy. *PLoS ONE* 12, e0179543. doi:10.1371/journal.pone.0179543

Pound, C. R., Partin, A. W., Eisenberger, M. A., Chan, D. W., Pearson, J. D., and Walsh, P. C. (1999). Natural history of progression after PSA elevation following radical prostatectomy. *JAMA* 281, 1591–1597. doi:10.1001/jama.281.17.1591

Qiu, F.-N., Huang, Y., Chen, D.-Y., Li, F., Wu, Y.-A., Wu, W.-B., et al. (2016). Eukaryotic elongation factor-1α 2 knockdown inhibits hepatocarcinogenesis by suppressing PI3K/Akt/NF-κB signaling. *World J. Gastroenterol.* 22, 4226–4237. doi:10.3748/wjg.v22.i16.4226

Regua, A. T., Najjar, M., and Lo, H.-W. (2022). RET signaling pathway and RET inhibitors in human cancer. *Front. Oncol.* 12, 932353. doi:10.3389/fonc.2022.932353

Rennebeck, G., Martelli, M., and Kyprianou, N. (2005). Anoikis and survival connections in the tumor microenvironment: is there a role in prostate cancer metastasis? *Cancer Res.* 65, 11230–11235. doi:10.1158/0008-5472.CAN-05-2763

Sakamoto, S., McCann, R. O., Dhir, R., and Kyprianou, N. (2010). Talin1 promotes tumor invasion and metastasis via focal adhesion signaling and anoikis resistance. *Cancer Res.* 70, 1885–1895. doi:10.1158/0008-5472.CAN-09-2833

Sattari Fard, F., Jalilzadeh, N., Mehdizadeh, A., Sajjadian, F., and Velaei, K. (2023). Understanding and targeting anoikis in metastasis for cancer therapies. *Cell Biol. Int.* 47, 683–698. doi:10.1002/cbin.11970

Sfanos, K. S. (2022). Immune cell infiltrates and prognosis in localized prostate cancer. *J. Pathology* 256, 135–138. doi:10.1002/path.5817

Shahid, M., Lee, M. Y., Piplani, H., Andres, A. M., Zhou, B., Yeon, A., et al. (2018). Centromere protein F (CENPF), a microtubule binding protein, modulates cancer metabolism by regulating pyruvate kinase M2 phosphorylation signaling. *Cell Cycle* 17, 2802–2818. doi:10.1080/15384101.2018.1557496

Siegel, R. L., Miller, K. D., Wagle, N. S., and Jemal, A. (2023). Cancer statistics, 2023. *CA A Cancer J. Clin.* 73, 17–48. doi:10.3322/caac.21763

Sun, Y., Du, C., Wang, B., Zhang, Y., Liu, X., and Ren, G. (2014). Up-regulation of eEF1A2 promotes proliferation and inhibits apoptosis in prostate cancer. *Biochem. Biophysical Res. Commun.* 450, 1–6. doi:10.1016/j.bbrc.2014.05.045

Sung, H., Ferlay, J., Siegel, R. L., Laversanne, M., Soerjomataram, I., Jemal, A., et al. (2021). Global cancer statistics 2020: GLOBOCAN estimates of incidence and mortality worldwide for 36 cancers in 185 countries. *CA A Cancer J. Clin.* 71, 209–249. doi:10.3322/caac.21660

Taddei, M., Giannoni, E., Fiaschi, T., and Chiarugi, P. (2012). Anoikis: an emerging hallmark in health and diseases. *J. Pathol.* 226, 380–393. doi:10.1002/path.3000

Tolcher, A. W., Quinn, D. I., Ferrari, A., Ahmann, F., Giaccone, G., Drake, T., et al. (2012). A phase II study of YM155, a novel small-molecule suppressor of survivin, in castration-resistant taxane-pretreated prostate cancer. *Ann. Oncol.* 23, 968–973. doi:10.1093/annonc/mdr353

Urakami, S., Igawa, M., Kikuno, N., Yoshino, T., Kishi, H., Shigeno, K., et al. (2002). Combination chemotherapy with paclitaxel, estramustine and carboplatin for hormone refractory prostate cancer. *J. Urol.* 168, 2444–2450. doi:10.1097/01.ju.0000036356.87513.bc

VanDeusen, H. R., Ramroop, J. R., Morel, K. L., Bae, S. Y., Sheahan, A. V., Sychev, Z., et al. (2020). Targeting RET kinase in neuroendocrine prostate cancer. *Mol. Cancer Res.* 18, 1176–1188. doi:10.1158/1541-7786.MCR-19-1245

Wang, L., Li, C., Wang, J., Yang, G., Lv, Y., Fu, B., et al. (2022a). Transformable ECM deprivation system effectively suppresses renal cell carcinoma by reversing anoikis resistance and increasing chemotherapy sensitivity. *Adv. Mater* 34, e2203518. doi:10.1002/adma.202203518

Wang, M., Xia, H., Yan, Q., Liu, W., Liu, M., and Wang, X. (2022b). Identification of pyroptosis-related gene signatures and construction of the risk model to predict BCR in prostate cancer. *Front. Mol. Biosci.* 9, 850758. doi:10.3389/fmolb.2022.850758

Wen, S., Niu, Y., Lee, S. O., and Chang, C. (2014). Androgen receptor (AR) positive vs negative roles in prostate cancer cell deaths including apoptosis, anoikis, entosis, necrosis and autophagic cell death. *Cancer Treat. Rev.* 40, 31–40. doi:10.1016/j.ctrv.2013.07.008

Woo, J. R., Liss, M. A., Muldong, M. T., Palazzi, K., Strasner, A., Ammirante, M., et al. (2014). Tumor infiltrating B-cells are increased in prostate cancer tissue. *J. Transl. Med.* 12, 30. doi:10.1186/1479-5876-12-30

Worst, T. S., Waldbillig, F., Abdelhadi, A., Weis, C.-A., Gottschalt, M., Steidler, A., et al. (2017). The EEF1A2 gene expression as risk predictor in localized prostate cancer. *BMC Urol.* 17, 86. doi:10.1186/s12894-017-0278-3

Xu, C., Hu, D., and Zhu, Q. (2013). eEF1A2 promotes cell migration, invasion and metastasis in pancreatic cancer by upregulating MMP-9 expression through Akt activation. *Clin. Exp. Metastasis* 30, 933–944. doi:10.1007/s10585-013-9593-6

Ye, G., Yang, Q., Lei, X., Zhu, X., Li, F., He, J., et al. (2020). Nuclear MYH9-induced CTNNB1 transcription, targeted by staurosporin, promotes gastric cancer cell anoikis resistance and metastasis. *Theranostics* 10, 7545–7560. doi:10.7150/thno.46001

Zelefsky, M. J., Kelly, W. K., Scher, H. I., Lee, H., Smart, T., Metz, E., et al. (2000). Results of a phase II study using estramustine phosphate and vinblastine in combination with high-dose three-dimensional conformal radiotherapy for patients with locally advanced prostate cancer. *J. Clin. Oncol.* 18, 1936–1941. doi:10.1200/JCO.2000.18.9.1936

Zhan, B., Huang, L., Chen, Y., Ye, W., Li, J., Chen, J., et al. (2020). miR-196a-mediated downregulation of p27 ^{kip1} protein promotes prostate cancer proliferation and relates to biochemical recurrence after radical prostatectomy. *Prostate* 80, 1024–1037. doi:10.1002/pros.24036

Zhang, K., Myllymäki, S.-M., Gao, P., Devarajan, R., Kytölä, V., Nykter, M., et al. (2017). Oncogenic K-Ras upregulates ITGA6 expression via FOSL1 to induce anoikis resistance and synergizes with αV-Class integrins to promote EMT. *Oncogene* 36, 5681–5694. doi:10.1038/onc.2017.177

Zhang, W., Shu, P., Wang, S., Song, J., Liu, K., Wang, C., et al. (2018). ZNF154 is a promising diagnosis biomarker and predicts biochemical recurrence in prostate cancer. *Gene* 675, 136–143. doi:10.1016/j.gene.2018.06.104

Frontiers in Endocrinology

Explores the endocrine system to find new therapies for key health issues

The second most-cited endocrinology and metabolism journal, which advances our understanding of the endocrine system. It uncovers new therapies for prevalent health issues such as obesity, diabetes, reproduction, and aging.

Discover the latest Research Topics

See more →

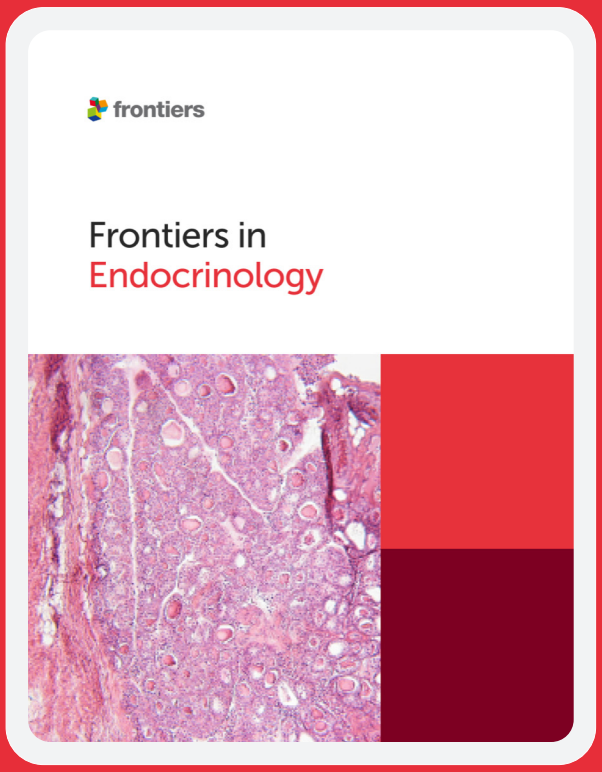

Frontiers

Avenue du Tribunal-Fédéral 34
1005 Lausanne, Switzerland
frontiersin.org

Contact us

+41 (0)21 510 17 00
frontiersin.org/about/contact